THE CONTACT ANGLE

AND

TWO-PHASE FLOW

\+ + + +

A Thesis submitted

for the degree of Doctor of Philosphy

in the University of Bristol

by

Terence Desmond Blake

Department of Physical Chemistry,

University of Bristol.

February, 1968.

S Y N O P S I S

The purpose of this work was to investigate the behaviour of the interfacial region between two immiscible fluid phases undergoing displacement through a porous material. In order to escape problems arising from the geometric complexities of naturally occurring systems, the studies have been confined to the interaction of capillary and hydrodynamic effects within the limited context of immiscible displacement in the simplest of all porous media: a single, uniform, cylindrical capillary.

In a preliminary investigation, benzene-water displacements were carried out in horizontal, Pyrex capillaries of small diameter (less than 1 mm). The predicted linear relationship between interfacial velocity and applied hydrostatic pressure was verified for rates of displacement in excess of 0.3 mm sec^{-1}, but at lower speeds, interfacial motion became unsteady. This was interpreted as the result of haphazard contamination of the capillary wall, and experiments were therefore begun in alkylchlorosilane-treated capillaries, whose surfaces were thought to be relatively inert. This approach was successful, and it was eventually possible to maintain steady displacement rates below 1μ sec^{-1}.

In these experiments, a micro-ciné apparatus was employed which *permitted* ~~enabled~~ the first, direct and simultaneous observations of interfacial velocity, applied hydrostatic pressure and the

contact angle. Results indicated that at sufficiently low displacement rates the moving interface is governed by the same two boundary conditions that govern the equilibrium state: namely the Laplace equation and a three-phase boundary condition represented by the contact angle. It was found that the dynamic behaviour of the contact angle is a major influence upon the character of the displacement, making it necessary to distinguish two types of two-phase flow, designated respectively consecutive and concentric flow. Transitions from one flow regime to the other were observed in systems having a high viscosity ratio and a low interfacial tension.

Data were also obtained on the velocity dependence of the contact angle over a greater range of velocities and under conditions of greater sensitivity than hitherto. This has prompted a theoretical treatment of contact angle velocity dependence in terms of a molecular displacement process in the three phase zone.

The value of the contact angle in the system benzene/water/trimethylchlorosilane-coated glass was dependent upon the duration of contact between water (or benzene saturated with water) and the treated glass surface. In general, the contact angle and its velocity dependence fell whilst contact angle hysteresis increased with increasing time of contact. In order to investigate this behaviour further, a period of research was devoted to the measurement of adsorption/desorption isotherms

of water on treated and untreated Vycor porous glass. This revealed that trimethylchlorosilane reacts with slightly less than half the available surface hydroxyl groups in fully hydrated porous glass, that the consequent reduction in B.E.T. monolayer capacity to water is largely due to the restriction of water adsorption at low relative pressures to unreacted hydroxyl groups, and that subsequent exposure of the treated surface to water vapour causes a reduction in its hydrophobic character.

Finally, techniques have been developed for the manufacture, calibration and utilisation of capillaries having diameters of less than 20μ. Benzene-water displacements have been carried out in two tubes of respectively 2 and 10μ radius. Determination of liquid viscosities and interfacial tensions have revealed no significant deviations from the accepted values.

CONSULTATION RECORD

UNIVERSITY OF BRISTOL

THE LIBRARY

All readers must sign their names in the space below, in confirmation that they understand and agree to observe the above conditions.

NAME (block capitals)	PERMANENT ADDRESS	SIGNATURE	DATE
DR C.E. BROWN	BP RESEARCH CENTRE, SUNBURY	C.E. Brown	16/3/76
J. S. PASAK	BRISTOL UNIVERSITY	J. S. Pasak	11/3/77
R. A. DAWS	IMPERIAL COLLEGE	R.A. Daws	4/7/77
MIR ASADULLAH	ESSEX UNIVERSITY	M. Asadullah	24/9/84
MIR ASADULLAH	ESSEX Univ.	M. Asadullah	2/9/85

THE CONTACT ANGLE

AND

TWO-PHASE FLOW

+ + + +

A Thesis submitted

for the degree of Doctor of Philosophy

in the University of Bristol

by

Terence Desmond Blake

Department of Physical Chemistry,

University of Bristol.

February, 1968.

To my Parents

and

to my Wife

MEMORANDUM

The work described in this thesis was carried out by me in the Department of Physical Chemistry of the University of Bristol between September 1964 and September 1967, under the joint supervision of Professor D. H. Everett, M.B.E., M.A., D.Sc. and Dr. J. M. Haynes. No part of this thesis has previously been submitted by me for any other higher degree, and the work described herein is original and unaided except where specific reference or acknowledgement has been made.

19th February, 1968.

T. D. Blake

I acknowledge with gratitude my debt to all those who have helped me during the course of this work. Special thanks are due to:

The Iraq Petroleum Company whose financial aid has made this work possible;

Professor D. H. Everett for his encouragement and unfailing interest;

Dr. J. M. Haynes, my mentor, for his help and guidance so generously given;

My Wife for her forbearance during the preparation of this dissertation.

C O N T E N T S

I N T R O D U C T I O N

Two-phase flow in porous media has been the object of increasing activity in recent years. This is largely as a result of its technological importance in the field of petroleum recovery, but soil science, groundwater hydrology and chemical engineering have provided additional impetus[98,167,168,169,170].

Much of this increased activity has centred on systems of such geometric complexity that they can be described only statistically and, as a result, rather imperfectly. However, the problems encountered in a detailed phenomenological description of two-phase flow originate only partly in the complicated geometric structure of the pore system, which is involved in both the capillary and hydrodynamic aspects of the problem: a more basic obstacle is the complexity of each of these aspects considered independently of the geometric intricacies. The present purpose is, therefore, to consider the interaction of capillary and hydrodynamic effects within the limited context of immiscible displacement in the simplest of all porous media: a single, uniform cylindrical capillary.

This approach is by no means original, the earliest work[124] located by the author was done in 1911; nevertheless, one aspect has received less attention than it merits,

and in the present work particular emphasis will be laid upon the importance of the contact angle.

The first two chapters will be concerned with the historical background and present status of the contact angle in relation to heterogeneous systems at equilibrium, although the early sections will be devoted to the more basic concept of surface tension.

In Chapter 3 the relevance of the contact angle to dynamic systems will be considered, and it will be shown that the particular problem of the contact angle makes it necessary to distinguish two types of two-phase flow.

Some detailed experimental studies of two-phase flow will be reported in Chapter 4, and in Chapter 5 space will be given to the development of a simple theory to account for the observed behaviour of the contact angle under dynamic conditions.

The concluding chapter will comprise a report of some preliminary studies of two-phase flow in microscopic capillaries.

During the course of study, a side issue has developed regarding the behaviour of certain alkyl chlorosilanes as surface modifying agents. A period of research has therefore been devoted to water adsorption on treated and untreated Vycor porous glass. A brief experimental description and a discussion of the results of this work appear in Appendix II.

C H A P T E R O N E

Capillary Systems at Equilibrium

Introduction

Whenever two immiscible phases exist in mutual contact they will in general be separated by an interface, interfacial zone or interphase in which there will be a more or less discontinuous transition from the properties of one phase to those of the other. In a capillary system the configuration of the interface plays a significant part in determining the thermodynamic state of the whole system. Any complete description of such a system must, therefore, account adequately for the experimental properties of the interfacial region as well as for those of the bulk phases.

In descriptions of this kind it is convenient to distinguish factors which govern mechanical equilibrium from those responsible for physico-chemical equilibrium and it is the contribution of the former to the, more general, thermodynamic equilibrium that will be the primary concern of this chapter. However, the treatment of individual equilibrium conditions inisolation has resulted in some confusion in the work of some authors - especially in relation to the mechanical stability of systems containing both fluids and solids. In this chapter, therefore, it is intended to give due consideration to all factors which

influence the particular stability conditions discussed.

1.1 Systems Containing Only Fluids

Surface Tension

In the absence of external macroscopic fields, such as gravity, the equilibrium stress tensor in a bulk fluid is isotropic and identical in magnitude (though opposite in sign) to the hydrostatic pressure. At the interface between two immiscible fluids, however, there exists, in addition, an anisotropic component normal to the interface. Furthermore, an exact formulation of this component is very difficult since it can only follow an exact knowledge of the change in molecular properties in going from one bulk phase to the other.[1] Without this detailed knowledge, it is necessary to devise a model in order to explain the experimental properties of the interface.

It so happens that the system behaves, from a mechanical standpoint, as if it consisted of two homogeneous fluids separated by a surface of uniform tension and zero thickness[2]. This "surface of tension" is, of course, purely fictitious; it is simply an artifact which fits the experimental facts and stands in place of the real molecular dynamic system.

Dividing Surfaces

Problems similar to those noted above are also

inherent in an exact physico-chemical specification of the interphase and they have been met in an analogous way.

Gibbs[3] has proposed a model in which both bulk phases remain homogeneous up to a geometrical dividing surface, parallel to the surface of tension and also of zero thickness. The differences in energy, entropy and mass between the model and the real system are made up by ascribing to the former, excess quantities of these properties.

Whilst, in principle, the position of the dividing surface is quite arbitrary, in practice it is found that the surface excess quantities are very sensitive to the position chosen[4]. Gibbs, therefore, makes the choice in such a way that the surface excess of one component becomes zero: relative excess quantities can then be defined which are invariant with respect to the position of the dividing surface. If, however, it is desired to make the model both physicochemically and mechanically equivalent to the real system, then the dividing surface must be placed coincident with the surface of tension. Fortunately, this condition only applies to curved surfaces and may often be relaxed providing the curvature is not great (i.e. not greater than, say, $10^4 cm^{-1}$). To some extent surface tension may also be regarded as an excess quantity[5], but it is important to remember that, whilst, experimentally, the surface of tension may be ill defined, its location and properties

are, in principle, completely defined by the real microscopic state of the interfacial zone and are in no way arbitrary.

In general, the use of a dividing surface is quite fundamental to the treatment of curved surfaces since only then is precise meaning given to the concepts of area and curvature. In the case of a plane interface the concept of a dividing surface is still useful, but not necessary, and valid alternatives exist[6,7,8].

Surface Tension: a Hydrostatic Property

The derivations of equations governing hydrostatics are all to be found in the standard texts[9]. However, a brief survey of those equations specific to the mechanical equilibrium of fluid/fluid interfaces will be useful for the present purposes. The two-dimensional principle of hydrostatics, which governs the mechanical equilibrium of a single surface, is given by the Laplace formula:[10]

$$(p'' - p') = \sigma \left(\frac{1}{r_1} - \frac{1}{r_2}\right) \qquad 1.1\text{-}1$$

where p'' and p' are the bulk hydrostatic pressures on opposite sides of the interface of surface tension σ, and r_1 and r_2 are the two principal radii of curvature of the surface at the point considered. Before proceeding, if the mean curvature is defined by

$$\frac{1}{r_m} = \frac{1}{2}\left(\frac{1}{r_1} + \frac{1}{r_2}\right) \qquad 1.1\text{-}2$$

Then Eq. 1.1-1 becomes

$$(p'' - p') = \frac{2\sigma}{r_m} \qquad 1.1\text{-}3$$

By convention, σ is taken to be positive so that the pressure on the concave side of the interface, p", is greater than that on the convex side, p'. Thus Eqs. 1.1-1 and 1.1-3 give an experimental definition of surface tension. (Note, however, that σ is left experimentally undefined when the interface is planar). Laplace[10] (1806) in fact used potential theory and not the concept of surface tension to derive Eqs. 1.1-1 and 1.1-3; however, Young's macroscopic concept of surface tension can also be used to obtain them and it seems likely that Young (1805) independently arrived at similar conclusions, though they lacked Laplace's mathematical rigour.

Laplace's equation is valid at every point on the surface, regardless of gravitational forces, provided only that the weight of the surface phase itself can be neglected.*

---

* Gibbs[3] (pp. 276-281) has shown that if the weight of material adsorbed at the interface is taken into account then Laplace's equation gains another term: thus Eq. 1.1-1 becomes

$$p'' - p' = \sigma\left(\frac{1}{r_1} + \frac{1}{r_2}\right) + g\Gamma\cos\alpha$$

where Γ is the total adsorption in gm cm^{-2} <u>at the surface</u>

In the absence of gravitational effects, the pressures p' and p" are uniform throughout their respective phases; σ also remains constant. At equilibrium, therefore, the mean radius, r_m, will be the same for all points in the surface. The surface is then said to have constant mean curvature. The sphere is the simplest of such surfaces.

The one-dimensional hydrostatic principle for three fluid phases which meet along a line of contact is given by an equation often called "The Law of Neumann's Triangle[12]." In vectorial notation, the equation is

---

footnote continued

of tension, g is the acceleration under gravity and α denotes the angle which the normal to the surface (at the point considered) makes with the vertical. Furthermore, the interfacial tension will vary with the height of the interface according to the equation

$$\frac{d\sigma}{dZ} = g\Gamma$$

However, since Γ is unlikely ever to exceed 10^{-8} gm cm^{-2} both effects are usually quite negligible - but this will not always be the case. For example, in a centrifugal field or in a near-critical system gravitational terms could play a dominant role in determining interfacial stability and the variation of σ with the spatial coordinates would then require explicit consideration.

$$\bar{\sigma}_{12} + \bar{\sigma}_{23} + \bar{\sigma}_{31} = 0 \qquad 1.1\text{-}4$$

where $\bar{\sigma}_{ij}$ is the surface tension vector acting normal to the line of contact within the ij interface. In connection with this equation, Defay and co-authors[4](p 10) have stated "It may be remarked that this condition is not a necessary and sufficient condition (for equilibrium), since the line of contact might itself be subjected to a tension. A curved line of contact in tension could be in equilibrium with the resultant of three surface tensions (σ_{ij}). There is, however, no convincing evidence for the existence of a tension of this kind." Gibbs, on the other hand, has suggested that such a line tension does exist and has outlined a thermodynamics for a line phase. (Gibbs[3] p.288 (footnote) et seq.)

Surface Tension: a Thermodynamic Property.

The thermodynamics of capillary systems has been fully dealt with in several recent texts[4, 8, 13, 14, 15]; the present purpose is merely to illustrate the thermodynamic nature of surface tension.

The superscript σ will be used to signify the surface excess of a quantity: thus, the terms U^{σ}, F^{σ}, S^{σ} and n_i^{σ} will denote respectively the excess internal energy, Helmholtz free energy, entropy, and number of moles of component i associated with the interface of area A. Then, for all isothermal, reversible

variations of a system initially at equilibrium at temperature T,

$$dU^\sigma = TdS^\sigma + \sigma dA + \sum_i \mu_i dn_i{}^\sigma \qquad 1.1\text{-}6$$

and

$$dF^\sigma = dU^\sigma - TdS^\sigma$$

$$= \sigma dA + \sum_i \mu_i dn_i \qquad 1.1\text{-}7$$

where μ_i is the chemical potential of component i.

It is convenient to use lower case symbols to denote quantities referred to unit area of surface, so that

$$\left.\begin{aligned} u^\sigma &= \frac{U^\sigma}{A} \\ s^\sigma &= \frac{S^\sigma}{A} \\ f^\sigma &= \frac{F^\sigma}{A} \end{aligned}\right\} \qquad 1.1\text{-}8$$

and the integrated form of Eq. 1.1-6 describing the isothermal, reversible production of unit surface is

$$u^\sigma = Ts^\sigma + \sigma + \sum_i \mu_i \Gamma_i \qquad 1.1\text{-}9$$

where Γ_i is the adsorption of component i:

$$\Gamma_i = \frac{n_i}{A} \qquad 1.1\text{-}10$$

The specific Helmholtz free energy of the surface is given by $f^\sigma = u^\sigma - Ts^\sigma$

$$= \sigma + \sum_i \mu_i \Gamma_i \qquad 1.1\text{-}11$$

It is sometimes possible to choose the dividing surface so that $\sum_i \mu_i \Gamma_i = 0$. <u>If</u> this is done then

$$f^\sigma = \sigma \qquad 1.1\text{-}12$$

However, this choice is not always convenient and in

general the surface tension is not equal to the specific Helmholtz free energy as is sometimes assumed[41]. Other, similar misconceptions occur in the literature. As Melrose has pointed out[16], the specific internal energy u is often referred to as a surface enthalpy: "This usage appears to rest on the frequently adopted view that in the case of interfaces involving but a single component the surface tensions can be regarded as Gibbs free energies." More generally, it would seem appropriate to define specific surface enthalpies by

$$h^\sigma = u^\sigma - \sigma$$

$$= Ts^\sigma + \sum_i \mu_i \Gamma_i \qquad 1.1\text{-}13$$

and specific Gibbs free energies by

$$g^\sigma = h^\sigma - Ts^\sigma$$

$$= \sum_i \mu_i \Gamma_i \qquad 1.1\text{-}14$$

"Unfortunately, the practice of referring to the surface excess internal energy as the enthalpy and the interfacial tension as the Gibbs free energy is almost universal in the literature." Some examples of the confusion resulting from this failure to exploit to the full the analogy between surface and bulk fundamental equations have been cited by Johnson[17].

Nevertheless, σ can still be regarded as the <u>total</u> change in free energy of a closed system containing a plane surface accompanying the isothermal, reversible

creation of fresh surface of unit area: that is

$$\left(\frac{\partial F}{\partial A}\right)_{T,V,n_i} = \sigma \qquad 1.1\text{-}15$$

This can be demonstrated by separating the various contributions to the free energy using primes to distinguish the two bulk phases: thus

$$F = F' + F'' + F^{\sigma} \qquad 1.1\text{-}16$$

and the total differential free energy is then given by

$$\begin{aligned} dF &= dF' + dF'' + dF^{\sigma} \\ &= -S'dT - p'dV' + \sum_i \mu_i' dn_i' \\ &\quad -S''dT - p''dV'' + \sum_i \mu_i'' dn_i'' \\ &\quad -S^{\sigma}dT + \sigma dA + \sum_i \mu_i^{\sigma} dn_i^{\sigma} \end{aligned} \qquad 1.1\text{-}17$$

If the interface is planar, $p' = p''$ and since V is held constant $dV' = -dV''$ and the volume work terms cancel. Further, the system is at equilibrium, therefore

$$\mu_i' = \mu_i'' = \mu_i(\sigma) \qquad 1.1\text{-}18$$

and the system is closed so that

$$dn_i' + dn_i'' + dn_i^{\sigma} = 0 \qquad 1.1\text{-}19$$

Hence $dF = \sigma dA$ and Eq. 1.1-15 follows. This explains why σ and not f^{σ} appears in formulae such as Laplace's equation and Neumann's law (and, as we shall see in section 1.3, Young's equation).

It can be shown that the hydrostatic principles noted above and Pascal's laws for bulk fluids are necessary conditions for the more general thermodynamic

equilibrium of fluid systems. They are as much part of Thermodynamics as, for example, Eq. 1.1-18. To illustrate this complementary role, Eq. 1.1-17 may be written, for all isothermal, reversible changes in a closed system of constant volume containing a closed spherical interface of radius r. The pressure inside the sphere is p" and that outside p'. Conditions 1.1-18 and 1.1-19 apply here also, but in this case

$$dV' = -dV'' = 4\pi r^2 dr$$

and

$$dA = 8\pi r dr$$

Substitution of these values for dV', dV" and dA in Eq. 1.1-17 and utilization of the condition for thermodynamic equilibrium $(\partial F)_{V,T,n_i \text{ etc}} = 0$ yields

$$4\pi r^2 dr(p'' - p') + 8\pi r\sigma dr = 0$$

which simplifies to

$$p'' - p' = \frac{2\sigma}{r} \qquad 1.1\text{-}20$$

Eq. 1.1-20 can at once be recognised as a particular case of the more general Laplace equation.

Finally in this section it is emphasised that the only condition both necessary and sufficient for thermodynamic equilibrium is that the <u>total</u> free energy of the whole system is a minimum. This condition can be expressed mathematically in numerous ways: four are

listed below:

$$\left(\frac{\partial U}{\partial n_i}\right)_{V,S,n_j \text{ etc}} = 0 \qquad 1.1\text{-}21$$

$$\left(\frac{\partial H}{\partial n_i}\right)_{P,S,n_j \text{ etc}} = 0 \qquad 1.1\text{-}22$$

$$\left(\frac{\partial G}{\partial n_i}\right)_{P,T,n_j \text{ etc}} = 0 \qquad 1.1\text{-}23$$

$$\left(\frac{\partial F}{\partial n_i}\right)_{V,T,n_j \text{ etc}} = 0 \qquad 1.1\text{-}24$$

1.2 The Surface Tension of a Solid

For an amorphous solid in a uniform state of stress, in equilibrium with its surroundings and possessing a mechanism for remaining so, the problem of thermodynamic description reduces to that for a fluid at rest. The mechanical equilibrium of such a "solid" body will therefore be governed by the various principles of hydrostatics.

The solids commonly encountered are not generally of this type, since they lack the mechanism enabling them to adjust to the conformation required for thermodynamic equilibrium; furthermore, their rigidity allows them to remain in mechanical equilibrium whilst accommodating non-uniform states of stress both within the solid and at the surface. The work of formation of the surface of a solid is therefore not the same as the work of stretching it, and, for all normal solids, the surface tension is

not equal to the surface stress* (See Gibbs[3], p.315). Nevertheless, there exist good experimental reasons for ascribing to a solid surface a tension analogous to that of fluids:[18,19] in particular, studies of the rate of homogeneous nucleation in supercooled liquids as a function of the amount of undercooling[20,21] are especially significant.

The definitions of surface tension given up to now, namely, Eqs. 1.1-1, 1.1-3 and 1.1-15, apply only to systems in thermodynamic equilibrium**. For the case of the non-equilibrium solid, Gibbs[3] (p.315) has proposed the definition

$$\sigma_s = f^\sigma - \sum_i \Gamma_i \mu_i^\sigma \qquad 1.2\text{-}1$$

This expression (which is the same as Eq. 1.1-11) involves only integral quantities which are indifferent as to whether or not the path taken in achieving them was isothermal and reversible. As Gibbs recognised, however,

---

*This is not generally true of fluids either <u>unless</u> the stretching process is done isothermally and reversibly. The point is that fluids <u>can</u> be stretched in this way, but normal solids <u>cannot.</u>

**For systems not in physico-chemical equilibrium see Defay and co-authors[4] pp. 55-70.

the quantities μ_i^σ and f^σ are only defined when the material and energy densities are uniform in the bulk of the solid. Such is clearly not the case when the state of internal strain varies from point to point and σ_s is as undefined as before.

A necessary and sufficient condition for thermodynamic equilibrium is that the total Helmholtz free energy of the system is a minimum: Eq. 1.1-24. This is the same for solids as for any other system, yet it is commonly assumed that minimisation of surface free energy only is sufficient. Once again the state of internal strain is ignored. In defence of this procedure it is argued that the elastic and configurational energy associated with the state of stress is only a very small part of the total internal energy (thermal, electrostatic, etc.) and may, therefore, safely be ignored.

Gibbs has recognised these problems and elegantly avoided them by choosing the dividing surface so that the adsorption of component 1, the solid, is reduced to zero. Eq. 1.2-1, written in terms of relative excess quantities, then becomes

$$\sigma_s = f_1^\sigma - \sum_{i=2}^{n} \Gamma_{i,1}\mu_i \qquad 1.2\text{-}2$$

where $\Gamma_{i,1}$ and μ_i are the relative adsorptions and chemical potentials of the n - 1 components comprising

the surroundings.* Provided only that the various energy and material densities of the solid, its state of strain etc., all remain constant and unaffected by changes in the surroundings, then the terms in Eq. 1.2-2 are completely defined.

If the solid is, for example, soluble in its surroundings, then this is the only rigorous definition of σ_s possible without detailed knowledge of the state of strain of the solid. If, on the other hand, it is wished to consider only the equilibrium of fluids at the surface of, as Gibbs put it, "an unchangeable solid," that is one whose <u>total</u> energy, mass, state of strain etc. all remain constant, then the following method of treating the subject is "more simple and at the same time more general" (Gibbs[3] p.328). Gibbs did not give σ_s a name; he did, however, define ξ "the superficial tension of the fluid in contact with the solid". According to his definition

$$\xi = \sigma_s - \sigma_{s,o} \qquad 1.2\text{-}3$$

where $\sigma_{s,o}$ is the value of σ_s if the solid were bounded by a vacuum: ξ may be either positive or negative and, for an immutable solid, will depend only upon temperature.

---

*The surroundings are assumed here to be fluids in equilibrium. For the situation in which the surroundings comprise solids see Eley[15] p.76 <u>et seq.</u>

By this means, the solid becomes merely a boundary condition upon the equilibrium of the contacting fluids.

1.3 Young's Equation and The Contact Angle

The System.

The system to be considered is illustrated below:

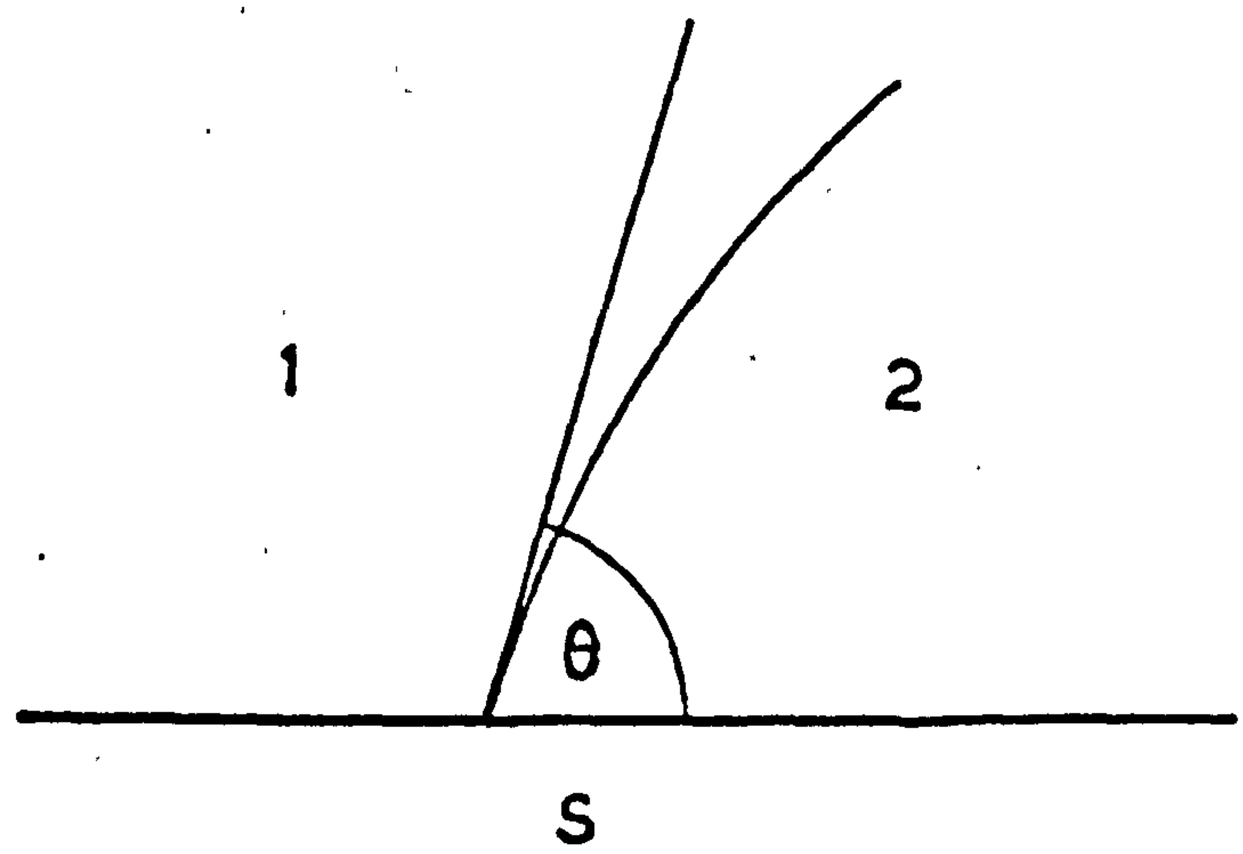

Fig. 1.1

Two immiscible fluid phases, 1 and 2, are simultaneously in contact with each other and a solid surface, S, at a line of three phase contact (the three phase line or TPL). In general, one of the fluid phases will be liquid whilst the other can be either liquid or gas. The various interfaces will be denoted by the subscripts S1, S2 and

12. The angle between the planes tangential to the solid surface and to the fluid/fluid (i.e. 12) interface at the TPL is called the contact angle θ. Unless otherwise stated, the convention adopted here is that θ be measured through phase 2.

If the 12 interface is considered to possess a tension σ_{12}, then it will exert a force $\sigma_{12} \cos\theta$ upon the TPL in a direction parallel to the solid surface. For the system to remain in mechanical equilibrium there must also exist forces of the same nature as surface tensions acting upon the TPL and associated with the S1 and S2 interfaces. Let them be denoted by σ_{1S} and σ_{2S} respectively; then, without making any assumptions about the mechanism by which they act, for equilibrium at the TPL

$$\sigma_{1S} - \sigma_{2S} = \sigma_{12} \cos\theta \qquad 1.3\text{-}1$$

The Historical Background.

The earliest statement of Eq. 1.3-1 is to be found in "An Essay on the Cohesion of Fluids" by Thomas Young[2] (p.84) - albeit in words rather than in algebraic form. Eq. 1.3-1 will therefore be designated Young's equation.

Ever since its appearance this relationship has aroused considerable, and at times quite heated, discussion[22,23]. Even the name is controversial. Adam[24] has suggested that Eq. 1.3-1 is too obvious to be worthy

of Young's name, and of late the appellation "The Young & Dupré equation" has enjoyed a certain vogue[14,25]. However, as Melrose[26] points out, "... no support for this latter description may be obtained from any adequate review of the classical work in this field, such as that of Bakker[(27)]." If any modification is justified it would seem far more suitable to refer to the relation as the Young-Gauss equation since Gauss was apparently the first to present it mathematically[28].

The concept of liquid surface tension was generally accepted in Young's time, for example by Segner[29](1751) and by Monge[30]; further, according to Bashforth and Adams[11], Clairault (1743) had appreciated that the height to which a liquid will rise in a capillary is determined by the relative attraction of the liquid particles for themselves and for the walls of the tube. He concluded that even if the former attractions were of greater magnitude than the latter, provided they were not twice as great, the liquid would still rise.

In 1869, Dupré[31] proposed the definition of the <u>work of adhesion</u>

$$W_{SL} = \sigma_S + \sigma_L - \sigma_{SL} \qquad 1.3\text{-}2$$

where σ_S, σ_L and σ_{SL} are supposed to be respectively the tensions of the solid surface, the liquid surface and the solid/liquid interface. Combined with a less general form of Young's equation,

$$\sigma_S - \sigma_{SL} = \sigma_L \cos\theta \qquad 1.3\text{-}3$$

the Dupré equation yields an expression relating W_{SL} to the contact angle:

$$W_{SL} = \sigma_L(1 + \cos\theta) \qquad 1.3\text{-}4$$

This expression (or rather its modern counterpart) is in some ways more useful than Eq. 1.3-3 since it involves only terms which are usually considered to be readily measurable, unlike Youngs equation for which σ_S and σ_{SL} are difficult even to define. Whilst Eq. 1.3-4 is clearly foreshadowed by Clairault's conclusions (above) the idea expressed, that competition between the cohesion of a liquid to itself and its adhesion to a solid gives rise to an angle of contact both constant and specific to a given system at equilibrium, was expounded for the first time in Young's original essay.

The extra utility and subtlety of Eq. 1.3-4 has prompted Adam[24] to suggest that "we should do more honour to Thomas Young by giving his name to equation (1.3-4) rather than to (1.3-3)". However, as Kitchener[33] notes, "Unfortunately, this plea seems unlikely to be heeded as the name is firmly attached to (Eq. 1.3-3) in innumerable text books. A practical compromise would be to call (Eq. 1.3-4) the "Young-Dupré equation" as it is normally arrived at by combining Dupré's equation with the so-called Young's equation".

Objections to Young's Equation

Adam's view[24] that Young's equation "... is obvious to anyone who regards surfaces as being in tension" is not universally accepted.

Bikerman[34] has repeatedly opposed the equation on the grounds that the equilibrium conditions are discussed only with respect to forces parallel to the surface and that no account is taken of the component of the stress tensor normal to the surface. Bikerman has published a booklet[35] containing two papers on Young's equation. In these he repeats all his objections and includes some experimental work in support of his views.

An analysis of the stresses in the region of three phase contact (the three phase zone or TPZ) performed by Lester[36] predicts that the normal component, $\sigma_{12} \sin \theta$, will cause distortion of the solid surface. If the solid is <u>easily</u> deformable, then the distortion may be sufficient to destroy the validity of Young's equation.

That distortion does occur has been elegantly demonstrated by Tabor and Baily[37]. They placed a few drops of mercury on a smooth mica sheet of 1 or 2μ thickness and observed that the mica was pulled up all round the edges of the drops. With mercury and this thickness of mica the deflection was of the order of 1 mm.

Michaels and Dean[38] have found similar effects when

paraffin oil is placed on unhardened silica-aquagel. The angle formed between the liquids in this case is close to the appropriate Neumann angle. However, on acid hardening, as the gel becomes more rigid, the deformation becomes smaller, and the angle eventually increases to the Young angle predicted by assuming the surface tension of a dilute gel to be close to that of the solution before gelation.

Melrose[26] has concluded that "The evidence provided by these experiments suggests that in most cases the defect in Young's equation arising from solid phase deformability is not important". It would seem, therefore, that Bikerman has overstated the case and that, in general, his objections are unrealistic.

The validity of Young's equation in a gravitational field has also been questioned[39,40]. Kitchener[33] has published a critical review on the subject in which he concludes that "the treatment of surfaces given by Gibbs in 1878 is still the most comprehensive and rigorous that has ever been presented". The treatment referred to includes a derivation of Young's equation, which, whilst apparently rather sketchy and spread over a number of pages, is, in fact, complete and explicitly allows for the effects of gravity as well as for those of adsorption and curvature. As Melrose observes, "His (i.e. Gibbs') discussion, although sufficiently extensive as to suggest

the subject is of some importance, has, apparently, not appealed to later writers. Thus the treatments given in presently available texts[14,41,42] and in recent reviews[43-45] do not, explicitly at least, refer to the existence of such conclusions".

Derivations of Young's Equation.

Much of the confusion concerning the function and validity of Young's equation, which has ensued since Gibbs' work, must be attributed to the many careless "derivations" present in more recent and otherwise respectable texts. Gray[46] has remarked on some notable examples. Misrepresentation of surface tension as variously surface Helmholtz or Gibbs free energy (the terms sometimes being interchanged indiscriminately[41]) or surface enthalpy has added immensely to the misunderstanding. The chaos in the literature is vast, and apparently self-regenerative[24,47]. In view of this, Johnson's recent and lucid restatement of Gibbs' proof, in modern terms, is all the more welcome.

Johnson[17] considers the equilibrium of a liquid drop resting on a "homogeneous, continuous and isotropic surface" in the presence of an equilibrium vapour phase and in a gravitational field. Gibbs makes his analysis using the equilibrium condition given by Eq. 1.1-21, whilst Johnson uses the equivalent condition Eq. 1.1-24. He shows that the necessary and sufficient condition for

thermodynamic equilibrium can be split up into two separate, though not independent, necessary conditions. One of these is necessary and sufficient for physico-chemical equilibrium, the other for mechanical equilibrium. Both take explicit account of gravity. The mechanical condition is then resolved into three, separate, hydrostatic principles relating to volume, surface and line, each of which is necessary for the thermodynamic equilibrium of the whole system. Thus appear Pascal's laws for bulk fluids, Laplace's equation for surfaces and Young's equation for the equilibrium of the TPL. If the system had contained three fluids, instead of two fluids and a solid, then Neumann's law would have resulted instead of Young's equation.

Derived in this way, the Laplace equation contains terms due to the weight of adsorbed material*, but Young's equation does not, simply because, in the Gibbs treatment, no adsorbed material is associated with the three phase line. However, had Gibbs chosen to adopt his own suggestion** "..... that a nearer approximation in the theory of equilibrium and stability might be attained by taking special account, in our general equations, of the

---

* See footnote pp. 5-6, this work

** Gibbs[3] p.288 (footnote) et seq.

lines in which surfaces of discontinuity meet", then not only would gravitational terms associated with line adsorption have appeared, but Young's equation would also have contained a line tension in a way analogous to that in which the Laplace equation contains a surface tension.

The various hydrostatic principles that result from Gibbs approach, and also from a more recent, statistical mechanical treatment by Buff[48], are simply necessary conditions that the total <u>differential</u> free energy of the system (at constant temperature volume and mass) is zero for all possible, infinitesimal displacements of volume, surface and line. This is the reason for the very <u>local</u> nature of Young's equation that has been emphasised by so many commentators[25,26,33]. Pascals laws, Laplace's equation and Young's equation all refer to mathematical <u>points</u> and therefore contain only the values of the intensive variables appropriate to the <u>point</u> under consideration.

<u>Further Implications</u>

As it has been remarked, Gibbs treatment of Young's equation is very comprehensive, and it contains certain further implications which have not been brought out by Johnson.

Firstly, Young's equation applies only when both solid-fluid interfacial tensions are co-planar, otherwise

the equilibrium condition is given by

$$\left.\begin{aligned} \sigma_{S1} - \sigma_{S2} &> \sigma_{12} \cos \alpha \\ \sigma_{S2} - \sigma_{S1} &> \sigma_{12} \cos \beta \end{aligned}\right\} \qquad 1.3\text{-}5$$

where α and β are the angles filled by fluids 1 and 2 respectively. This condition reduces to Eq. 1.3-1 when $\alpha + \beta = 180^{\circ}$ (Gibbs[3] p.326).

Secondly, Young's equation applies only when all the interfacial tensions are properly defined, and they are only so defined if there is a constant state of strain both within the bulk of the solid and at the surface. Thus unless the solid is in <u>this</u> sense "unchangeable," σ_{S1} and σ_{S2} are not defined and Young's equation is inapplicable. Notice, however, that in <u>this</u> usage the term "unchangeable" need not be taken to mean inert. For example, Young's equation certainly can apply to systems in which the solid is soluble, provided all the usual and other* conditions are fulfilled, because in this case σ_{S1} & σ_{S2} are well defined by equation 1.2-2. On the other hand, it certainly cannot apply where significant local strain of the Bikerman-Lester type obtains. In such a case not only are σ_{S1} & σ_{S2} undefined at the TPL, but the geometry is incorrect as well.

Johnson[17], in reply to Bikerman's criticism of his paper, says, "Whilst I have indeed considered the solid to

---

* See Gibbs[3] p.327

be rigid (but not necessarily plane) the proof would have to be modified only slightly for mobile surfaces, (e.g. gelatin). Equation (30)* would then contain an additional term depending upon the curvature of the solid, but Young's equation would still appear in the form given. Similarly, equations describing the internal stress in a solid would appear separate from Young's equation".

Such an extended analysis as Johnson suggests may indeed be possible, but it would be wrong to assert that it can be made using Gibbs' formalism.

An Alternative Form of Young's Equation

It was noted in Section 1.2 that the interfacial tension at a solid surface is unlikely to be sensitive to changes in the internal strain of the solid. Further, the Lester treatment shows that only surfaces of low elastic modulus are likely to be influenced by changes in the contacting fluids. If, therefore, the discussion is restricted to insoluble, rigid solids, i.e. solids which are for all practical purposes Gibbs "unchangeable" solids then it is possible to define** the "superficial tensions" of fluids 1 and 2 in contact with the solid S as, respectively,

---

* The total mechanical equilibrium condition for Johnson's system.

** See p. 15, this work, Eq. 1.2-3.

$$\left.\begin{aligned} \xi_{S1} &= \sigma_{S1} - \sigma_{S,0} \\ \xi_{S2} &= \sigma_{S2} - \sigma_{S,0} \end{aligned}\right\} \qquad 1.3\text{-}6$$

where, as before, $\sigma_{S,0}$ is the surface tension of the solid if bounded by a vacuum. Substitution in Eq. 1.3-1 then yields

$$\xi_{S1} - \xi_{S2} = \sigma_{12} \cos \theta \qquad 1.3\text{-}7$$

This equation was first derived by Gibbs[6](pp. 328-329) and it has been reproduced by Boyd & Livingstone[49] and by Johnson[17]. A similar approach has been suggested by Brown,[50] and Guastalla[51] has given a mechanical analogy for the equation which illustrates the ideas very clearly. It is perhaps interesting to note that this equation (i.e. Eq. 1.3-7) with the definitions given by 1.3-6 seems to be more in keeping with Young's own notion of the subject than equation 1.3-1. (See Young[2] p.83).

Eq. 1.3-7 seems conceptually much simpler than Eq. 1.3-1 and one wonders why it has not found greater appeal. Perhaps the lack of attraction is due to the fact that the definitions of ξ_{S1} and ξ_{S2} given by Eq. 1.3-6 serve only to emphasise the pessimistic view of Adamson and Ling[25] that "it is futile to seek a general thermodynamic connection between contact angle and the surface free energy of the pure solid. Any success in relating the two must come from a theory based on specific molecular models".

The Duplex Film Hypothesis

Many authors[14,17,41,52] have assumed some form of Eq. 1.3-1 to be applicable when one of the fluids completely wets the solid surface and spreading occurs. This is postulated to be the limiting case of Young's equation for which the contact angle is zero; thus

$$\sigma_{S1} - \sigma_{S2} = \sigma_{12} \qquad 1.3\text{-}8$$

where fluid 2 is understood to be the wetting phase. It is not evident, however, that Young's equation can be invoked in such a purely formal way, since the TPL, for which the equation represents the hydrostatic equilibrium condition, does not exist. An alternative designation for Eq. 1.3-8 that has certain semantic advantages is the "duplex film" hypothesis[52].

Gans[53] has suggested that, rather than referring to Eq. 1.3-8 as the case of zero contact angle, it would be more appropriate to use the term "no contact angle": "It must be expected that only fortuitously will the energy relations at three independent interfaces balance so nicely as to result in a contact angle of 0°." These remarks imply that, when no finite contact angle is formed, the situation is more likely to be accurately described by the expression

$$\sigma_{12} \leq (\sigma_{S1} \sim \sigma_{S2}) \qquad 1.3\text{-}9$$

than by Eq. 1.5-8. However, the work reported recently

by Johnson and Dettre[54] clearly shows that providing all the various interfacial tensions exhibit their equilibrium values*, then, for three fluid systems at least, Eq. 1.3-8 is <u>exactly</u> obeyed <u>whenever</u> spreading occurs. Furthermore, it does not seem unreasonable to expect this to be equally true for solid substrates since, when spreading occurs, both Young's equation and Neumann's Law formally reduce to the same equation (Eq. 1.3-8).

The paradox, thus posed, is perhaps resolved when it is remembered that there is plenty of evidence to show that the interfaces, whose tensions appear in Young's equation, are not as independent as Gans would suggest, either under spreading or non-spreading conditions. Bangham and Razouk[32] were the first to show the importance of the adsorption of the third phase at the interface between the other two, and knowledge of the existence of this adsorption has since played an increasingly large part in our understanding of three phase equilibria[25,26].

The definitions of solid/fluid interfacial tension so far employed (Eqs. 1.2-1 &1.2-2) have taken explicit account of this third-phase adsorption, but the nomenclature employed has not. It is therefore proposed to

---

* There must, therefore, be a mechanism by which the interfacial tensions can obtain their equilibrium values.

introduce, <u>for the remainder of this section only</u>, a notation similar to that used by Melrose[26]: thus $\sigma_{Si,j}$ is the interfacial tension of the interface between solid and component i at which component j is adsorbed with a ~~spread-~~ surface ~~ing~~ pressure of $\pi_{Si,j}$; σ_{Si} is now redefined at the interfacial tension of the Si interface when the adsorption of component j is zero. Hence

$$\pi_{Si,j} = \sigma_{Si} - \sigma_{Si,j} \qquad 1.3\text{-}10$$

The duplex film hypothesis is now stated as

$$\sigma_{S1,2} - \sigma_{S2,1} = \sigma_{12} \qquad 1.3\text{-}11a^{*}$$

and equation 1.3-9 becomes

$$\sigma_{12} \leqslant (\sigma_{1S,2} \sim \sigma_{S2,1}) \qquad 1.3\text{-}12$$

The conclusion to be drawn from the Johnson and Dettre experiments[54] is that, under equilibrium spreading conditions, Eq. 1.3-11 is more likely to be generally appropriate than Eq. 1.3-12. This perhaps becomes more obvious if Eq. 1.3-11 is written (using σ_{Si} in its new meaning) as

$$\sigma_{S1} - \sigma_{S2} - \sigma_{12} = \pi_{S1,2} - \pi_{S2,1} \qquad 1.3\text{-}11b$$

---

* In the formulation of this and subsequent equations using this notation it is tacitly assumed that the term $\pi_{12,S}$ is zero. Furthermore, experimental evidence[55] suggests that if, say, fluid 2 spreads, displacing fluid 1, then $\pi_{S2,1}$ is also zero.

It is the existence of the terms on the right of this equation that make it the appropriate equation under equilibrium spreading conditions.

The conceptual difficulties associated with the interpretation of Eq. 1.3-11 in the absence of a line of three phase contact can be overcome by the use of a model system designed to allow the coexistence of both the S1,2 and S2,1 interfaces in mutual equilibrium even under spreading conditions. Thus Gibbs treats the situation in the context of a vertical capillary tube up which the spreading liquid rises until it is just balanced by gravity.

Recently, Melrose[56] has made use of a model in which a thin, spread film and an adsorbed layer are separated by an inert movable barrier, but are in contact via a saturated third phase (solution or vapour). An external mechanical force applied to the barrier just prevents the film from spreading further. The duplex film hypothesis is shown to give the stability condition for the adsorbed film such that the system remains in equilibrium when the mechanical force is zero. Eq. 1.5-11 implies that $\pi_{S1,2}$ will increase until $\sigma_{S1,2}$ just balances $\sigma_{S2,1} + \sigma_{12}$. It will do this when the thickness of the film is such that regions of the film which contact respectively phase 1 and the solid substrate correspond to the 12 and S2,1 interfaces.

Although ~~spreading~~ surface pressures have been discussed here

only within the context of spreading systems, spreading pressures are by no means precluded by non-zero contact angles,[32,54,57-60] and Young's equation in the new terminology is

$$\sigma_{S1,2} - \sigma_{S2,1} = \sigma_{12} \cos \theta \qquad 1.3\text{-}13$$

However, it is only when Eq. 1.3-11 pertains that the adsorbed film can grow continuously until it becomes sufficiently thick to take on the properties of the bulk liquid.

A similar view was put forward by Frumkin[60] in 1938. He postulated that non-zero contact angles are only possible in equilibrium systems if the free energy of the liquid film in contact with the solid is a discontinous function of film thickness, that is, if there is no continuous transition from adsorbed phase to bulk phase through a series of increasing film thicknesses corresponding to thermodynamically stable states.

Behaviour of this type has been explained by Derjaguin and his collaborators[61,62] in terms of a "disjoining pressure" acting normal to the plane of the liquid film and preventing film thinning. The magnitude of the disjoining pressure is considered to vary with film thickness, and, in systems exhibiting finite contact angles, the particular mode of variation operative effectively destabilizes a range of film thicknesses with

respect to thinner films. In these circumstances a draining film, on reaching a certain thickness, will spontaneously separate into bulk liquid droplets and adsorbed multilayers.

Read and Kitchener[63] have recently examined the way in which, with favourable systems, disjoining pressures can be calculated using intermolecular force theory and considering only London dispersion forces and electrical double layer forces. They emphasise, however, that this procedure is not justified with polar liquids showing autophobism[43] nor with "highly associated liquids, notably water, with which various solids may be structurally incompatible". In both these cases behaviour is "... controlled by the local molecular structure ... in the vicinity of the solid surface and this factor still presents great difficulties for theoretical treatment".

Russian scientists[57,64,65] have laid a much greater emphasis on liquid structuring. Derjaguin and Zorin[57] have suggested that, in the vicinity of a solid surface, polar liquids can exist in two forms. One of these has greater structural order than the other - the ordinary bulk liquid phase - and therefore has a lower vapour pressure. They suggest that the transition from one form to the other is discontinuous and analogous to the melting of a crystal. For example, Fedyakin[66] has reported that water films

can exist in two forms on clean glass surfaces. One form, obtained by condensing the saturated vapour, gives a contact angle with bulk water of about 40°. The other form, which remains behind after bulk water has been moved across the glass surface, has the properties of the water mass and is completely wetted by bulk water.

C H A P T E R T W O

Contact Angle Hysteresis

Introduction

Young's equation admits of but one value of the contact angle for a given system in equilibrium, yet it is an experimental fact that contact angles may often adopt various values, between certain limits, without any apparent movement of the three phase line (the TPL). This phenomenon is usually called "contact angle hysteresis" a term coined by Sulman[67] in 1920.

Reported observations of contact angle hysteresis are numerous, and a bibliography[68] and several reviews[14,44,69] containing sections on this topic have been published in recent years. Various theories have been put forward to explain these observations, but these do not appear to have been recently reviewed.

The common methods of measuring contact angles (e.g. the tilting plate[70] and variable volume sessile-drop[71] methods) all involve some displacement of the TPL across the surface of the solid, and it is not always clear whether or not the TPL is stationary or slowly moving when the angle is determined[44]. Nevertheless, it is proposed here to limit the use of the term "contact angle hysteresis" to the situation in which a given system can adopt various equilibrium configurations each with a different contact

angle. Thus any variation of the contact angle with the speed with which the TPL moves across the surface of a solid will not be called contact angle hysteresis (see Fig. 3.9 Section 3.2). Likewise the term will not be applied to variation of the contact angle simply in response to changes in the physico-chemical properties of the system, e.g. its pH[72]. This definitive limitation, however, should not be taken to mean that unobserved kinetics of this kind may not be responsible for, at least, some cases of observed contact angle hysteresis.

It has become customary when discussing contact angle hysteresis to refer to the maximum andminimum observed angles as respectively the "advancing" and "receding" angles. In the present context, however, such terminology would be confusing, implying motion of the TPL when none is meant. The two limiting angles, i.e. the two extreme values which the contact angle can assume before the TPL begins to move are therefore better termed the "pre-advancing" and "pre-receding" contact angles, ϕ_{pa} & ϕ_{pr} respectively. Thus if there is no contact angle hysteresis $\phi_{pa} = \phi_{pr}$, otherwise $\phi_{pa} > \phi_{pr}$.

2.1 Classification of Theories

The Limitations of Young's Equation

Young's equation, as it stands (Eq. 1.3-1) is simply a relationship between the thermodynamically defined

quantities σ_{S1}, σ_{S2} & σ_{12}. As derived, it is an equilibrium condition for a particular <u>model</u> system. Its purpose is to describe a real situation, but its ability to do so will depend upon the degree of congruence between the model and the real system. Explanations of contact angle hysteresis will therefore be divided into two categories: those to which Young's equation is relevant and those to which it is not. One example of this latter type has already been met (see Section 1.3). It occurs when the TPL rests along an edge. In these circumstances, the correct three phase equilibrium condition is given by Eqs. 1.3-5 and not by Young's equation, and although θ is still abstractly defined by Eq. 1.3-1 it has no physical existence. However, the edge might be part of a submicroscopic step on an otherwise plane surface so that there would <u>appear</u> to be a contact angle; moreover, it would exhibit hysteresis, but the observed contact angle would have nothing to do with Young's equation.

This example serves to illustrate the fact that it is not generally valid to identify the observed contact angle with that defined by Young's equation. To emphasise this, observed contact angles have been designated by a separate symbol, ϕ, whilst θ has been expressly reserved for the intrinsic angle appropriate to Young's equation.

First Category: Young's Equation Relevant

To the first category defined above belong explanations in terms of surface roughness large enough for Young's equation to apply but small enough to go unobserved*, so that ϕ differs from θ but is related to it by the detailed geometry of the surface.

How this may happen is illustrated in Fig. 2.1. The diagram shows a section through a liquid drop at rest on an idealised rough surface. The system is circularly symmetrical about the z-axis and although drawn otherwise for visual clarity, the drop is assumed to be much larger than the individual corrugations.

If the slope angle of the surface at the point of contact shown is α then

$$\phi = \theta + \alpha \qquad 2.1\text{-}1$$

The maximum possible angle, ϕ_{max}, occurs where α is a maximum and the minimum angle, ϕ_{min}, where α is a minimum[73-75]. The value of ϕ actually observed will, therefore, depend on the location of the TPL and ,therefore, upon such factors as drop volume, gravitational forces, etc.

---

* If the roughness causing contact angle hysteresis is large enough to be seen, then the problem is considered to be trivial, although the difficulty in measuring the intrinsic angle, θ, may or may not be similarly so.

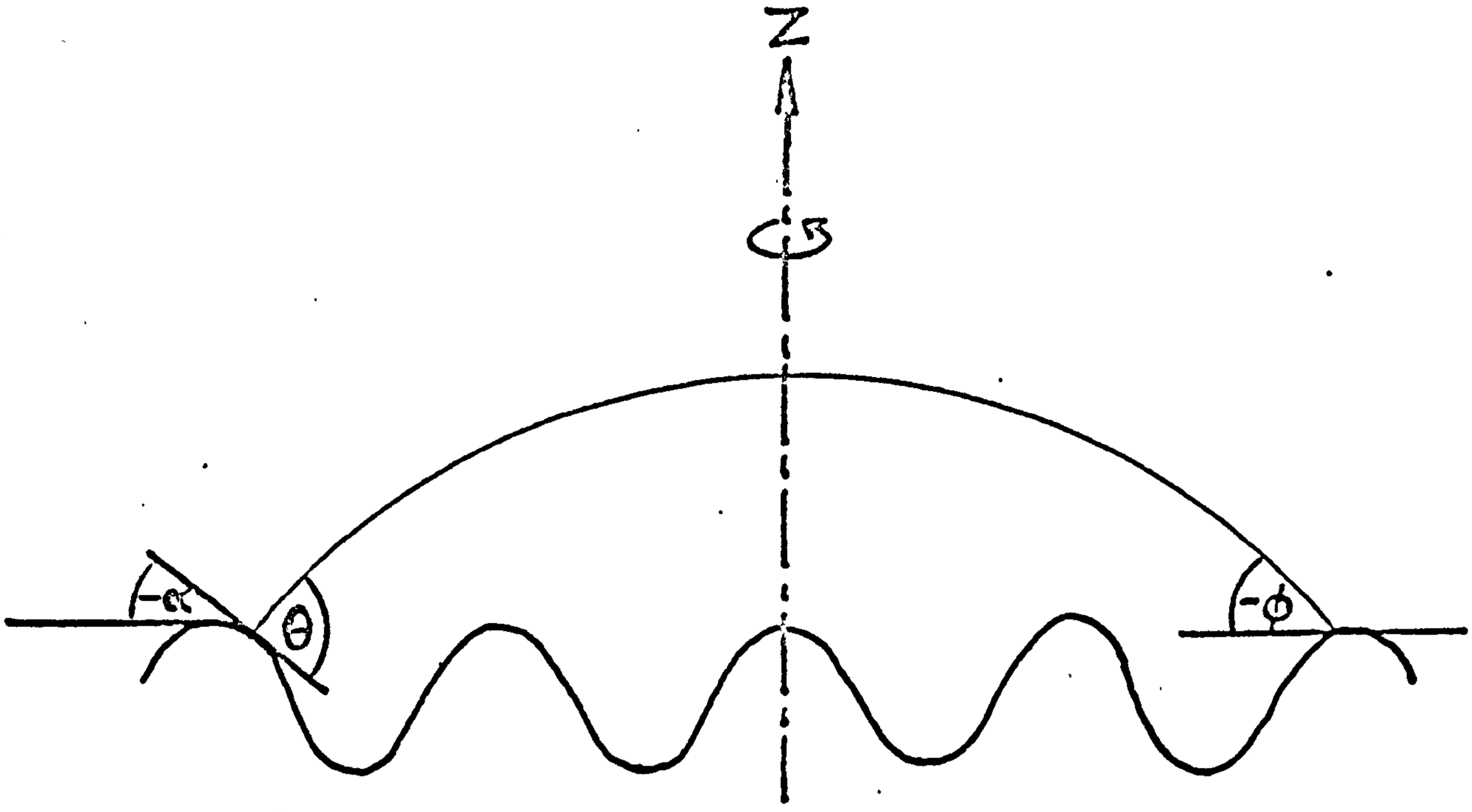

Fig. 2.1

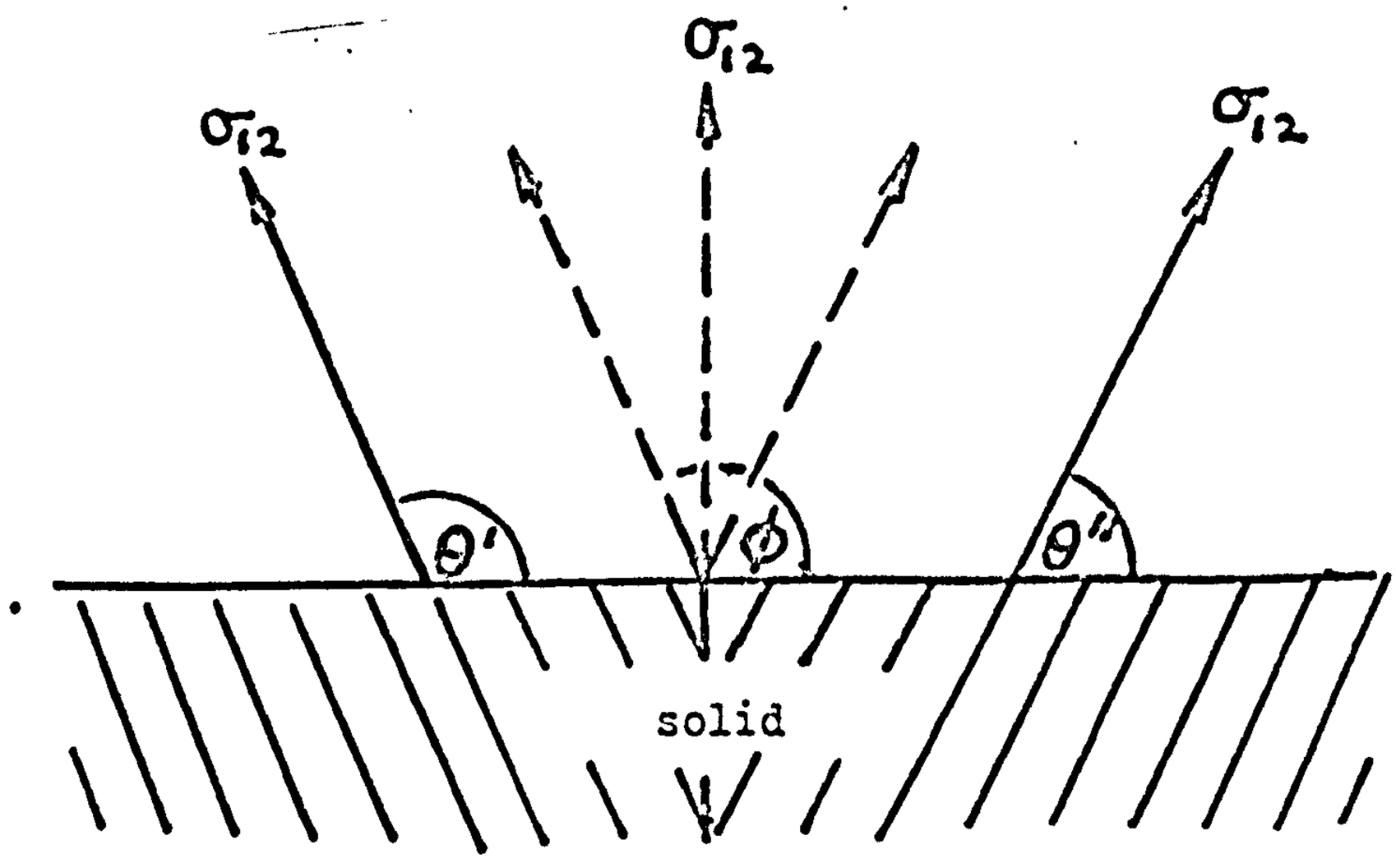

Fig. 2.2

Second Category: Young's Equation Irrelevant.

To the second category belong explanations in which the real situation differs in some fundamental way from the model system for which Young's equation is derived. Two examples will be discussed.

In the first of these, the difference is that whereas in the Young's equation model all the properties of the solid surface in the neighbourhood of the TPL are continuous, in the postulated real system they are not[76]. The discontinuity could be simply geometric, like the edge already mentioned, or it could be due to chemical heterogeneity[74]. Just how sharp the discontinuities need be is not yet clear but a grain boundary in a polycrystalline surface might suffice.

The situation could be visualised as follows. Fig. 2.2 shows the junction of two solid surfaces. On either side of the junction Young's equation applies at the TPL between fluid phases 1 and 2 and the solid surface. Thus contact angles θ' and θ'' are unambiguously defined for these two surfaces, but, at the junction, the surface properties change discontinuously and θ is therefore not defined. Nevertheless, if the discontinuity contributes nothing to the free energy or the material balance of the system then one might expect the observed contact angle to take any value between θ' and θ''. The precise value of ϕ, within

these limits, would then be determined by other considerations such as the volume of the fluid phases, gravitational forces, σ_{12}, etc.[76].

The second example considered in this category is that in which the real system is not in thermodynamic equilibrium. In this case the question is one of kinetics and contact angle hysteresis is only apparent.[77]

2.2 The Effect of Surface Roughness

The Roughness Factor.

In an attempt to correlate the observed contact angle of a liquid drop resting on a roughened surface with that observed when the drop rests on a smooth surface of the same material, Wenzel[78] has proposed the relationship

$$\sigma_{12} \cos \phi = R(\sigma_{S1} - \sigma_{S2}) \qquad 2.2\text{-}1$$

Where R, the "roughness factor", is defined by

$$R = \frac{\text{actual surface area}}{\text{geometric surface area}}$$

If the contact angle measured on the smooth surface is taken to be the intrinsic angle, θ, then

$$\cos \phi = R \cos \theta \qquad 2.2\text{-}2$$

Cassie and Baxter[79] have extended Wenzel's treatment to porous materials. They considered the equilibrium of a sessile drop resting on a model surface composed of parallel cylindrical rods. If θ exceeds 90° (and the

rods are sufficiently closely spaced so that the liquid interface between them is not distorted by gravity) then the liquid does not penetrate between the rods and the base of the drop has a composite surface consisting of alternately liquid/solid and liquid/air interfaces. Cassie and Baxter derived the equation:

$$\cos \phi = a_{SL} \cos \theta - a_{LA} \qquad 2.2\text{-}3$$

where a_{SL} and a_{LA} are respectively the areas of liquid/solid and liquid/air interface per unit area of the composite surface. If the surface were non-composite, then a_{LA} would equal zero and Eq. 2.2-3 would reduce to Wenzel's equation, Eq. 2.2-1. Cassie and Baxter also report some experimental observations in support of their equation.

Gray[80] has dismissed Eqs. 2.2-1 to 2.2-3 on the grounds that "... area roughness and heterogeneity conditions are assumed to influence the contact angle equilibrium whereas, since equilibrium occurs along a line, only roughness of that line can influence the equilibrium". This view seems to stem from the notion that Eqs. 2.2-1 to 2.2-3 are modifications of, or to, Young's equation. Certainly they have been derived in a similar way, and Eq. 2.2-1 shows a formal resemblance to Young's equation, but whereas the latter is simply the hydrostatic principle applicable to the various lines of three phase contact, Eqs. 2.2-1 to 2.2-3 can only be under-

stood as <u>mechanical conditions for free energy minima of whole systems</u> containing bulk phases and surfaces, as well as three phase lines. Their derivation as such[73,74,78,79] has, however, generally lacked sufficient rigour and this may have been partly responsible for the confusion.

Firstly, the common assumption that $\sigma_{ij} = f^{\sigma}_{ij}$ is made without specifying the position of the Gibbs dividing surface. Secondly, minimisation of surface free energy only is considered, whereas an adequate derivation on these lines must involve minimisation of the <u>total</u> free energy of the system. The two methods become equivalent only when the following are true:

(i) the solid is immutable;

(ii) the total free energy of the system is independent of interfacial curvature (<u>e.g.</u> the liquid is incompressible);

(iii) external macroscopic forces, <u>e.g.</u> gravity, are effectively zero;

(iv) the volumes of the bulk phases remain constant.

However, even if this more rigorous approach is adopted for the derivation of Eqs. 2.2-1 and 2.2-3, they still cannot be regarded as useful equations relating ϕ to the intrinsic thermodynamic properties of the system and can be objected to on still more fundamental grounds.

Metastable States

Shuttleworth and Bailey[73] and, more recently, Bikerman[81] and Good[74] have suggested that a sessile drop on a rough surface can adopt any one of a large number of metastable configurations.

This idea has been extensively developed by Johnson and Dettre[75]. Fig. 2.3 shows what may be taken to be an enlargement of the left hand side of Fig. 2.1. It illustrates the fact that there will be two positions in each trough, A and B, at which θ can assume its equilibrium value. At both these positions the vector sum of the forces acting at the TPL will be zero. If the drop edge is displaced from A to O or P then the resultant vector is such as to move the drop back to A. On the other hand, if the TPL is displaced from B to Q then the resultant is such as to move the edge still further from B until it eventually comes to rest again at C. Thus, associated with each trough, there are only two equilibrium positions, one metastable (or possibly stable) position, A, and one unstable position, B. Any two neighbouring metastable positions will be separated by an unstable one, and the unstable positions will correspond to the tops of potential energy barriers to the movement of the TPL across the rough surface. As Johnson and Dettre[75] point out, it is the existence of these metastable positions

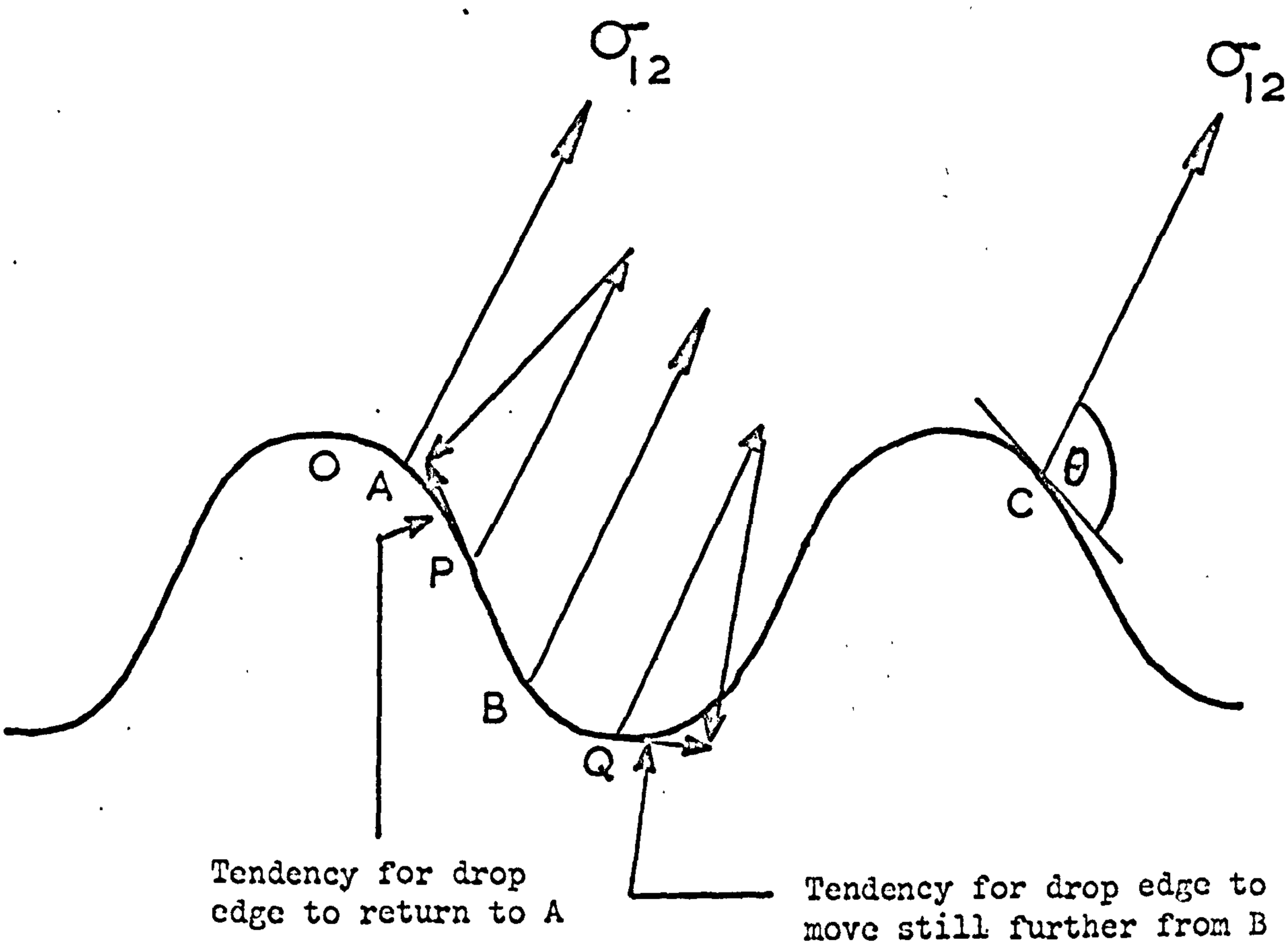
σ_{12}
O
A
P
B
Q
σ_{12}
C
θ
Tendency for drop edge to return to A
Tendency for drop edge to move still further from B

Fig. 2.3

or states, with their concomitant energy barriers, which renders the Wenzel and the Cassie and Baxter equations inadequate. It is only when the metastable states are considered that an explanation of the contact angle hysteresis emerges.

The Heights of The Energy Barriers

It is possible to calculate the heights of the energy barriers, E_ϕ, by considering the change in free energy associated with moving the TPL from a metastable (or stable) position to a neighbouring unstable one. This has been done by Johnson and Dettre[75] in an extensive computer study of a model system similar to that shown in Fig. 2.1. Gravity is ignored and the sessile drop is taken to be incompressible. Figs. 2.4a to 2.4e illustrate some of their conclusions.

As ϕ approaches ϕ_{min} or ϕ_{max} (Figs. 2.4a and 2.4e respectively) the stable and unstable states approach coincidence and E_ϕ diminishes to zero. Johnson and Dettre consider the drop to have a vibrational energy, E_D, such that unstable configurations will only present a barrier to the movement of the drop if $E_D < E_\phi$. Thus it is unlikely that either ϕ_{max} or ϕ_{min} will ever be achieved. If this concept is correct it invalidates the Shuttleworth and Bailey identification[73] of ϕ_{max} with ϕ_{pa} and ϕ_{min} with ϕ_{pr}.

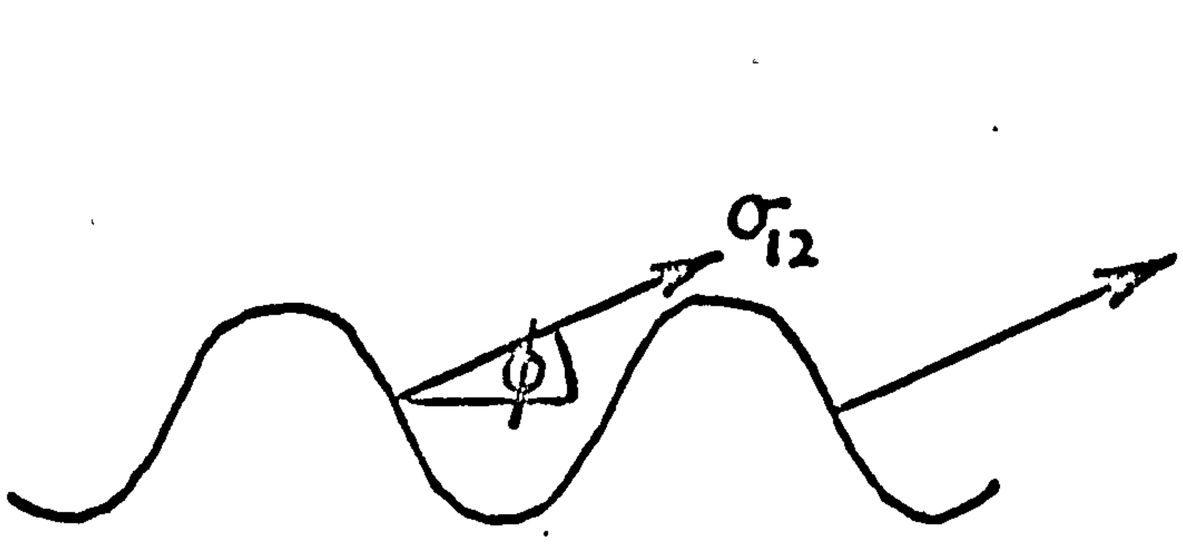

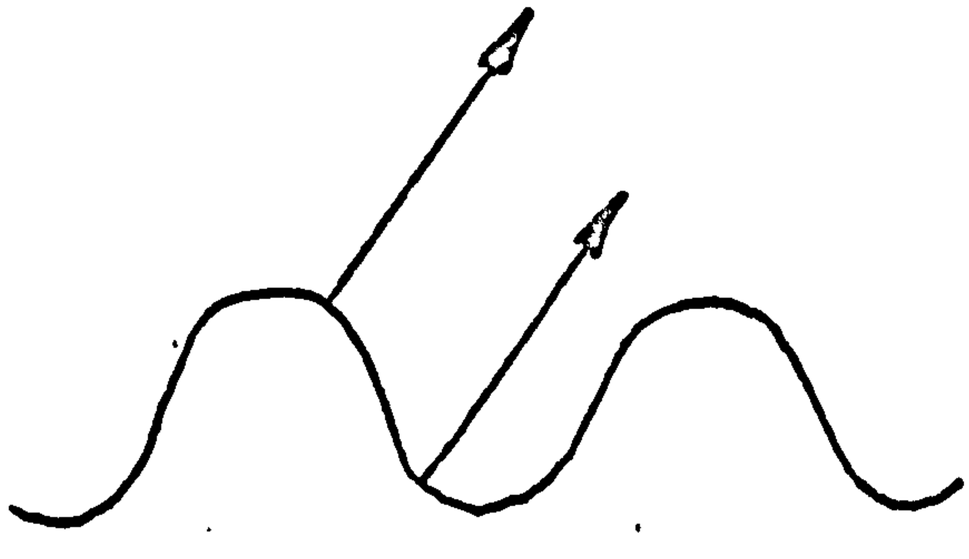

a

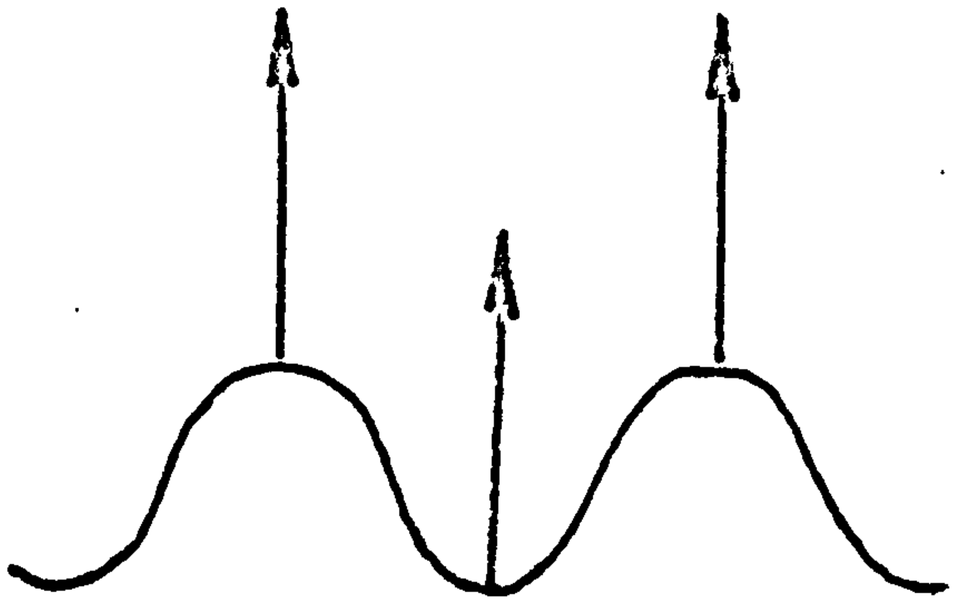

b

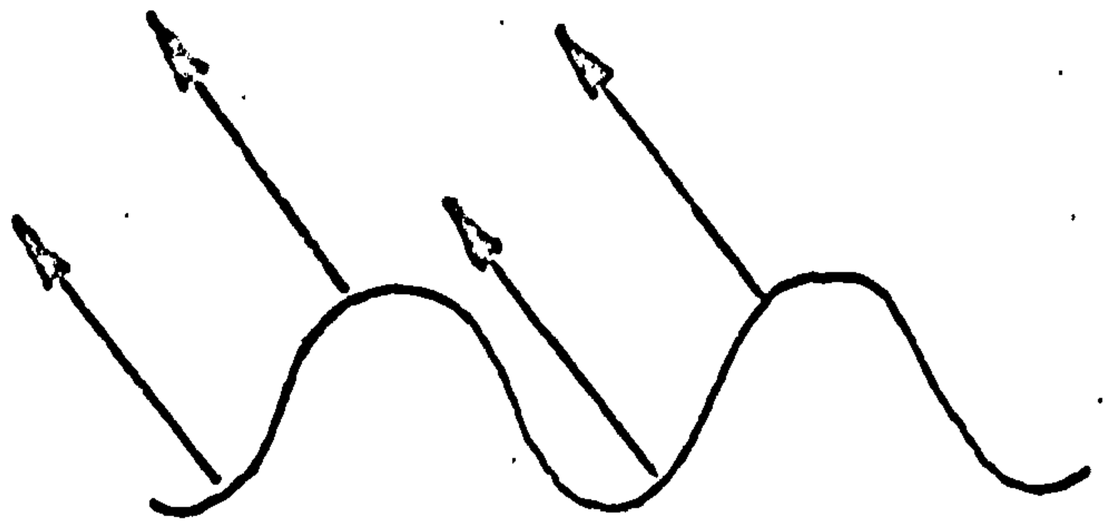

c

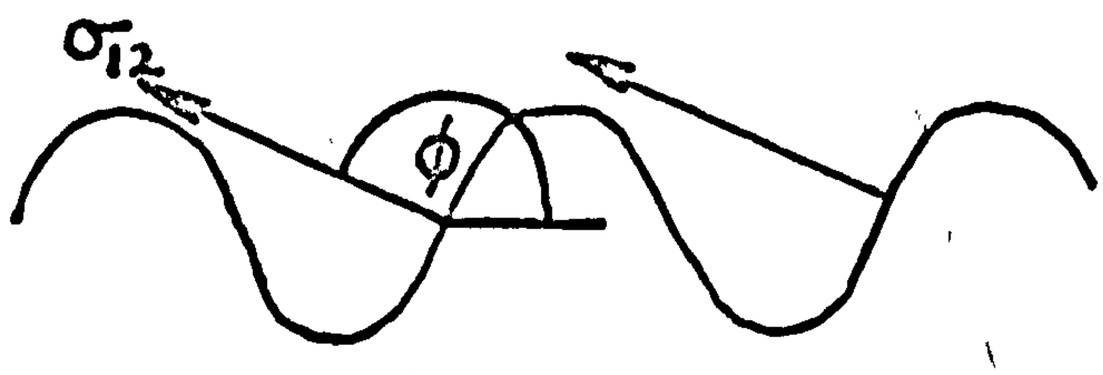

d

e

Fig. 2.4

Fig. 2.4c indicates the position of the TPL for which E_ϕ is a maximum. This configuration is thus the most stable and is, therefore, the configuration with the lowest free energy and the one which should correspond most closely with that predicted by Wenzel's equation. It will not necessarily correspond exactly, however, because the total free energy of the system is not a continuous function of ϕ. The computer study has confirmed this, and it has also shown that if R exceeds a certain value such that the slope angle, α, can satisfy the equation

$$\theta = 180^\circ - |\alpha| \qquad 2.2\text{-}4$$

then the configuration having the minimum free energy is given approximately by the Cassie and Baxter equation for a composite surface, Eq. 2.2-3. Once the composite configuration has been achieved, the energy barrier to the motion of the various three phase lines is drastically reduced, and so, therefore, is contact angle hysteresis.

Johnson and Dettre[82,83] have subsequently performed a series of ingenious experiments on artificially roughened and specially constructed surfaces. Their results qualitatively confirm their predictions. Qualitative support is also given by the results of earlier studies by Bartell and Sheppard[84] (See also Ray and Bartell[120]).

The major disadvantage with the Johnson and Dettre treatment is that whereas on generally rough surfaces

liquids can spread between as well as over the various asperities, in the idealised system, liquid movement takes place only over the crests and, moreover, the whole length of the TPL moves across any given barrier simultaneously. In the real system, if θ through the liquid is less than 90° then the liquid will spread between the various asperities in preference to over them. Indeed, a system of microscratches, for example, would considerably aid the process of spreading: it might well render $\phi = 0^{\circ}$ and eliminate contact angle hysteresis altogether. Bikerman's comment[34] that it is the nature of the roughness and not just the degree of roughness that effects the contact angle is thoroughly justified[25].

2.3 The Effect of Surface Heterogeneity

General Physico-Chemical Heterogeneity

Cassie[85] has extended Wenzel's treatment of rough surfaces to heterogeneous surfaces and has proposed the equation

$$\cos \phi = a' \cos \theta' + a'' \cos \theta'' \qquad 2.3\text{-}1$$

where a' and a'' are the fractions of the solid surface having intrinsic contact angles θ' and θ'' respectively for the particular three phase system considered. (If $\theta'' = 0^{\circ}$ and $\theta'' = 180^{\circ}$ then the Doss and Rao equation[86] is obtained:

$$\cos\phi = a' - a''$$

$$= a' - (1 - a')$$

$$= 2a' - 1 \qquad 2.3\text{-}2)$$

According to Cassie, hysteresis can be explained on the basis of Eq. 2.3-1 by assuming changes in a' and a" in the vicinity of the TPL as it advances or recedes over the solid surface. This is a rather curious notion, because, according to the derivation outlined by Cassie, Eq. 2.3-1, like Eqs. 2.2-1 and 2.2-3, can only be understood as the condition for minimisation of the free energy of the whole system and a' and a" refer to the whole solid-fluid interface, not just to the TPZ. Whilst changes in a' and a" in the vicinity of the TPL are quite likely to change the contact angle, there can be no interpretation of this fact in terms of Eq. 2.3-1.

In fact there is no need to postulate changes in a' and a" to explain hysteresis. Pease[87] has suggested that if the solid surface were composed of a mosaic of areas having different intrinsic contact angles with respect to the particular fluid-fluid combination considered, then ϕ_{pa} would be most closely associated with areas for which the intrinsic contact angles were high, and ϕ_{pr} would be most closely associated with areas for which the intrinsic contact angle was low.

Good[74] has pointed out that a smooth, but chemically

heterogeneous surface, having, for example, regions of polar and non-polar molecules, could give rise to energy barriers to the movement of the TPL and, therefore, to metastable states analogous to those produced by rough surfaces. Johnson and Dettre[76] have pursued this analogy and given a detailed analysis of the equilibrium configurations open to a liquid drop resting on a heterogeneous surface of idealised geometry.

Fig. 2.5 shows their system in plan and section. The surface is composed of concentric bands having, alternately, characteristic contact angles θ' and θ'' with the liquid, such that $\theta' > \theta''$. The boundaries between the bands are infinitely sharp and contribute nothing to the free energy of the system. If the drop periphery lies on such a boundary then the drop can assume any contact angle, ϕ, such that $\theta' \geqslant \phi$ and $\phi \geqslant \theta''$. If the drop is considered incompressible and gravity is ignored, then, at any given boundary, ϕ is determined, within the set limits, by the volume of the drop.

Fig. 2.6 provides an enlarged view of the left hand side of the drop and shows various positions for the TPL. The bands are taken to be narrow compared with the drop radius, and ϕ is therefore approximately constant for the positions shown. If the TPL rests at boundary C, then a slight displacement of the drop towards P or Q

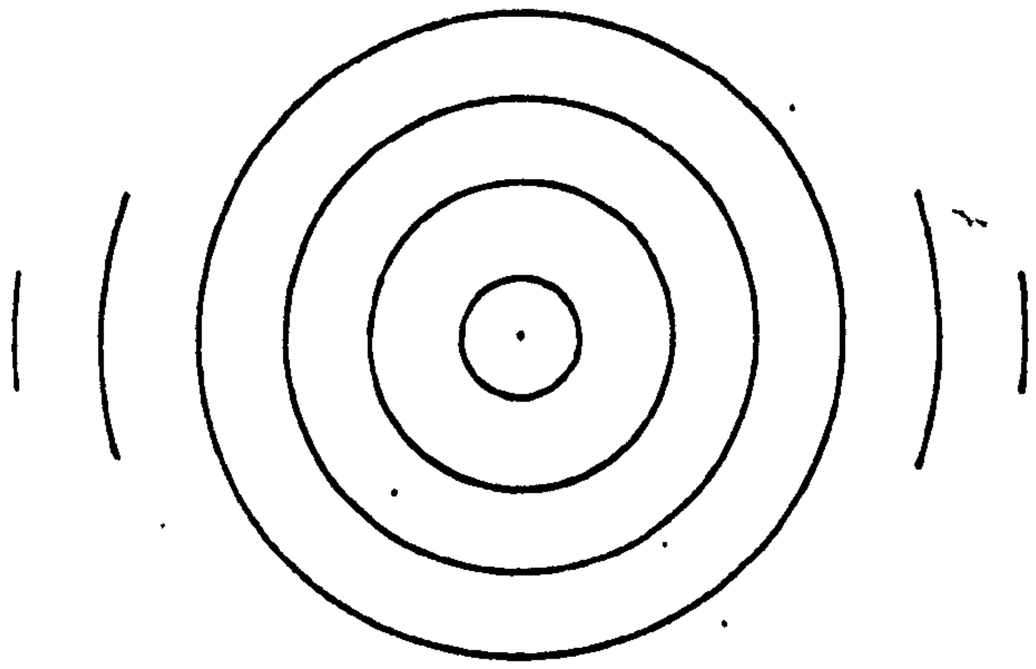

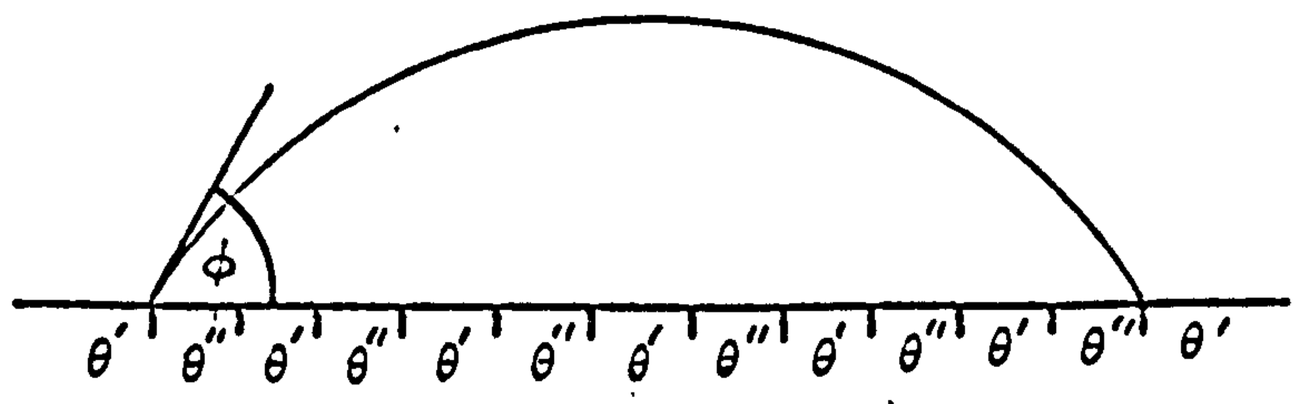

Fig. 2.5

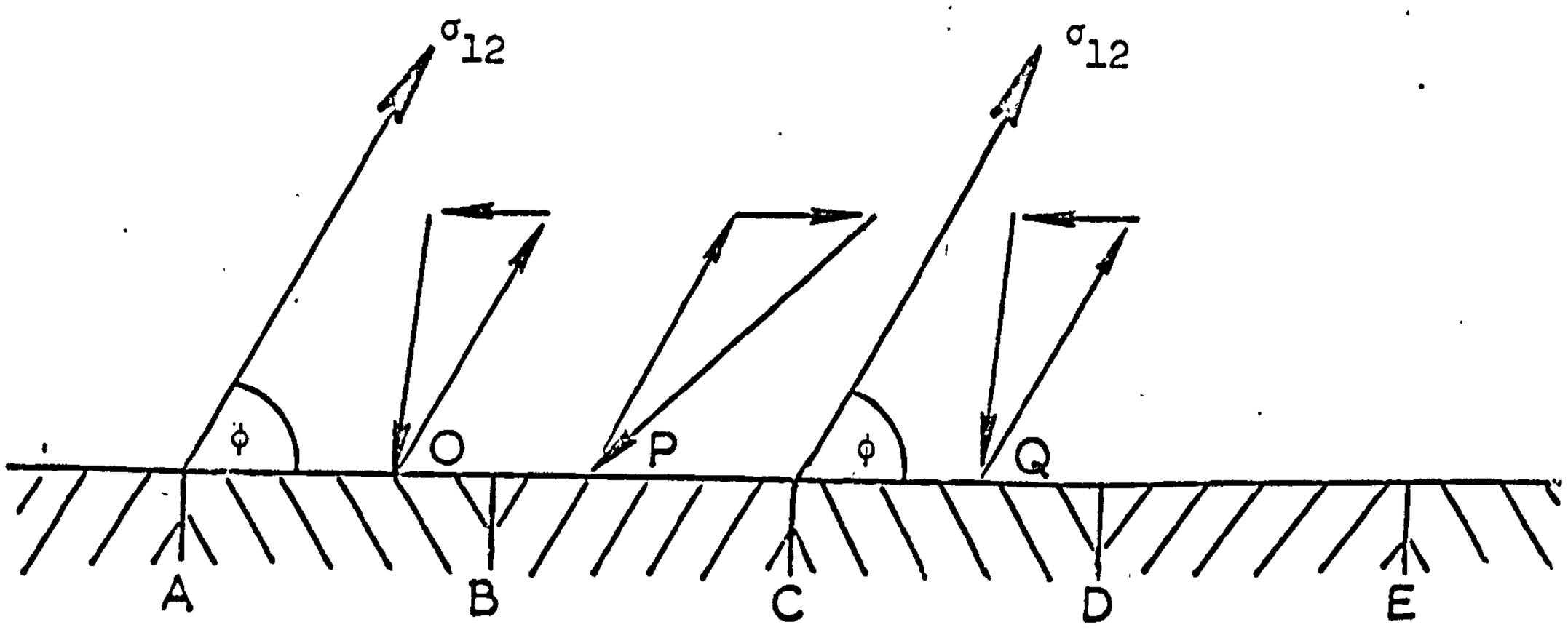

Fig. 2.6

will result in a restoring force tending to move the drop back to C. A slight displacement from boundary B, however, results in a force tending to move the drop edge still further from B, either through P to C or O to A. Thus A and C are positions of metastable (or possibly stable) equilibrium whilst B and D are positions of unstable equilibrium. All positions between are non-equilibrium positions, so that, in general, the TPL will rest at a boundary.

As with rough surfaces, positions of unstable equilibrium provide a series of energy barriers to the movement of the TPL across the solid surface. These are at a minimum when $\phi = \phi_{max} = \theta'$, or $\phi = \phi_{min} = \theta''$. As with rough surfaces, Johnson and Dettre consider that the value of ϕ which will actually be observed in any real system will depend upon the heights of the energy barriers, E_ϕ, and the ability of the TPL to cross them, represented by the "drop energy", E_D. The TPL will move if $E_D > E_\phi$, but will be stopped if $E_D < E_\phi$. Thus, once again, ϕ_{max} and ϕ_{min} are unlikely to be observed in any static system.

The configuration for which E_ϕ is a maximum is particularly interesting since this will correspond most closely to that predicted by the Cassie equation (Eq. 2.3-1). It will not necessarily correspond exactly, however, because, as with the idealised rough surface, the total free energy

of the system is not a continuous function of ϕ.

Johnson and Dettre suggest that it should ultimately be possible to relate E_D to such physical quantities as the vibrational energy of the liquid drop and the way in which it is moved over the surface of the solid. Indeed, the way in which the drop can move over the surface will be very important. In the model system the whole length of the TPL moves concertedly whereas in a real system, in which chemical heterogeneity is randomly scattered, such synchronism is unlikely and ϕ is more likely to be the result of some local averaging of the maximum and minimum available local values. In this connection, Adamson and Ling[25] have suggested that studies of contact angles on cleavage surfaces of pure and mixed crystals might shed light on the averaging that occurs with heterogeneities of molecular dimensions.

Penetration

One of the most frequently advanced explanations of contact angle hysteresis is penetration of the surface of the solid by one of the contacting fluids. The penetration of low energy (usually hydrocarbon) surfaces by water molecules is the most commonly cited example,[24,43,44,56,88] although recently Timmons and Zisman[71] claim to have found a more general relationship between the molar volumes of several liquids and the amount of contact angle hysteresis exhibited by them on certain surfaces. However, in spite

of the wide acceptance of the penetration hypothesis, its advocates are seldom very precise in their explanation of just why it should cause hysteresis.

One might suppose that a surface composed of an equilibrium dispersion of water in a hydrocarbon matrix would be highly heterogeneous and could cause hysteresis; however, it seems probable that heterogeneity of this type would posses too fine a structure to produce any significant effect. This latter view is supported by some results cited by Zisman[43] as evidence in favour of the penetration hypothesis. He reports that water shows no contact angle hysteresis ($\phi_{pa} = \phi_{pr} = 90^{\circ}$) on long chain fatty acid, alcohol or primary amine monolayers retracted from aqueous solution (and, therefore, presumably saturated with water), but hysteresis does result if the monolayer is retracted from a non-aqueous medium. Moreover ϕ_{pr} (through the water) was the same, in this latter case, as ϕ_{pr} and ϕ_{pa} in the former case.

Perhaps a more likely explanation of how penetration could cause contact angle hysteresis is that penetration (or at least penetration via the vapour phase) is a slow process, and that the observed contact angle hysteresis simply reflects the non-attainment of thermodynamic equilibrium. This view is compatible with the results noted above and also with those of other workers[44,66,89-91].

2.4 Kinetic Factors

As stated, the measurement of a contact angle usually involves the prior displacement of the TPZ across the surface of the solid. Such displacements are likely to cause departures from thermodynamic equilibrium and hence changes in the contact angle. Elliott and Riddiford[90,92] have used the term "relaxation phenomena" to describe the way in which the contact angle, disturbed in this way, subsequently returns to equilibrium. If the relaxation process is sufficiently slow then non-equilibrium angles may be sustained in apparently stable systems which will then apparently exhibit contact angle hysteresis.

Relaxation phenomena are well known in many branches of science, e.g. rheology, spectroscopy, and studies of chemical kinetics. Once hypothesised, therefore, it is not so much the principle of relaxation that is of interest as the possible mechanism. It is of interest to know, firstly, by what mechanism can movement of the TPZ influence the contact angle, i.e. what causes contact angle velocity dependence, and secondly, by what mechanism can the contact angle "relax"?

One simple mechanism by which movement of the TPZ can influence the contact angle arises from the fact that the adsorption at both liquid/solid interfaces will not, in general, be identical. Displacement of, say, phase 1 by

phase 2 will involve destruction of S1 interface and creation of fresh S2 interface. If adsorption/desorption processes (or possibly the transport processes to and from the surface) are slower than the rate of displacement then there will be a non-equilibrium contact angle. If they are sufficiently slow then the non-equilibrium angle will persist. In this connection, Gregg[113] has stated that the elimination of hysteresis requires that sufficient time be allowed for the attainment of adsorption equilibrium. Saka and Gaudin[122] have provided supporting experimental evidence. In a recent and very thorough study of the system nitrogen/water/galena, containing the surfactant potassium ethyl xanthate, they demonstrated that failure of the system to adjust to equilibrium surfactant adsorption accounted for at least half the observed contact angle hysteresis (80°).

Hansen and Miotto[77] have suggested that displacement of the TPZ may involve molecular disorientation. They assume that associated with displacement there is a natural length, namely the "peripheral thickness", δ. If there is also a natural time, τ, the relaxation time of the most slowly relaxing molecules at the TPZ, then there will be a natural displacement velocity for the TPZ :

$$\dot{x}_n = \frac{\delta}{\tau} \qquad 2.4\text{-}1$$

Hansen and Miotto state that if $\dot{x} \ll \dot{x}_n$, where $\dot{x}$ is the actual displacement velocity, then the displacement should be "quasi-static": i.e. all the tensions operating at the TPL should have their equilibrium values and ϕ should equal θ. If, on the other hand, $\dot{x} \gg \dot{x}_n$, then at least the most slowly relaxing molecules will be disoriented and the tensions of interfaces involving them will exceed their equilibrium values. In this case, therefore, ϕ is unlikely to equal θ. On standing, the disoriented molecules will orientate and the TPL will move, but at a velocity approximating $\dot{x}_n$, until ϕ once more equals θ.

Kinetic theory[93] predicts relaxation times in bulk liquids of the order 10^{-10} to 10^{-14} sec. The relaxation times of molecules in the TPZ would have to be much longer than this if the Hansen and Miotto theory is to warrant serious consideration. For example, if one assumes that δ is of the order of molecular dimensions, say 10^{-8} cm, and that many observers would consider a contact angle system to be stable if they saw no movement of the TPL in, say, $2\frac{1}{2}$ hr, and that 1 or 2μ of movement is all that could go unnoticed in such a period, then the Hansen and Miotto explanation would require a relaxation time of from 0.5 to 1 sec! On the other hand the figures used in this example are perhaps unfairly

chosen, and it is a fact that many experimenters* are prepared to accept data obtained with systems in which the TPL is visibly moving, albeit slowly, as evidence for contact angle hysteresis. Moreover, Clifford and Lecchini[94] have recently reported the results of NMR studies of water adsorbed on several silica surfaces. Spin-lattice relaxation times obtained at room temperature varied from 0.1 to 1 sec. If the same sort of molecular reorientation processes are involved in spin-lattice relaxation as in relaxation following movement of the TPZ then even the value of τ obtained above is not unreasonably high for at least one system, and the Hansen and Miotto theory must be considered as a viable explanation of contact angle hysteresis.

2.5 Conclusion

Although the various explanations of contact angle hysteresis have been examined individually, there is no reason why they should necessarily operate thus. One might easily envisage circumstances in which, for example, surface roughness, chemical heterogeneity and kinetic factors all play an important part in determining the contact angle. However, whatever the circumstances, if

---

* See, for example, Elliott and Riddiford[90], Macdougal and Ockrent[70], and Saka and Gaudin[122].

the observed contact angle exhibits hysteresis then, in terms of the known explanations, there is no justification for identifying any particular value of ϕ with θ, and any thermodynamic deductions based on any such identification must be held suspect.

C H A P T E R T H R E E

Two-Phase Flow

Introduction

In Chapter 1 it was seen that the mechanical equilibrium of a fluid system at rest is governed by certain hydrostatic principles. Pascal's law governs the bulk phases and the boundary conditions are supplied by the Laplace equation and Neumann's law. If one of the boundaries is formed by an immutable solid then Young's equation replaces Neumann's law at the perimeter of contact.

In the following chapter, two-phase flow will be discussed within the limited context of the steady immiscible displacement of one fluid by another within uniform, cylindrical capillaries.

One method of approach is to regard the motion of the interface between the fluids as being controlled by the same boundary conditions as govern the equilibrium state. However, the applicability of the Laplace equation, and also the significance of the contact angle are uncertain in non-equilibrium systems. Indeed, as was shown in the last chapter, the status of the contact angle is poor enough even when the interface is thought to be stationary, let alone when the TPZ is known to be moving.

The solution to the hydrodynamic problem of single-phase streamline flow in an infinite, uniform, cylindrical tube is well known and given by the Poiseuille formula. Rigorous solutions for a few other simple geometries are known[95]; however, more sophisticated models can lead to intractable mathematical problems, as is well known in studies of single-phase permeability[96,97]. This is one of the reasons for the "limited context" of this chapter.

In the single-phase case, the only boundary requirement is that of no slip at the wall. In the two phase case, a further problem arises from the interaction of capillary and hydrodynamic effects. The disparity between the normally parabolic velocity distribution for laminar flow of fluids in cylindrical capillaries and the constant rate of displacement necessitates some radial flow in the vicinity of the moving phase boundary (Figs. 3.1 and 3.2). This radial flow not only causes additional energy dissipation, but may also prevent the interfacial tension from reaching its equilibrium value[98]. Possibly still more important, interfacial curvature is dependent upon the contact angle, and if this is, in turn, dependent upon interfacial velocity then so too will be the curvature.

In the author's view, the particular problem of the contact angle makes it necessary to distinguish two types of flow.

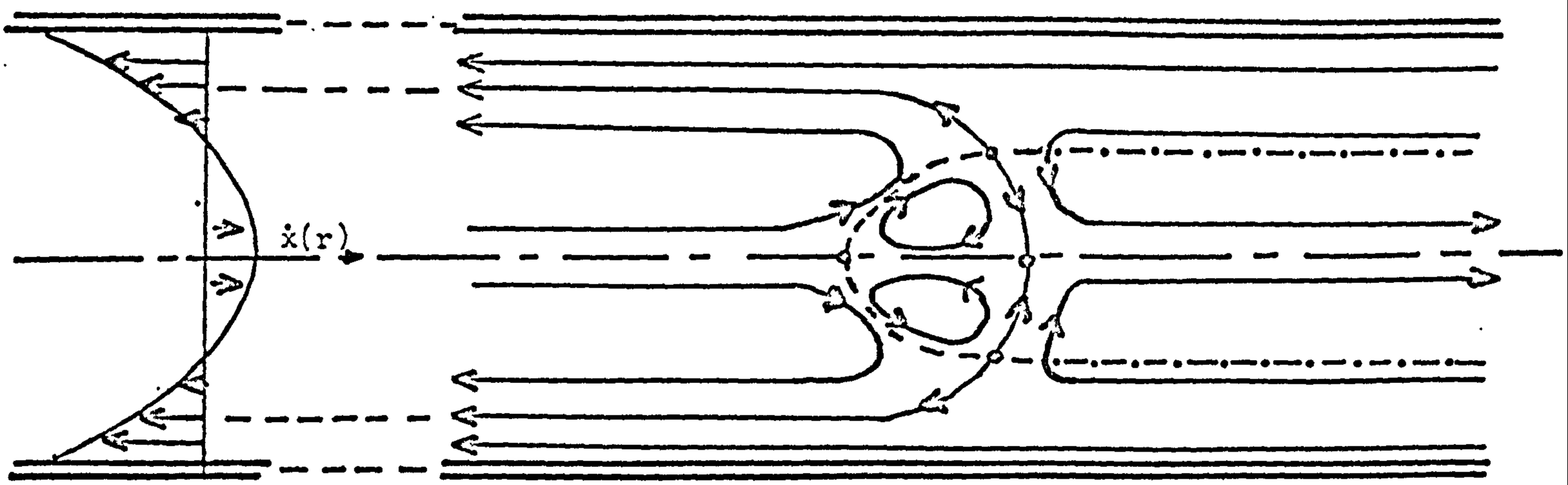

Fig. 3.1 Concentric flow

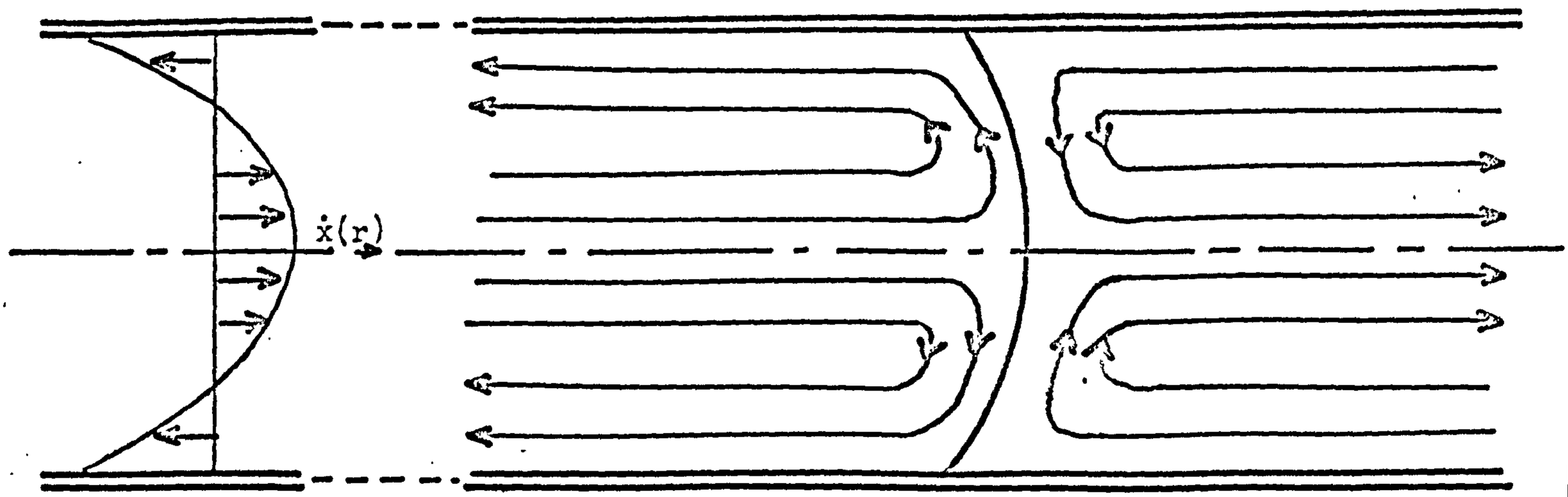

Fig. 3.2 Consecutive flow

In flow of the first type, concentric flow, there is no discontinuity in the longitudinal flow close to the wall. Displacement is essentially incomplete, and one of the fluids always flows within an annulus of the other (Fig. 3.1). By definition there is no contact angle with concentric flow because there is no three phase contact.

Conversely, flow of the second type, consecutive flow, is characterised by the existence of a finite contact angle. Displacement may or may not be absolutely complete, but any remaining film does not have fluid properties and there is, therefore, a discontinuity in longitudinal flow close to the wall, i.e. in the TPZ (Fig. 3.2)

3.1 Concentric Flow

Film Thickness

The first quantitative studies of concentric flow were made by Fairbrother and Stubbs[99]. Their interest centred on whether or not the velocity of a bubble of air in a horizontal capillary through which a liquid is flowing is a true index of the volume flow rate. The possibility that it might not be so arises from the existence of a thin film of liquid surrounding the bubble (Fig. 3.3). When the bubble is in motion this film, which has been left behind by the liquid moving in fromt of the bubble, eventually becomes part of the liquid behind the rear

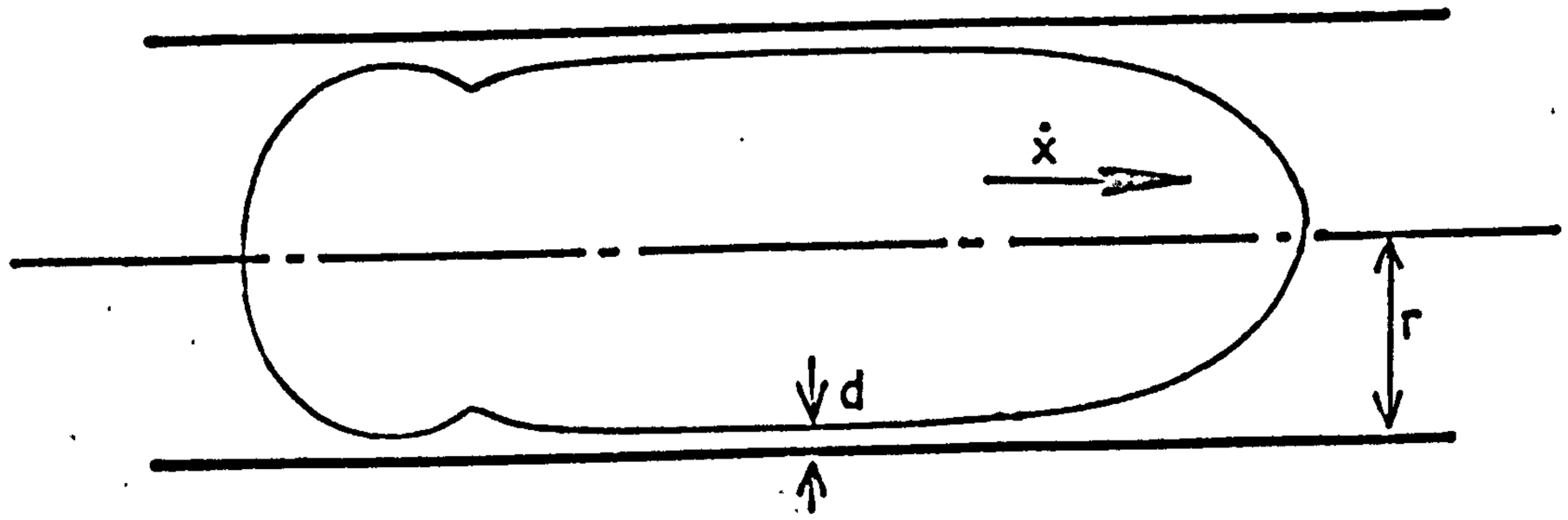

Fig. 3.3

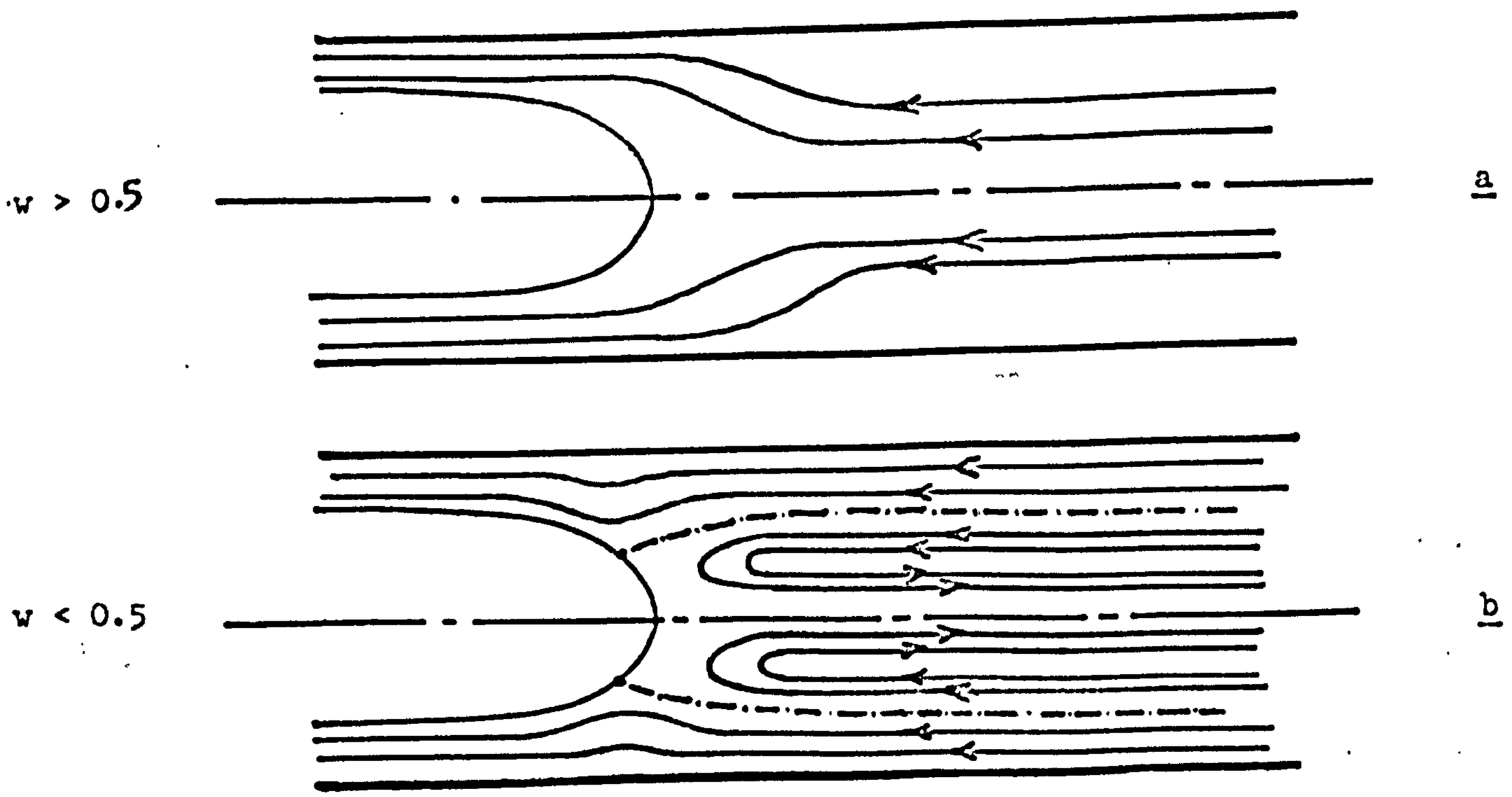

Fig. 3.4

meniscus. The velocity of the bubble is therefore greater than the mean velocity of the liquid ahead of it, $\dot{x}_m$. Thus if the volume flow rate is calculated from $\dot{x}$ and the total cross-sectional area of the tube, the value obtained will be too high.

Let it be assumed, for the moment without justification, that the film is at rest, and that $\dot{x}$ exceeds $\dot{x}_m$ by an amount $w\dot{x}$, such that

$$\dot{x}_m = \dot{x}(1 - w) \qquad 3.1\text{-}1$$

Then if d is the film thickness and r the radius of the tube (assumed uniform and cylindrical),

$$w = \frac{\dot{x} - \dot{x}_m}{x}$$

$$= \left(\frac{r^2}{(r-d)^2} - 1\right) \Big/ \left(\frac{r^2}{(r-d)^2}\right)$$

$$= \frac{2d}{r} - \frac{d^2}{r^2} \qquad 3.1\text{-}2$$

Further, if $r \gg d$ then

$$w = \frac{2d}{r} \qquad 3.1\text{-}3$$

Fairbrother and Stubbs measured w as a function of $\dot{x}$ for air bubbles in tubes containing various liquids. They found that, for each liquid, w^2 was proportional to $\dot{x}$ and the proportionality constant was simply the ratio of the liquid's viscosity, n, to its surface tension σ. Thus

$$w = \frac{2d}{r} = 1.0 \left(\frac{\dot{x}n}{\sigma}\right)^{\frac{1}{2}} \qquad 3.1\text{-}4$$

As Fairbrother and Stubbs remark, it is to be expected that w should be a function of $(\frac{n\dot{x}}{\sigma})$ since this is the only non-dimensional combination of these three relevant quantities, but that w should be proportional to $(\frac{n\dot{x}}{\sigma})^{\frac{1}{2}}$ has not been explained, nor has the coincidence that the empirically determined constant is 1.0. This empirical relationship can, in any case, only be valid when w is small, for when $(\frac{n\dot{x}}{\sigma}) > 1$ then $w > 1$ and Eq. 3.1-4 is meaningless.

Taylor[100] has extended this work to cover liquids of greater viscosities and faster flow rates. He concluded that Eq. 3.1-4 is a good approximation providing $0 < (\frac{n\dot{x}}{\sigma}) < 0.09$.He does not, however, report any measurements for which $(\frac{n\dot{x}}{\sigma}) < 10^{-3}$; thus, in fact, Eq. 3.1-4 is only verified in the range $10^{-3} < (\frac{n\dot{x}}{\sigma}) < 0.09$. The Fairbrother and Stubbs experiments were well within this range.

Taylor found that when $(\frac{n\dot{x}}{\sigma})$ increases beyond 0.09, w is less than predicted and asymptotically approaches a value of about 0.56 when $(\frac{n\dot{x}}{\sigma}) > 1.9$,that is when the stresses due to viscosity are greater than those due to surface tension. He notes that when $w = 0.5$, the flow velocity on the axis of the tube at points far from the meniscus is identical with that of the meniscus, so that if $w > 0.5$, the central filament is moving towards the meniscus, whereas if $w < 0.5$, the central filament is moving away from it. If the flow is reduced to steady

motion relative to the bubble by superposing a velocity $-\dot{x}$, it is only when $w > 0.5$ that flow with one stagnation point is possible. This is shown in Fig. 3.4a. The two simplest possible types of flow when $w < 0.5$ are shown in Figs. 3.4b & c. In Fig. 3.4b there is one stagnation point on the axis and a stagnation ring on the meniscus. In Fig. 3.4c there are two stagnation points on the axis.

Merchessault and Mason[101] have measured film thicknesses conductimetrically in the range $7\times10^{-6} < (\frac{n\dot{x}}{\sigma}) < 2\times10^{-4}$ and obtained the empirical equation.

$$w = 1.78 \left(\frac{n\dot{x}}{\sigma}\right)^{\frac{1}{2}} - 0.1 \left(\frac{n}{\sigma}\right)^{\frac{1}{2}} \qquad 3.1\text{-}5$$

The appearance of the term $(\frac{n}{\sigma})^{\frac{1}{2}}$ is rather peculiar since it implies that the empirical constant 0.1 has dimensions $(\text{length/time})^{\frac{1}{2}}$. Goldsmith and Mason[102] have since concluded that deviations from Eq. 3.1-4 were probably due to errors inherent in the experimental method employed.

Bretherton[103], in an invaluable theoretical study of the problem, has derived the equation,

$$w \simeq 2.69 \left(\frac{n\dot{x}}{\sigma}\right)^{\frac{2}{3}} \quad \text{as} \quad \left(\frac{n\dot{x}}{\sigma}\right) \to 0 \qquad 3.1\text{-}6$$

which should be in error by no more than 10% provided $(\frac{n\dot{x}}{\sigma}) < 5\times10^{-3}$. Unfortunately, the extensive experimental results given in his paper for the range $10^{-7} < (\frac{n\dot{x}}{\sigma}) < 10^{-2}$ "... agree well neither with theory nor with previous experiments by other workers", the values of w being less than that given by Eq. 3.1-4 but still inexplicably greater

than that predicted by theory. Bretherton is unable to explain these results either in terms of surface roughness or surface tension gradients resulting from contamination[98]. Disjoining pressure may possibly account for the discrepancies at the slowest speeds, when the absolute magnitude of w is small, but he concludes that this explanation is incomplete.

Bubble Shape

In spite of its lack of experimental support, Bretherton's paper does provide the most complete theoretical analysis to date, both of the problem and of the approximations necessary for a simple solution. In fact it provides the only analytical expression for d that does not contain both $\dot{x}$ and $\dot{x}_m$. Much of what is to be said here will therefore be based on Bretherton's conclusions. However, the approach will be considerably less detailed as the intention is merely to discover what factors influence the shape of bubbles rather than to deduce exact analytical expressions describing them.

The problem concerns the balance between surface tension and viscous forces for a steadily moving interface between two incompressible fluids, 1 and 2, having viscosities η_1 and η_2. The fluids are contained within a uniform cylindrical tube of radius r. Fluid 1 is assumed to completely wet the tube wall, and the interfacial tension σ_{12} is taken to be well defined and constant. The approxi-

mate magnitude of inertial, gravitational and viscous forces, relative to surface tension, are then given respectively by the dimensionless numbers:
$\frac{\rho r \dot{x}^2}{\sigma_{12}}$, $\frac{\rho g r^2}{\sigma_{12}}$ and $\frac{\eta_i \dot{x}}{\sigma_{12}}$, where ρ is a representative density and i takes values 1 or 2 according to which fluid the viscous stresses are to be evaluated for.

It will be assumed that

$$\frac{\rho r \dot{x}}{\eta_i} \ll 1 \qquad 3.1\text{-}7a$$

and that

$$\frac{\rho g r^2}{\sigma_{12}} \ll 1 \qquad 3.1\text{-}7b$$

The first condition is that the Reynolds number based on the tube radius is small, i.e. inertial forces are negligible in comparison with viscous forces; the second lays down that surface tension forces are much more important than gravitational forces.

For a bubble at rest, Fig. 3.5, there are no viscous stresses. The front and rear menisci must therefore assume shapes of constant mean curvature. Further, since fluid 1 is assumed to completely wet the tube wall, they must be hemispheres of curvature $\frac{2}{r}$. At any point on the cylindrical part of the interface the mean curvature is $\frac{1}{r}$. Since the pressure within the bubble is uniform the film will experience a pressure $\frac{\sigma_{12}}{r}$ causing it to thin until it is stabilized by disjoining pressure.

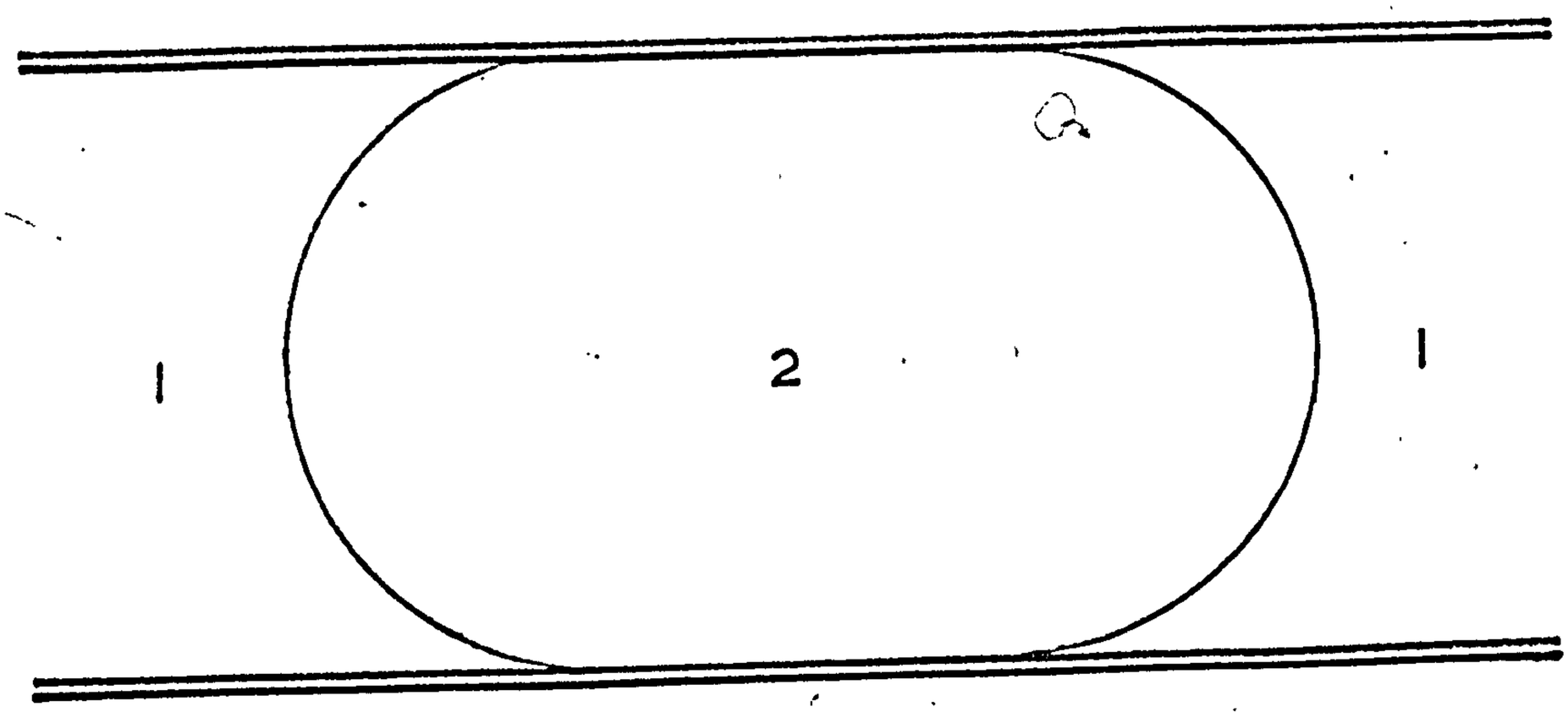

Fig. 3.5

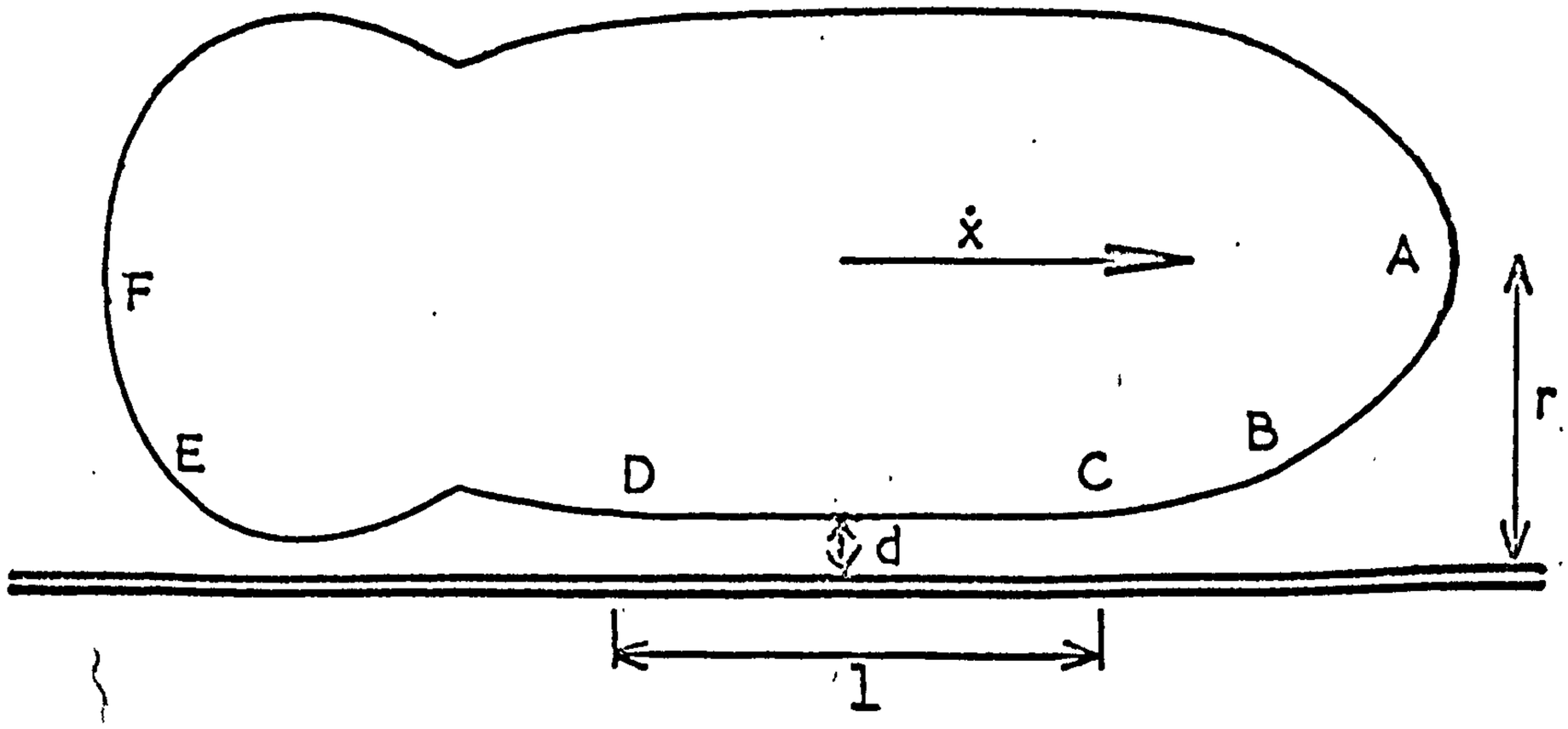

Fig. 3.6

For sufficiently small, non-zero $(\frac{\eta_1 \dot{x}}{\sigma_{12}})$ the interface is conveniently divided into several regions (Fig. 3.6). The front and rear menisci are separated by a region CD of length ℓ in which there is a uniform annular film of fluid 1. The thickness of the film, d, is such that $\ell \gg d$ and $r \gg d$. The mean curvature of the interface in this region is constant and of order $\frac{1}{r}$ i.e. $O(\frac{1}{r})$. If $\eta_1 \gg \eta_2$ then the film is in a region of approximately uniform pressure, with negligible tangential stress on its free surface. It will therefore be sensibly at rest, as has been verified experimentally by Goldsmith and Mason[102].

At the menisci, but away from the wall, (regions AB and EF) the viscous stresses are $O(\frac{\eta_1 \dot{x}}{r})$, whereas stresses due to surface tension are $O(\frac{\sigma}{r})$. Thus in regions AB and EF the fractional change in mean curvature due to motion will be $O(\frac{\eta_1 \dot{x}}{\sigma_{12}})$ and, if this is small, these regions will be, to a first approximation, spherical.

On the other hand, in the transitional regions, BC and DE, the viscous stresses are $O(\frac{\eta_1 \dot{x}}{d})$ * and the

---

*The approximation involved here is that for sufficiently small $(\frac{\eta_1 \dot{x}}{\sigma_{12}})$ the interface in these regions is almost parallel to the tube wall: the fluid thickness is therefore much less than r and O(d). This approximation is the basis of the "lubrication approximation" adopted by Bretherton.

curvature changes from approximately $^2/r$ at B,E to approximately $^1/r$ at C,D.

If the length of the regions ED and BC are O(ar) then the stress gradient induced by surface tension will be $O\left(\frac{\sigma}{ar^2}\right)$ whilst that due to viscous stresses will be $O\left(\frac{\eta_1 \dot{x}}{d^2}\right)$. For hydrodynamic stability, these stress gradients must balance and the resulting condition is therefore

$$\left(\frac{\eta_1 \dot{x}}{d^2}\right)\left(\frac{ar^2}{\sigma_{12}}\right) = 1 \qquad 3.1\text{-}8$$

This condition is not unique, however, since it may be factorized into two dimensionless groups and the numerical constant a. The more general equation is, therefore,

$$a\left(\frac{\eta_1 \dot{x}}{\sigma_{12}}\right)^b \left(\frac{r}{d}\right)^c = 1 \qquad 3.1\text{-}9$$

Comparison with Bretherton's equation (Eq. 3.1-6) gives: $a = 1.34$, $b = \frac{2}{3}$ and $c = 1$; whilst Fairbrother and Stubbs equation (Eq. 3.1-4) yields: $a = \frac{1}{2}$, $b = \frac{1}{2}$ and $c = 1$.

Bretherton's detailed analysis of the curvature of the two menisci predicts that the true mean curvature of the region AB is

$$\frac{1}{r_m} = \frac{2}{r}\left[1 + 3.73\left(\frac{\eta_1 \dot{x}}{\sigma_{12}}\right)^{\frac{2}{3}}\right] \qquad 3.1\text{-}10$$

and the associated pressure drop Δp_{Front} is, therefore,

---

*One of the constants b or c is of course redundant, since it can always be chosen equal to 1, but both have been included for clarity.

given by

$$\Delta p_{Front} = \frac{2\sigma_{12}}{r}\left[1 + 3.73\left(\frac{\eta_1 \dot{x}}{\sigma_{12}}\right)^{\frac{2}{3}}\right] \qquad 3.1\text{-}11$$

This arises partly from viscous stresses in neighbourhood of the meniscus and partly from the pressure drop across the interface itself due to surface tension.

At the rear meniscus the situation is different. The pressure drop across a moving rear meniscus exceeds the static value, $\frac{2\sigma_{12}}{r}$, only if $\left(\frac{d}{r}\right)\left(\frac{\eta_1 \dot{x}}{\sigma_{12}}\right)^{-\frac{2}{3}} < 1.87$. For larger values, it tends to assist rather than hinder motion. The necessary energy comes from the finite volume of liquid in the film of thickness d at a pressure $\frac{\sigma_{12}}{r}$ higher than the liquid behind the meniscus. For values of $\left(\frac{d}{r}\right)\left(\frac{\eta_1 \dot{x}}{\sigma_{12}}\right) < 1.87$ the energy dissipated in the transition region DE exceeds this amount and external work has to be done to make the meniscus move. If (d/r) is defined by front meniscus travelling with the same velocity (Eq. 3.1-6) then the dynamic pressure drop is found to be $- 1.94 \left(\frac{\eta_1 \dot{x}}{\sigma_{12}}\right)^{\frac{2}{3}} \left(\frac{\sigma_{12}}{r}\right)$.

Thus the rear meniscus contributes to the total dynamic pressure drop down the tube which is

$$\Delta p_{Total} = 9.4\left(\frac{\sigma_{12}}{r}\right)\left(\frac{\eta_1 \dot{x}}{\sigma_{12}}\right)^{\frac{2}{3}} \qquad 3.1\text{-}12$$

Film Instability

Providing the thin liquid annulus left on the walls of a tube following incomplete displacement is long compared with its diameter and has a thickness greater than the range

of surface forces, it will have no inherent mechanical stability[105-106].

Goldsmith and Mason[102] observed that when liquid bubbles were brought to rest, film thinning did not take place uniformly. Instead, wavelike disturbances could be seen to travel in towards the bubble centre from both ends. If the bubble was short (less than about 4 diameters long) this produced a dumb-bell shape, (Fig. 3.7a) with the wetting liquid being gradually squeezed out via the ends. For longer bubbles the amplitude of the waves increased and resulted in the formation of a series of uniformly spaced unduloids (Fig. 3.7b). These eventually closed and produced a string of approximately uniform bubbles (Fig. 3.7c). The length of these smaller bubbles was found to be in agreement with the theoretical predictions of Goren[107].

Similar wave-like disturbances can be seen near the trailing end of moving bubbles (as has been anticipated in Figs. 3.3 and 3.6). In Goren's view, these are possibly due to the liquid annulus in that region having been in existence long enough to afford small disturbances a chance to grow. However, providing the bubble is long enough for his method to be valid, Bretherton's theoretical study of bubble profiles predicts that these variations in film thickness will be independent of bubble length and that if $(\frac{d}{r})$ is defined by a leading meniscus travelling with the

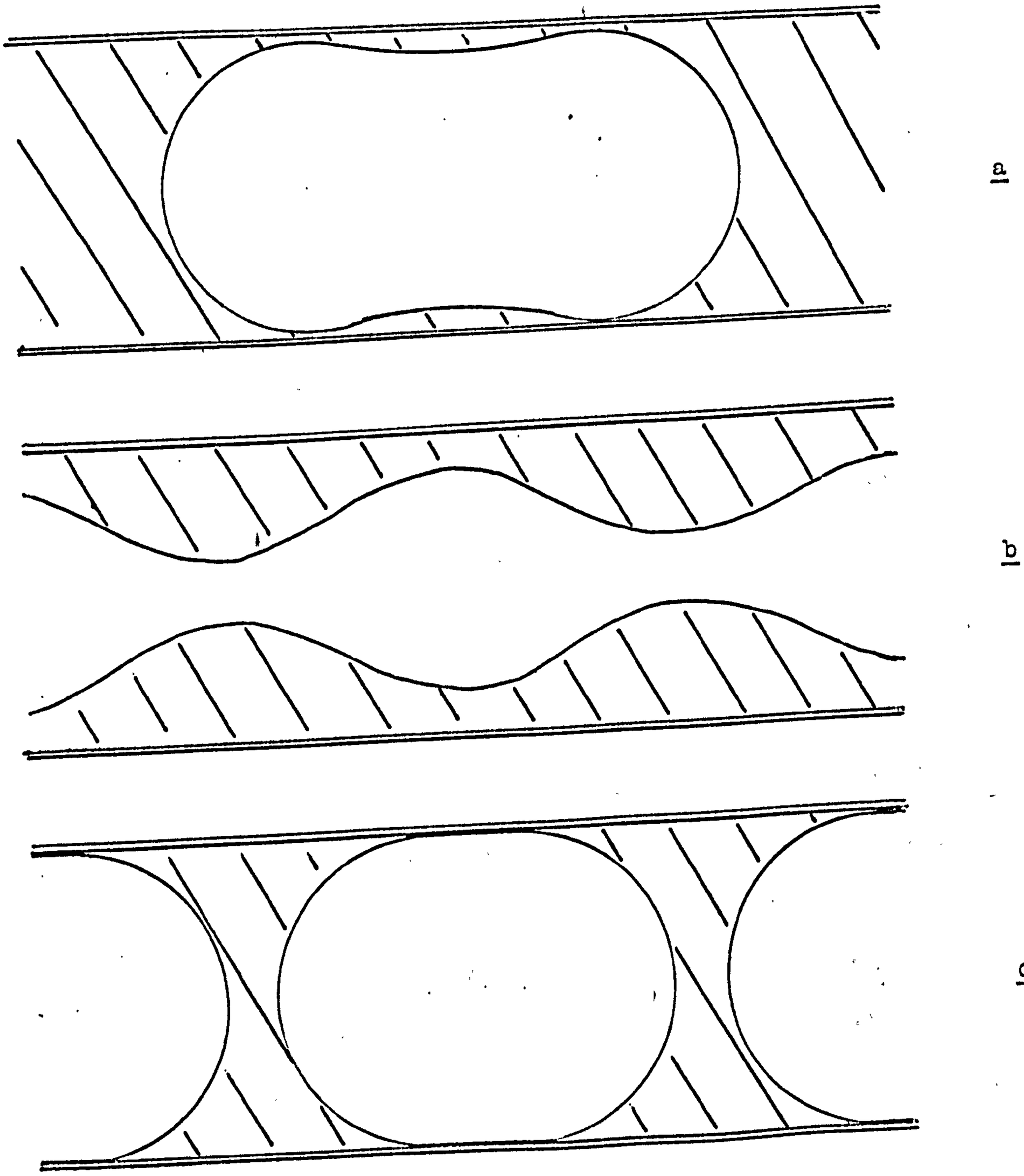

Fig. 3.7

same velocity then the minimum film thickness will be 0.716d.

Velocity Profiles and Streamline Patterns

Mason and co-workers[102,108,109] have made an extensive investigation of velocity profiles and streamline patterns within both bubbles and their surrounding liquids. Their ingenious technique involved ciné studies of the movement of tracer particles introduced into the appropriate phase. The theoretical analysis provided[102], however, is only valid at positions "... sufficiently far removed from the bubble ends..." Thus, apart from information on tube radius, liquid viscosities and bubble velocity, $\dot{x}$, either the film thickness, d, or the average velocity, $\dot{x}_m$, must be known before a velocity profile or streamline pattern can be calculated. It is only when the bubble ends are taken into consideration, as in Bretherton's paper, that just one of the variables $\dot{x}$, $\dot{x}_m$ or d is sufficient. Figs. 3.8a, b & c show velocity profiles and velocity gradients for concentric flow of liquids with various viscosity ratios. They represent positions sufficiently far removed from the meniscus for radial flow to be neglected.

Isolated Menisci

Although interface shape has hitherto been discussed only with respect to the flow of complete bubbles, the majority of what has been said applies equally well to isolated menisci involved in concentric flow. The similitude

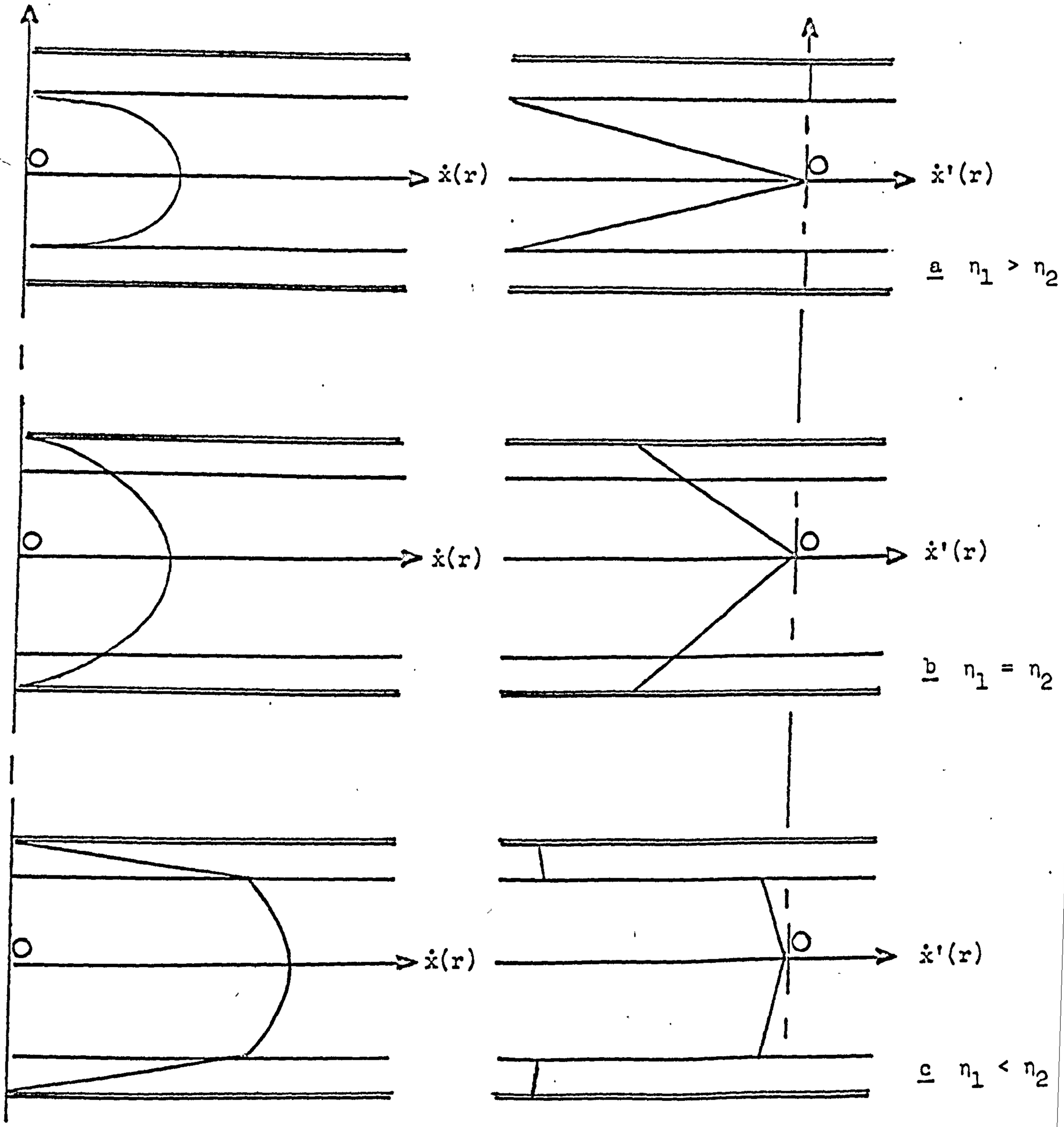

Fig. 3.8 Velocity profiles, $\dot{x}(r)$, and velocity gradients, $\dot{x}'(r)$ (after Goldsmith and Mason[102])

is not quite complete, however, for whilst the rear meniscus of a uniformly moving bubble always advances into a region in which the fluid distribution is defined, in part at least, by the associated front meniscus travelling with the same velocity, the fluid distribution in front of an isolated trailing meniscus is not similarly defined and will, in general, be quite arbitary. Furthermore, if the previous history of the system is unknown, it may be difficult to distinguish, experimentally, whether ~~or not~~ concentric flow or consecutive flow is responsible for the shape of the moving interface, i.e. whether or not there is a moving line of three phase contact.

3.2 Consecutive Flow

The Three-Phase Boundary Condition

In the last section capillary displacement was discussed only for systems in which one fluid completely wets the tube wall. The existence of a finite angle of contact between the moving interface and the tube wall presents additional problems: (i), by what mechanism does the TPZ move across the solid surface, and (ii), how, as a boundary condition, does the TPZ modify hydrodynamic behaviour?

The hydrodynamic aspect of the problem would not appear to present any insuperable difficulties[110].

Bretherton[103] has asserted that complete displacement of one fluid by another from the surface of a solid is impossible as it "... would involve infinite viscous stresses at the wall." However a non-zero fluid velocity at a solid boundary, which consecutive flow may or may not require, is not prescribed by hydrodynamics. One example has been described by Taylor,[111] and this and related phenomena have been discussed in detail by Moffat.[112] What is required now is a detailed working model of the TPZ, and, to this end, molecular dynamics rather than hydrodynamics is the more likely tool.

Contact Angle Velocity Dependence

The term "dynamic contact angle" will here be applied only to contact angles associated with three phase lines which move or are caused to move across the surface of the solid*. Elliott and Riddiford[44] have asserted that Young's equation is applicable even when the TPL is moving, providing that appropriate non-equilibrium values of the various interfacial tensions are used. However, in the

---

* (i) This term has been used in an alternative sense[113]. See Elliott and Riddiford[44].

(ii) It will be noticed that this definition presupposes that the TPL can move; indeed this supposition is fundamental to the distinction between concentric and consecutive flow.

absence of any proof of the validity of this assertion, it seems inappropriate to use the symbol θ to denote the dynamic contact angle; rather, since, at present, the dynamic contact angle is essentially an observed quantity, it will be more in keeping with previous notation (Section 2.1) if the symbol ϕ be used instead.

In accordance with common usage the term "advancing contact angle", ϕ_a, will be used when referring to the angle measured through a fluid which is displacing another from the surface of a solid, and the designation "receding contact angle", ϕ_r, will be applied to the angle measured through a fluid which is being displaced (see Fig. 3.9).

Ablett[114] (1923) reported the variation of ϕ with the velocity of the TPL between air, water and paraffin wax. He found that advancing angles increased and receding angles fell to certain, well defined, limiting values as the rate of displacement increased.

Yarnold and Mason[91] obtained results in general agreement with Ablett's, but they also observed that ϕ was markedly dependent upon how long the three phases (air/water/wax) had been in contact. In their opinion the velocity dependence of the contact angle was due to the disturbance of adsorption equilibria at the solid/fluid boundaries in the TPZ. Cassie[85] has suggested a similar cause, and the conclusions of Bartell and Bristol[115] lend further support to this hypothesis. Adam and Livingstone[116],

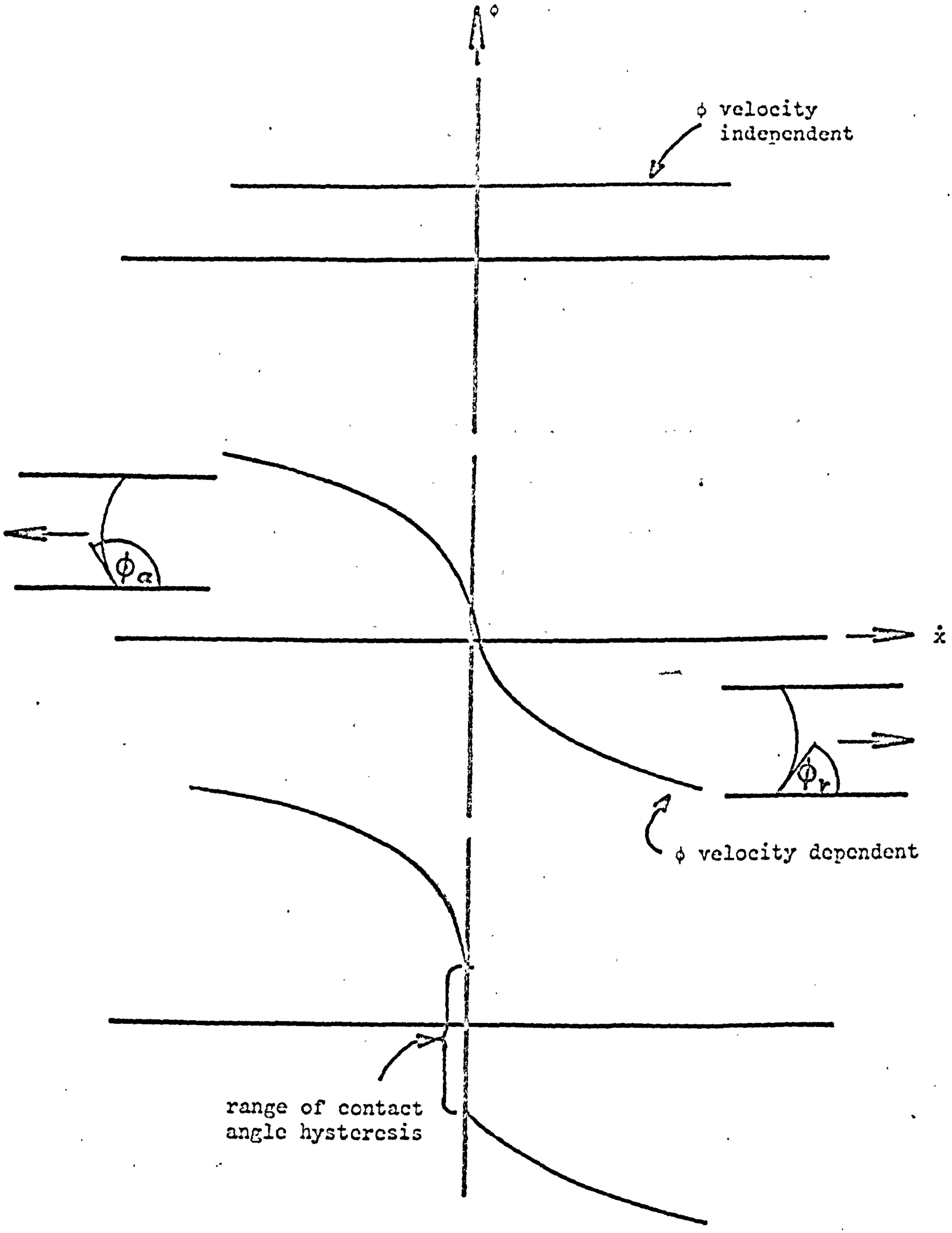
ϕ
ϕ velocity independent
ϕ_a
ẋ
ϕ_r
ϕ velocity dependent
range of contact angle hysteresis

Fig. 3.9

however, believe that the area in the immediate vicinity of the TPL is likely to be in adsorption equilibrium, even if other parts of the system are not. Similar conclusions have been drawn by Melrose[26]. On this reckoning, only interfaces that were advancing rapidly would show contact angle velocity dependence.

Bartell and Bjorklund[117] have found a dynamic effect in the system mercury/water/benzene, but conclude that for sufficiently small rates of displacement ($< 0.3\mu$ sec^{-1}) the contact angle was independent of velocity*. However, their precision ($\pm 2^{o}$) does not appear to have been sufficient to entirely justify this assertion. More recently, Gaudin and Witt[72] have shown that when oxygen is excluded from the system the contact angle is not dependent upon velocity, but when oxygen is admitted both contact angle hysteresis and velocity dependence appear. This latter behaviour is attributed to the formation of a comparatively rigid oxide film covering the mercury surface, which then no longer has the properties of liquid mercury. Such an oxide film, if present in the Bartell and Bjorlund

---

* N.B. A contact angle which is velocity independent is, ipso facto, independent of both rate and direction of displacement and, therefore, does not exhibit contact angle hysteresis (see Fig. 3.9).

experiments, would nullify their rejection of the "friction" hypothesis[118].

Rose and Heins[119] have investigated Nujol/glass/air and oleic acid/glass/air systems over a moderate range of interfacial velocities (c. 5×10^{-3} to 0.5 cm sec^{-1}). The receding angles for both liquids were close to zero in all cases, but the advancing angles increased with increasing velocity over the whole range. The data, however, are very scattered. Rose and Heins were unable to give any hydrodynamic explanation of their results although a dimensional analysis was attempted.

Elliott and Riddiford[90,92] have made an intensive study of the polyethylene/water/air + water vapour, and siliconed glass/water/air + water vapour systems. Over a velocity range of approximately 20 to 400μ sec^{-1}, their experimental observations confirm that advancing and receding angles respectively rise and fall with increasing rate of displacement. Above 200μ sec^{-1} the advancing angle (measured through the water) tends to a limiting value. No similar trend was observed with the advancing air interface. The authors state that at the lowest speeds (17μ sec^{-1}) the contact angle was constant for both advancing and receding conditions although about 22° of hysteresis persisted. Their published data, however, are inconclusive.

Elliott and Riddiford go on to suggest that this result may be interpreted in terms of the Hansen and Miotto theory (see Section 2.4). If the natural length associated with displacement, δ, were of order 10^{-8} cm then, with a natural displacement velocity, x_n, of roughly 10^{-3} cm sec^{-1}, the relaxation time for the process would be of the order of 10^{-5} sec. A Frenkel[93] type expression is used to obtain the temperature dependence of τ:

$$\tau = \tau_o \exp \frac{E}{RT} \qquad 3.2\text{-}1$$

or

$$\dot{x}_n = \frac{\delta}{\tau_o} \exp \frac{-E}{RT} \qquad 3.2\text{-}2$$

where τ_o is the relaxation time appropriate to bulk water, and E is the activation energy for the relaxation process at the TPZ. Then, taking τ_o as about 10^{-10} sec, they obtain a value for E of about 1.7×10^3 Joules $mole^{-1}$. Elliott and Riddiford state that although this value is not unreasonable it is "... predicted on the assumption that during advance, water does not penetrate the solid surface". In this connection[92] they report that freshly advanced and recessed contact angles, on standing, tended to relax towards a common value over periods of up to 18 hr. This they attribute to penetration of the silicone layer by water rather than to a Hansen and Miotto process. On the other hand, they remark that it is tempting to suppose that the limiting values of the contact angles observed at the

highest rates of displacement might correspond, in the Hansen and Miotto scheme, to total disorientation at the TPZ.

Elliott and Riddiford have also studied systems similar to those noted above with the vapour phase replaced by Bayol. Experimental difficulties were found to be much greater, but results were qualitatively similar to those given previously, although no lower speed range was found in which ϕ was independent of the rate of TPL displacement.

It is interesting to note that Zisman and co-workers[43] have reported that, within experimental error ($\pm 2^{\circ}$ maximum), contact angle hysteresis is absent from many carefully prepared liquid/vapour/organic polymer systems providing "the liquid drop was advancing or receding sufficiently slowly to be reasonably close to an equilibrium condition".

Chittenden and Spinney[121] have found that the character of the contact angle velocity dependence, in the system: water/cyclohexane/glass, is itself dependent upon the pre-treatment of the glass surface. Velocity dependence is greatest when the glass is first outgassed at c. 200°C and then exposed to cyclohexane (saturated with water). It is thought that cyclohexane is strongly adsorbed at the glass surface after this treatment and that the displacement of cyclohexane by water at high velocities leaves behind a thick non-equilibrium film of cyclohexane

which increases the contact angle measured through the water. At lower velocities, the rate of desorption of the non-equilibrium film more nearly approaches its rate of deposition, and a lower, more nearly equilibrium value of the contact angle therefore results.

In contrast with Ablett, and Elliott and Riddiford, Chittenden and Spinney find, like Rose and Heins, that contact angle velocity dependence is still apparent at rates of displacement in excess of 1 cm sec^{-1}.

In conclusion, it may be remarked that contact angle velocity dependence has received much less attention than contact angle hysteresis, and has been explained in terms of displaced equilibria rather than surface roughness or heterogeneity.

Interface Shape

The unknown effect of displacement upon the three-phase boundary condition at the wall is not the only problem encountered with consecutive flow. As with concentric flow, the energy loss and associated radial variations in interfacial curvature produced by radial flow in the vicinity of the moving two-phase boundary have also to be considered.

Figs. 3.10a and b show two simple types of flow pattern such as might be found in this region. The meniscus is considered stationary and the tube moves from

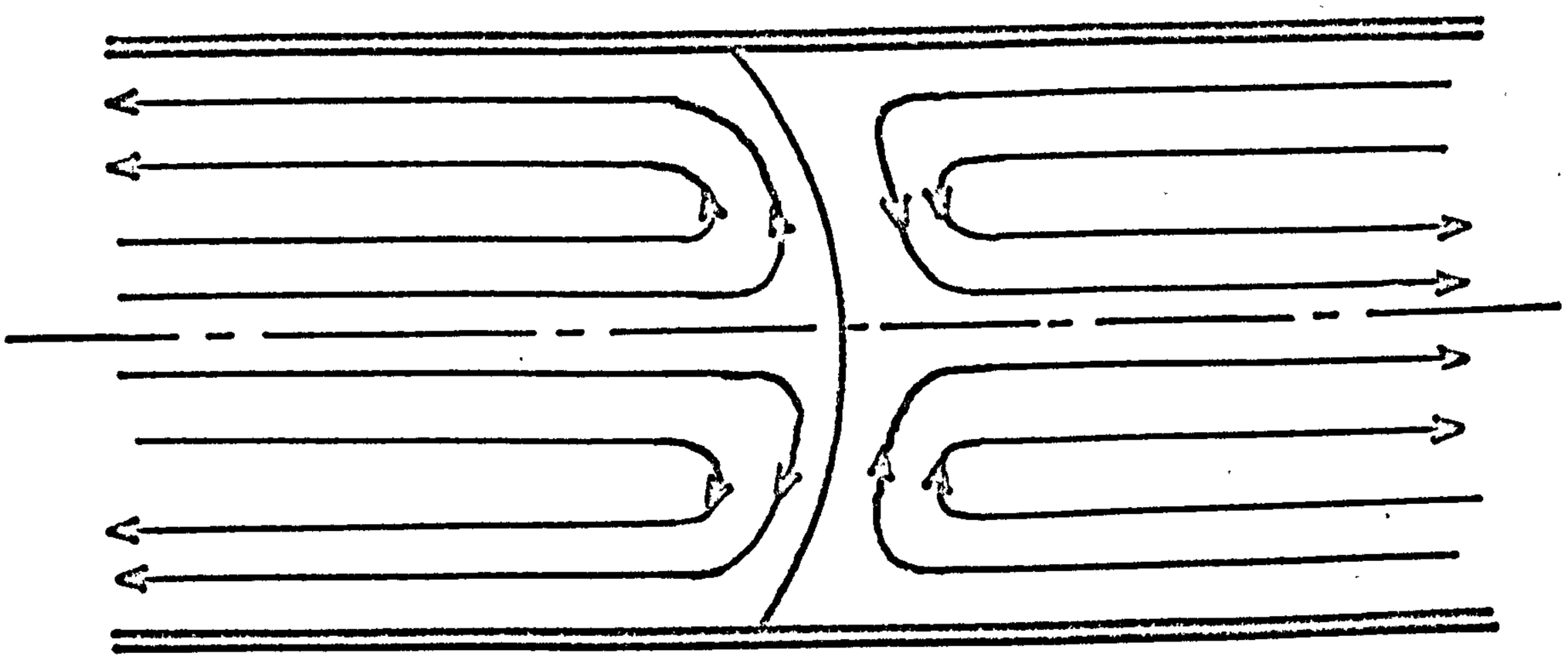

Fig. 3.10a

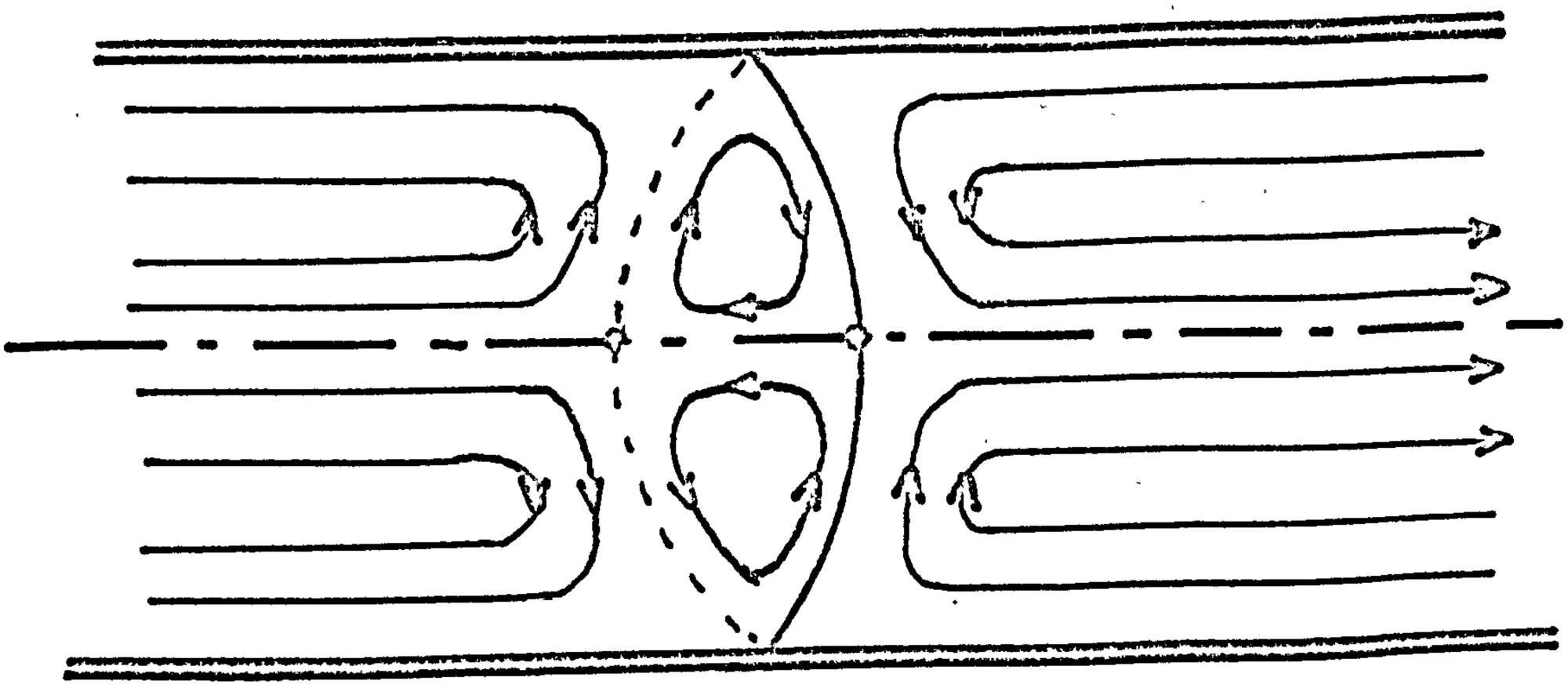

Fig. 3.10b

left to right. No particular significance is attached to the curvature of the meniscus.

Under flow conditions of type a, the tangential shear stress at the fluid-fluid interface will be zero and there will be no flow in the interface. The tangential velocity component at the interface will, nevertheless, be continuous[98].

In the other type of flow pattern illustrated, b, an eddy has formed on one side of the meniscus; there is circulation in the interface, two stagnant points on the tube axis and a stagnant ring at the TPL.

There is no way of predicting a priori which (if either) flow pattern will be adopted, although if there is significant adsorption at the moving phase boundary then interfacial circulation will be inhibited (see Levich[98] pp. 380-394). The experimental studies by Goldsmith and Mason have revealed only flow patterns of type a, but it must be emphasised that they were concerned with concentric and not consecutive flow.

Rose[123] considers flow patterns of type a only. He deduces that the tangential velocity component at the interface will be zero, but then goes on to state that if this is so, "it will be readily apparent that ... no pressure gradients exist in either phase tangential to the surface". On the contrary, this is not readily apparent. The stress tensor in the neighbourhood of the interface

must have a component normal to the interface, or the interface would not move at all, and there is no obvious reason why this normal component should be the same at all points on the interface - especially near the tube wall[110]. Rose therefore appears to be arguing from incorrect premises when he states, "In consequence, the capillary pressure differences between wetting and non-wetting fluids at each point in the interface region will have a constant value; hence the moving interface will have constant curvature throughout".

A dimensional approach similar to that used in concentric flow might prove more fruitful. If, once again, inertial and gravitational forces are ignored (conditions 3.1-7a & b), then, except perhaps in the unknown region of the TPZ, the only important forces to be considered are viscous and surface tension forces.

Away from the tube wall the viscous stresses are $O\left(\frac{\eta_1 \dot{x}}{r}\right)$ whereas stresses due to surface tension are $O\left(\frac{\sigma_{12}}{r_m}\right)$, where $\frac{1}{r_m}$ is the mean curvature of the interface. If the interface is assumed spherical, then to a first approximation

$$r_m = r \sec \phi . \qquad 3.2\text{-}3$$

where ϕ is the dynamic contact angle. Thus over the majority of the interface the fractional change in mean curvature due to motion is $O\left(\frac{\eta_i \dot{x}}{\sigma_{12}}\right)\left|\sec \phi\right|$. Deviations from

sphericity are therefore unlikely providing

$$\left(\frac{\eta_i \dot{x}}{\sigma_{12}}\right)|\sec \phi| \ll 1 \qquad 3.2\text{-}4$$

As yet there are no reported instances of consecutive flow in systems in which condition 3.3-2 is violated and the interface shape is known. The highest values of $\left(\frac{\eta_i \dot{x}}{\sigma_{12}}\right)|\sec \phi|$ obtained by Rose and Heins[119] in their ciné study of consecutive flow in Nujol-air and oleic acid-air systems was about 0.02. That no deviations from sphericity have been reported is therefore not surprising.

3.3 A Simple Equation for Two-Phase Flow

In view of the concluding remarks of the last section, providing conditions 3.1-7a, 3.1-7b and 3.2-4 are complied with, and providing also that ϕ is known as a function of $\dot{x}$, then a simple combination of the Laplace and Poiseuille equations should provide an approximate, but nevertheless useful, equation for two-phase flow in systems of cylindrical geometry. Numerous equations of this type appear in the literature, and this chapter will conclude with a resumé of the principal results of their application.

Equating the capillary driving force and the viscous resistance to unaccelerated flow yields, for the steady-state interfacial velocity,

$$\dot{x} = \frac{-r\sigma_{12} \cos \phi}{4(\eta_1 x + \eta_2(1 - x))} \qquad 3.3\text{-}1$$

where x and (1 - x) are the lengths of the capillary occupied by fluids 1 and 2 with viscosities η_1 and η_2 respectively. If the capillary pressure is opposed by an applied hydrostatic pressure, Δp, then

$$\dot{x} = \frac{r^2 \Delta p - 2r\sigma_{12} \cos \phi}{8(\eta_1 x + \eta_2 (1 - x))} \qquad 3.3\text{-}2$$

If $\dot{x}$ is found as a function of Δp then it is possible to calculate ϕ as a function of $\dot{x}$.

One of the earliest* equations of this type was derived by West[124] (1911): "On the Resistance to the Motion of a Thread of Mercury in a Glass Tube", and a similar equation was proposed by Yarnold[125] (1938). Their equations necessarily took into account two mercury-air interfaces and were, therefore, of the form

$$\dot{x} = \frac{r^2 \Delta p - 2r\sigma_{12} (\cos \phi_r + \cos \phi_a)}{8\eta_1 l} \qquad 3.3\text{-}3$$

where l is the length of the mercury thread of viscosity η_1, and the viscosity of the air is ignored.

Eley and Pepper[128] have studied water/Nujol, water/benzene, and nitrobenzene/Nujol displacements in a single capillary as a preliminary to an investigation of two phase flow in powder packings.

In all the investigations noted above, surprisingly good agreement is reported between the simple theory and

---

* Brittin[126] refers to an even earlier study by Decharme[127] (1874).

experiment. Both West and Yarnold found indications of a large contact angle hysteresis, but no dynamic effect. Once a certain critical driving pressure Δp_c was reached, the mercury slug began to move with $\dot{x}$ proportional to $(\Delta p - \Delta p_c)$. Eley and Pepper calculated that in their experiments ϕ was always close to zero, and suggested that this was probably due to the practice, found necessary, of giving the capillary a preliminary wetting with the displacing liquid. When this was not done the advance of the interface was much slower and much less reproducible, being occasionally halted completely at patches of contamination on the surface of the capillary. In one such case, with water/Nujol, ϕ was calculated to be c. 70°!

The resistance to motion of the TPZ, described by West and others, corresponds to the well-known Jamin[130] effect. Recently Schwartz and co-workers[131] have carried out extensive measurements on systems exhibiting this phenomenon. Their results indicate the presence of a considerable contact angle velocity dependence.

Calderwood and Mardles[129] have studied the rate of movement of liquid indices down inclined tubes under gravity. Their results show both contact angle hysteresis and velocity dependence.

Washburn[132] has investigated the capillary rise of a single liquid against gravity. If ρ is the density of

the liquid and z is the height to which it rises in time t, then ignoring the density and viscosity of vapour,

$$\frac{2\sigma_{12}\cos\phi}{r} - \rho g z - \frac{8\eta z\dot{z}}{r^2} = \rho\,(\dot{z}^2 + \ddot{z}z) \qquad 3.3\text{-}4$$

An approximate solution to this equation has been proposed by Bosanquet[133]. Washburn, however, considered that if $\dot{z}$ and $\ddot{z}$ are both small then the inertial terms on the right may be neglected. Further, if ϕ is independent of velocity and

$$z = 0 \text{ at } t = 0$$

$$z = z_f \text{ at } t = \infty$$

then

$$\rho g(z_f - z) = \frac{8\eta}{r^2} z\dot{z} \qquad 3.3\text{-}5$$

and integration yields,

$$t = \frac{8\eta}{\rho g r^2}\left[z_f \ln\left(\frac{z_f}{z_f - z}\right) - z \right] \qquad 3.3\text{-}6$$

Expansion of the logarithm yields the result, well known in soil studies[128], that in the early stages of capillary rise $\dot{z} \propto \sqrt{t}$ or, more exactly,

$$z = \left(\frac{r^2 \rho g\, z_f}{8\eta}\right)^{\frac{1}{2}} t^{\frac{1}{2}} \qquad 3.3\text{-}7$$

This last equation has been experimentally verified by Peek and McLean,[134] and more recently by Ligenza and Bernstein[135] for capillaries of small radius (20 to 50μ) (see also Rosano and Gristalla[136]).

Le Grand and Rense[137] have made a very careful study of capillary rise of water, ethanol and glycerol in glass

capillaries. Some data were obtained in the very early stages of liquid ascent ($t < 0.1$ sec) in the hope of detecting inertial effects associated with the terms on the right of Eq. 3.3-4, circulation at the interface and turbulence at the entrance to the capillary. Their results, plotted according to Eq. 3.3-6, do show divergences when $t < 1$ sec. Thereafter, however, Eq. 3.3-6 is obeyed within experimental error.

A detailed analysis of the hydrodynamic aspect of the problem has been attempted by Brittin[126]. The equation arrived at takes into account most of the inertial effects expected by Le Grand and Rense and, although the equation is unwieldy (and in practice semi-empirical), it does give better agreement with their data than Eq. 3.3-6 when $t < 1$ sec.

Rose and Heins[119] have studied the movement of liquid indices in horizontal tubes. Contact angles were measured directly from photographs and were in fair agreement with those predicted on the basis of Eq. 3.3-3; ϕ_r was close to zero in all cases. This result has since been used by Chittenden and Spinney[121] in a study of water-cyclohexane displacements in glass capillaries (see Section 3.2).

Templeton[138,139] has conducted a series of experiments involving gas-liquid and liquid-liquid displacements in

single, uniform glass capillaries having diameters ranging from 4 to 40μ. Capillary radii were determined from the pressure required to maintain the interface at rest against capillary pressure, assuming $\phi = 0$ and σ_{12} independent of tube radius. Radii were compared with values measured visually to $\pm 0.1\mu$, and the two methods were reported to agree within 2%.

The fluids used were air or water against benzene, Nujol or various refined hydrocarbon oils. Whilst an equation similar to 3,3-2 gave values for the viscosities of water and benzene close (no details given) to the bulk values, those given for Nujol and the refined hydrocarbons were up to 30% low. Templeton attributes this to the presence of an annular water film about the oil column, as postulated by Yuster, but this does not explain a 15% reduction in viscosity reported for the oil phase in oil-air displacements; nor does it explain an apparent 30% increase in oil phase viscosity for the first water displacing oil run following only oil-air displacements. In an attempt to explain this latter observation, Templeton postulates an irregular fluid distribution following a first, incomplete, water displacing oil run. Such a distribution, if present, might well be sufficient to impede flow[140], but it seems curious that phenomena of this type were not actually observed. Street[143] has

suggested an explanation of some of these anomalies in terms of electroviscous effects.

Over the last ten years, Derjaguin and Fedyakin[65,141,142], have reported a series of remarkable and intriguing experiments with capillaries having diameters in the range 300Å to 10μ. In one experiment the viscosities of water and benzene were determined using an equation similar to Eq. 3.3-2 to describe the rate at which the liquids penetrated capillaries against the pressure of entrapped air, the capillaries being closed at one end. The contact angle was assumed to be zero at all times. Viscosity was found to be a linear function of tube radius for both liquids. Values are reported ranging from 10% of the bulk value for r ≈ 200Å to close to 90% for r ≈ 0.15μ. Similar variations are also given for surface tension, ranging from about 30% of the normal value for r ≈ 200Å to approximately 100% for r ≈ 0.15μ. These results are attributed to the influence of the capillary wall upon the structure of the liquids. The inference is that in tubes of diameter less than c. 0.1μ, liquids have a diminished structural order, e.g. in the case of water a diminished state of hydrogen-bonding. This is surprising, particularly in view of Derjaguin's insistence on the importance of structuring in polar liquids close to glass or silica surfaces[64].

C H A P T E R F O U R

Displacement Studies in Macroscopic Capillaries

Introduction

Liquid-liquid displacements have been carried out in horizontally mounted, cylindrical, Pyrex capillaries of between 0.4 and 1 mm bore. Initially, simple measurements were made of interfacial velocity, $\dot{x}$, as a function of applied hydrostatic pressure, Δp, using a benzene/water interface in a chemically cleaned capillary. Later, in an attempt to introduce velocity dependence of the contact angle in a controlled way, experiments were begun in silane-treated tubes, and in all but the preliminary experiment, P3, a micro-ciné technique was used which ~~enabled~~ permitted direct measurements of all the observable parameters, $\dot{x}$, Δp and the contact angle, ϕ. At first, interest centred on the verification of Eq. 3.3-2 and the interdependence of ϕ and $\dot{x}$; however, at a later stage, experiments were carried out using benzene/glycerol and cyclohexane/aniline interfaces in order to investigate the effects of respectively a high viscosity ratio and a low interfacial tension upon the stability of the moving phase boundary.

4.1 Alkyl Chlorosilanes as Surface Modifying Agents

Dimethyldichlorosilane is believed to react with

hydroxyl groups of hydrated glass surfaces by elimination of HCl to give a chemically bonded organophilic layer[90,143-146].

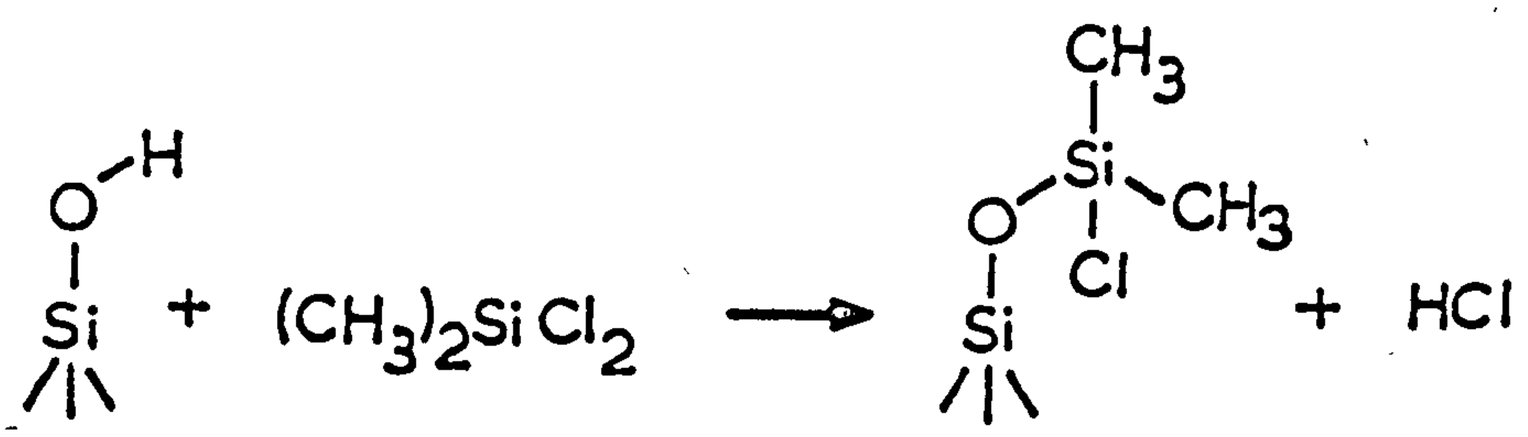

It has been suggested[148] that the reaction is facilitated by the removal of the HCl by alkali oxides (e.g. Na_2O) present in or near the glass surface. The lack of such oxides in silica may explain the conclusion reached by White[149] that, at room temperature, chlorosilane molecules interact only physically and reversibly with the hydroxyl groups of a silica surface from which physically adsorbed water has been removed by evacuation. Armistead and Hockey[150] have very recently published a paper on the reactions of methylchlorosilanes with hydrated Aerosil silicas which suggests that, for steric reasons, only non-hydrogen-bonded hydroxyls are available for chemical reaction.

In the preliminary experiments described here, silane coating was achieved simply by drawing a continuous stream of air saturated with dimethyldichlorosilane vapour through the acid-cleaned capillary; a chemically resistant, hydrophobic surface resulted and it was, therefore, thought

unnecessary to resort to the high-temperature curing process recommended by some authors[143,149]. In subsequent experiments, a more refined, high vacuum technique was employed (described in a later section) and, in series E experiments, tubes were treated with trimethylchlorosilane. This final modification was introduced because of the likelihood of dimethyldichlorosilane polymerising in the presence of water during the coating process[144,149]:-

$$nMe_2SiCl_2 + (n-1)H_2O \quad Me_2SiCl(-OSiMe_2-)_{n-2}-OClSiMe_2 + (2n-2)HCl$$

Polymerisation, it was thought, might produce random variations in the nature and thickness of the silane coating, and in its bonding to the glass, and hence be responsible for observed contact angle hysteresis. Trimethylchlorsilane is unlikely to produce larger polymers than the dimer $Me_3Si-O-SiMe_3$. This ether is expected to be sufficiently volatile to be removed under vacuum, leaving only a monolayer of chemisorbed silane molecules.

4.2 Experimental Methods

Cleaning and Preparation of Materials

All glassware was constructed from Pyrex borosilicate glass (composition: SiO_2 80.6%; B_2O_5 12.6%; Al_2O_3 2.0%; Na_2O 4.2%) and carefully cleaned before use. At first, chemical cleaning methods were used - usually hot chromic acid or ethanol/nitric acid treatment followed by multiple

rinsings with conductivity water. However, after some experience these methods were abandoned because:-

(i) they were only partially effective;

(ii) they are hazardous and messy;

(iii) glass is leached by this treatment (even distilled water will do this) and probably acquires a highly porous surface[161,162] which may continue to retain foreign matter. The method eventually adopted involved rinsing the apparatus in distilled water (in order to remove loosely held dust and soluble material), and then placing it in an annealing oven where it was subjected to a circulating current of air at temperatures between 500 and 560°C for a minimum of 1½ hr before being allowed to cool slowly in a clean atmosphere.

Methylchlorosilanes were supplied by Hopkin and Williams in purified form, but were used as received only in Exp. P3. For all other experiments methylchlorosilanes were further purified by trap-to-trap distillation under vacuum in a grease free apparatus, and either used directly or distilled into evacuated sample tubes fitted with an internal break-seal. Purity, as checked by gas chromatography, was at least 99%.

The conductivity water used for both cleaning purposes and displacement studies was twice distilled in all-Pyrex stills fitted with fractionating columns packed with glass

beads. After an initial running-in period, this method was found to provide a uniform product with a conductivity of less than 2μ mho and a surface tension of 72.0 ± 0.2 dyne cm^{-1}. The use of ion-exchange columns for this purpose was avoided[151]. Water used for surface rehydroxylation (described later) was redistilled into evacuated, break-seal bulbs.

Benzene was May and Baker "Crystallisable" grade, sulphur free, having a boiling range of 79.5 to 80.5°C. This was used as received in Exps. P2, P3 and A1. For the remainder, it was redistilled and the middle fraction further purified by successive recrystallisation.

The glycerol used in Exp. F2 and also as an immersion liquid was BDH "Analar" grade. It was used as received. The aniline and cyclohexane were BDH "Laboratory Reagent" grade and were used as received.

Pairs of liquids used in displacement studies were mutually saturated and stored in closed glass vessels. When required, samples were withdrawn by syphon.

The benzene/water interfacial tension was checked by the method of Harkins and Brown[152] and found to be 34.9 ± 0.1 dyne cm^{-1} at 20°C. The benzene/glycerol interfacial tension was measured using a du Noüy tensiometer and found to be 19.5 dyne cm^{-1} at 20°C.

Exp. P2: Preliminary, Benzene-Water Displacements in Uncoated Capillary

The apparatus is illustrated in Fig. 4.1. A 150 cm

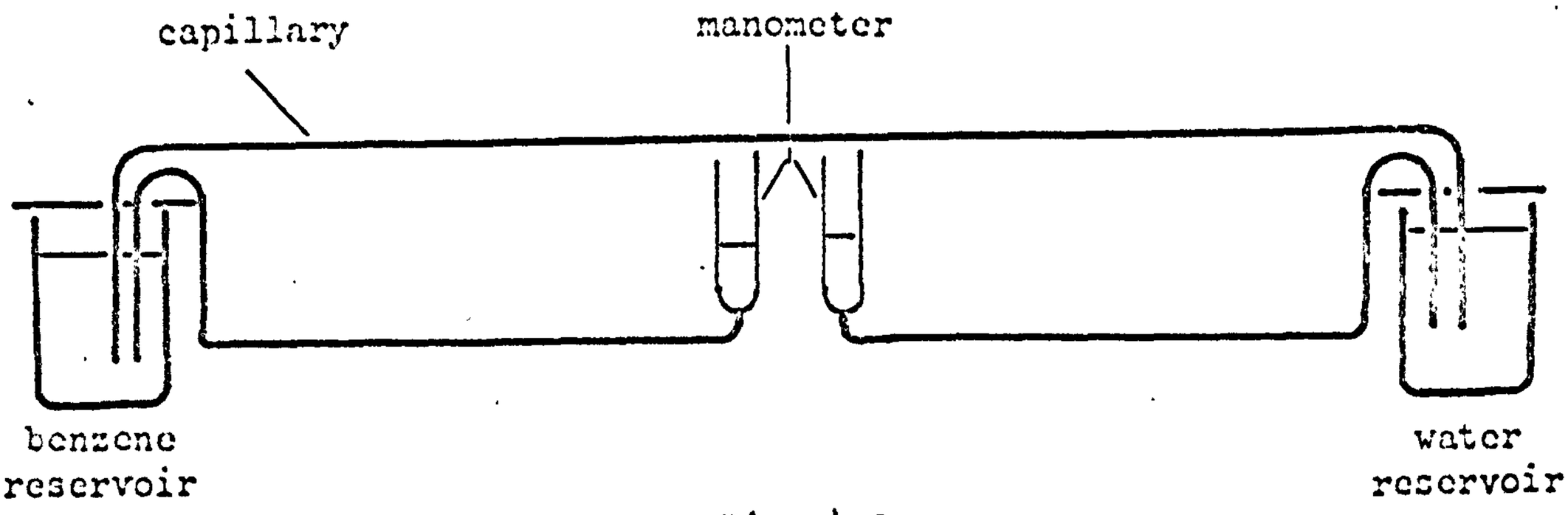

Fig. 4.1

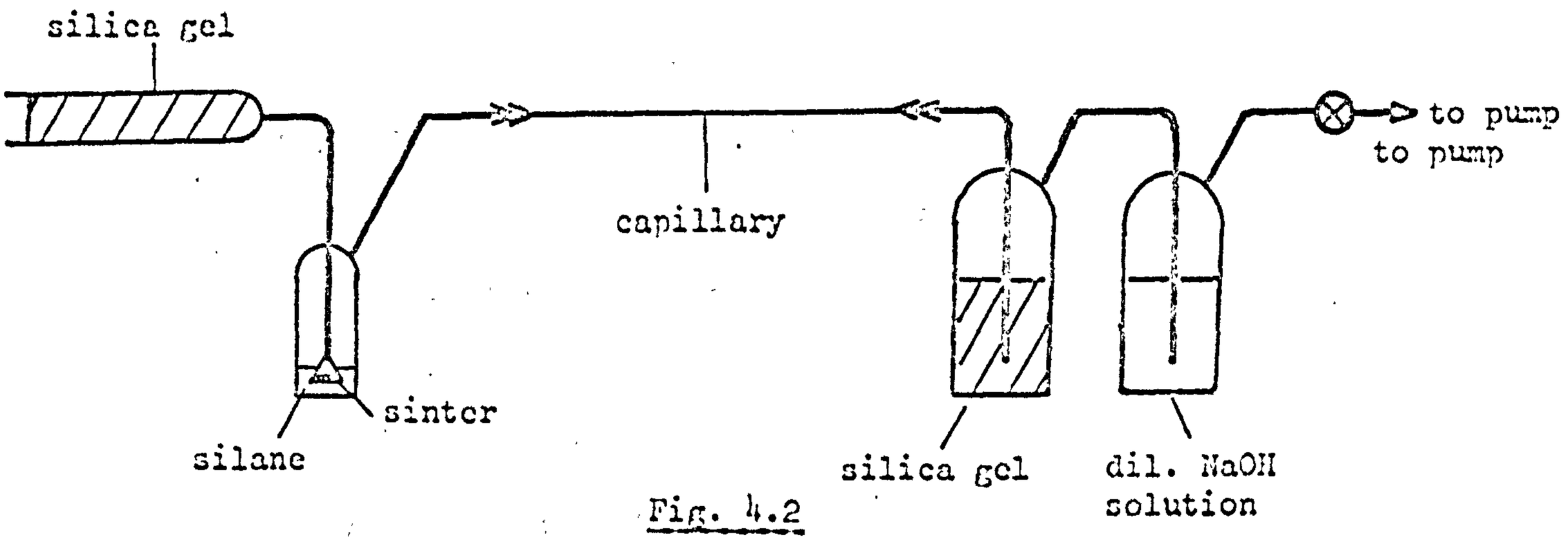

Fig. 4.2

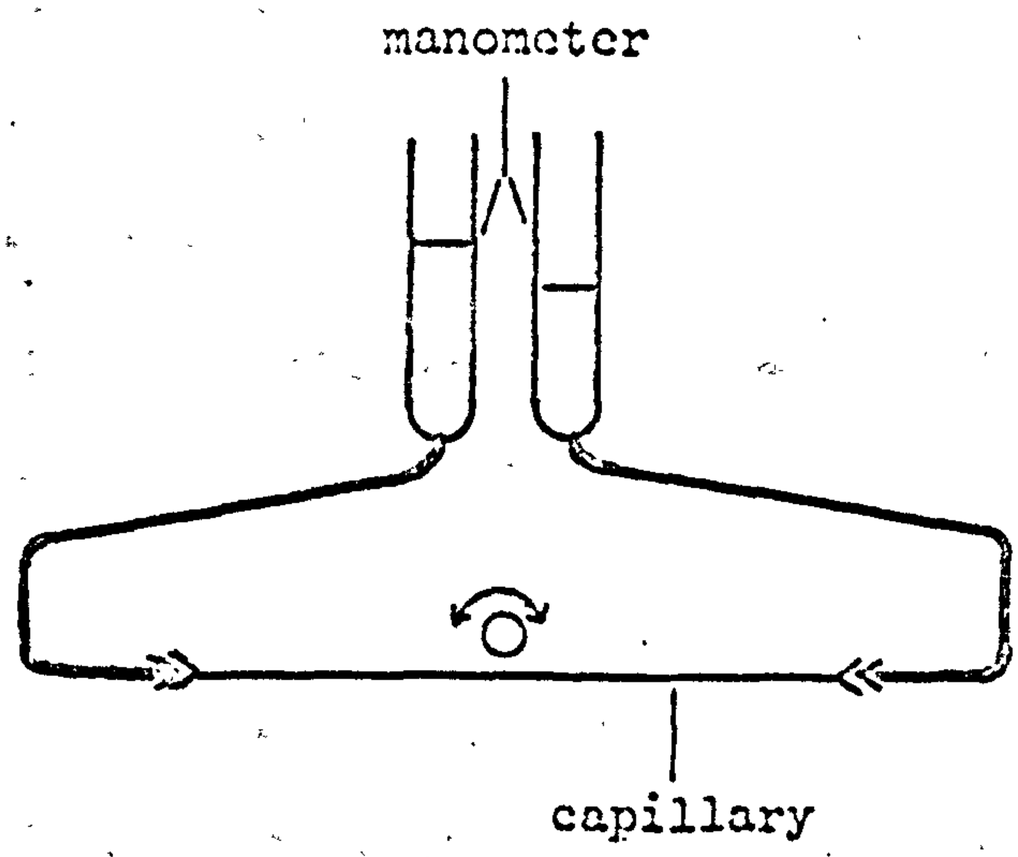

Fig. 4.3

length of nominally 1 mm bore glass capillary was calibrated with mercury and found to have an average diameter of 0.90 mm. Uniformity was checked by measuring the exact length of an approximately 2 cm index of mercury at different positions in the tube. The maximum variation in index length was $\pm$0.06 cm, equivalent to $\pm$1.5% in radius. Short sections at each end of the tube were then bent at right angles. After chemical cleaning, the capillary was set up so that its ends dipped into beakers containing respectively benzene and water. Two 16 mm bore glass tube, mounted vertically near the centre of the capillary, were connected with the contents of the beakers by glass syphons, thus forming a manometer.

A benzene/water interface was formed in the following way. The beaker containing the benzene was removed and a degreased rubber teat was applied to the exposed end of the capillary and manipulated so as to fill the capillary with water. The teat was removed and water was allowed to syphon over for a few minutes. The benzene beaker was then replaced and its height adjusted until a steadily moving benzene/water interface formed just inside the capillary. By raising or lowering the beakers, and thereby adjusting Δp, the interface could be moved in either direction or be held stationary in any part of the tube.

Before measurements were begun, the manometer arms were filled and the capillary was carefully levelled against a

hydrostat; Δp could then be conveniently determined by measuring capillary and manometer heights with a well levelled cathetometer, which could be read to ± 0.002 cm. The densities of benzene and water were obtained from tables[147].

During the displacements, the interface was timed between etch-marks to the nearest 0.2 sec. If interfacial motion became unsteady, the run was abandoned. The velocity at the mid-point of the capillary was found by interpolation. The results of several displacements in each direction are given in Table 4.1.

Exp. P3: Preliminary, Benzene-Water Displacements in Dimethyldichlorosilane-Treated Tubing.

Two B10 sockets were attached to an approximately 28 cm length of 0.4 mm, precision bore (Veridia) tubing. The diameter was found by mercury calibration to be within 1% of the nominal value. After chemical cleaning the capillary was mounted in the apparatus shown in Fig. 4.2. Air drawn in at A was dried over silica-gel, saturated with dimethyldichlorosilane vapour and sucked through the capillary. A second bed of silica-gel removed most of the excess silane and prevented backflow of water vapour from the final washbottle. The latter, containing a dilute solution of sodium hydroxide, removed any remaining silane and also indicated the flow rate. The silane, about 2 cc, was exhausted within 10 min but the flow of air was

continued for a further 2 hrs to remove most of the unreacted silane from the capillary wall.

After treatment, the tube was connected to two 16 mm bore manometer arms as shown in Fig. 4.3, and clamped to a supporting framework which could be tilted about the axis O. Water was added via the right-hand manometer tube. When the meniscus reached the left-hand end of the capillary, benzene was introduced via the left-hand manometer tube so that a benzene/water interface formed just beyond the end of the capillary. Any air bubbles were easily removed by tilting the apparatus about O. During displacements, Δp was set in the same way.

Two marks were made about 2.5 cm apart along a selected portion of the tube. The distance between them, Δx, the total length of the capillary, l, and the distance from the water end to the point mid-way between the marks were measured to within ± 0.01 cm with a horizontal cathetometer. Δp was set and the moving interface (observed through the horizontal cathetometer) was timed between the marks to the nearest 0.1 sec. Δp was determined by measuring the manometer heights above the point mid-way between the two marks to the nearest 0.01 cm with a vertical cathetometer. The average interfacial velocity between the marks $\Delta x/t$, differs very little from the actual velocity at the mid-point, providing the angle of tilt is small and $\Delta x \ll l$.

The results of several displacements in both directions are recorded in Table 4.2.

The Micro-ciné Apparatus

Subsequent experiments were carried out in an improved apparatus which had the following major advantages:-

(i) direct microscopic observation of the contact angle;

(ii) a photographic record of both contact angle and displacement velocity;

(iii) accurate control of temperature.

The cell in which capillaries were mounted during displacements is shown in Plate 1 and in section in Fig. 4.4. The lower half (A) is machined from aluminium and the upper half (B) from Perspex. Jointing surfaces are lapped and polished. Both windows (C) were originally of optically flat glass cemented in place with Araldite; however, owing to repeated failure of the Araldite/Perspex bond, the upper window was replaced with Perspex. Capillaries (D) and a 0-50°C thermometer (E) are held in place with No. 17 rubber bungs (F) which are accurately bored on a lathe after being frozen in liquid nitrogen. Before final assembly bungs and jointing surfaces are lightly smeared with silicone grease. Countersunk socket-headed screws lock the two halves of the cell together, compressing the bungs and forming an air-tight seal. The extended base of the cell carries two adjustable

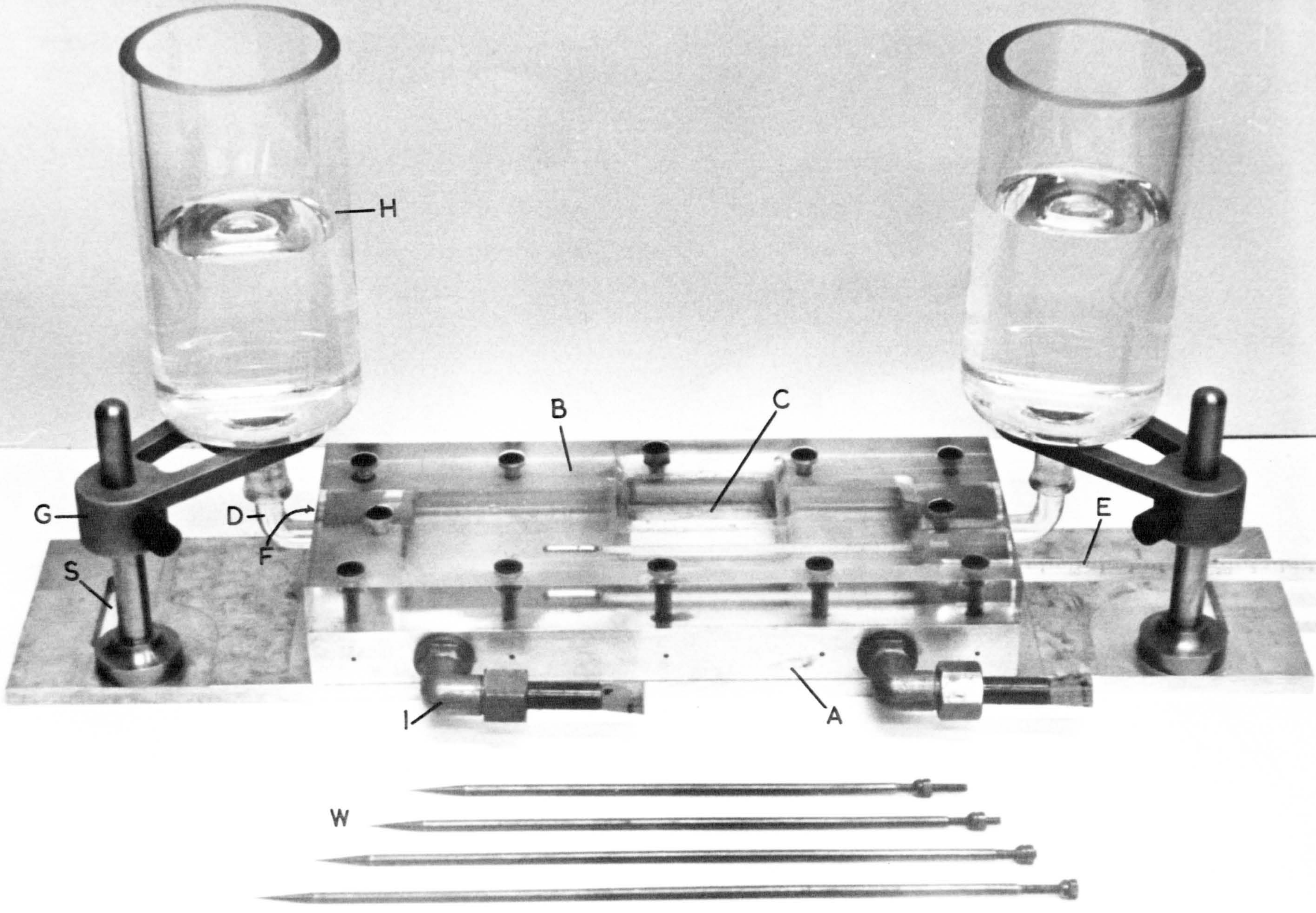

PLATE I

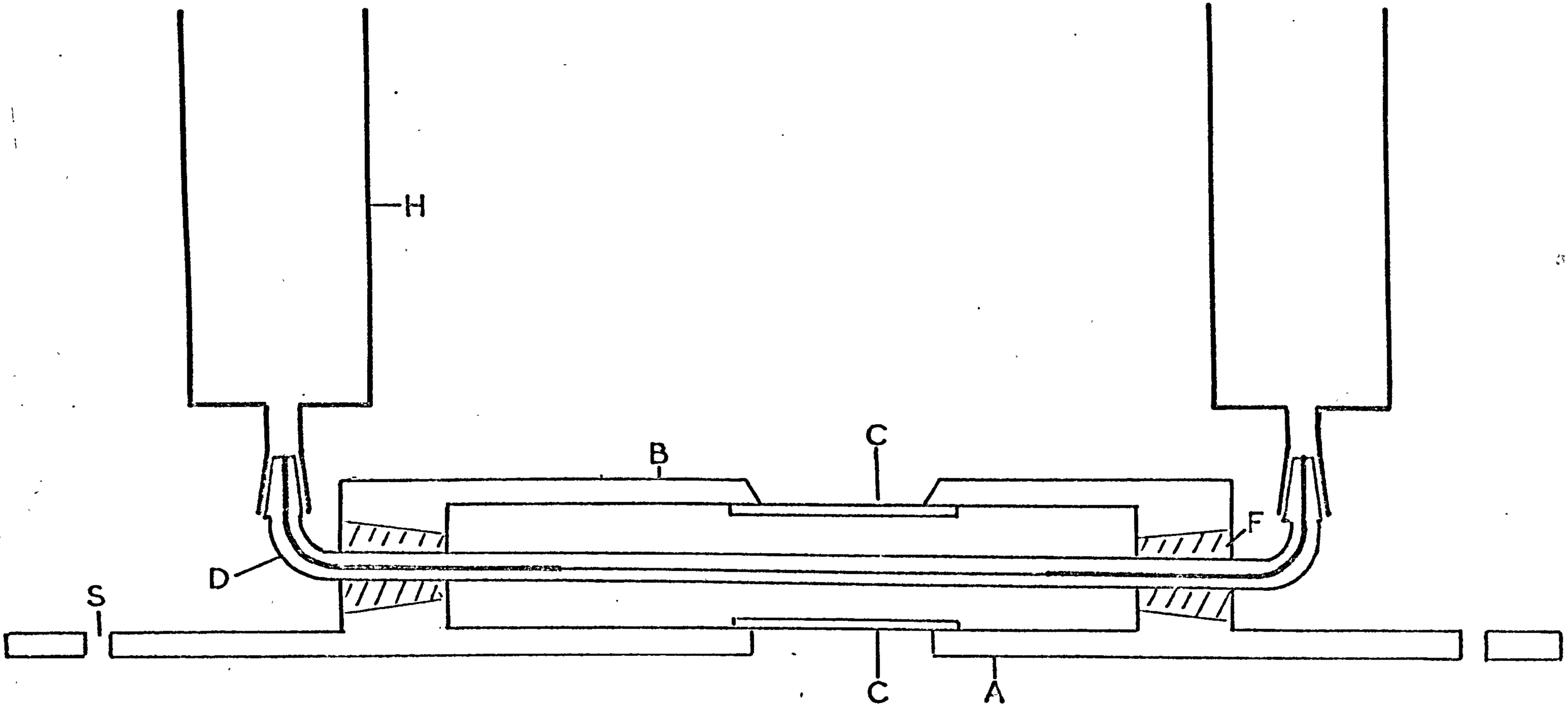

Fig. 4.4

brackets (G) which support the manometer vases (H). The latter are constructed from 15 cm lengths of 5 cm internal diameter Veridia glass tubing and fitted with B10 sockets which form satisfactory, grease-free seals between vases and capillary.

Plate 2 shows the cell mounted on the modified stage of a Vickers "Patholux" microscope. Two $\frac{1}{2}$ in. Simplefix elbow couplings (I) and short lengths of PVC tubing (J) (wrapped in insulating material, not shown) are used to connect the cell in circuit (Fig. 4.5) with a large reservoir of glycerol immersed in an oil thermostat. Glycerol circulation is maintained by a single-action peristaltic pump (K) (WAB - Gallenkamp) on the return line from the cell to the reservoir. Under working conditions, the cell can be held within $\pm 0.1^{\circ}C$ of any temperature between 20 and $45^{\circ}C$ for long periods.

Glycerol was chosen as the thermostat liquid in spite of its high viscosity (c. 1500 cp at $20^{\circ}C$) because:-

(i) within the temperature range 15 to $45^{\circ}C$ its refractive index is within 0.5% of that of Pyrex glass (1.475), and it thus eliminates both the lens effect of the capillary walls and total internal reflection at the outer surface of the capillary;

(ii) the cell materials are unaffected by it.

To prevent changes in the refractive index of the glycerol because of moisture gain by the hygroscopic liquid, the

PLATE 2

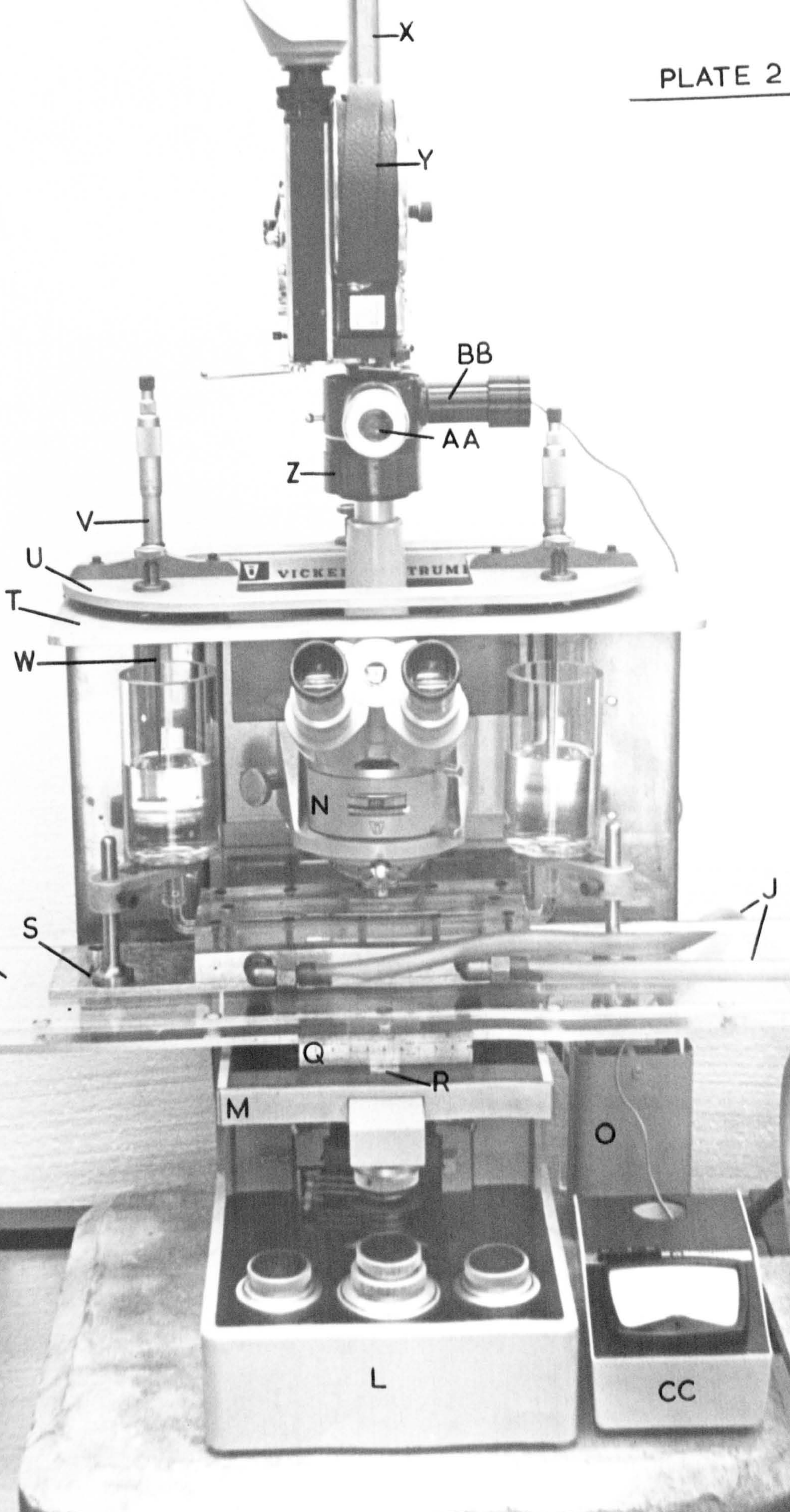

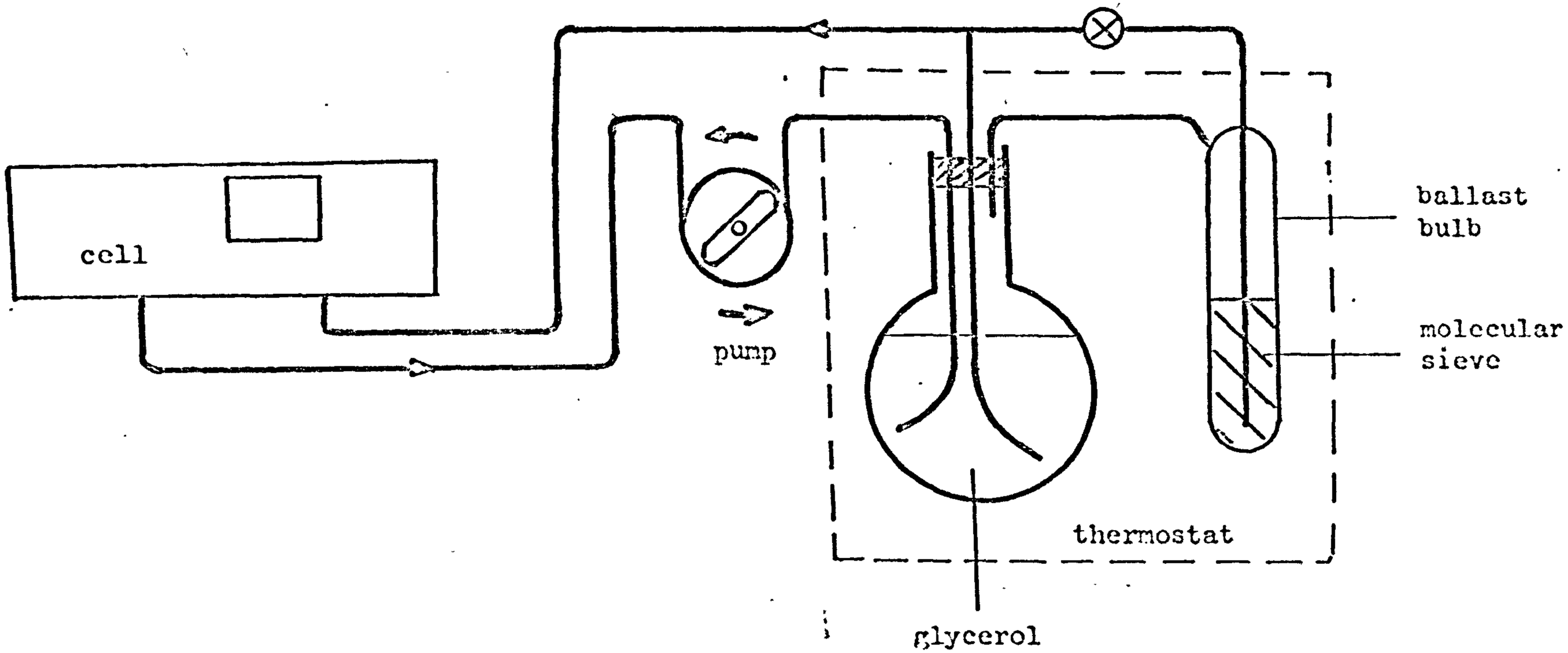
cell
pump
ballast
bulb
molecular
sieve
thermostat
glycerol

Fig. 4.5

circulating system was closed and incorporated a ballast bulb containing a quantity of molecular sieve (BDH, type 4A.XW).

The microscope has a heavy diecast body (L) carrying a substantial stage (M) capable of fore-and-aft and transverse movements. Focusing is achieved by raising or lowering the counterbalanced barrel (N) which carries the lens system (objective, intermediate lens and binocular eyepiece). There is an integral system of Köhler illumination terminating in an adjustable Abbe condenser below the stage. The light source, a 12 v 100 w quartz-iodine lamp, is contained in a ventilated housing at the rear of the microscope. The intensity of illumination is controlled by a rheostat and filters. The 12v supply is provided by a transformer (O). This was originally housed within the body of the microscope, but was later removed to reduce heat transfer to the stage.

A table (P) was added to the microscope stage to carry the cell. It is made of Perspex (for low thermal conductivity) and is supported across the back on inverted V-shaped Teflon slides. These are carried on a length of $\frac{1}{2}$ in. diameter stainless steel rod which is clamped to the microscope stage. The front of the table, braced with a light aluminium beam, is locked to the existing traversing-mechanism, and carries an engraved millimetre scale (Q) perpendicular to the stage vernier (R). The bolts securing the cell to the table pass

through slots (S) in the extended base of the cell allowing it to be freely aligned under the microscope.

An aluminium platform (T) cantilevered forward from the top of the main body of the microscope carries a levelling table (U) to which are attached two micrometer depth-gauges (V). These are positioned immediately above the manometer vases and are equipped with a set of stainless steel needles (W, Plate 1) of various lengths and covering overlapping depth ranges. Manometer heights are determined by lowering the needles until they just touch the surface of the liquid.

A stout pillar (X) emerges from the top of the microscope body and supports the camera (Y) and camera adaptor (Z). The adaptor contains a subsidiary eyepiece and a beam-splitting prism which directs light either to the camera focusing eyepiece (AA) or to the photoelectric cell (BB) of the photometer (CC).

The 16 mm cine camera (Bolex H16) has clockwork and electric drives, providing framing speeds between 12 and 64 f.p.s. and single shots. It is used either with a Switar 75 mm telephoto lens or with no lens and a short extension tube (as shown).

Exp. A1: Benzene-Water Displacements in Dimethyldichlorosilane-Treated Tubing.

The capillary used in this study was constructed from two, extended, 2 mm capillary cones (B10) and a length of

0.50 mm precision bore tubing (Veridia). A reference mark was etched near the middle of the Veridia section, and the position of this mark and the lengths of the 2mm and Veridia sections of the capillary were measured to the nearest 0.01 cm. Right-angled bends were made close to the base of each cone. Fig. 4.4 (above) shows a capillary of similar construction. After annealing, the completed capillary was flushed with conductivity water and connected to the grease-free apparatus shown diagrammatically in Fig. 4.6.

With cut-offs 1,2 and 3 raised, dimethyldichlorosilane was outgassed and subjected to trap-to-trap distillation under vacuum until a few cc of purified product remained in bulb C (bulbs A and B, containing the less pure fractions, having been successively removed at the constrictions). With cut-offs 3 and 4 raised, the remainder of the system was flamed out and evacuated to 10^{-5} torr.

The capillary was cleansed of organic impurities by flaming in a stream of oxygen generated by heating potassium permanganate (cut-offs 1, 3 and 4 raised). A sintered glass disc (Joblings No. 4) prevented solid decomposition products from reaching the capillary. As the oxygen was pumped away via the capillary, the latter was carefully heated, using a gas/air flame, so that most of the tubing was maintained at a temperature high enough to give a slight sodium coloration to the flame.

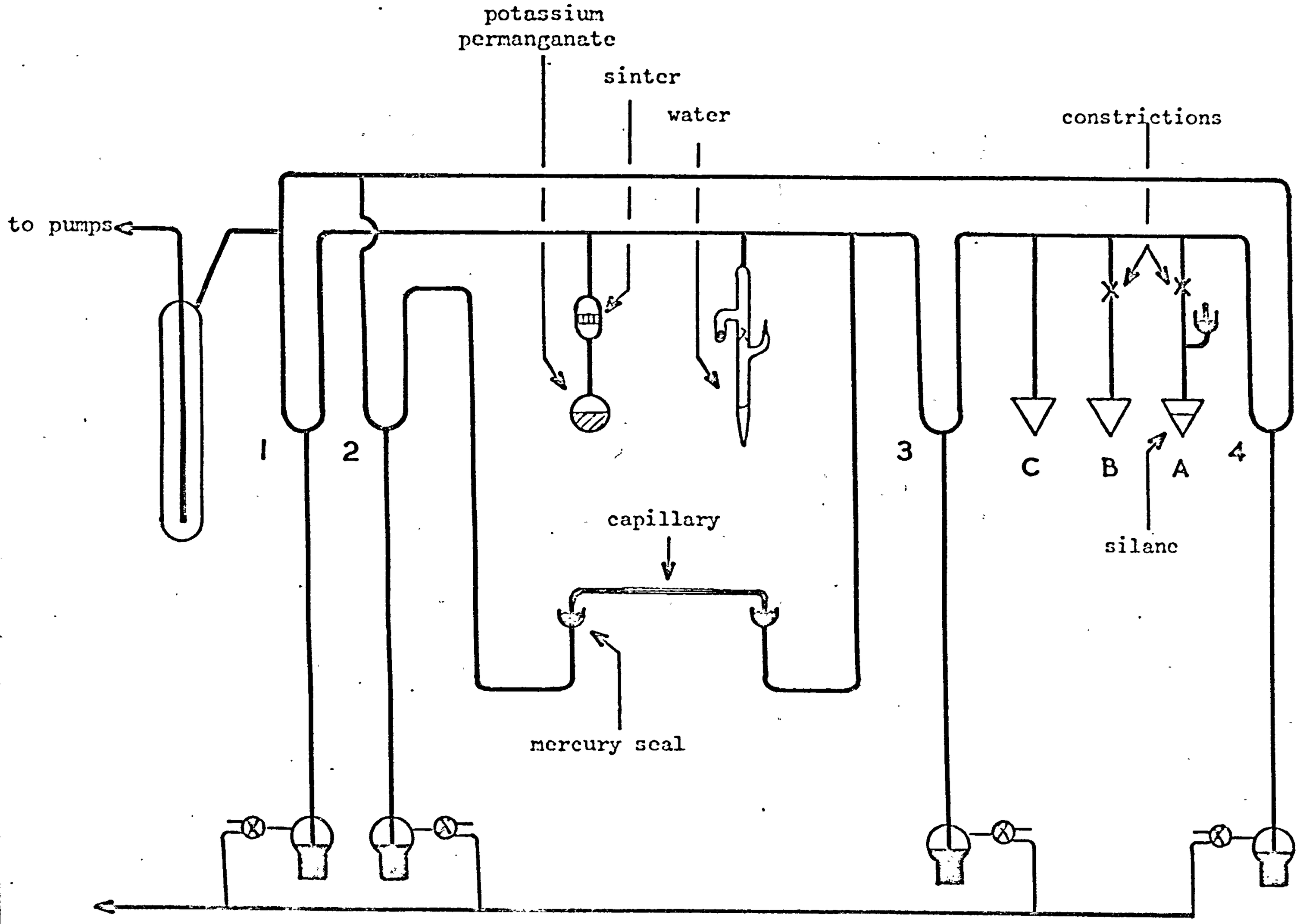
potassium
permanganate
sinter
water
constrictions
to pumps
1
2
3
4
C
B
A
silane
capillary
mercury seal

Fig. 4.6

Heating was stopped after 15 min. and the internal seal on the water reservoir was broken, allowing the few cc of water contained therein to evaporate away slowly via the capillary. This was done in order to rehydroxylate the glass surface prior to silane treatment, and took approximately 24 hrs. Cut-off 3 was then lowered and a stream of silane vapour was drawn through the capillary until bulb C had emptied. Finally, all cut-offs were lowered and the system was evacuated to 10^{-5} torr over a period of 48 hours.

Displacement studies were performed in a constant temperature room held at 20.5 $\pm$0.2°C. Because of this, although the cell was filled with glycerol to eliminate undesirable optical effects, it was not necessary to connect the circulating system and thermostat. To minimise vibration, the micro-ciné apparatus was placed on a massive brick pillar.

A dummy capillary, with both manometer vases filled with water, was used to check the levelling of a cathetometer, and this, in turn, was used to check the alignment of the cell and levelling table. Depth-gauge needles were calibrated against the cathetometer and cross-checked against each other.

All glassware used in the experiment was cleaned in the annealing oven as described. Depth gauge needles were thoroughly degreased in an acetone vapour bath.

The freshly treated capillary was removed from the vacuum system and rapidly transferred to the displacement cell. A benzene/water interface was formed by first partly filling one manometer vase with water, then, when the capillary had completely filled, the other vase was filled with benzene. Adjustments to the manometer heights, and hence to Δp, were made using glass pipettes. Changes in Δp were readily determined to within ± 1 dyne cm^{-2} with the depth gauges, and one absolute value was measured using the cathetometer. Owing to an uncertainty in the exact height of the capillary (± 0.025 cm), absolute values of Δp were only reliable to ± 10 dyne cm^{-2}. Liquid densities were obtained from tables.

The moving interface was usually photographed at 16 f.p.s. The camera was operated for timed intervals of not less than 3 sec. Stationary or very slowly moving interfaces were photographed using single shots at timed intervals of up to 15 minutes. Reported displacements were carried out at three positions in the Veridia section of the tube. These positions were determined relative to the etch mark to within ± 0.005 cm using the microscope stage scale and vernier. The diameter of the capillary was measured directly, to the nearest 5 μ, using a calibrated graticule in the microscope eyepiece.

After displacements had been completed the capillary

and vases were emptied, dried and refilled, but this time with water only. Measurements were then made of the rate of flow through the capillary under a known hydrostatic pressure. In this way it was possible to determine the effective length of the capillary, i.e. that length of the Veridia tubing which would have the same resistance to flow as the whole capillary assembly.

Velocities and contact angles were obtained from the film of the displacements. The processed film was back-projected onto a horizontal drafting table using a Specto 16 mm "Motion Analysis Projector (Mk. 2)" and a series of mirrors (Fig. 4.7). Measurements were facilitated by covering the table with translucent, millimetre-ruled graph paper which was calibrated against the projected image of the capillary tube. In this way the resolution obtained was between 4 and 5μ , or approximately 1% of the tube radius.

Interfacial velocities ($\dot{x}$) were deduced from the distance moved (between 100 and 500μ) in a known time. The latter was calculated from the ratio of the number of frames in which the interface travelled the measured distance to the number of frames shot in the measured time. The constancy of the camera's framing-speed was checked independently by filming a stopwatch. With the clockwork drive, speeds were found to vary by less than 3% during the first 400 frames after rewinding. The estimated uncertainty upon reported values

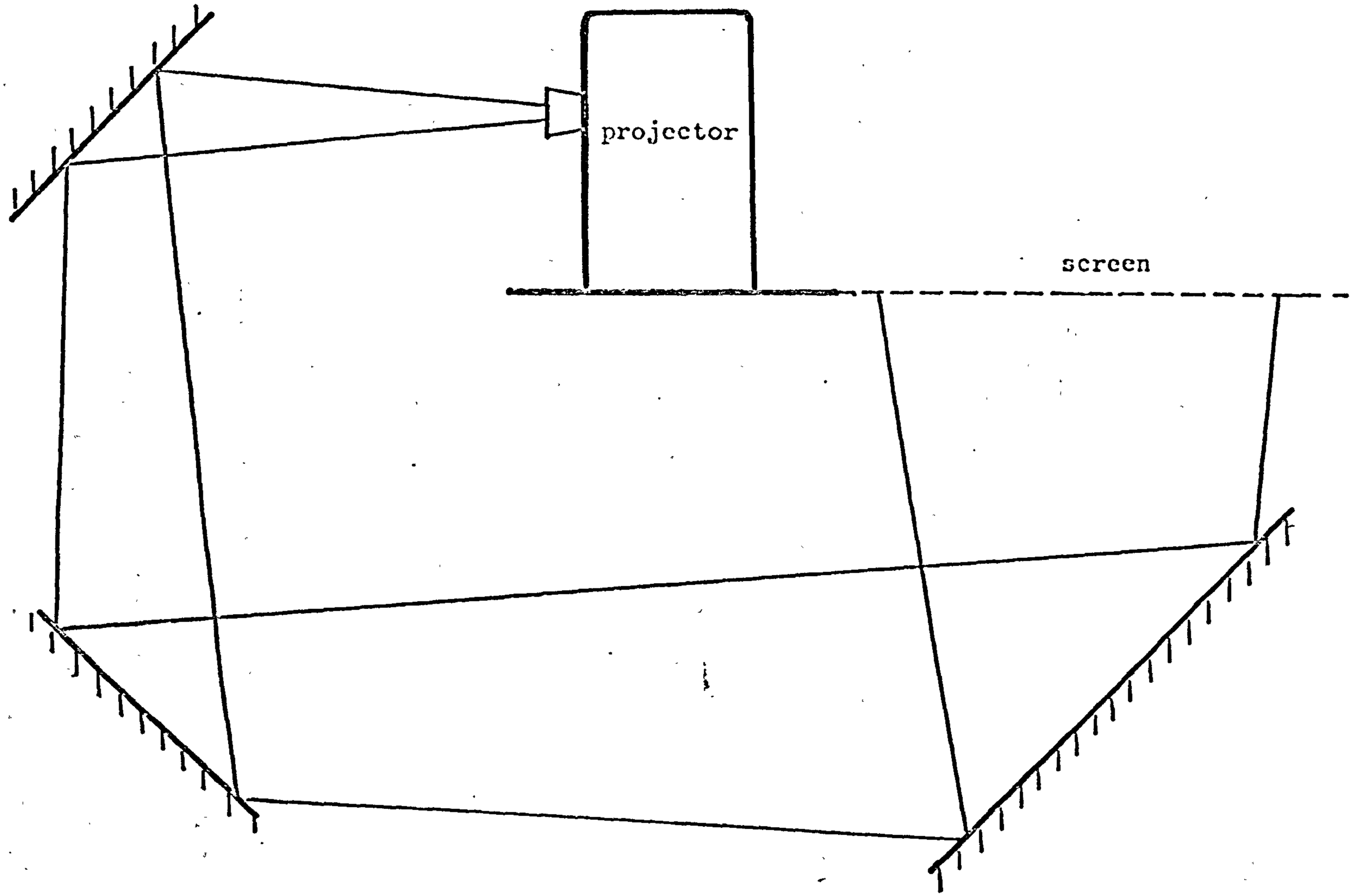

Fig. 4.7

of $\dot{x}$ was $\pm 5\%$ for speeds in excess of 1000μ sec^{-1}, falling to $\pm 3\%$ at 100μ sec^{-1} and increasing again to about $\pm 8\%$ below 10μ sec^{-1}.

Contact angles (ϕ) were calculated from the meniscus height, h, and the tube radius, r. Assuming a spherical interface,

$$\cos \phi = \frac{2rh}{r^2 + h^2} \qquad 4.2\text{-}1$$

Where practicable, interfaces were checked for sphericity by curve matching. The recorded values of ϕ are averages of at least five measurements in each case. The uncertainty is about $\pm 3^\circ$ at 90° falling to $\pm 2^\circ$ below 80° and above 100°.

Contact angles (ϕ_{cal}) were also calculated from the values of $\dot{x}$ and Δp using Eq. 3.3-2. The benzene/water interfacial tension was taken to be 35 dyne cm^{-1}, and viscosities were obtained from tables[147].

All results are set out in Table 4.3.

Exp. E1: Benzene-Water Displacements in Trimethylchloro-silane-Treated Tubing.

The following "annealing" process was found to be effective in eliminating longitudinal scratches found on the inner surface of Veridia tubing. A 10 cm length of nominally 0.65 mm Veridia capillary was attached to two lengths of stock tubing of similar bore, and mounted on a lathe. The capillary was rotated at c. 50 r.p.m. and heated with an electric furnace until it could be seen to sag

slowly if the rotation was momentarily stopped. It was held at that temperature (c. 700°C) for a few minutes before being slowly cooled. An 8 cm portion of the annealed Veridia tubing was then connected to two, extended, 2 mm capillary cones (B10) which were bent at right angles as in Exp. A1.

After a further annealing at 560°C, the completed capillary was mounted in the simplified silane-coating apparatus depicted in Fig. 4.8. This apparatus was also used in Exps. E2 and CX. The limb carrying the trimethyl-chlorosilane, water and potassium permanganate samples was prepared afresh for each treatment. The remainder of the apparatus was cleaned in the annealing oven immediately before each run.

The system was evacuated to c. 5×10^{-6} torr. The magnetic valve was then closed and a low pressure of oxygen was generated by heating the potassium permanganate. The temperature of the capillary was raised to 510°C using the electric furnace, and maintained at that temperature for 1 hr, after which the magnetic valve was opened and the temperature reduced to 100°C. This cleaning procedure was exactly reproducible, unlike the rather arbitrary flaming technique used previously (Exp. A1).

After the oxygen had been pumped away, the valve was closed and the internal seal on the water reservoir broken. The capillary was exposed to water vapour at 100°C

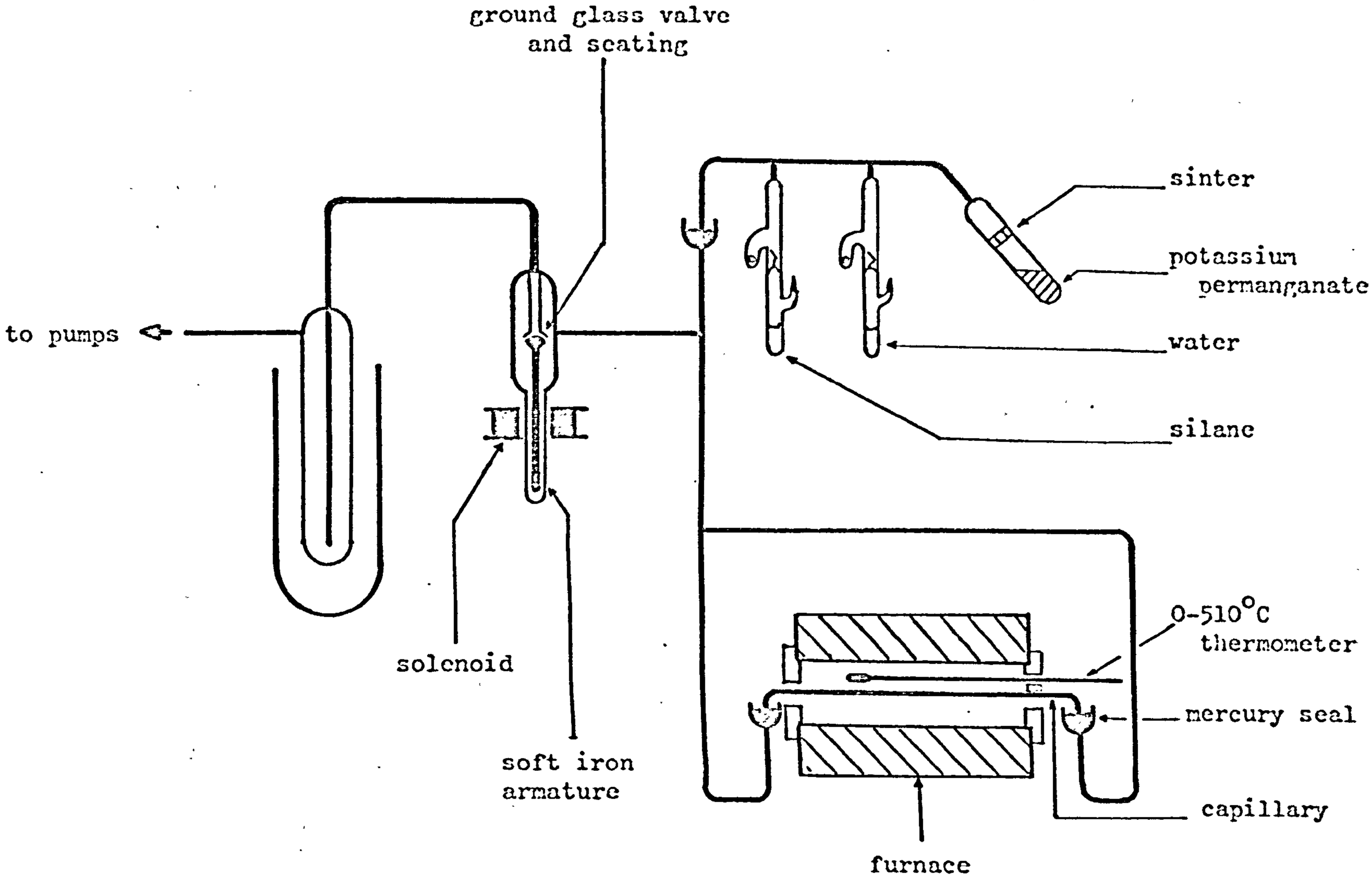
ground glass valve
and seating
to pumps
sinter
potassium
permanganate
water
silane
solenoid
soft iron
armature
0-510°C
thermometer
mercury seal
capillary
furnace

Fig. 4.8

for 2 hrs and then at room temperature for a further 15 hrs before being evacuated once more. Finally, the valve was closed for a third time and the seal broken on the silane bulb. Silane treatment was carried out for 6 hrs at room temperature. The capillary was then pumped for 48 hrs before being opened to the atmosphere and incorporated in the displacement cell.

Benzene-water displacements were performed in a manner similar to that of Exp. A1; however, no direct measurements were made of the hydrostatic pressure across the capillary, and liquid levels were adjusted using 100 ml all-glass syringes (Excelo). This procedure allowed a far more rapid adjustment of Δp.

The experiment was carried out using the glycerol circulation system and thermostat to control the cell temperature. The capillary was first filled with benzene which was then displaced by water at various speeds along successive lengths of the Veridia section of the tube until approximately half the total length of the visible portion had been traversed (c. 2 cm). One hour later, the displacements were continued in the same direction at various speeds over the remaining half. Subsequent displacements in both directions were performed during the next 4 hrs, and a further series of displacements was carried out after a period of three weeks during which the capillary remained filled with water (satur-

ated with benzene).

The exact framing speed used when filming displacements (nominally 18 f.p.s.) was determined by filming a stopwatch.

Interfacial velocities and associated contact angles were determined from the processed film using the apparatus described for Exp. A1. Velocities were calculated from the distance moved by the interface during a specified number of frames (the exact number used was dependent upon interfacial speed, but was usually between 10 and 50). Very slow speeds ($< 5\mu$ sec^{-1}) were determined from single frames taken at timed intervals. Contact angles were measured as in Exp. A1. Estimated errors on $\dot{x}$ are the same as for Exp. A1. However, the probable error on ϕ was reduced to $\pm 2^{\circ}$. For a single displacement carried out at 0.7 cm sec^{-1}, the estimated uncertainty upon $\dot{x}$ and ϕ rose to $\pm 7\%$ and $\pm 4^{\circ}$ respectively. The results obtained in this experiment are listed in Table 4.4.

Exp. E2: Benzene-Water Displacements in a Second Trimethylchlorosilane-Treated Tube.

A capillary tube of 0.70 mm bore was prepared in exactly the same way as the tube used in Exp. E1. Displacement experiments were performed largely as before. On this occasion, however, the tube was first filled with water, and displacements were carried out during an initial period of 4 hrs, and then again after a further 20 hrs. Results

are given in Table 4.5.

Exp. F2: Benzene-Glycerol Displacements

Benzene-glycerol displacements were made in the tube used in Exp. E1. Between the two experiments, however, the tube was evacuated to 10^{-5} torr for 24 hrs in order to remove as much adsorbed water as possible. Results are recorded in Table 4.6.

Exp. CX: Cyclohexane-aniline Displacements

Cyclohexane-aniline displacements were studied, at temperatures close to the consolute point, in 0.5 mm bore stock capillary treated with trimethylchlorosilane as described above (Exp. E1). Results are described in the next section.

4.3 Discussion of Results.

Throughout this section, contact angles referred to in connection with a benzene/water interface are measured through the water. With other systems, contact angles will be specified as necessary. The use of the terms "advancing and receding angles", ϕ_a and ϕ_r respectively, will be in accord with the convention adopted in section 3.2.

Exps. P2 and P3

The results of these preliminary experiments have already been discussed in detail elsewhere[140], but they are, nevertheless, included here for completeness.

Eq. 3.3-2 predicts that the interfacial velocity $\dot{x}$, measured at a given point along a cylindrical capillary of radius r, should be a linear function of the applied hydrostatic pressure Δp, with a zero velocity intercept of $\frac{2\sigma_{12}}{r} \cos \phi$, and a slope which should be calculable from the viscosities of the fluids 1 and 2 and the position of the interface.

The results obtained with the uncoated tube (Fig. 4.9) show a linear dependence of $\dot{x}$ upon Δp. The gradient (5.5×10^3 dyne sec cm^{-3}) is in good agreement with the calculated value (5.35×10^3 dyne sec cm^{-3}); the intercept, however, is dependent upon the sign of $\dot{x}$. If energy losses due to circulatory flow are negligible, this indicates firstly that the contact angle is independent of displacement rate in the range studied, and secondly that, if this independence extends down to $\dot{x} = 0$, there is a large contact angle hysteresis. From the measured intercepts at $\dot{x} = 0$, and with $\sigma_{12} = 35.0$ dyne cm^{-1}, it is found that ϕ is 43° for water displacing benzene (W → B), but 96° for benzene displacing water (B → W). Thus, the interfacial curvature actually changes sign as the direction of displacement is reversed - a conclusion which was confirmed by direct observation.

Because of irregular movement of the interface, velocities below about 0.03 cm sec^{-1} could not be maintained

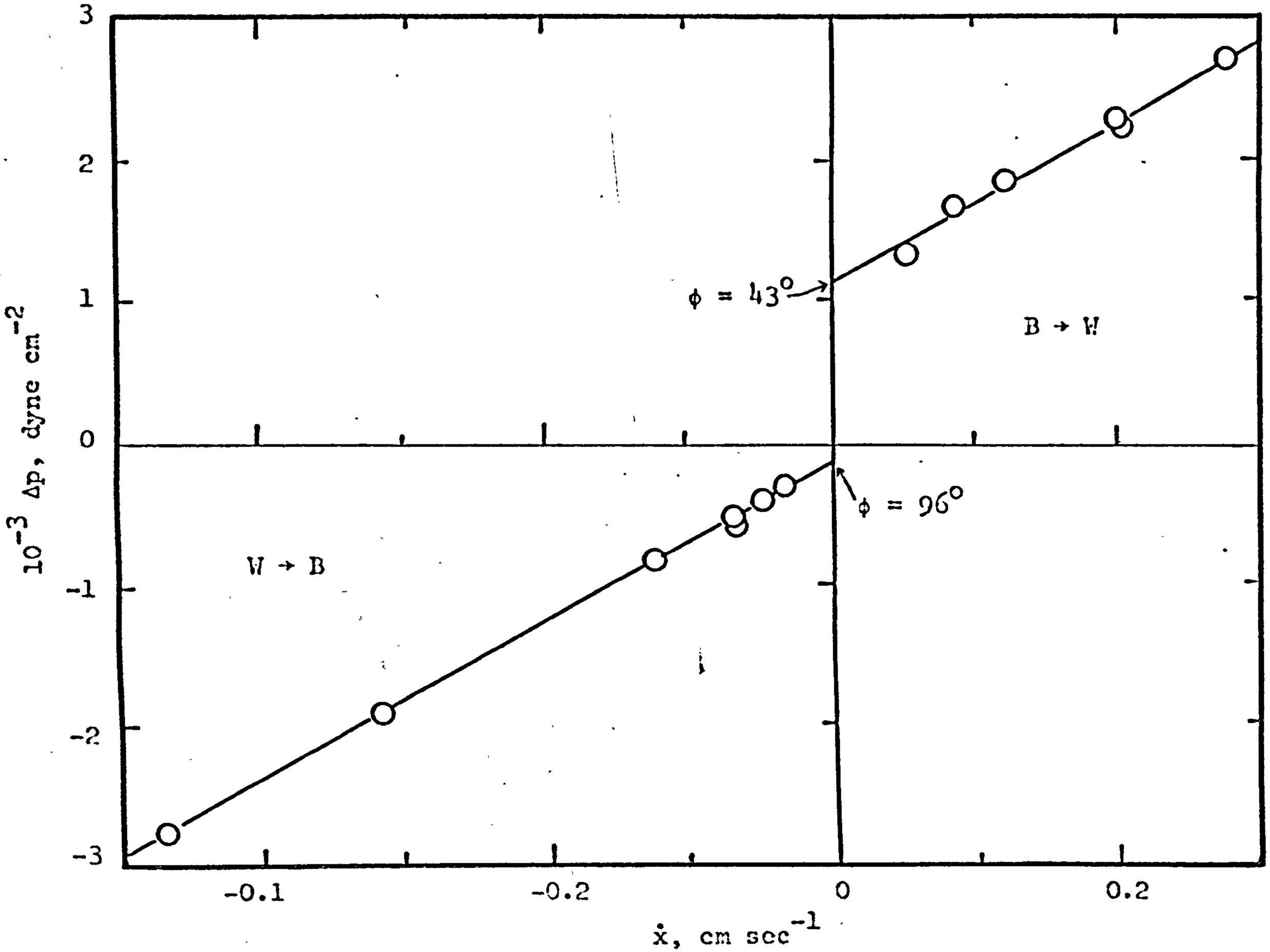

Fig. 4.9

in these experiments over sufficiently long periods for reliable measurements to be made. This was attributed to microscopic variations in the surface properties of the tube, probably arising from haphazard contamination. Indeed, the high-energy "clean" glass surface would not be expected to survive for long without far more elaborate precautions than those taken here. At this stage, therefore, experiments were begun in silane-treated tubes, whose surfaces were thought to be relatively inert.

Fig. 4.10 shows that in the dimethyldichlorosilane treated capillary, stable velocities of a few μ per second could be maintained. Again there are two regions where Eq. 3.3-2 is obeyed, although with generally increased contact angles (161° with W → B and 99° with B → W). However, ϕ_r is velocity dependent at rates below 1.5×10^{-2} cm sec^{-1}, and appears to have risen to at least 121° before motion ceases. On the other hand, ϕ_a would seem to show no velocity dependence down to 4×10^{-4} cm sec^{-1}, the lowest velocity studied.

Contact Angles: Calculated v. Measured.

In Exp. A1, despite the introduction of a more sophisticated silane treatment, steady interfacial velocities below 4μ sec^{-1} were still unobtainable. At the other extreme, the maximum velocity studied was 0.11 cm sec^{-1}.

The ciné technique enabled studies of all the

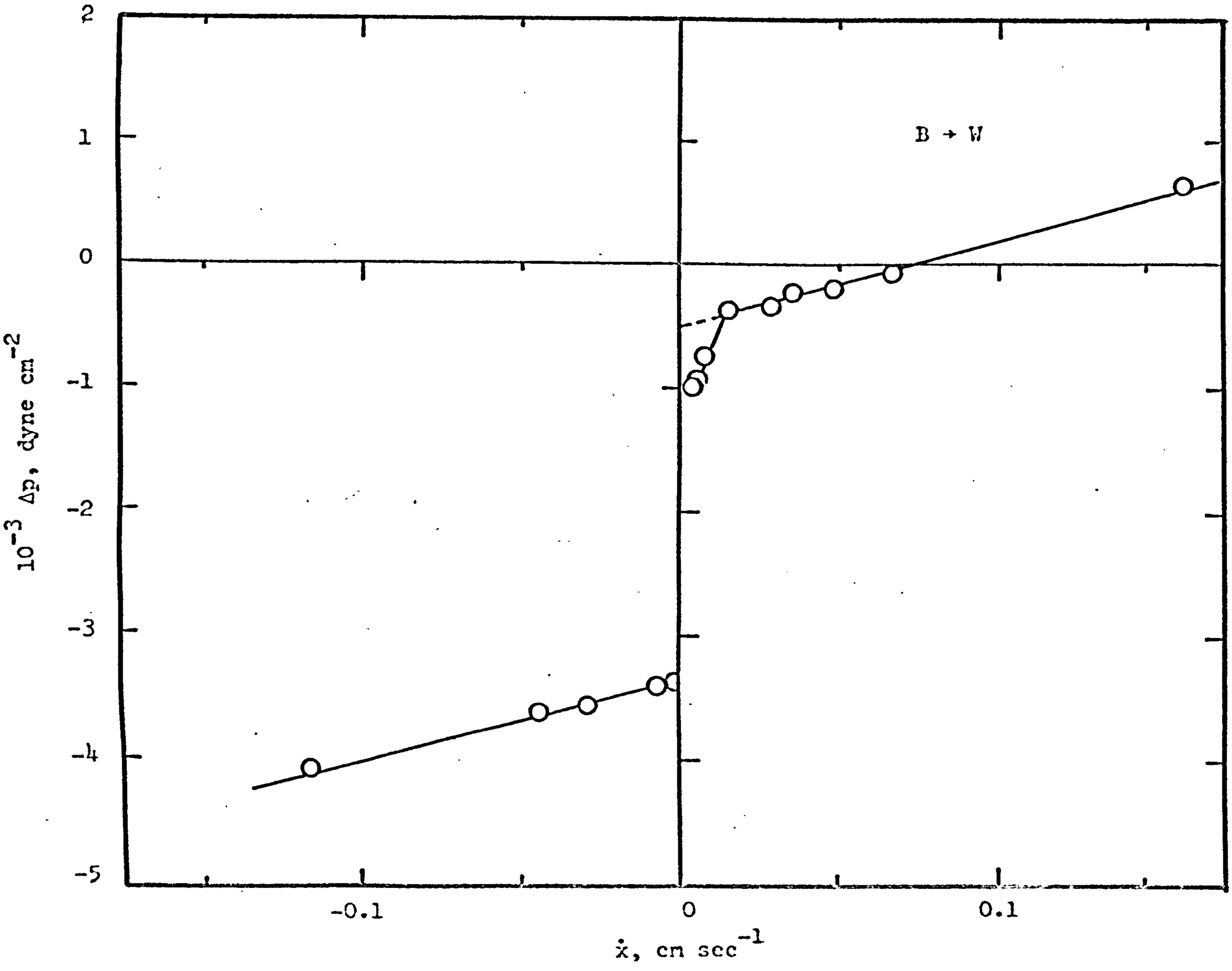

Fig. 4.10

observable parameters, $\dot{x}$, Δp and ϕ, to be made in the same experiment, thus permitting, for the first time, a direct comparison between the observed contact angle and that calculated according to Eq. 3.3-2.*

Fig. 4.11 shows that there is, in fact, good agreement between the angles from the two sources. The deviations that do exist are attributable to experimental error. The tendency for points for stationary interfaces to fall below the line representing total congruence suggests a small, systematic error amounting to about 1 or 2°. Alternatively, this result may indicate the presence of surface active impurities at the benzene/water interface causing a lowering of the benzene/water interfacial tension to about 33 dyne cm^{-1} (normal value: 35 dyne cm^{-1} at $25^{\circ}C$).

During displacements, no departures of interface shape from sphericity were detected. Since the expression $\frac{n\dot{x}}{\sigma_{12}}|\sec\phi|$ never exceeded 10^{-3} this is as expected.**

The results reported above, together with those obtained by Rose and Heins[119], confirm that for sufficiently small, non-zero interfacial velocities, energy losses due to circulatory flow are negligible, and the interface is

---

* The earlier work by Rose and Heins[119] was with liquid indices and not with a single, moving interface.

** See Section 3.2 pp. 79-80.

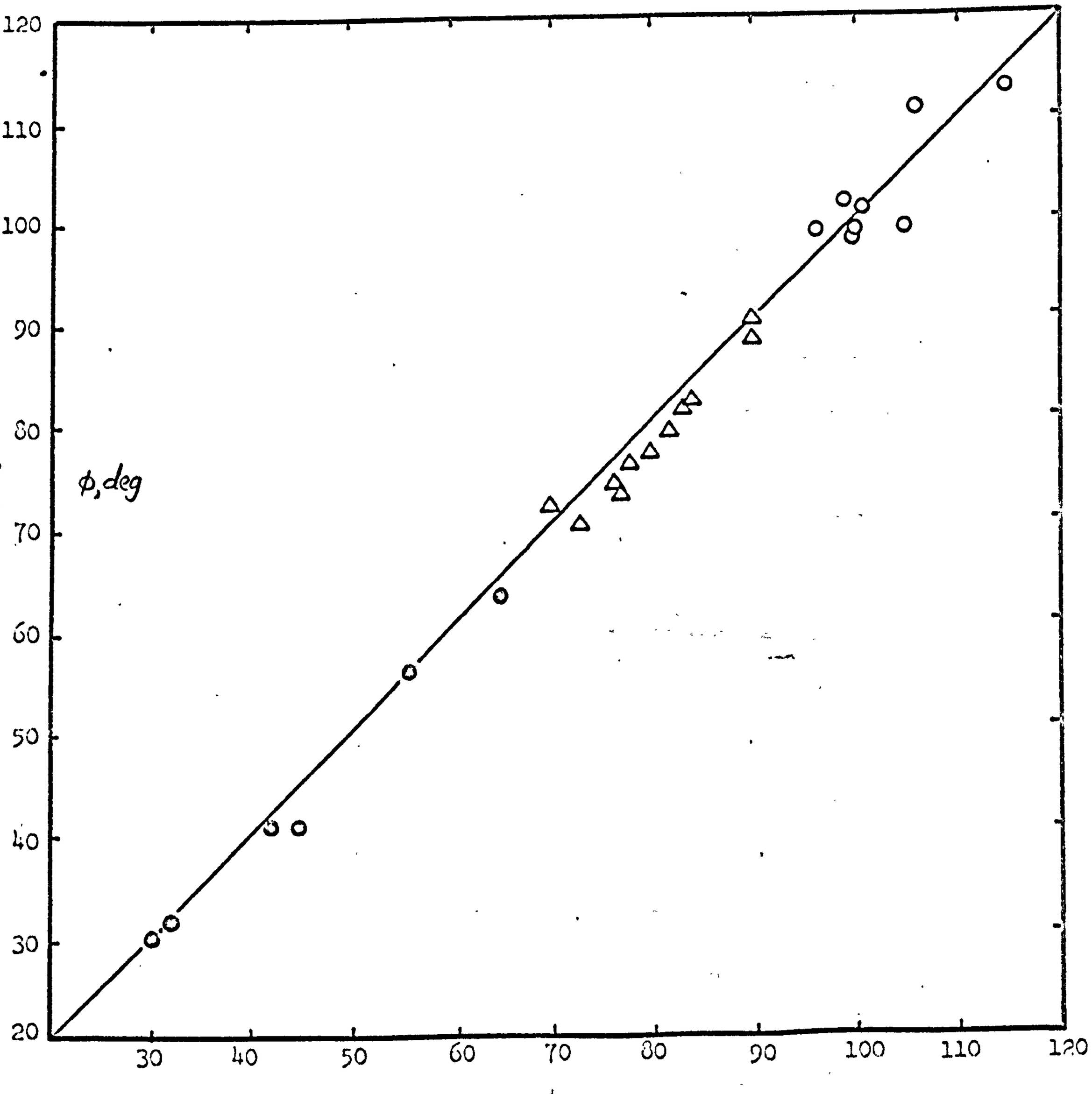

Fig. 4.11 ○ W → B; △ stationary interface; ● B → W

governed by the same two conditions that govern the equilibrium state of the interface. Thus the pressure drop across the moving interface is given by

$$\Delta p = \frac{2\sigma_{12} \cos \phi}{r} \qquad 4.3\text{-}1$$

Veridia Tubing: Longitudinal Roughness.

An unexpected problem was encountered in the use of Veridia precision bore tubing. All the small diameter (<1 mm) samples examined were found to be badly scored in a longitudinal direction. This is apparently the result of the manufacturing process. Plate 3 shows every sixth frame from film of a high-speed displacement taken at 64 f.p.s. The rearrangement of benzene left behind in the grooves in the wake of a receding benzene interface can clearly be seen. Regular longitudinal roughness of this type may have been responsible for the anomalously thick films found by Bretherton[103] in his concentric flow experiments which were also performed in Veridia tubing. Certainly, extra difficulties are added to the measurement of contact angles, since those greater than 90° will be apparently increased, and those less than 90° apparently decreased by "fingering" along the grooves[81]. This effect will not show up in Fig. 4.11, however, because both the calculated and the observed angles are, in this case, derived from the mean curvature of the whole interface.

In subsequent experiments, Veridia tubing was subjected

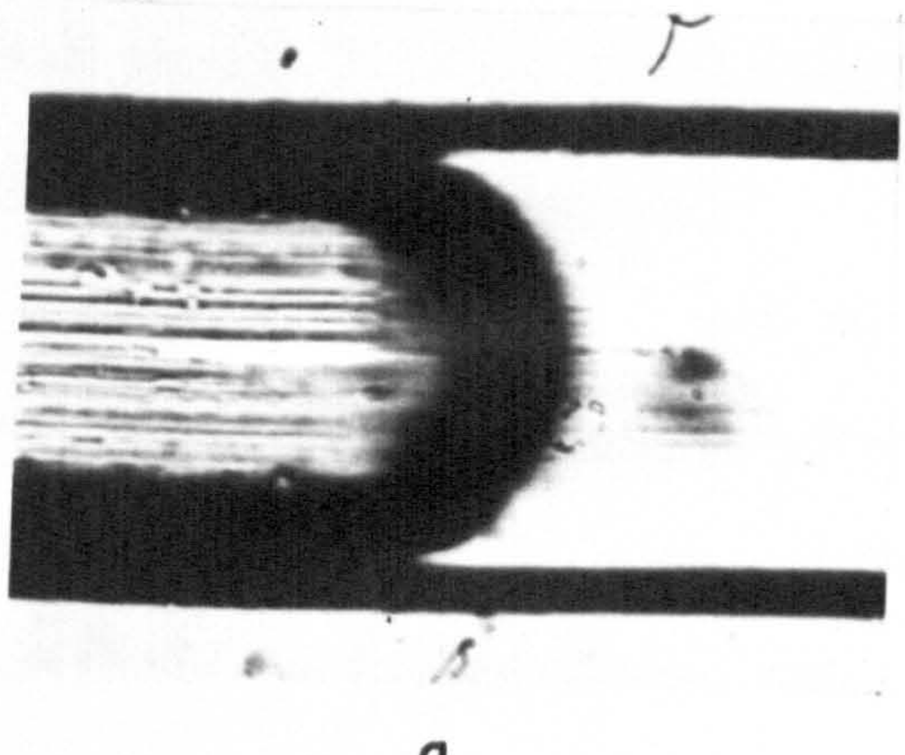

a

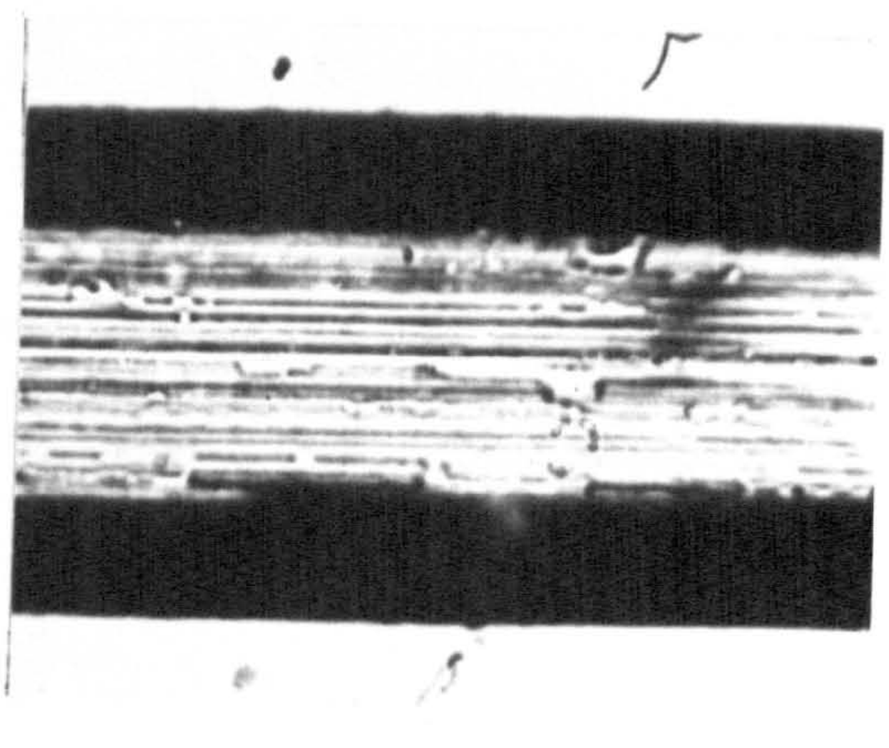

b

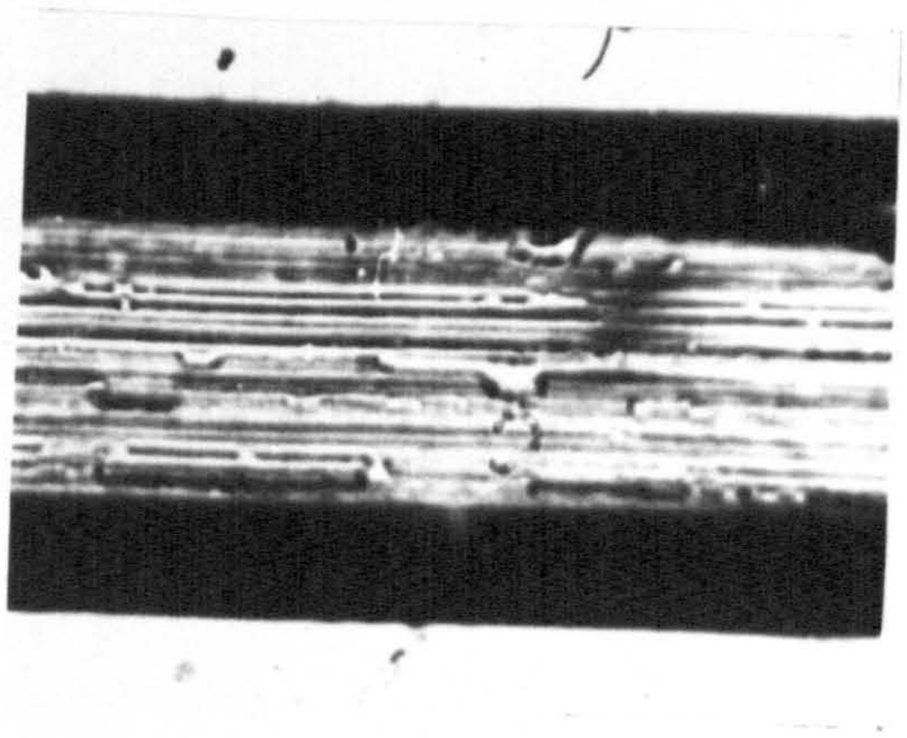

c

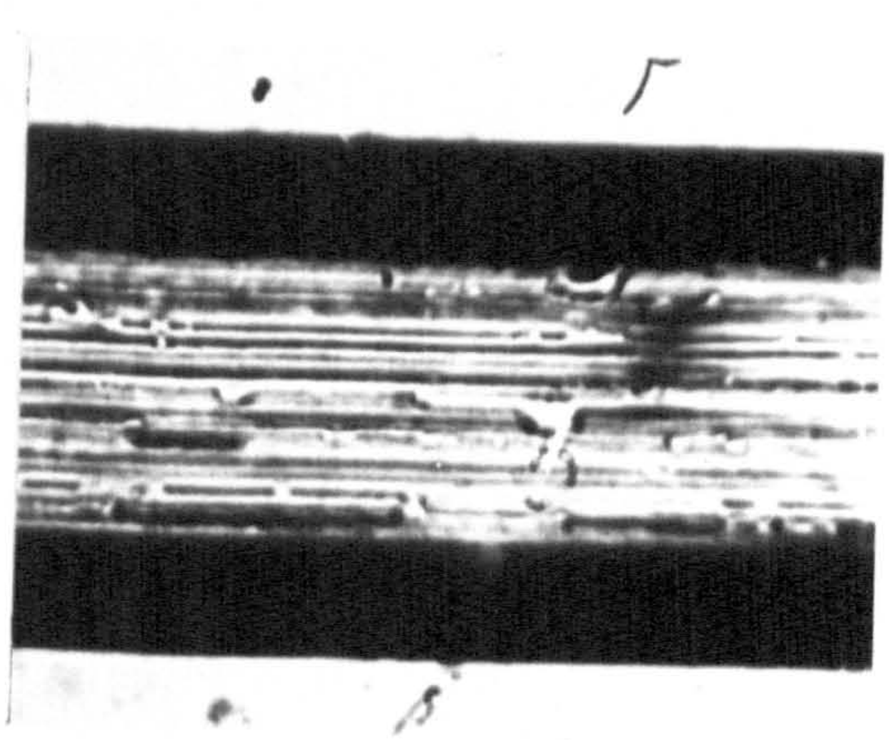

d

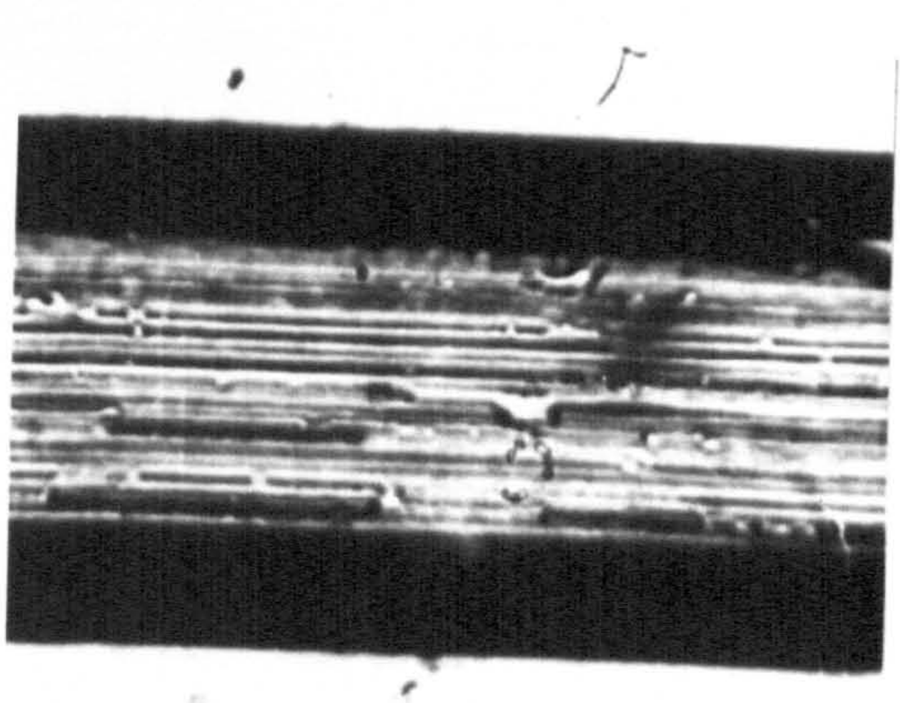

e

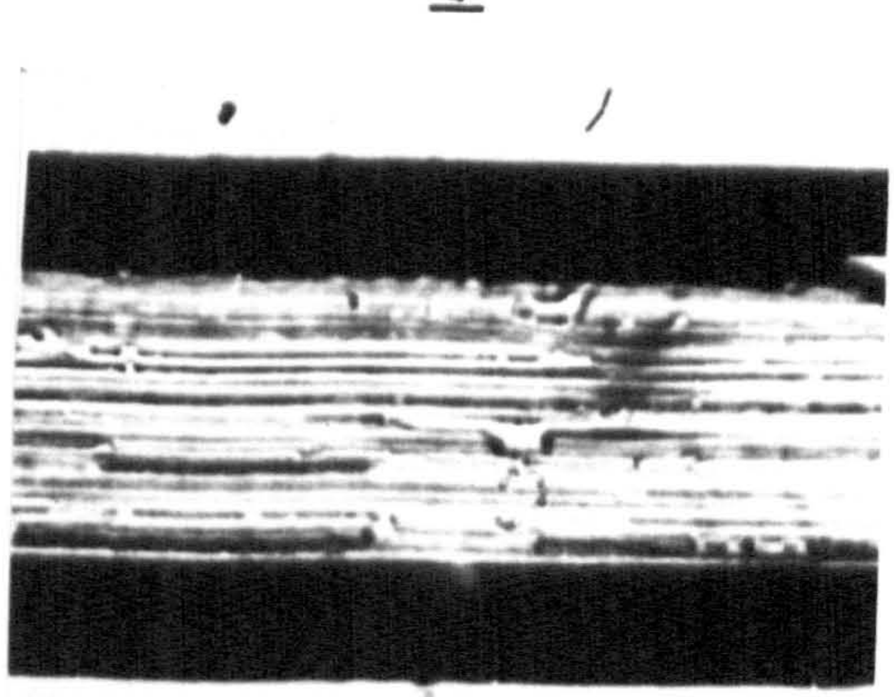

f

PLATE 3

to the annealing process described in the previous section. This treatment was very effective in removing the grooves, but did result in some small variations in tube radius.

The Contact Angle in Exp. A1.

A plot of ϕ against $\dot{x}$ can be seen in Fig. 4.12. The contact angle is clearly dependent upon both the rate and the direction of displacement. As in Exp. P3, dependence is particularly marked in the case of B → W, with ϕ_r decreasing from 70° at 4μ sec^{-1} to 43° at 150μ sec^{-1}; although from 150 to 640μ sec^{-1} further variation is insignificant. The 27° of hysteresis may reflect large scale surface heterogeneity. This conclusion is supported by the fact that speeds of less than 1μ sec^{-1} could be sustained over only very short distances (< 10μ). When this occurred, ϕ lay in the region otherwise associated with a static interface. Two such points are plotted in Fig. 4.12.

Elliott and Riddiford[90,92] also observed a large contact angle hysteresis and velocity dependence (81 to 105°) in the system water/air + water vapour/dimethyldichlorosilane-coated glass. In their experiments, the silane was applied from solution in carbon/tetrachloride, and the range of speeds studied was from 8 to 300μ sec^{-1}. Their results are plotted in Fig. 4.12 for comparison.

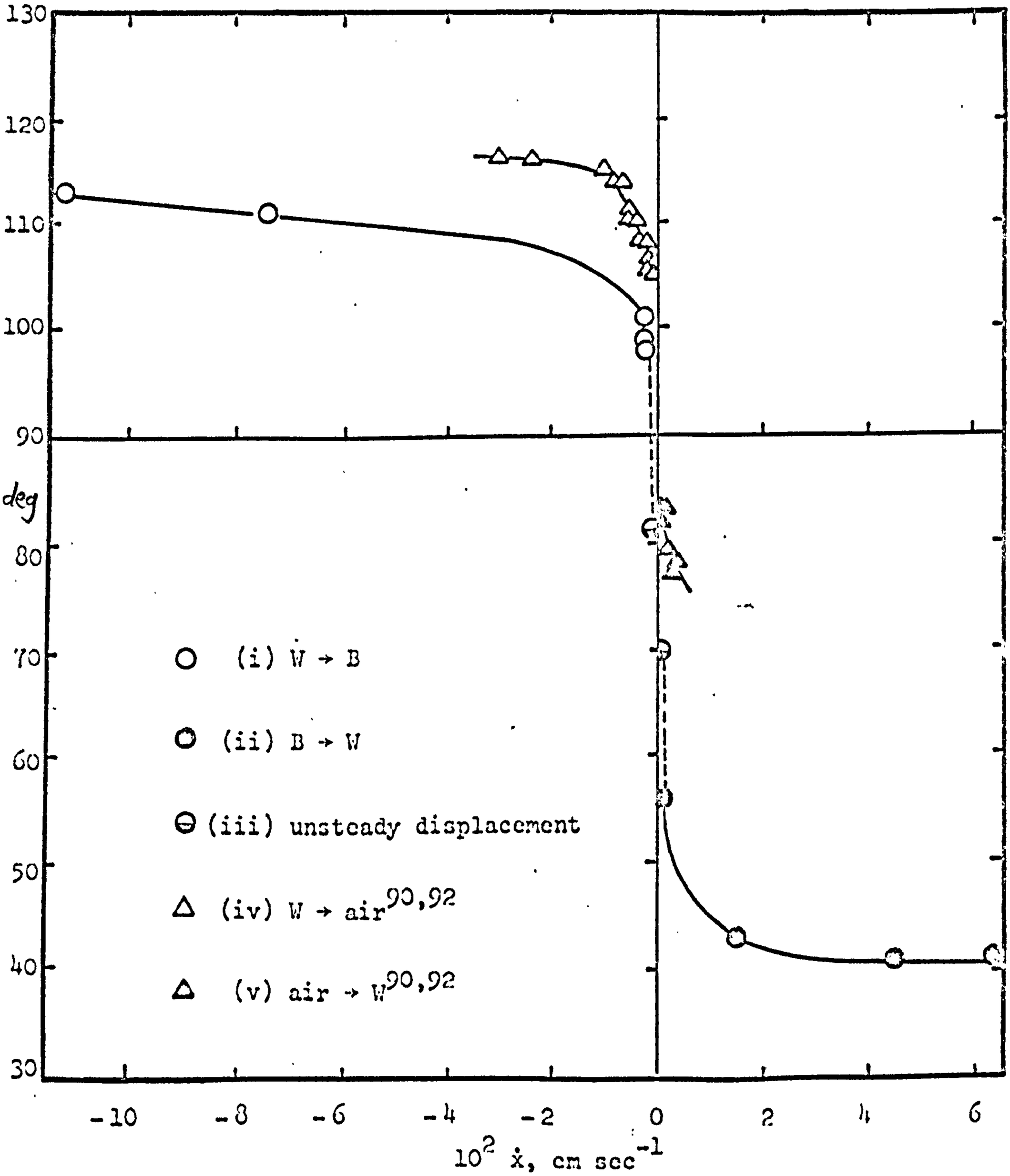
130
120
110
100
90
φ, deg
80
70
60
50
40
30
(i) W → B
(ii) B → W
(iii) unsteady displacement
(iv) W → air 90,92
(v) air → W 90,92
-10
-8
-6
-4
-2
0
2
4
6
10² ẋ, cm scc⁻¹

Fig. 4.12

The Contact Angle in Exp. 1E.

After the adoption of trimethylchlorosilane as coating agent, it became possible to study displacement rates below the previous lower limit of 4μ sec^{-1}. The results of the first W → B runs prior to direct contact between tube wall and water (Fig. 4.13,(i)) show some scatter but little or no significant rate dependence - the contact angle remaining at 160° ±3° over the whole range of velocities (9 to 314μ sec^{-1}). After one hour had elapsed, a more marked rate dependence developed, and the contact angle fell by about 10° overall (Fig. 4.13,(ii)). This may have been due to the action of the low concentration (c. 0.15%) of water, dissolved in the benzene, upon the silane coated surface.

Subsequent displacements in both directions support this view (Fig. 4.13,(iii)). Plate 4 shows frames typical of those from which measurements were taken. (The absence of grooves is noticeable.) Frames a, b and c show respectively,

B → W at 103μ sec^{-1} with $\phi_r = 124°$,

W → B at 19μ sec^{-1} with $\phi_a = 146°$ and

W → B at 175μ sec^{-1} with $\phi_a = 158°$

Two important factors emerge: firstly that following direct contact between tube wall and bulk water, a further, even larger drop in the contact angle ensued; secondly that whilst both advancing and receding angles show a rate dependence which is qualitatively similar to that observed

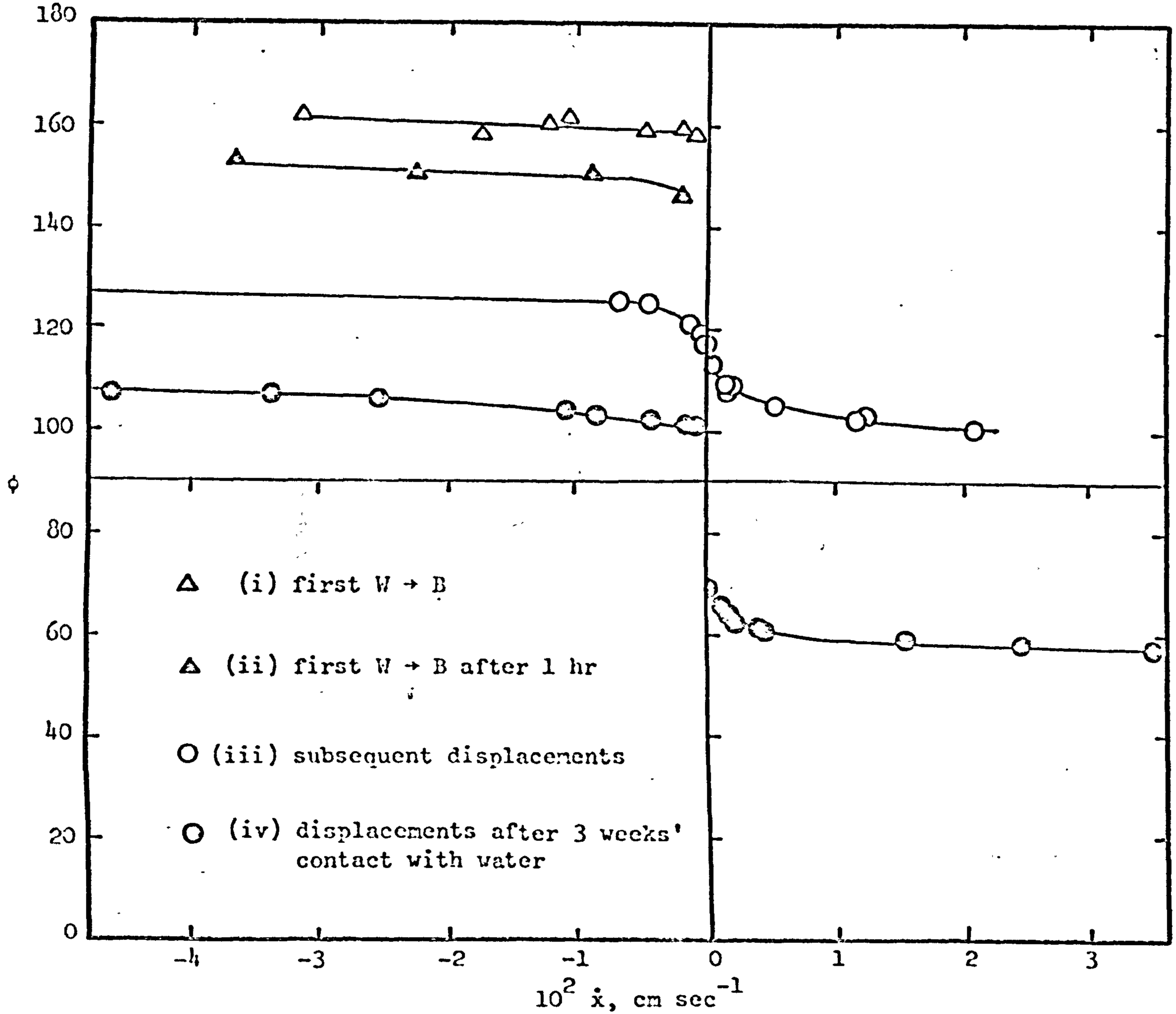
180
160
140
120
100
80
60
40
20
0
φ
(i) first W → B
(ii) first W → B after 1 hr
(iii) subsequent displacements
(iv) displacements after 3 weeks' contact with water
-4
-3
-2
-1
0
1
2
3
10² ẋ, cm sec⁻¹

Fig. 4.13

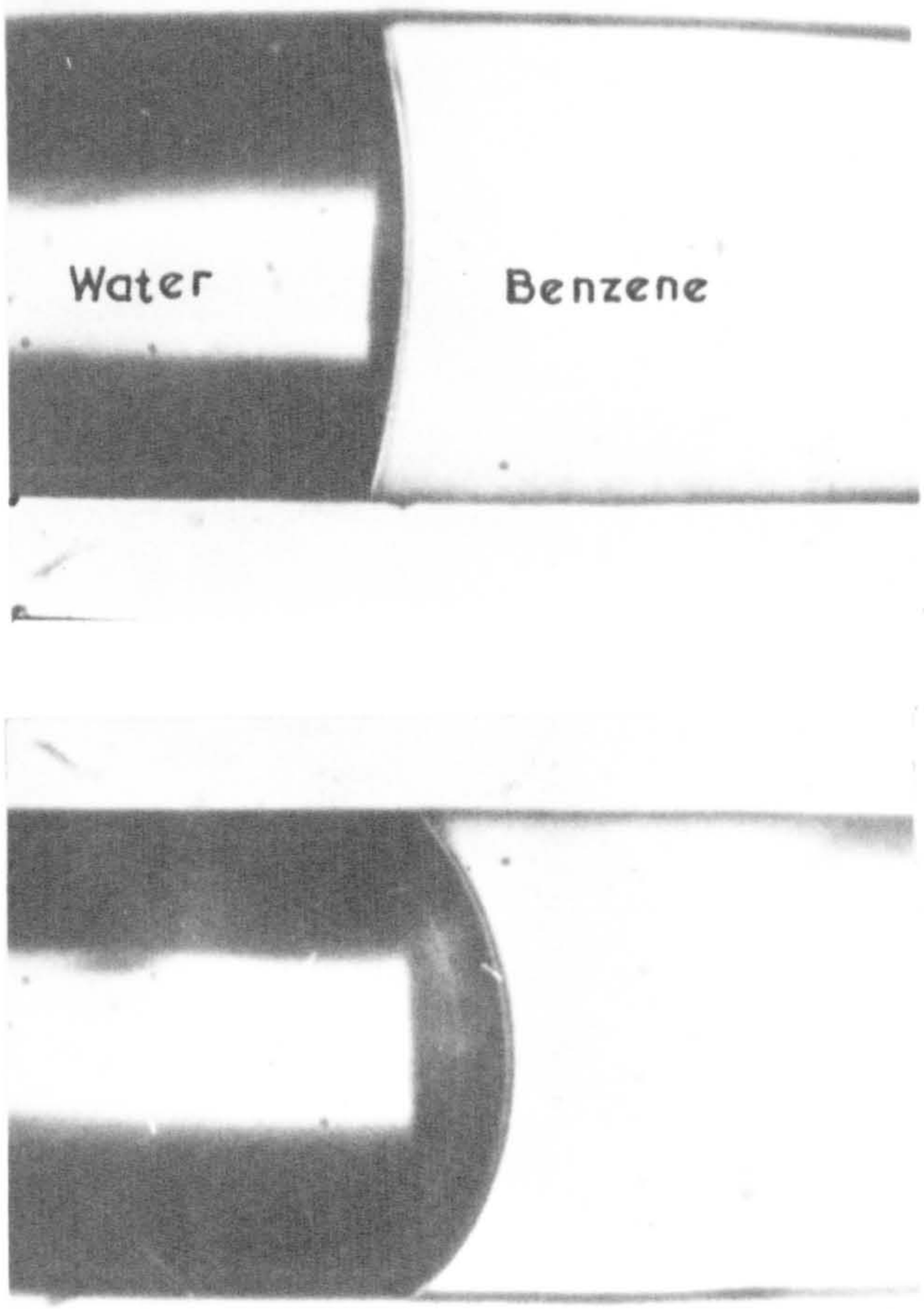

a

b

PLATE 4

c

in the dimethyldichlorosilane-treated tube, hysteresis is less than 4°. Indeed, a value of $117^{\circ} \pm 2^{\circ}$ was recorded for both stationary interfaces and those moving slowly in either direction (i.e. with $\dot{x}$ between -1 and $+2\mu$ sec^{-1}).

The data obtained after direct contact with water for three weeks (Fig. 4.1 3,(iv)) show a reduced velocity dependence but a greatly enhanced hysteresis. The lowest maintainable velocities were 2μ sec^{-1} for B → W with $\phi_r = 68^{\circ}$, and 5μ sec^{-1} for W → B with $\phi_a = 101^{\circ}$. The interface could be constrained to adopt any contact angle between these limits without any detectable movement over periods of up to 2 hrs. There is also a further large drop in ϕ that adds further weight to the notion that water has the ability to modify the properties of the silane-coated surface.

The Contact Angle in Exp. E2.

In this experiment, with the capillary initially filled with water, no change was observed in ϕ_r between the first and subsequent displacements (Fig. 4.14, (iii)). On the other hand, ϕ_a fell by about 7° during the first two hours of study, although no further changes had resulted after 20 hr. During this latter period, however, hysteresis doubled and it became impossible to maintain steady displacement rates below 14μ sec^{-1}. Thus, once again, there is evidence for a profound effect associated with the duration of contact between water and silane-treated glass.

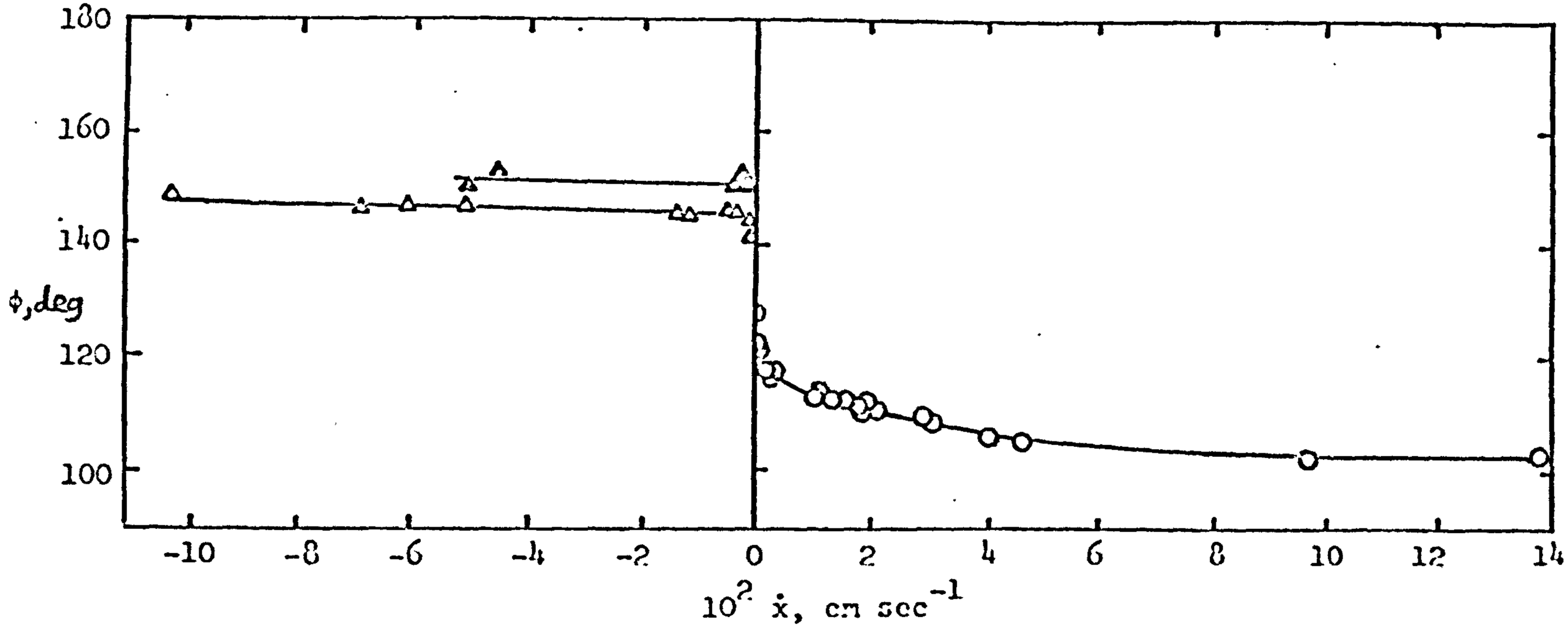

Fig. 4.14 △ early W → B; △ subsequent W → B; ○ B → W;
□ W → B after 22 hr; ● B → W after 22 hr

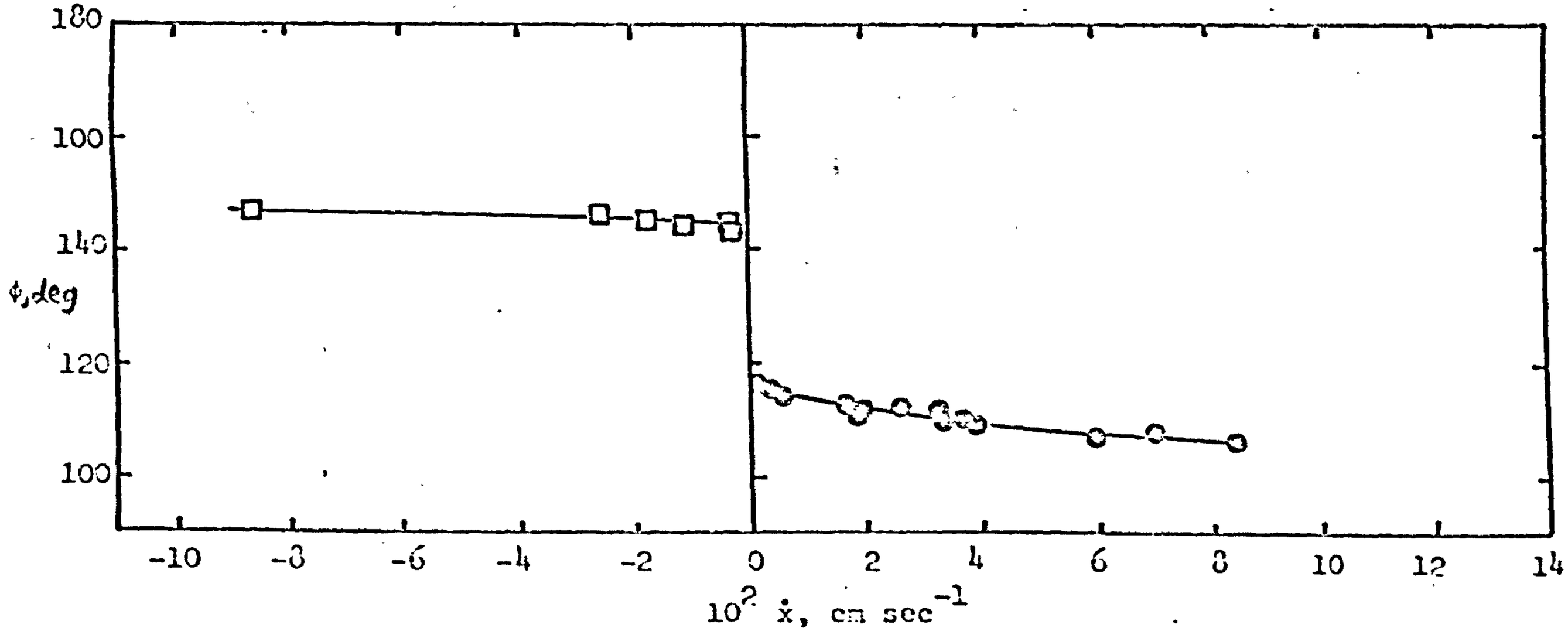

One possible explanation is that water (or at least, water saturated with benzene) is capable of hydrolysing the chemisorbed silane molecules. A second possibility is that the lowering of ϕ and the increase in hysteresis is due to the slow adsorption of surface active impurities at the silane-coated glass/water interface. Alternatively, the changes may simply be due to penetration of the silicone layer by water, as suggested by Elliott and Riddiford[90] to explain qualitatively similar, though less dramatic, changes in ϕ observed with their system. In support of this latter hypothesis is the report by Kiselev[153] of an increase in the amount of water adsorbed by rutile after it had been exposed to various organochlorosilanes. This is interpreted as being due to capillary condensation in micropores between silane residues. An analogous effect appeared in the measurement of water adsorption on silane-treated porous glass reported in Appendix II

Contact Angle Velocity Dependence.

Although in both experiments E1 and E2 displacements were made at random positions in the tube, scatter was never more than $\pm 3^{\circ}$, indicating that the silane treatment employed provided a uniform coating on any one tube. On the other hand, reproducibility from tube to tube is not good. (Compare, for example, early B→W data: Figs. 4.13, (iii), and 4.14,(iii).) Furthermore, the contact angles are

strongly dependent upon the age of the system, with ϕ_a, ϕ_r and the velocity dependence of those angles decreasing, and the amount of contact angle hysteresis ($\phi_{pa} - \phi_{pr}$) increasing with age (Table 4.7). Nevertheless, the experiments do provide a considerable amount of coherent data on the velocity dependence of ϕ over a much greater range of velocities than before.

No evidence has been found to support the conclusion reached by Elliott and Riddiford[90,92] that, even when a system exhibits contact angle hysteresis and velocity dependence, there exists a lower range of velocities (0 to 17μ sec^{-1} with their system) within which the contact angle is independent of displacement rate. On the contrary, it has been found that, where there is contact angle hysteresis, there is often a range of velocities which cannot be achieved experimentally, and within which contact angles are therefore indeterminate and not velocity independent. In deference to Elliott and Riddiford, however, it must be noted that they report the existence of such a range of velocities only for liquid/vapour/solid systems and not for liquid/liquid/solid systems. The summary of results given in Table 4.7 shows a slight trend that indicates that difficulties in maintaining low velocities are greatest when contact angle hysteresis is large, and that an increase in hysteresis generally results in a

Table 4.7

Exp.	Sense	$(\phi_{pa} - \phi_{pr})$, deg.	Estimated change in ϕ from lowest velocity to		Lowest steady velocity, μ sec^{-1}
			100μ sec^{-1}	500μ sec^{-1}	
A1	W → B	42	7	11	-22
	B → W		9	15	+13
E1 initial	W → B	4(max)	9	11	-1
	B → W		16	24	+2
E1 after 3 weeks	W → B	33	4	9	-5
	B → W		8	12	+2
E2 initial	W → B	13	4	6	-2
	B → W		15	24	+5
E2 after 22 hr	W → B	27	4	4	-24
	B → W		4	7	+14

decrease in the corresponding velocity dependence.

At the other extreme, one non-zero contact angle system has been found in which neither hysteresis nor a dynamic effect were detectable at velocities between -1 and $+2\,\mu\,sec^{-1}$. This agrees favourably with the observations of Zisman and co-workers[43], and is also fully compatible with the Hansen and Miotto theory of hysteresis[77].

Although contact angles have been measured at considerably higher interfacial speeds than in previous work, no convincing evidence has been found for the sharp cut-off in rate dependence at high speeds reported by Ablett[114], and also inferred by Elliott and Riddiford[90,92]. Instead, contact angles were observed to tend, roughly logarithmically, towards a limiting value. A similar trend is to be found in the data published by Rose and Heins[119] and by Chittenden and Spinney[121]. Further support for this view is provided by the results of Exp. F2.

<u>Exps. F2 and CX: Transitions between Consecutive and Concentric Flow.</u>

The advancing glycerol interface in Exp. F2 (Fig. 4.15, (i)) showed a large, roughly logarithmic, contact angle velocity dependence with ϕ_a ranging from 99° at $11\mu\,sec^{-1}$ to 140° at $2200\mu\,sec^{-1}$. Hysteresis was also large (55°), and the rate dependence of ϕ_r with B → G was equally marked. In this case, ϕ_r changed from 44° at $3\mu\,sec^{-1}$ to 27° at

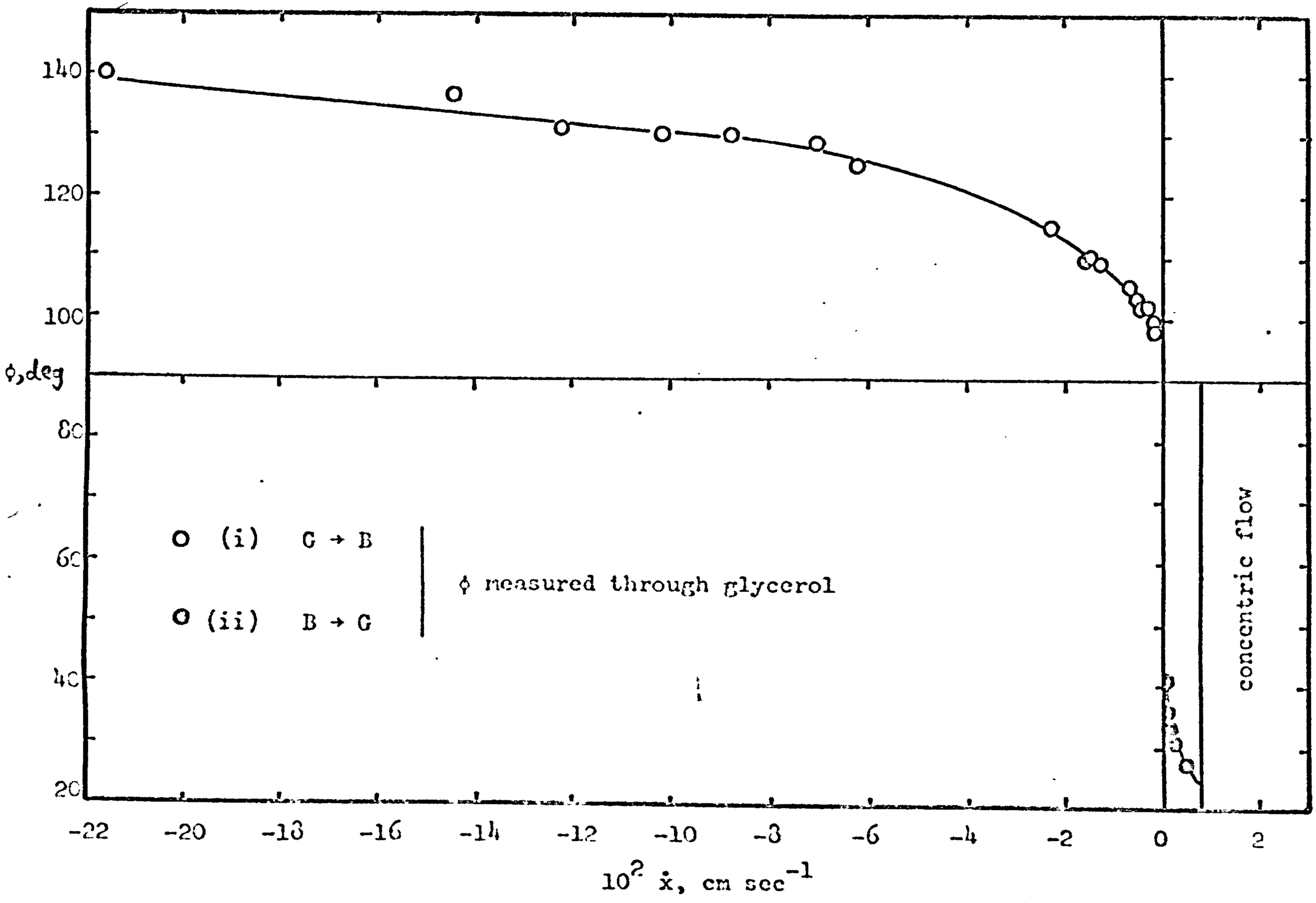
140
120
100
φ, deg
80
60
40
20
(i) C → B
(ii) B → C
φ measured through glycerol
concentric flow
-22
-20
-18
-16
-14
-12
-10
-8
-6
-4
-2
0
2
10² ẋ, cm sec⁻¹

Fig. 4.15

only 48μ sec^{-1}. Above 70μ sec^{-1}, however, there was a spontaneous transition from consecutive to concentric flow. This is shown in Plate 5.

The thickness of the glycerol film remaining after the transition was in accord with the Fairbrother and Stubbs equation, Eq. 3.14, although the liquid in the film was not at rest. In fact, following the transition, the edge of the remaining glycerol film continued to move in the same direction as the meniscus, but at a velocity of about 60μ sec^{-1}, i.e. slightly less than the transition velocity. If the meniscus was halted not more than two diameters away from the moving periphery, the latter eventually caught up with the stationary phase boundary and adopted a contact angle of about 44^{o}.

If a thick (i.e. visible) film was produced with a length greater than three or four tube diameters then unduloids formed. If these were of sufficient size, they closed to form short glycerol indices with hemi-spherical ends. Plate 6 shows the sequence of closure. The glycerol film between two indices of this type slowly thinned and eventually ruptured at some point. Liquid remaining in the film was then drawn back into the two indices until they both adopted contact angles of approximately 44^{o}. Each newly formed interface exhibited the same contact angle hysteresis and velocity dependence as the original

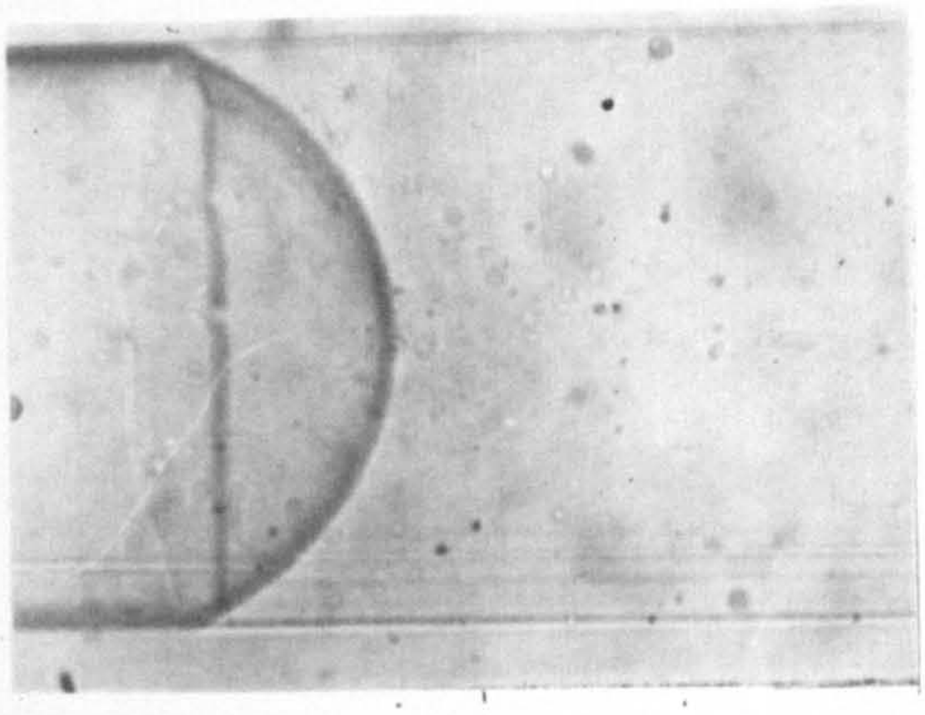

a

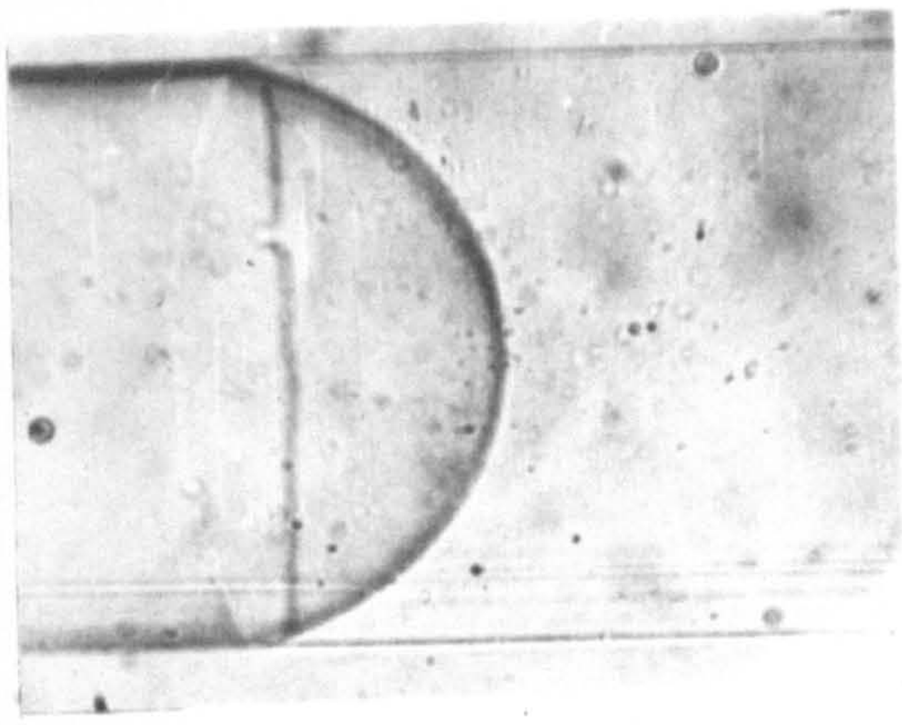

b

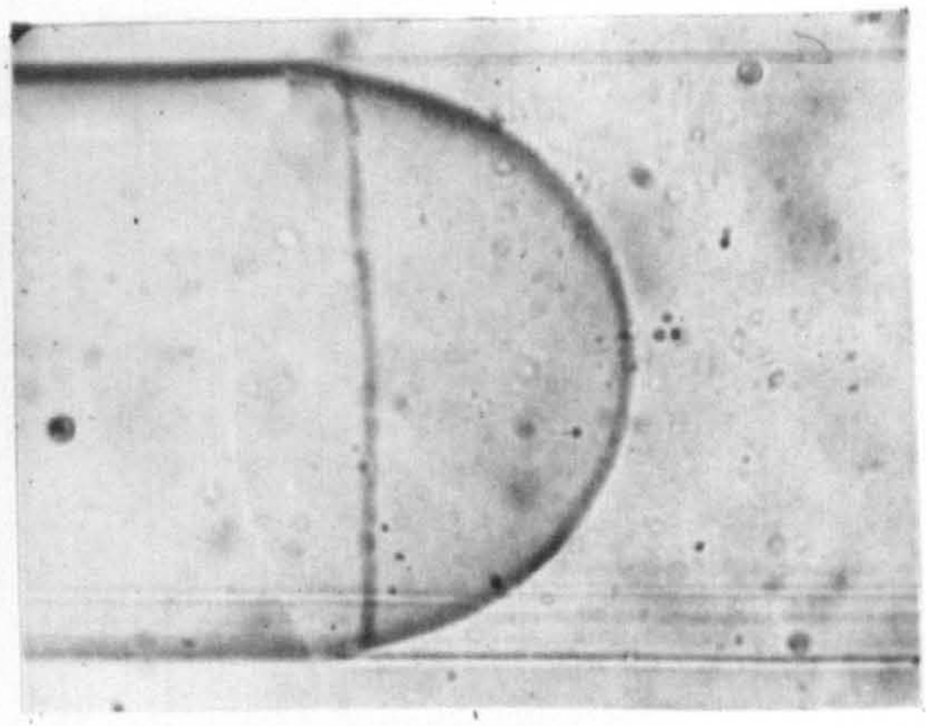

c

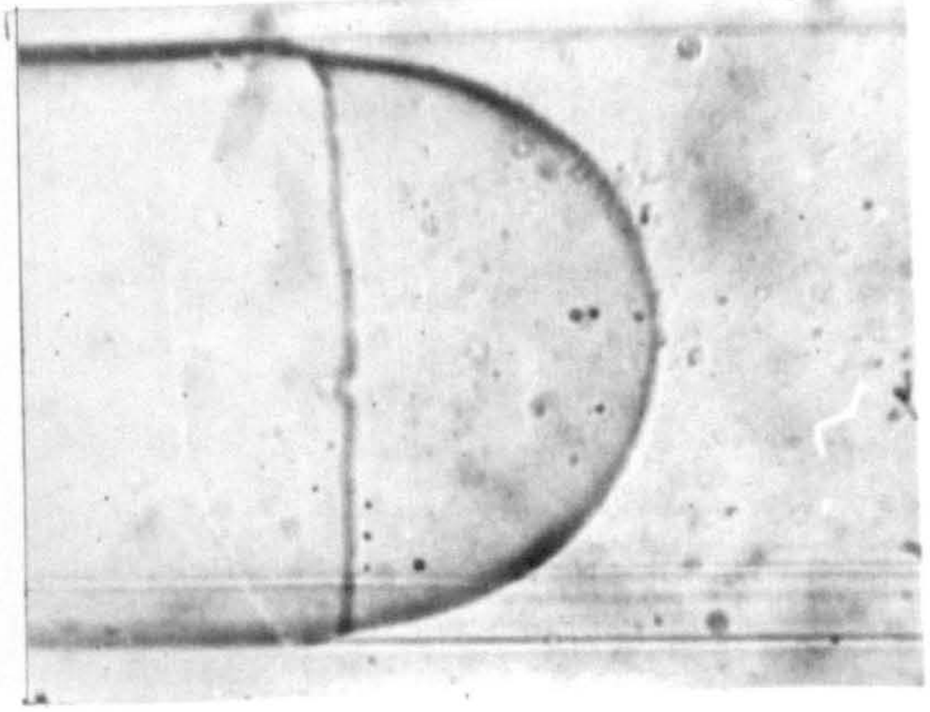

d

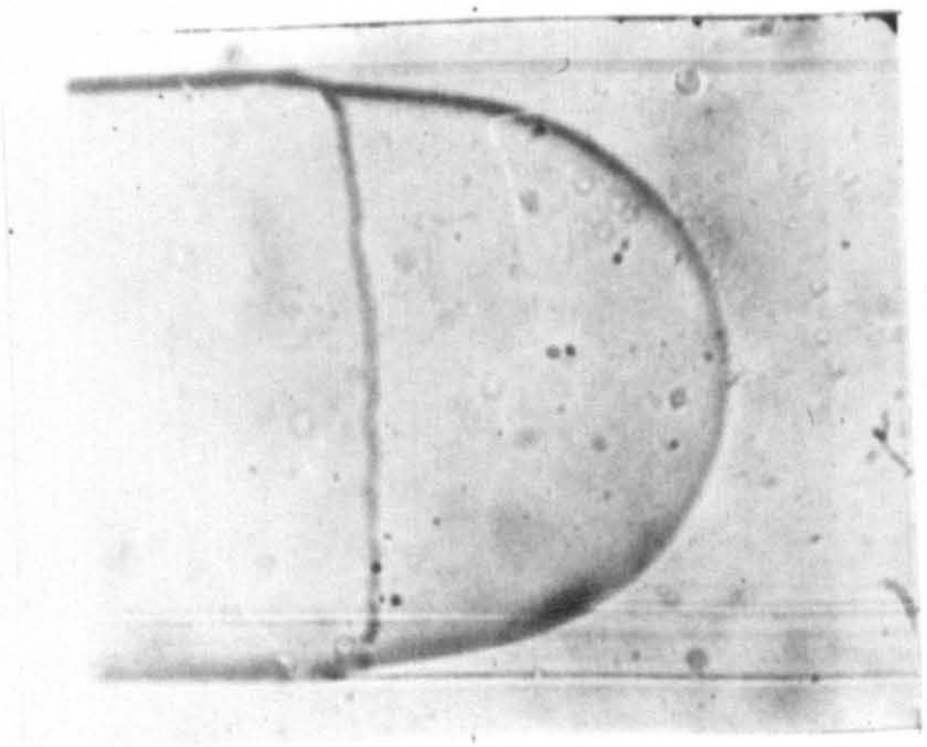

e

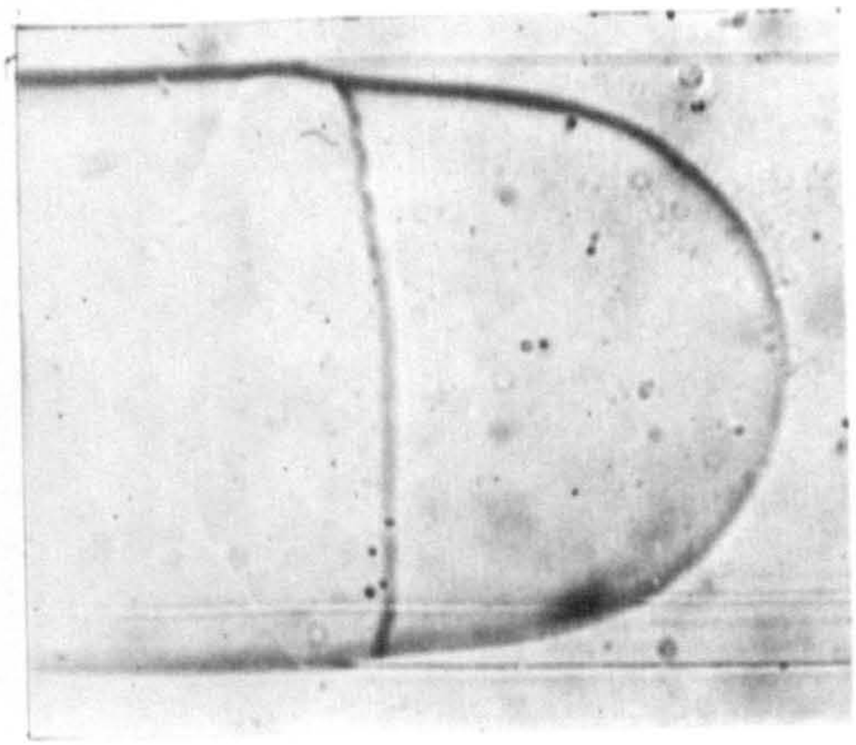

f

PLATE 5

PLATE 6

consecutive flow interface - the whole chaplet providing a much enhanced Jamin effect[130,131].

A spontaneous transition was also observed in Exp. CX. The particular samples of aniline and cyclohexane used had a consolute point at 29.5°C, so that at the temperature of the experiment, 28.7°C, the interfacial tension was very low. Pressure measurements across a stationary interface indicated a value of between 1 and 2 dyne cm^{-1}. The transition occurred when cyclohexane was displacing aniline at approximately 70μ sec^{-1}. The contact angle (through the aniline) just prior to the transition, was 24°.

It seems reasonable to suppose that transitions from consecutive to concentric flow are favoured by high velocities and systems in which the displacing liquid is considerably less viscous than that being displaced. In Exp. F2, for example, the viscosity of glycerol was *c.* 1000 cp, whereas that of benzene only 0.6 cp. Thus one would expect a large asymmetric stress gradient across the moving phase boundary - particularly near the wall. Similarly, in Exp. CX the viscosities of aniline and cyclohexane were respectively 0.8 and 3.2 cp[147]. Thus again the displaced liquid had the higher viscosity, although in this case the ratio was only 4:1 as compared with 1700:1 in Exp. F2. On the other hand, in Exp. CX the surface tension stress, $\frac{\sigma_{12}}{r_m}$, which will oppose a transition, was only about 40 dyne cm^{-2} compared with *c.* 570 dyne cm^{-2} for the glycerol/benzene interface.

The fact that in both systems transitions occurred at the same velocity is probably coincidental.

Film Thickness and Continuity in Flow Transitions.

In his discussion of what has been termed here "consecutive flow", Bataille[110] has asserted that there will always be an extremely thin film of liquid left behind on the tube wall even when $\phi = 90^{\circ}$. Some such residual film was allowed for in the definition of consecutive flow in Chapter 3, but it was pointed out then that the remaining film would not have the properties of a bulk fluid.

Large equilibrium spreading pressures are known to exist with non-zero contact angles[32,54,57-60], and movement of the TPL provides a far more direct, a far more rapid, and probably a far more liberal mechanism for the deposition of an adsorbed film than, say, diffusion. Witness, for example, the success of the retraction method in depositing surface active films[43]. Nevertheless, the potential energy of an adsorbed film is a steep function of its thickness, whereas the potential energy of a thick film of the type produced by concentric flow is a function only of the change in surface curvature with thickness (providing gravitational forces may be neglected). Transition from consecutive to concentric flow therefore requires the transfer of the control over the system's configuration, from intermolecular forces of the type responsible for adsorption and disjoining pressure,

to the macroscopic forces normally considered in hydrodynamics. Thus, unless the interface reaches a configuration having a zero contact angle as transition occurs, film thickness will be a discontinuous function of velocity.

Elliott and Riddiford[90] appear to be the only authors to report having observed what may have been a continuous transition. Their data show that, in the system Bayol/water/siliconed glass, ϕ_r (measured through the Bayol) fell from 16° at 9μ sec^{-1} to 0° at about 85μ sec^{-1}. They note, however, "... that it is difficult to correlate an advancing angle of 180° with any particular velocity. The rate of advance of the foremost part of the liquid/liquid interface does not truly reflect the relative motion between the advancing liquid and the solid surface when the line of three-phase contact is stationary".

The type of interrelationship expected to exist between consecutive and concentric flow is shown in Fig. 4.16. The height OA is the equilibrium film thickness with $\phi_r > 0$; AD represents the variation of film thickness with the velocity of a consecutive flow interface. AG represents film thickness as a function of the velocity of the meniscus in concentric flow. Lines BE and CF represent transition situations.

BE is the possible relationship between film thickness and displacement velocity for an interface which, having

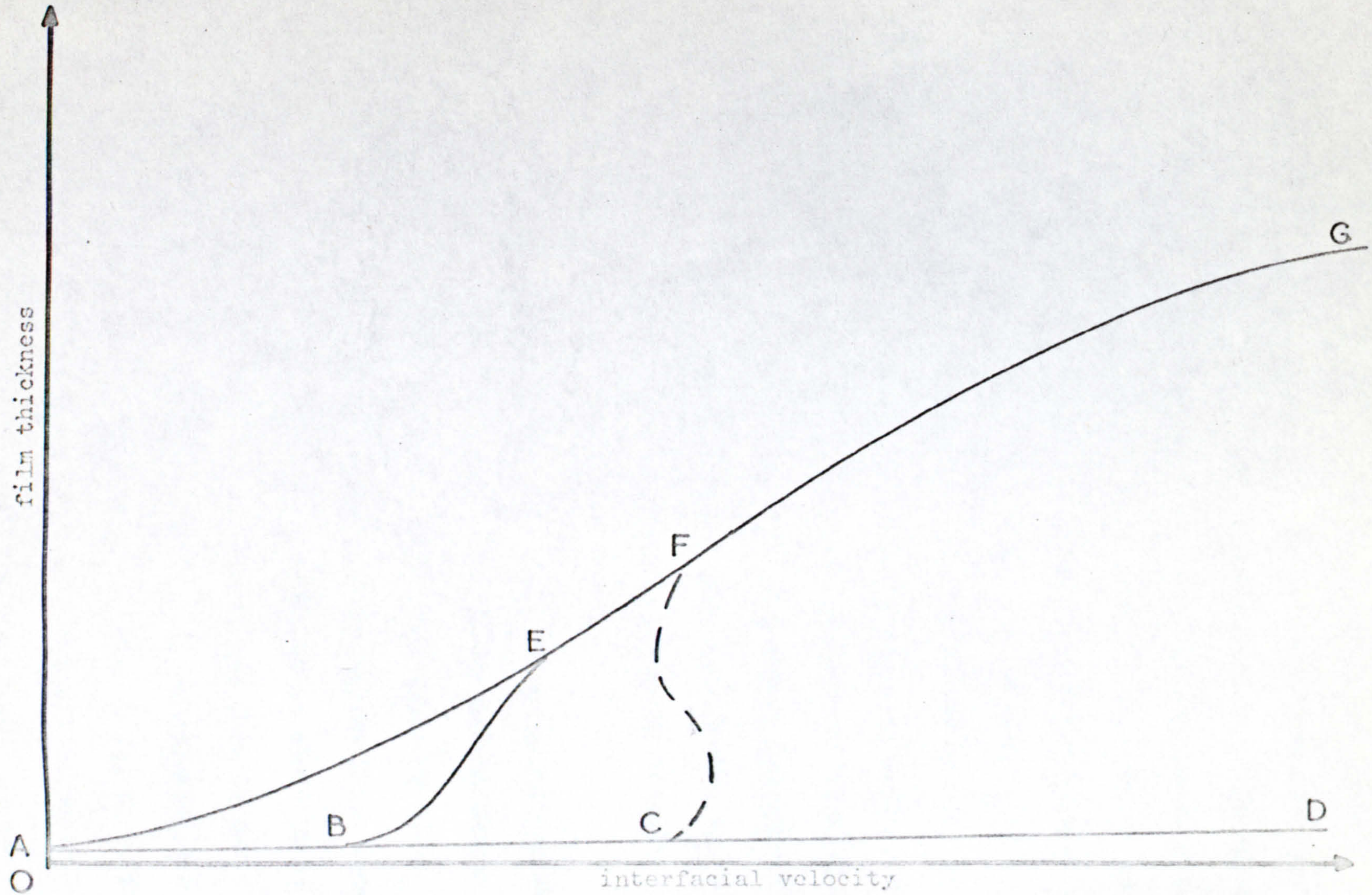

Fig. 4.16

attained a receding contact angle of 0^{o}, undergoes a continuous transition from consecutive to concentric flow.

CF is the possible relationship between film thickness and velocity for an interface which, having attained some receding contact angle greater than 0^{o}, undergoes a spontaneous, discontinuous transition from consecutive to concentric flow. In broad terms, such a transition is the manifestation of sudden interfacial instability brought about by an imbalance of surface tension and viscous forces. A more precise formulation of the cause is difficult, and it is likely that such can only follow detailed knowledge of the potential energy distribution both before and after the transition. It is, nevertheless, interesting to speculate.

Fig. 4.17 illustrates the various relationships that might exist between the potential energy and thickness of the films being left behind in the two types of flow. Solid lines indicate concentric flow, dotted lines consecutive flow. Fig. 4.17a shows a system in which there is no transition at any velocity (turbulent flow is not considered). Fig. 4.17b indicates the relationships likely for a discontinuous transition, and Fig. 4.17c those for a continuous transition; $\dot{x}_c$ is the transition velocity. Fig. 4.17d represents the wetting situation; consecutive flow is totally absent.

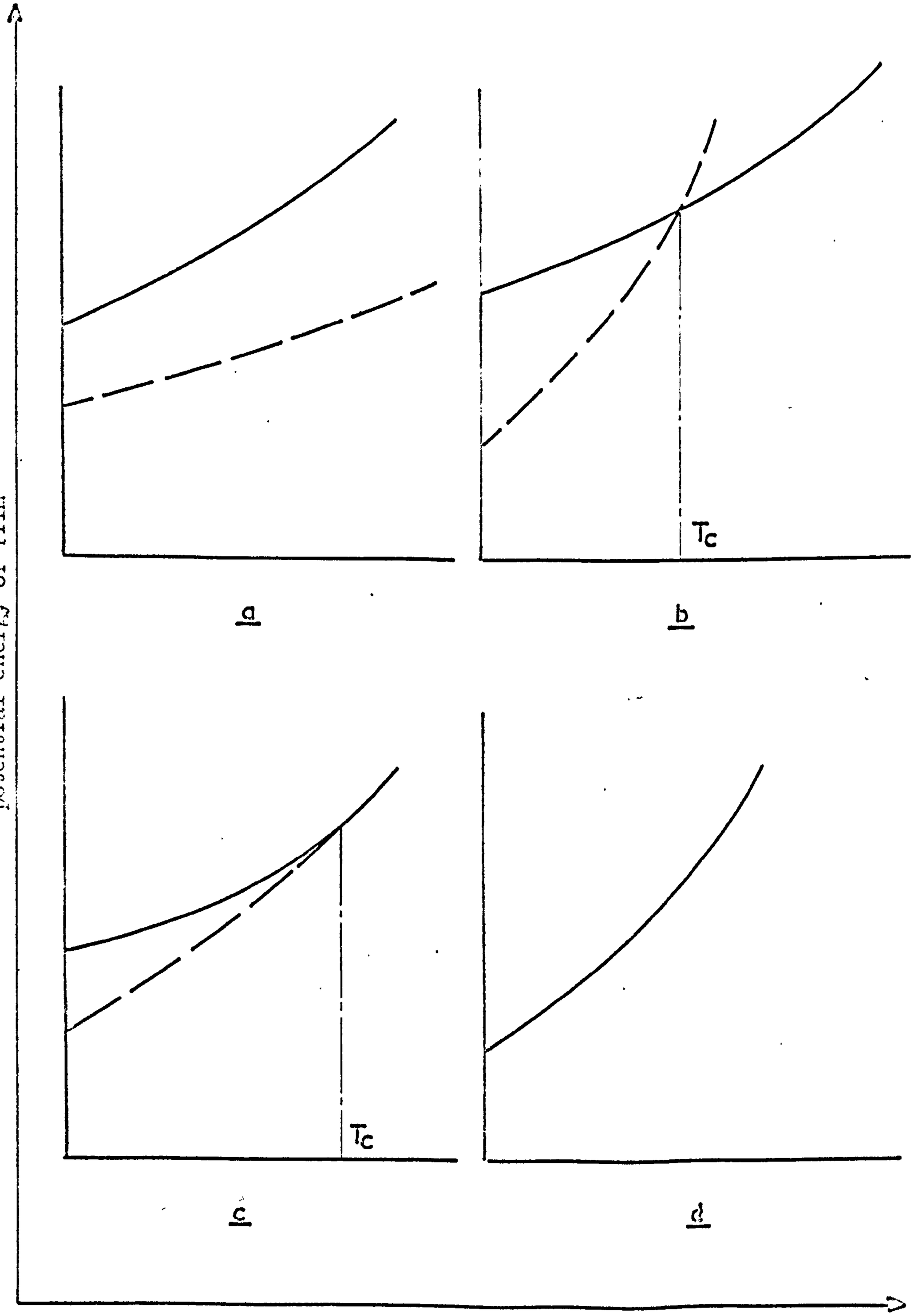

Fig. 4.17

C H A P T E R F I V E

Contact Angle Velocity Dependence: a Theory

Introduction

It is suggested that the theory of absolute reaction rates can be applied to the movement of the TPZ across the surface of the solid in a way analogous to that in which it is currently applied to the rheology of bulk and surface phases[154]. Although this approach derives, in part, from the Hansen and Miotto theory[77] of contact angle hysteresis, it owes much more to the relaxation theory of transport processes developed extensively by Eyring[155-157] and by Frenkel[93].

5.1 The Model

The theory is conveniently discussed within the context of the consecutive flow of two, mutually-saturated liquid phases, 1 & 2, in a uniform cylindrical capillary. The capillary is horizontal and of such a radius, r, that gravitational forces may be neglected (condition 3.1-7b). Displacements of phase 2 by phase 1 will be defined as being in the positive direction and all contact angles will be measured through phase 2 (Fig. 5.1). Initially, the system is at rest and the pressure drop across the 12 interface is simply

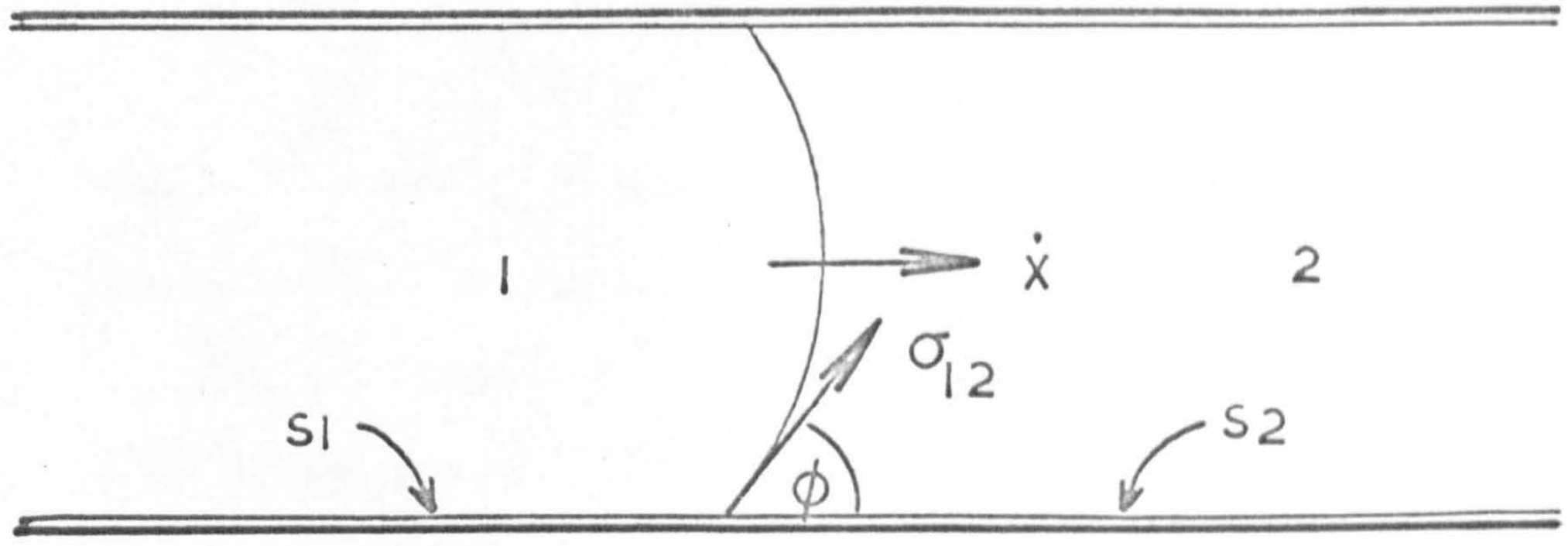

Fig. 5.1

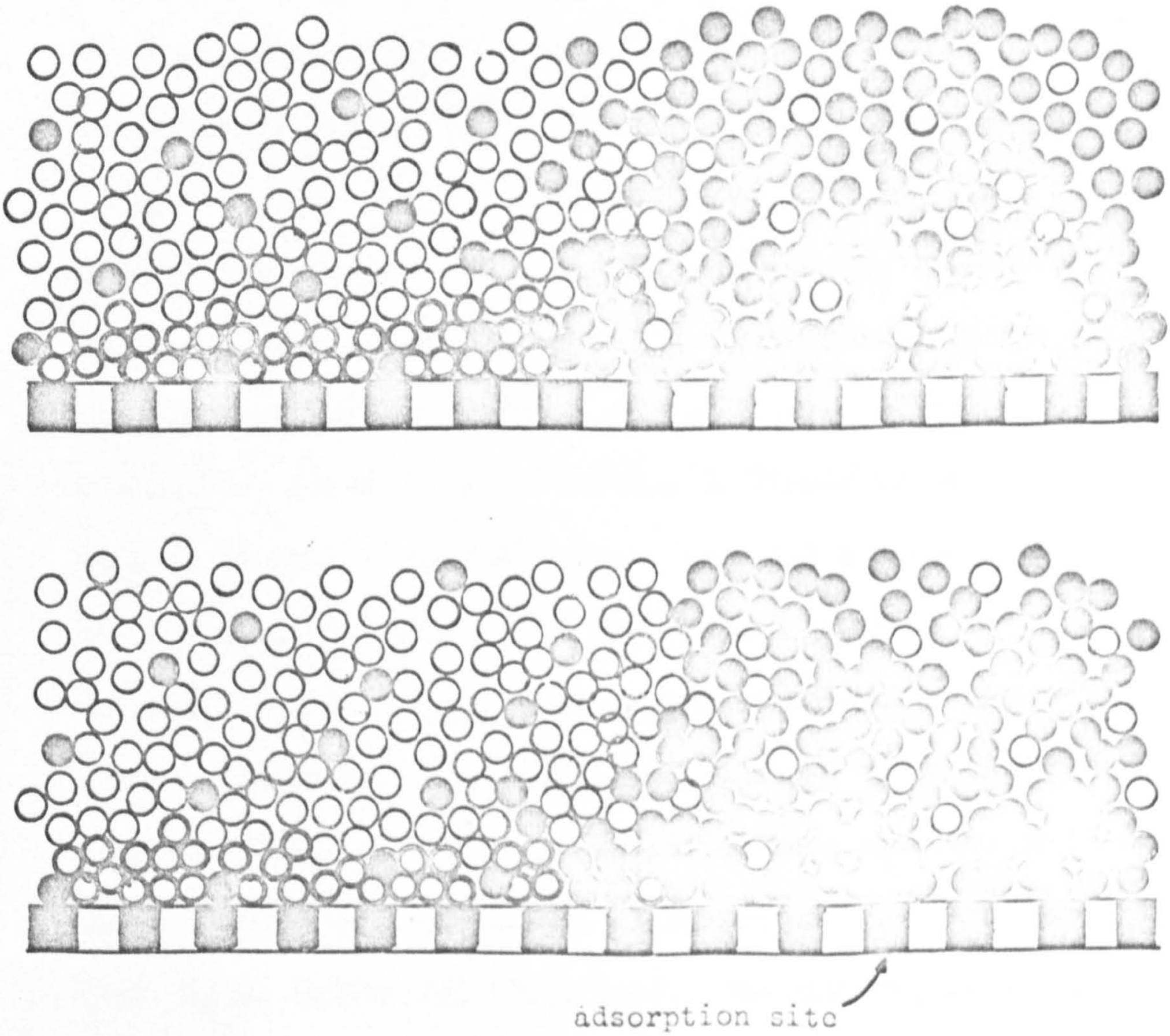

Fig. 5.2 Representation of moving TPL

$$\Delta p^{\circ} = \frac{2\sigma_{12} \cos \phi^{\circ}}{r} \qquad 5.1\text{-}1$$

where ϕ° is the equilibrium value of the contact angle and hysteresis is absent.

Suppose that on the internal surface of the capillary (i.e. the solid surface, S,) there are a large number of identical sites at which molecules of either liquid phase are adsorbed. Suppose also that the displacement of one molecule by another from such a site is equivalent to the passage of the system over a potential energy barrier. Since neither liquid completely wets the capillary wall, the adsorption at the S1 interface is different from that at the S2 interface, and the TPZ constitutes a transitional region in which the adsorption varies in some unknown way from that appropriate to one interface to that appropriate to the other. Viewed on a molecular scale, this transition is likely to be abrupt. Recent estimates[171] suggest that the thickness of the interfacial region, in a non-critical system, is between 2 and 5 Å, i.e. of the order of molecular dimensions. One might reasonably expect the TPZ to be of a similar thickness, and to encompass no more than two or three adsorption sites in the direction of the solid surface normal to the TPL (Fig. 5.2). The picture, however, will not be static, for, at this molecular level, the TPZ will fluctuate constantly about some mean position

as molecules of one species interchange with those of the other. Nevertheless, when the TPL is stationary, the nct§ rate of molecular exchange will be zero.

Let the displacement of a molecule of phase 1 by one of phase 2 be defined as the forward (i.e. positive) direction, and let the number of times this occurs in unit time along unit length of the TPL be K_+. Then, according to the theory of absolute reaction rates,

$$K_+ = K_+' \exp\left(\frac{-\varepsilon_+}{kT}\right) \qquad 5.1\text{-}2$$

where ε_+ is the activation energy for the process and K_+' is a temperature dependent "frequency factor"[*].

Similarly, the rate of molecular displacement in the backward direction will be

$$K_- = K_-' \exp\left(\frac{-\varepsilon_-}{kT}\right) \qquad 5.1\text{-}3$$

where K_-' and ε_- are, respectively, frequency factor and activation energy for the displacement of a molecule of phase 1 by one of phase 2 from an adsorption site in the TPZ. When the TPL is stationary, the net rate of molecular exchange must be zero;

thus $K_+ = K_-$

i.e. $$K_+' \exp\left(\frac{-\varepsilon_+}{kT}\right) = K_-' \exp\left(\frac{-\varepsilon_-}{kT}\right) \qquad 5.1\text{-}4$$

Suppose that there is an increase in the pressure drop across the 12 interface, i.e. in Δp, there will be little or no change in K_+' or K_-', but the increase

---

[*] See Glasstone Laidler and Eyring[157] p.5 et seq.

in the potential gradient across the TPZ will lower the energy barrier to displacement in one direction and, at the same time, raise the energy barrier to displacement in the opposite direction. The result will be a net movement of the TPZ in the favoured direction. Without the change in Δp, the energy barriers (i.e. ε_+ and ε_-) would be unaltered and the TPL would not move. Thus, if the TPL is to move with a finite velocity, extra, irreversible work must be done on each adsorption site as it passes through the TPZ. This result expresses the fact[158] that movement of the TPL can only occur isothermally if it also occurs infinitely slowly.

It has been experimentally shown (Section 4.3) that, at sufficiently low velocities, the pressure drop across the moving interface between two mutually saturated liquids undergoing consecutive flow in a uniform cylindrical capillary is given by

$$\Delta p = \frac{2\sigma_{12}}{r} \cos \phi \qquad 5.1\text{-}5\ (4.3\text{-}1)$$

where σ_{12} is the equilibrium surface tension, and ϕ is the appropriate dynamic contact angle. Since the system is supposed to show contact angle velocity dependence, for non-zero $\dot{x}$,ϕ is less than ϕ^{o}. The difference between the pressure drop in the dynamic case and that in the static case, $(\Delta p - \Delta p^{o})$, thus gives a measure of the additional force necessary to move the

interface at a finite velocity in excess of that required if it is moved infinitely slowly. The work done by this additional force per unit displacement of unit length of the TPL is given by

$$\psi = \sigma_{12}(\cos\phi - \cos\phi^{o}) \qquad 5.1\text{-}6$$

If it is assumed that this work is used entirely in raising or lowering the energy barriers ε_+ and ε_- then

$$\psi = n_o \delta\varepsilon \qquad 5.1\text{-}7$$

where n_o is the number of adsorption sites per unit area of the solid surface and $\delta\varepsilon$ is the work done on each site. This, of course, implies that the same amount of work is done on each site irrespective of whether or not it is occupied by a molecule of phase 1 or one of phase 2. This is possibly equivalent to the assumption that the molecules of both phases are of equal size. However, if the validity of Eq. 5.1-7 is, for the moment, accepted, then, for positive ψ, ε_+ and ε_- will be respectively lowered and raised by the same amount, $\frac{\psi}{n_o}$, and the net displacement will be in the forward direction, and given by

$$K_{net} = K'_+ \exp\left(\frac{\psi - n_o\varepsilon_+}{n_o kT}\right) - K'_- \exp\left(\frac{-\psi - n_o\varepsilon_-}{n_o kT}\right)$$

$$= K_+ \exp\left(\frac{\psi}{n_o kT}\right) - K_- \exp\left(\frac{-\psi}{n_o kT}\right) \qquad 5.1\text{-}8$$

But, from Eq. 5.1-4, $K_+ = K_- = K$, say. Hence

$$K_{net} = K\left[\exp\left(\frac{\psi}{n_o kT}\right) - \exp\left(\frac{-\psi}{n_o kT}\right)\right]$$

$$= 2K \sinh\left(\frac{\psi}{n_o kT}\right) \qquad 5.1\text{-}9$$

and the velocity of the TPL is

$$\dot{x} = 2K\lambda \sinh\left(\frac{\psi}{n_o kT}\right) \qquad 5.1\text{-}10$$

where λ is the average distance between the centres of adsorption sites.

Combination of Eqs. 5.1-6 & 5.1-10 yields

$$\dot{x} = 2K\lambda \sinh\left(\frac{\sigma_{12}}{n_o kT}\right)(\cos\phi - \cos\phi^o) \qquad 5.1\text{-}11$$

Now, if $\left(\frac{\sigma_{12}}{n_o}\right)(\cos\phi - \cos\phi^o) \ll kT$ then Eq. 5.1-11 simplifies to

$$\dot{x} = \frac{2K\lambda\sigma_{12}}{n_o kT}(\cos\phi - \cos\phi^o) \qquad 5.1\text{-}12$$

so that $\dot{x}$ is a linear function of $\cos\phi$ * and

$$\frac{d\phi}{d\dot{x}} = \frac{-n_o kT}{2K\lambda\sigma_{12}\ \mathrm{Sin}\ \phi} \qquad 5.1\text{-}13$$

On the other hand, if $\frac{\sigma_{12}}{n_o}(\cos\phi - \cos\phi^o) \gg kT$,

Eq. 5.1-11 simplifies to

$$\dot{x} = K\lambda \exp\left[\frac{\sigma_{12}}{n_o kT}(\cos\phi - \cos\phi^o)\right] \qquad 5.1\text{-}14$$

whence,

$$\log\dot{x} = \log K\lambda - \frac{\sigma_{12}}{2.303\ n_o kT}\cos\phi^o + \frac{\sigma_{12}}{2.303\ n_o kT}\cos\phi \qquad 5.1\text{-}15$$

In this case a plot of $\log\dot{x}$ against $\cos\phi$ should give a straight line of slope $\frac{\sigma_{12}}{2.303\ n_o kT}$.

---

* C.f. Newtonian flow equations: Glasstone Laidler and Eyring[157] p.483.

5.2 Testing the Equations

Figs. 5.3, 5.4 & 5.5 show data, from, respectively Exps.E1, E2 & F2, plotted according to Eq. 5.1-15. These particular sets of data were chosen because they all show a large velocity effect. Each graph has a long linear region, although, in the case of glycerol displacing benzene (Fig. 5.5), this curls over at velocities below 100μ sec^{-1}. Table 7.1 shows values of n_o calculated from the slopes of the linear regions.

Table 7.1

Exp.	Fig.	Sense	$n_o \times 10^{-13}$, cm^{-2}
E1 (iii)	5.3	B → W	5
		W → B	2
E2 (iii)	5.4	B → W	5.2
F2	5.5	G → B	3.6

With σ_{12} 35 dyne cm^{-1} for the water/benzene interface, and 19.5 dyne cm^{-1} for the benzene/glycerol interface, $\frac{\psi}{n_o} \gg kT$, providing $(\cos \phi - \cos \phi^o) > 0.1$. The use of Eq. 5.1-15 is thus internally consistent for these data in this respect. However, the systems in Exps. E2 and F2 both showed considerable contact angle hysteresis whereas this was assumed to be absent in deriving Eq. 5.1-15. The apparent success of Eq. 5.1-15 in accounting for the results of these experiments suggests

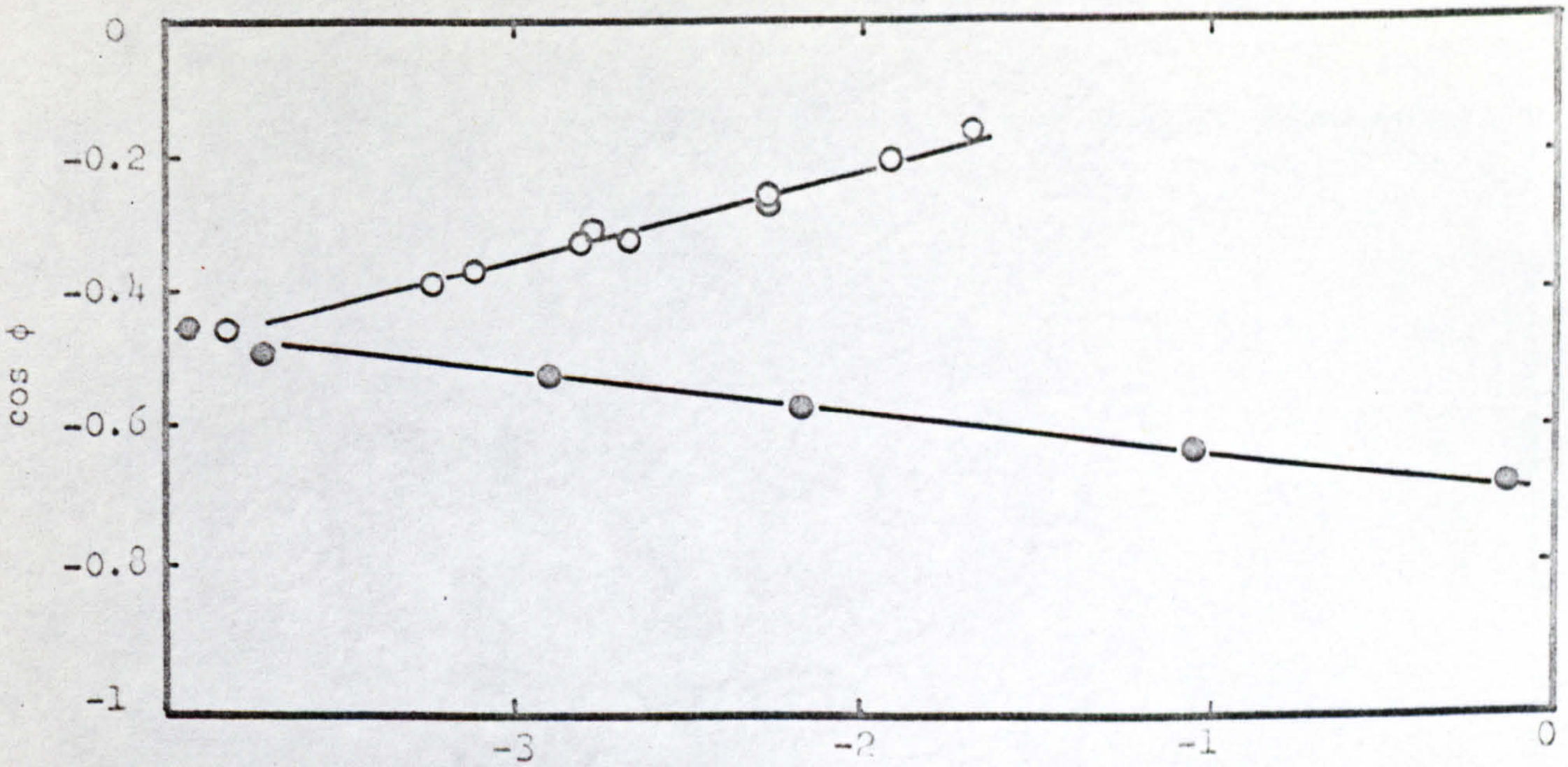

Fig. 5.3 ○ B → W; ● W → B; data from Exp. E1(iii) plotted according to Eq. 5

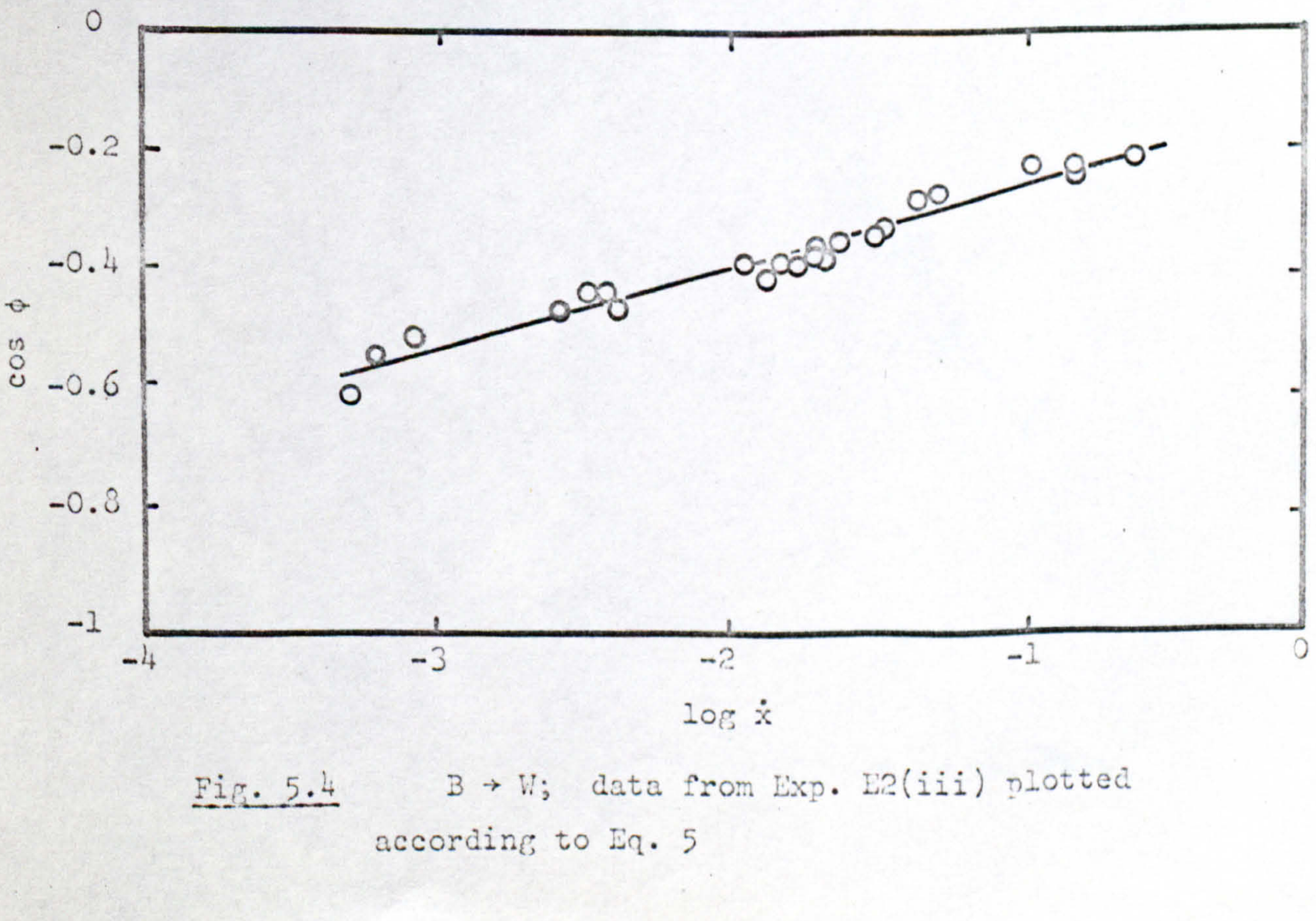

Fig. 5.4 B → W; data from Exp. E2(iii) plotted according to Eq. 5

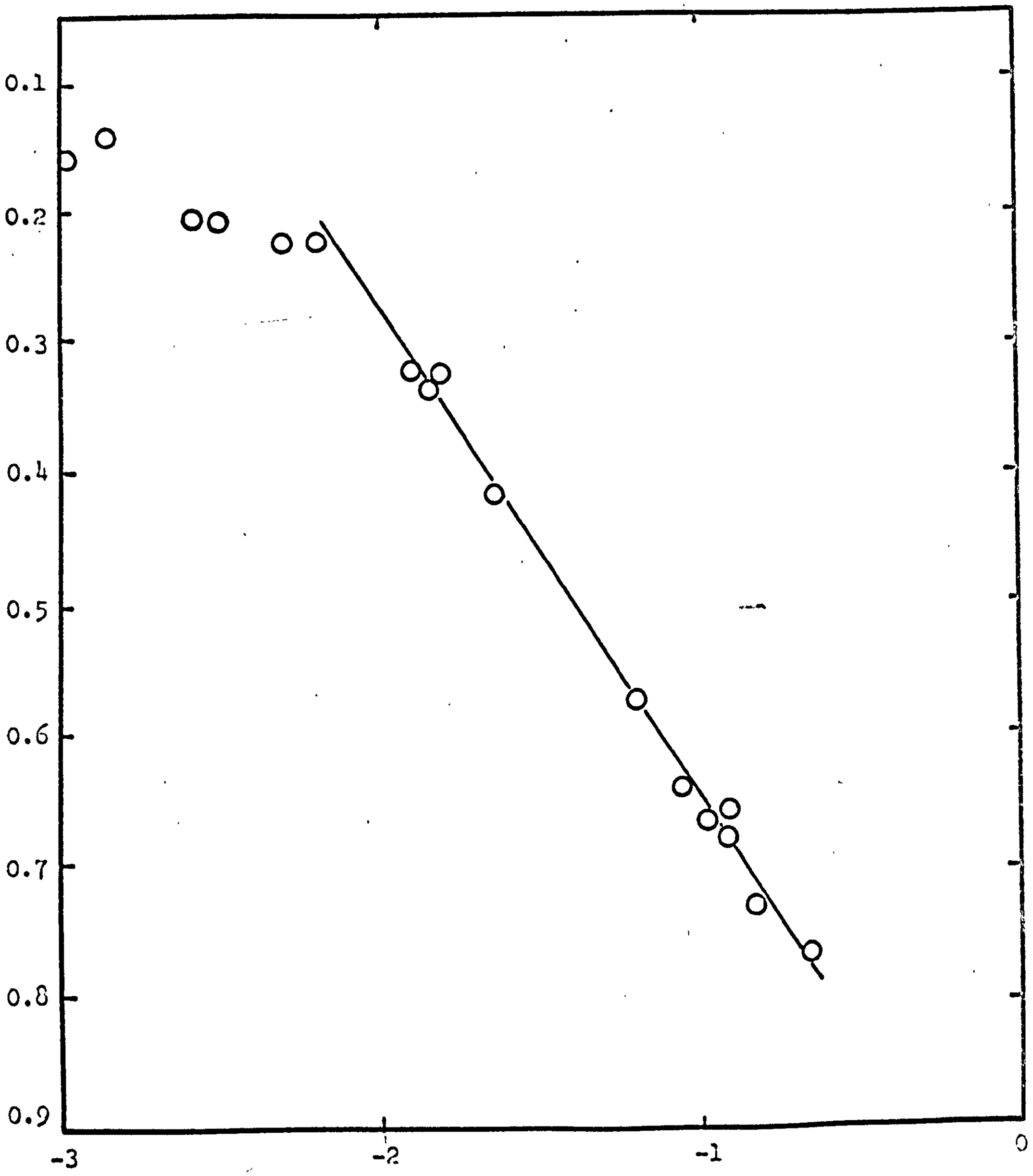

Fig. 5.5 G → B; Data from Exp. F2 plotted according to Eq. 5.1-15.

that this inadequacy is unimportant except at low velocities.

The close agreement between the values of n_o obtained from the B → W data of Exps. E1 & E2 is encouraging. On the other hand, the difference between the values obtained from B → W and W → B data of Exp. E1 is disappointing. It is possible that this difference is the direct result of the assumptions made when formulating Eq. 5.1-7.

As noted above, the model used in the development of Eqs. 5.1-12 & 5.1-15 does not admit the possibility of contact angle hysteresis. Just as with the Hansen and Miotto theory, given sufficient time, contact angles should relax back to their equilibrium values. The speed with which this will occur will depend upon the rate constant, K, and how far the system is removed from equilibrium. Fig. 5.3 is, therefore, of particular interest. Because there is little or no hysteresis, it is possible to determine $\cos \phi^o$ with some precision (0.48 ± 0.02) and hence determine $K\lambda$, the equivalent of the Hansen and Miotto natural velocity, $\dot{x}_n$. The value obtained, 1 μ sec^{-1}, can be used to calculate K providing λ can be estimated. If, as a rough guide, λ is taken to be $n_o^{-\frac{1}{2}}$ then $K \approx 5 \times 10^2$ sec^{-1}, and $1/K$, the equivalent of the Hansen and Miotto relaxation time, τ, is 2×10^{-3} sec. In this connection, it is important to note that

there exist significant differences between the model used in deriving the theory presented here, and that used by Hansen and Miotto. In particular, whilst the latter theory predicts that

$$\lim_{\dot{x} \to 0} \frac{d\phi}{d\dot{x}} = 0 \qquad 5.2\text{-}1$$

Eq. 5.1-13 shows that

$$\lim_{\dot{x} \to 0} \frac{d\phi}{d\dot{x}} = \frac{-n_o kT}{2K\lambda\ \sigma_{12}\ \sin\ \phi} \qquad 5.2\text{-}2$$

Thus any equivalence between $K_f^{\neq}$ and $\dot{x}_n$, and between $^1/K$ and τ is purely superficial.

The calculation of the activation energy, ε_+, is more difficult since the value of K_+' must be ascertained first, and this requires knowledge of the partition functions for the activated and initial states, $\mathcal{Z}^{\ddagger}$ and $\mathcal{Z}_+$ respectively:*

$$K_+' = \frac{kT}{h}\ \frac{\mathcal{Z}^{\ddagger}}{\mathcal{Z}_+} \qquad 5.2\text{-}3$$

However, by utilizing the identity

$$K^{\ddagger} = \frac{\mathcal{Z}^{\ddagger}}{\mathcal{Z}_+}\ \exp\left(\frac{-\varepsilon_+}{kT}\right) \qquad 5.2\text{-}4$$

where $K^{\ddagger}$ is the equilibrium constant relating the activities of molecules in the initial and activated states, and the thermodynamic relationship

$$K^{\ddagger} = \exp\left(\frac{-\Delta F^{\ddagger}}{RT}\right) \qquad 5.2\text{-}5$$

where $\Delta F^{\ddagger}$ is the standard Helmholtz free energy of activation per mole, Eq. 5.1-2 may be written in the

---

* See Glasstone, Laidler and Eyring[157] p.482

form $K_+ = \frac{kT}{h} \exp\left(-\frac{\Delta F^{\ddagger}}{RT}\right)$ 5.2-6

with the value of K given above, $\Delta F^{\ddagger}$ is found to be 2.5×10^4 Joules mole^{-1}. This does not appear to be unreasonable for a process which is envisaged as the desorption of a water molecule and the adsorption of a benzene molecule. For example, the difference between the latent heats of vaporization of water and benzene is of the same order of magnitude: 1.2×10^4 Joules mole^{-1}.

5.3 Residual Films

With sufficiently high energy barriers, the rate of TPZ displacement will be negligible even for large values of ψ. However, a significant rate of displacement might become possible in, say, the second adsorption layer at a much lower value of ψ. Once disruption of the TPZ has occurred, the periphery of the 1,2 interface will slip across the surface of the first adsorption layer comparatively unhindered, leaving the latter to reach equilibrium concentration by diffusion. The extent to which the contact angle will still be velocity dependent will be determined by how strongly the second layer interacts with the adsorption sites.

This type of behaviour may be responsible for the difficulty in maintaining low displacement velocities experienced in all experiments but E1, for, not until

a certain, limiting value of ϕ is reached will the TPZ break down and measurable displacement occur; thereafter, if the displacement velocity is reduced, the TPZ, including the first adsorption layer, reforms, and, once again, displacement ceases to occur at a significant rate.

If the residual film were chiefly non-polar, it might be more efficient at screening the long-range effects of the adsorption sites than if it were chiefly polar. The low rate dependence generally found for W → B, compared with that observed with B → W, might thus be simply explained in circumstances where a large degree of contact angle hysteresis is also apparent. In support of this view, it is worth noting that, in the one instance where contact angle hysteresis is negligible (Exp. E1), the W → B rate dependence is comparatively large at low velocities.

5.4 The Adsorption Sites

The question of what precisely constitutes an adsorption site is difficult to answer with certainty. With n_o of order 5×10^{13} cm^{-2}, there is approximately one site every $200 Å^2$. One possibility is that the silane layer is imperfect and that there are numerous small patches of exposed glass surface at which, in particular, water molecules are adsorbed. Certainly

the behaviour of the silane surface on exposure to water, reported in Chapter 4, lends support to this view. Another possibility arises from the fact that a glass surface is usuaully covered with sub-microscopic cracks[159,160] and is easily corroded by water[161,162]. Corrosive attack of this type might well lead to the production of adsorption centres to which the comparatively large chlorosilane molecules have no access but which can interact with the much smaller water molecules.

Although it has been assumed for simplicity that all adsorption sites are equivalent, there may, in fact, be a distribution of activation energies. Indeed this would seem inevitable, and a low concentration of sites with high activation energies could become the controlling influence over the behaviour of the contact angle.

5.5 Conclusion

The apparent success of Eq. 5.1-11 in relating the data reported here is no guarantee of the correctness of the model used. The theory has been developed around a particular molecular mechanism - namely the desorption/adsorption of molecules of the principle fluid components at the surface of the solid in the TPZ. There is, however, no reason why alternative activated processes might not be involved. For example, molecular reorientation (as

suggested by Hansen and Miotto); viscoelastic deformation of a soft substrate[36]; or the adsorption/desorption of an additional, surface active, component. Nor is there any need for the activated process to occur principally in the first adsorption layer. For example, where one of the phases is aqueous, forces opposing displacement of the TPZ could originate from the disruption of a comparatively thick electrical double layer. Similarly, liquid structuring as extensive as that suggested by Derjaguin[64] is likely to result in massive contact angle velocity dependence. Derjaguin and Shcherbakov[163] have argued that the contact angle is not formed with the surface of the solid, but with the overlaying adsorbed multilayers. This would seem particularly likely with high energy surfaces and polar liquids. In these circumstances the TPZ, if such existed, would not be tied to the fluid/fluid interface and the controlling influence upon the observed contact angle would be the mechanism by which the periphery of the interface moved across the surface of the adsorbed film. A better phenomenological approach would then be to consider the effects of non-Newtonian flow in the upper levels of the adsorbed multilayers.

These latter possibilities pin-point the need to know precisely how far the influence of the solid surface extends in systems in which $\phi \neq 0$; just how thick are

the adsorbed films left behind by a consecutive flow interface?

C H A P T E R S I X

Microcapillary Studies

Introduction

Benzene-water displacements were conducted in two Pyrex capillaries of nominally 2 and 10μ radius. They were done primarily to determine the magnitude of any "wall effect" upon liquid viscosity and interfacial tension as measured in tubes of this size. The extensive work in this field by Derjaguin and Fedyakin[65,141,142] has aroused a good deal of controversy, and it was therefore of the utmost importance that any results obtained should be capable of unambiguous interpretation. To this end, a considerable effort was made to ensure that capillary radii were known with the maximum precision. In addition, the glass surface was prepared using a technique which, it is believed, almost totally eliminates uncertainties arising from contact angle hysteresis and velocity dependence by ensuring that the capillary wall is completely wetted by water.

The experimental techniques used are described here in some detail, since neither Derjaguin nor Fedyakin gives an adequate account of the methods used to produce and examine microcapillaries.

6.1 Production and Calibration of Microcapillaries

Drawing the Capillaries

A length of 5 cm diam., heavy-walled, Pyrex tubing was worked in a lathe using a large hot flame until a section of capillary was produced having an internal diameter of 1 to 2 mm, an external diameter of about 3 cm and a length of between 4 and 6 cm. A smaller flame was then concentrated on the central section of the capillary until the channel was barely visible to the naked eye. At this point, which was determined only after much practice, the lathe was stopped and one end of the tube was released and withdrawn to a distance of about 10 feet. The resulting capillary was cut into convenient sealed lengths and stored for future use.

Capillaries produced in this way had internal diameters of anything up to 50μ tapering away to less than 1μ. Outside diameters, however, were usually several millimeters. Heavy-walled capillaries were deliberately produced for mechanical strength.

Basic Calibration Technique

None of the microcapillaries was of perfectly uniform bore. Thus, although, in most cases, the variation was less than 1% in 100 diameters, it was necessary to obtain the radius of the microcapillary at every point along its length in order to interpret the results of subsequent

displacement studies with the maximum precision.

The method adopted was based upon that described by Fedyakin[142]. A length of microcapillary is formed in such a way that it terminates in a closed space like a thermometer bulb. The tube is then evacuated and filled with water. If the volume of the bulb is known then, given the specific volume of water as a function of temperature, it is possible to calculate the volume of liquid displaced from the bulb as a result of thermal expansion. Determination of the position of the water meniscus in the capillary as a function of bulb temperature then permits the calculation of the cross-sectional area of the tube. If this is assumed circular in section then its radius may be obtained.

Blowing and Filling Bulbs.

A length of between 2 and 4 cm was cut from a selected microcapillary and sealed at one end. The open end was connected to a cylinder of compressed argon. A pressure of between 10 and 30 lb. in^{-2} (according to the thickness of the capillary wall) was applied to the capillary and its closed end was softened with a small flame applied axially and evenly from all sides. If this was done correctly, the capillary opened out into a small, nearly spherical bulb of suitable capacity. This capacity was judged to be such that, during calibration, a change in temperature of about 10°C would cause an approximately

1 cm displacement of the meniscus. The coefficient of cubical expansion of water at 25°C is approximately 0.3×10^{-3} deg^{-1} so that, as a rough guide, the desired capacity is about $10^3 r^2 cm^3$, i.e. for a 1μ rad. capillary approximately 10^{-5} cm^3..

Several tubes were prepared in this way and built into the apparatus shown in Fig. 6.1. The system was evacuated, and conductivity water (prepared as described in section 4.2) was outgassed in the reservoir. Whilst still under vacuum, the reservoir and tube container were sealed off and removed from the remainder of the system at the constriction. The water was tipped into the tube container which was then opened restoring atmospheric pressure and forcing water into the capillaries until all bulbs were completely filled.

The Thermistor

A Standard Telephone and Cables (STC), No. F23 thermistor was used to monitor bulb temperature in place of the thermocouple used by Fedyakin. It was connected in series with a 1,000Ω ($\pm$1Ω) standard resistance (Sullivan) and the circuit was completed by a 2 volt accumulator (Exide DTP). The resistance of the thermistor, R_t was determined by comparing the potential drop across it, E_t, with that across the standard resistance, E_s, using a Pye 0 to 1.7 volt potentiometer graduated in divisions of 10^{-4} volt. If the standard resistance is taken to be

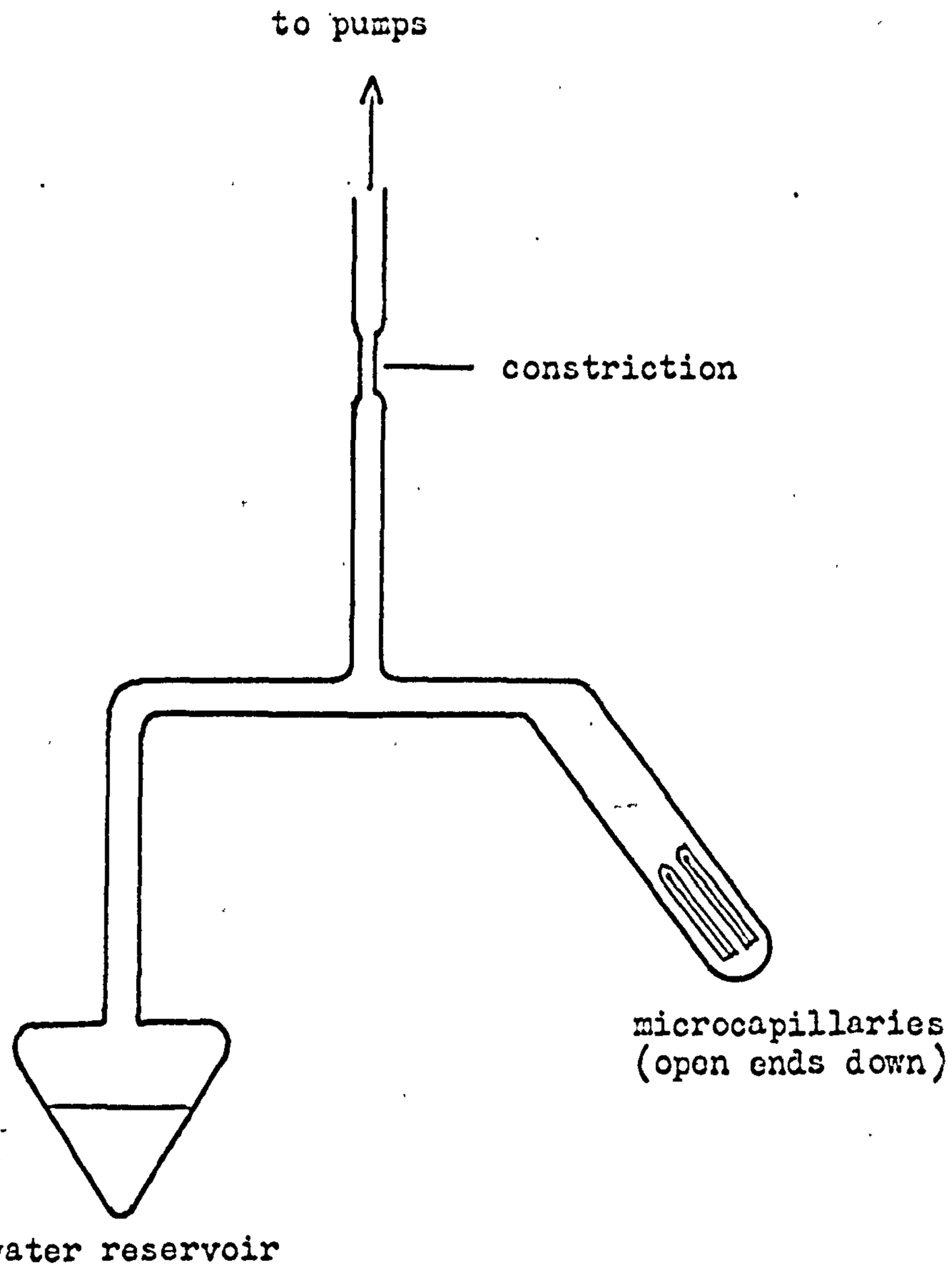
to pumps
constriction
microcapillaries
(open ends down)
water reservoir

Fig. 6.1

exactly 1000Ω then R_t is given by

$$R_t = \frac{E_t}{E_s} \times 1000 \qquad 6.1\text{-}1$$

Before use the thermistor was aged for two days at 80°C and 4x normal loading (0.5 to 1 milliwatt), and then calibrated over the temperature range 0 to 50°C against N.P.L. standardised thermometers which were read with a cathetometer to the nearest 0.01°C. The calibration was also checked at the ice point. As expected, R_t varied with the absolute temperature, T, according to the equation:

$$\log R_t = \log a + {}^{b}/_{T} \qquad 6.1\text{-}2$$

The constants, a and b, were determined by a least squares fit of $\log R_t$ as a linear function of ${}^{1}/_{T}$ using a digital computer. The values obtained were

$$a = 6.9904\ (\pm 0.0027) \times 10^{-2}$$

and $$b = 1284.17\ (\pm 0.03)^{\circ}K$$

Over the range of calibration, the thermistor was reliable for measuring absolute temperatures to within ±0.01°C and temperature differences to within ±0.005°C. The calibration was checked after the thermistor had been in continuous operation for some weeks. No significant drift was detected.

Assembling the Calibration Apparatus

A fine scratch mark was made near the middle of a selected microcapillary. The bulb of the latter was then inserted into the small mercury filled jacket shown in Fig. 6.2 so that it was in contact with the tip of the

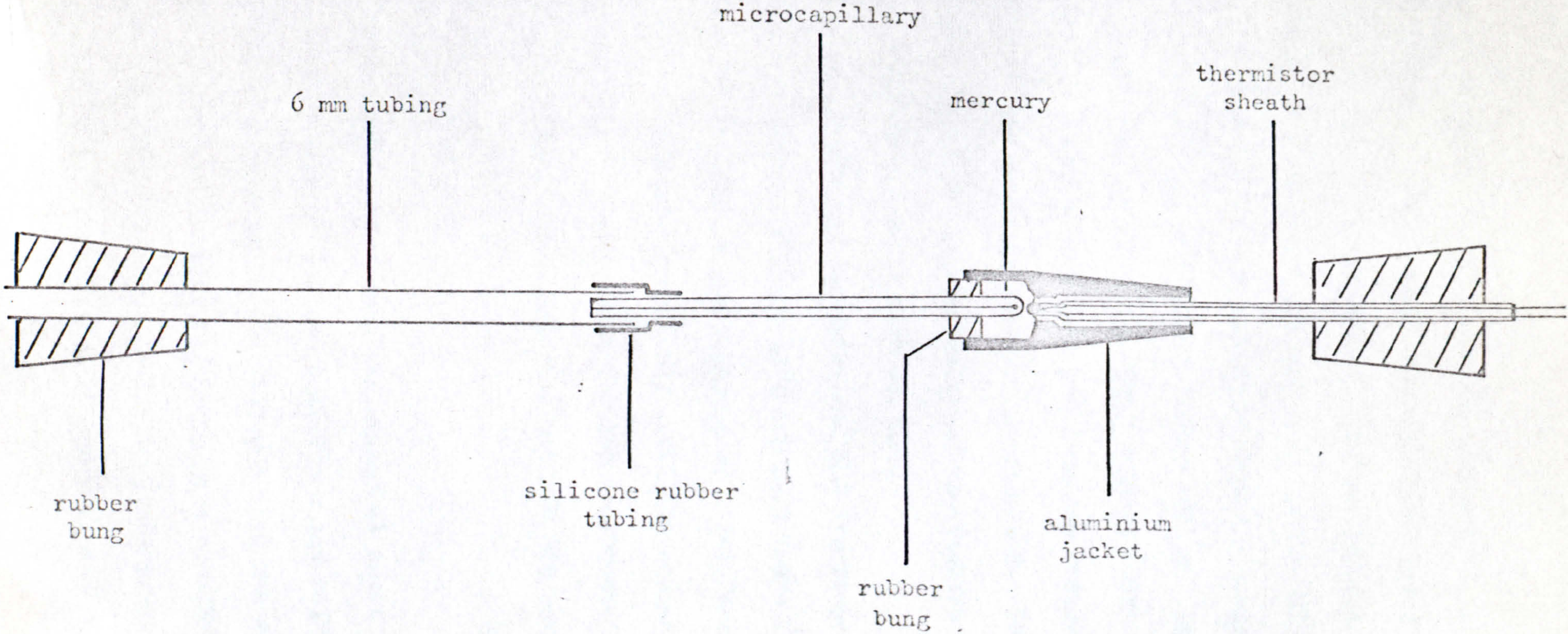

Fig. 6.2 Microcapillary calibration assembly

thermistor cemented in position at the far end. The jacket was made of aluminium for rapid thermal conduction and sprayed with a thin layer of PTFE to prevent corrosion.

A length of 6 mm glass tubing was slipped a little way over the open end of the microcapillary and sealed to it with a short length of silicone rubber tubing. Two concentrically bored rubber bungs were used to mount the microcapillary (scratch mark upwards) into the thermostatically controlled cell described in Section 4.2. This was then secured to the adapted stage of the Vickers microscope also described in that section.

Glycerol circulation was commenced, and the temperature of the cell was raised to about 45°C and held there for an arbitary period to expel a small amount of water from the capillary. The cell was then cooled until the meniscus reached a suitable starting point for the calibration (usually a few tenths of a millimetre outside the thermistor jacket).

Measurements

The temperature of the cell was raised at about 0.1°C per min. As the water in the microcapillary and bulb expanded, the moving meniscus was followed with the microscope and a record was kept of: (i) the time at which a measurement was made; (ii) the potential differences E_t and E_s; and (iii) the position of the meniscus relative

to the scratch mark, X'. The last was determined compositely using a calibrated graticule and the microscope-stage scale and vernier. In this way distances down to 0.01 cm were measurable to within ±0.5%. Corresponding values of E_t, E_s and X' were obtained later by linear interpolation against time.

The meniscus was usually followed a distance of 1.5 to 2.5 cm from the starting point, X'_o. Heating was then stopped and the calibration process repeated, but this time with the capillary cooling at about 0.1 °C per min., until the meniscus reached X'_o once more.

To minimise errors due to backlash in the stage drive and mountings, X' was always measured with the microscope cross wires apprcaching the meniscus in the same direction irrespective of whether the system was warming or cooling. In spite of this precaution, during the calibration of the first microcapillary, a small difference (0.02 cm) was found in the position of the interface at the starting temperature before and after the first warming/cooling cycle. This small difference corresponded to a slight loss of water and was therefore attributed to evaporation. In subsequent calibrations, the difficulty was overcome by inserting a few drops of water into the 6 mm tubing.

Determination of Bulb Volume

The microcapillary was pulled from the thermistor

jacket, and, with magnification and illumination suitably adjusted, the bulb was photographed through the microscope using the 35 mm camera attachment supplied by Vickers. The bulb was then rotated through approximately 45° and re-photographed. This procedure was repeated twice more to produce a total rotation of 180°. In addition, a slide graduated in divisions of 0.005 cm was photographed at the same magnification in two mutually perpendicular orientations. Finally, the position of the closed end of the bulb was determined relative to the scratch mark.

The processed film was projected on to a drafting table covered with graph paper (see Section 4.2). For each photograph, the width of the projected image of the bulb, 2y', was measured as a function of x', the distance from the closed end of the bulb. In this way four values of y' were obtained for each value of x'. Variations within each set of y' were usually less than 5% indicating that the bulbs were, to a modest approximation, cylindrically symmetrical about the x" axis. Plate 7 shows two typical images, one photographed at 90° to the other (magnification x 54).

The square root of the product of each set of y" values was plotted against x' and the resulting curve was integrated by weighing. Multiplication by π and a scaling factor gave the bulb volume V_{bulb}. The appropriate scaling factor was found by calibrating the graph paper used on the drafting

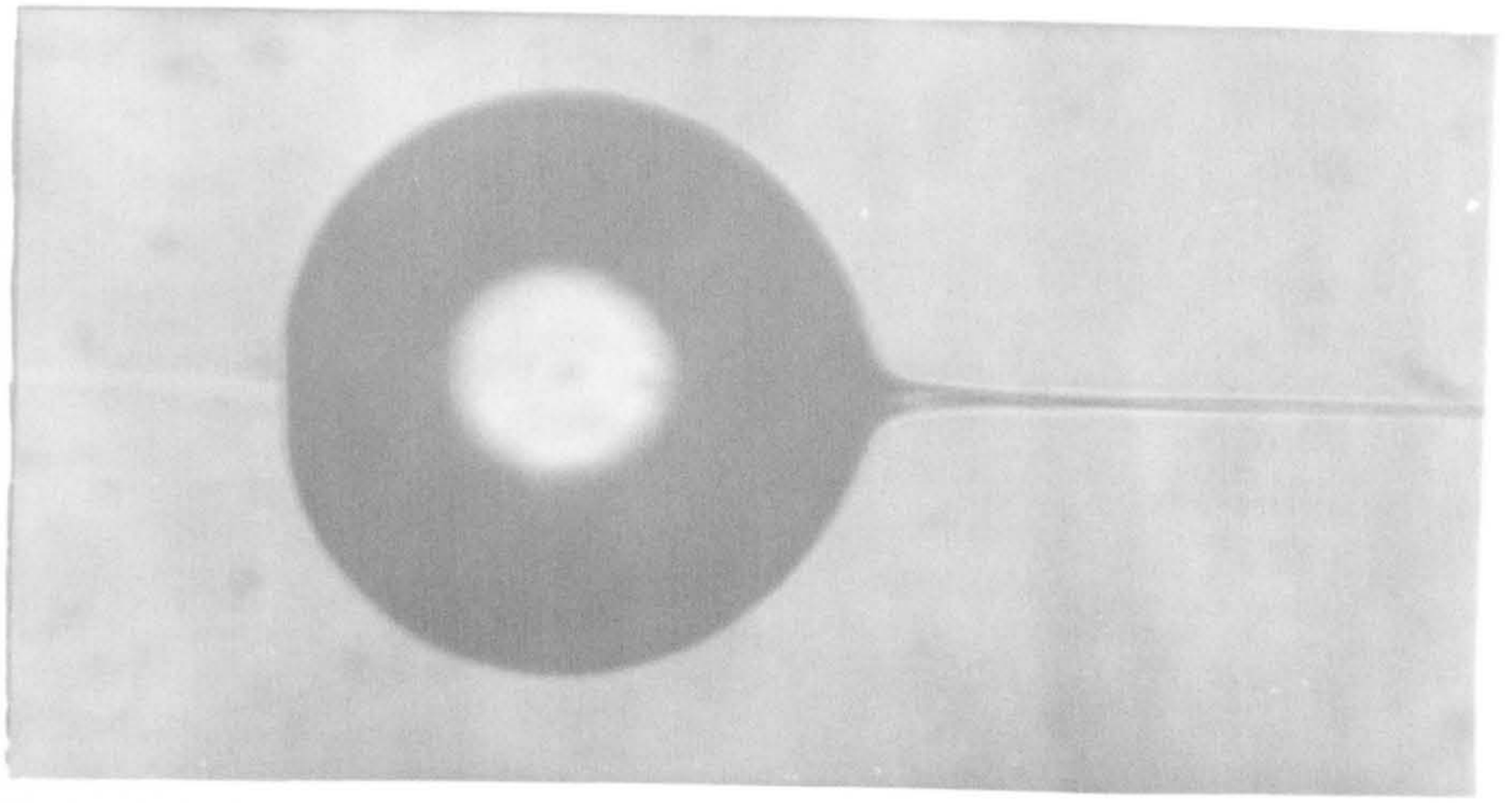

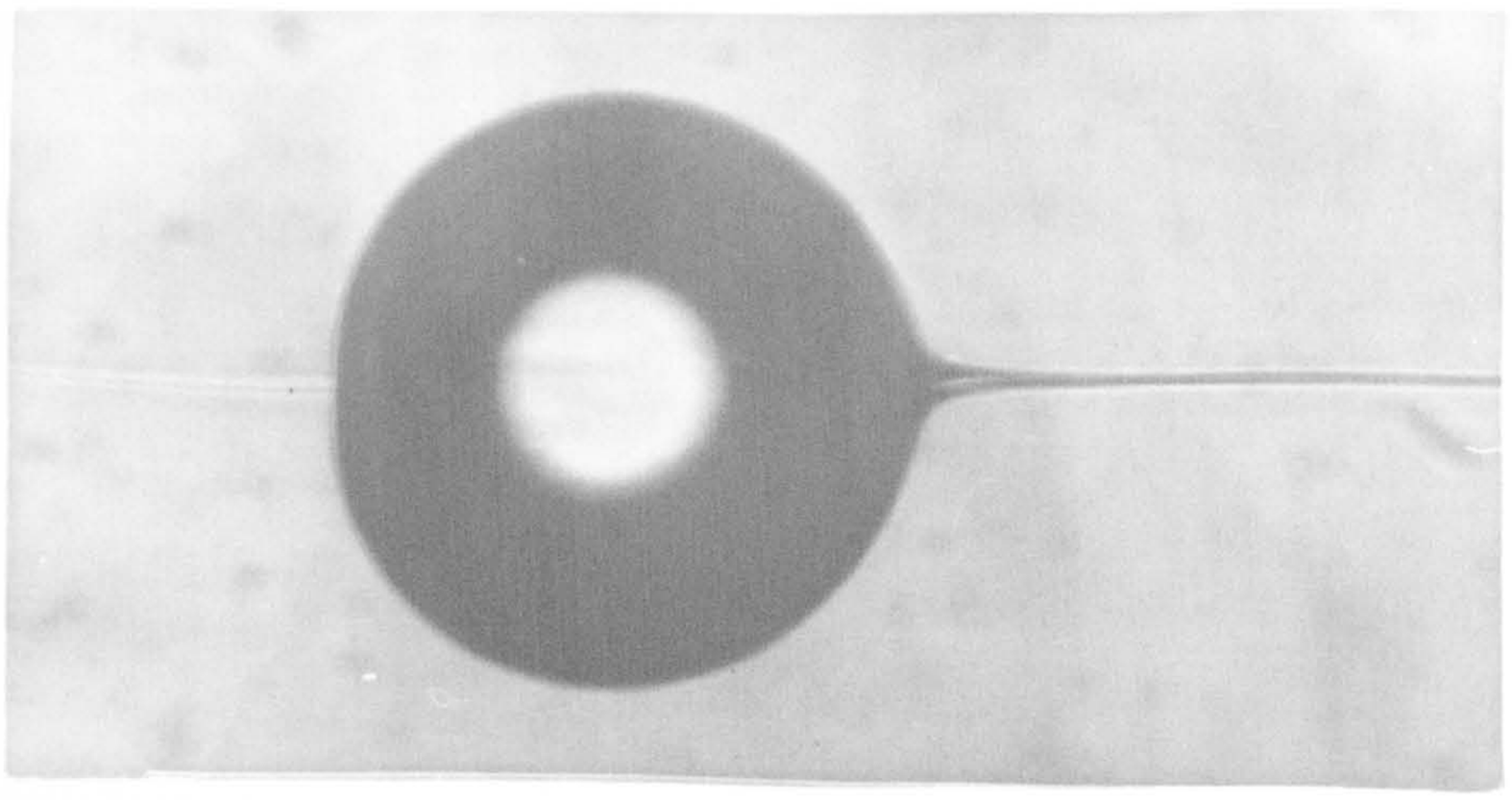

PLATE 7

table against the two projected images of the graduated slide.

As an accuracy check the "sectioning" method, described above, was used to calibrate the bulb of a capillary of nominally 20μbore. The value obtained was $1.79(5) \times 10^{-3}$ cm^3. The bulb was then cut from the capillary and weighed, first empty, and then after it had been filled with mercury using a commercial porosimetry apparatus. The difference in weights (0.0243(2) gm) divided by the appropriate density of mercury gave the capacity of the bulb as $1.795(\pm 0.005) \times 10^{-3}$ cm^3. Such close agreement, though gratifying, was somewhat surprising in view of the numerous stages and the several approximate methods inherent to the sectioning technique. The estimated error on the latter method is $\pm 1.5\%$ for a cylindrically symmetrical bulb. This value was arrived at on the assumption that by far the largest errors ($\pm 0.5\%$) were introduced in the measurement of x' and y'. If the bulb is not cylindrically symmetrical then the total error on V_{bulb} could be much greater.

In passing, it may be noted that the weighing technique would be unsuitable for bulbs of less than 10^{-4} cm^3 unless an exceptionally sensitive balance were used and the wall of the tube made extremely thin.

Calculation of Capillary Radius

Eqs. 6.1-1 and 6.1-2 were used to calculate the

temperature appropriate to each experimentally determined position of the meniscus, $X = X' - X'_o$.

The specific volume of water, v_w as a function of temperature was obtained from the Tilton-Taylor equation[163].

$$v_w = \frac{508929.2(T + 68.12963)}{1 - (T - 3.9863)^2(T + 288.9414)} \qquad 6.1\text{-}3$$

where T is in ^oC. This equation is accurate in the range 0-42^oC to one part in 10^6. The effect of dissolved air is negligible[163].

An approximate value of the tube radius (from direct microscopic measurement) was used to calculate the volume of water in the microcapillary alone when X = 0. This was never more than 1% of V_{bulb} and was added to the latter to give V_o, the total volume of water present when X = 0. It was then possible to calculate V, the total volume of water present for all other values of X using

$$V = V_o \frac{v_w}{v_{wo}} \qquad 6.1\text{-}4$$

where v_{wo} is the specific volume of water at the temperature for which X = 0.

Figs. 6.3a and 6.3b show plots of V against X for the two micro capillaries subsequently used in displacement studies. If each tube is assumed circular in section then its radius is given by

$$r = \sqrt{\frac{1}{\pi}\frac{dV}{dX}} \qquad 6.1\text{-}5$$

(The coefficient of cubical expansion of Pyrex glass used for the microcapillaries is less than 0.3% that of water

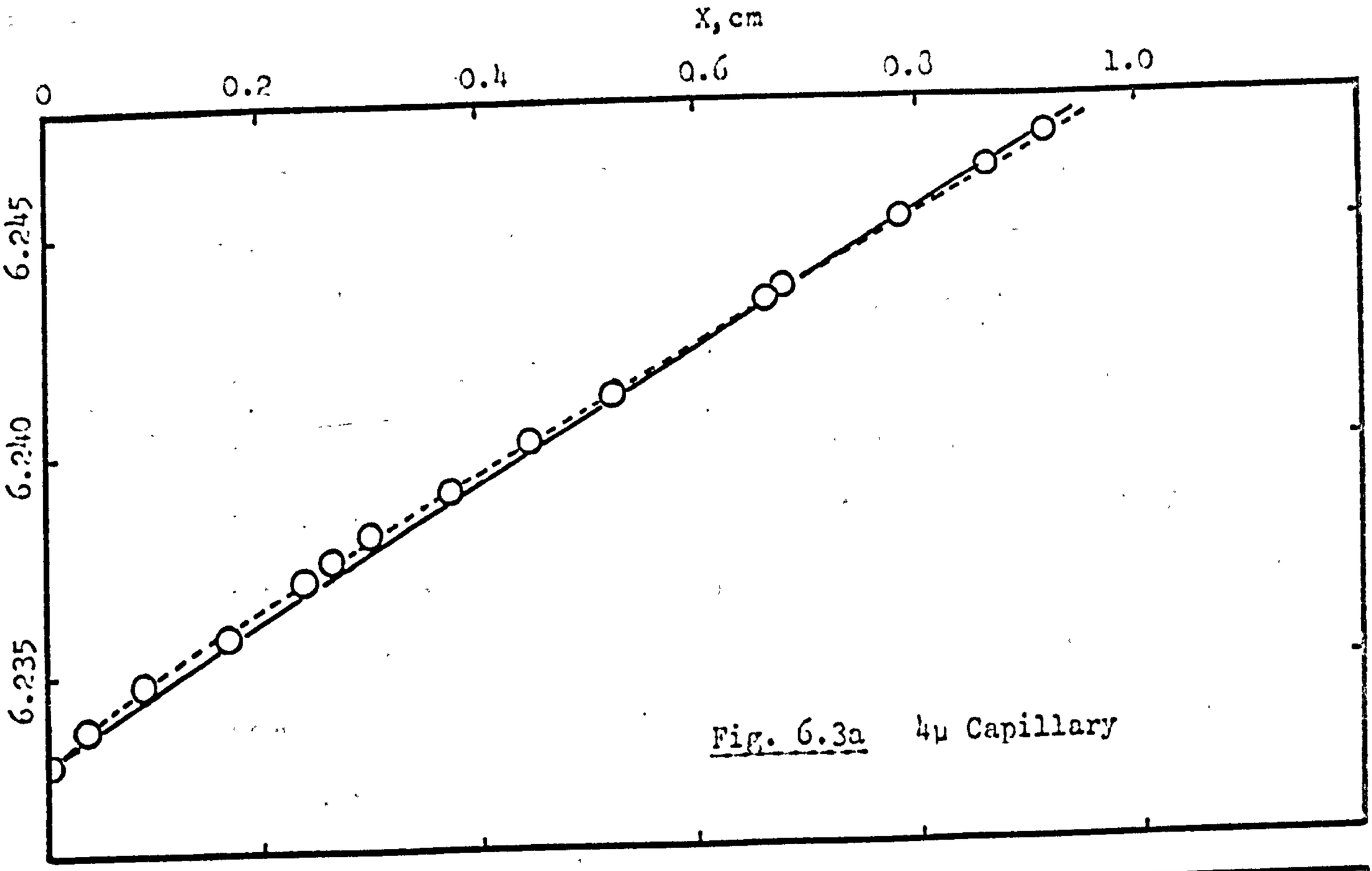

Fig. 6.3a 4μ Capillary

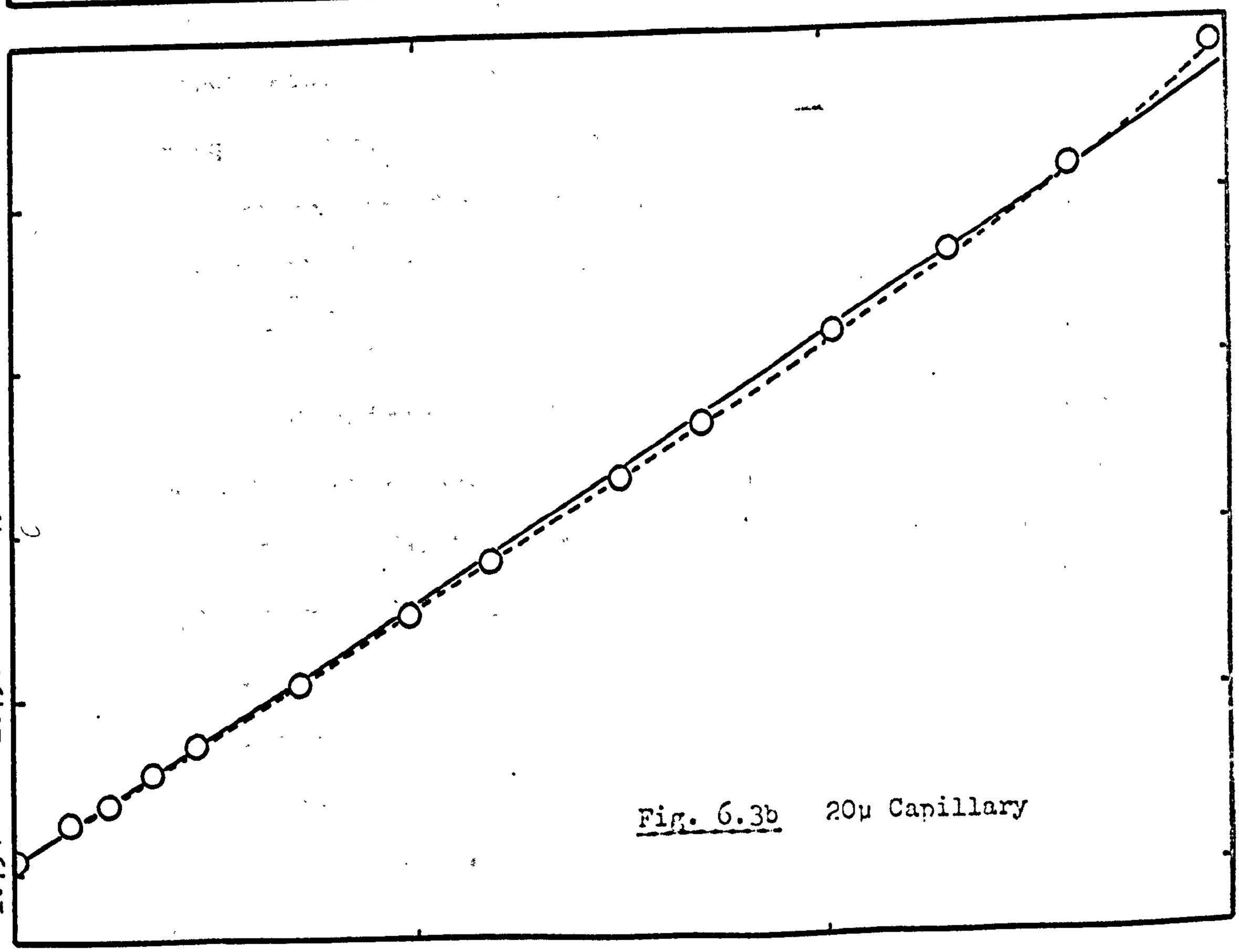

Fig. 6.3b 20μ Capillary

and can, therefore, be neglected). The graphs deviate only slightly, but, nevertheless, significantly, from a straight line (solid line in Figs. 6.3), and differentiation by tangent drawing would be difficult to perform with any accuracy. Accordingly, a digital computer was programmed to fit the data to a suitable polynomial, $V = V(X)$, by the method of least squares, and then to evaluate the first differential to obtain r. The order of the polynomial was chosen by inspection of trial runs on each set of data. The lowest order was chosen, consistent with a small standard deviation and sensible behaviour both inside and outside the range of input data. In all cases a cubic expansion was found adequate (dotted line in Figs. 6.3).

After curve fitting the computer tabulated values of r and $\sum_{X=0}^{X} \frac{\delta X}{r^4}$ for values of X at 0.1 cm intervals between zero and the maximum value of X. The summations were evaluated in increments of 0.001 cm. and, to a good approximation, provided solutions to the integrals $\int \frac{dx}{r^4}$ in Eq. 6.4-1 (see later). Tables 6.1 and 6.2 give the computer output for the two microcapillaries used in displacement studies.

An estimate was made of the probable error on any value of r by assuming that uncertainties in the measurement of bulb temperature were negligible, and that the only significant errors were those introduced in the determination of V_o and X. If the uncertainty on V_o is placed at $\pm 2\%$ and

that upon any value of X and ±1% (maximum), then, assuming that the curve-fitting technique is efficient in smoothing random errors in X, the uncertainty upon r is probably slightly less than ±1%. If this is so then the summations $\sum_{X=0}^{X} \frac{\delta X}{r^4}$ will be within ±4% of their true value.

6.2 Surface Treatment

During the development of the silane treatment used in Exps. E1 and E2, it was observed that if cleaning and rehydroxylation were carried out as described, but exposure to silane vapour was omitted, then the resulting capillary was completely wetted by water. Indeed the observed contact angle remained indistinguishable from 0° for all velocities between ±1 mm sec^{-1}. Moreover capillary treated in this way was singularly resistant to contamination. It was therefore decided to adapt this method for use with micro-capillaries.

Treatment was carried out using the apparatus shown in Fig. 6.4.

A calibrated section of microcapillary was slid, in a known orientation, into a sheath consisting essentially of a 30 cm length of 9 mm Pyrex tubing. The microcapillary was lodged at a narrow, slightly tapering, section some 12 cm from the closed end. Constriction C was made near the open end which was then connected to the remainder of

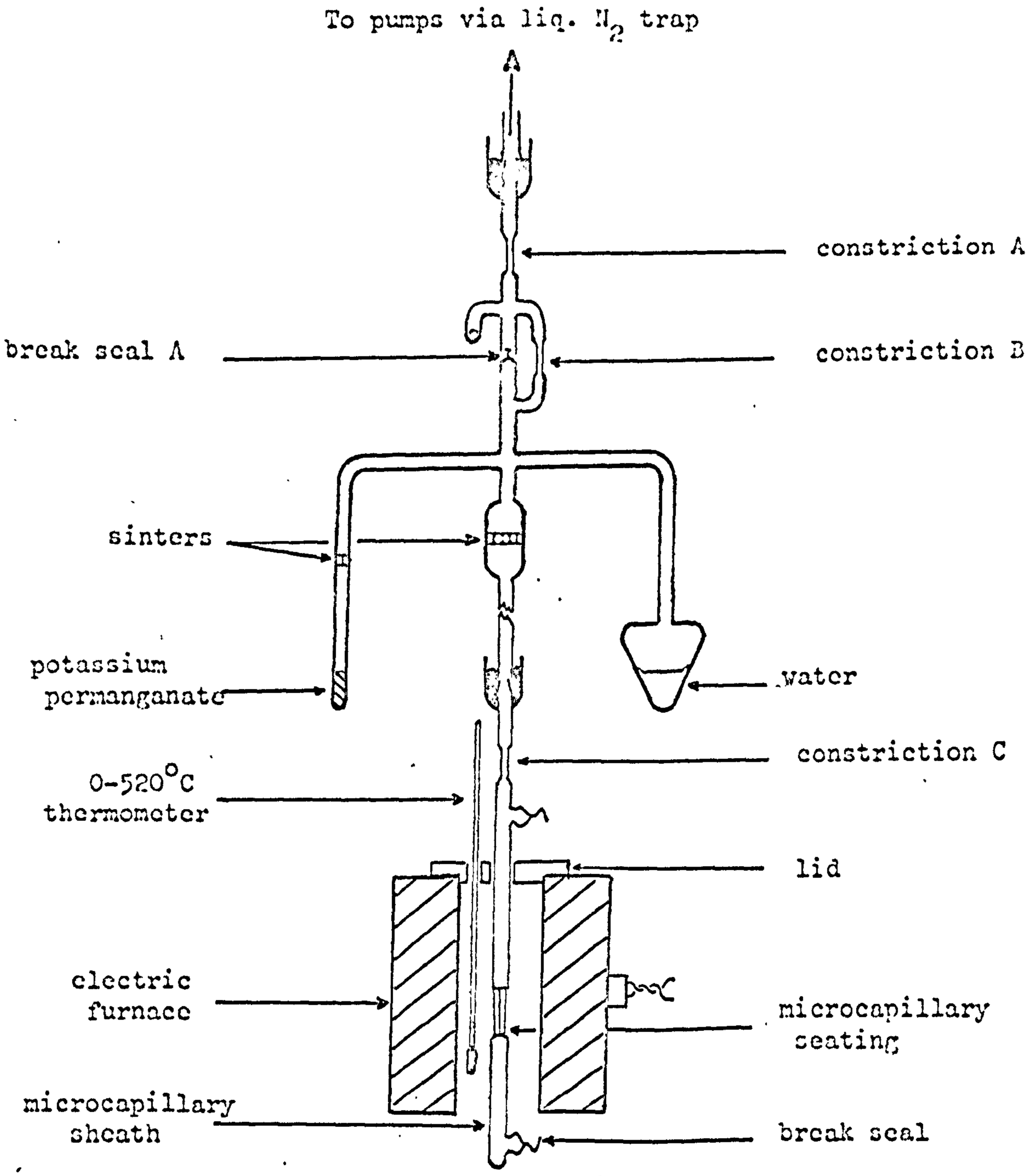
To pumps via liq. N_2 trap
A
constriction A
break seal A
constriction B
sinters
potassium permanganate
water
constriction C
0-520°C thermometer
lid
electric furnace
microcapillary seating
microcapillary sheath
break seal

Fig. 6.4

the apparatus,

After outgassing the conductivity water and evacuating the system for 1 hour, constriction A was sealed, and a low pressure of oxygen was generated by cautiously heating the potassium permanganate (0.5 gm). Two sintered glass discs (Joblings No. 4) prevented solid decomposition products from reaching the capillary. The latter was then heated to 510°C and maintained at that temperature for at least two hours to oxidise organic contamination. After evacuation via break seal A, the furnace was lowered, and a small flame was evenly applied to the microcapillary seating until the latter could be seen to constrict tightly around the microcapillary - thus providing it with two wide bore connections. Rehydroxylation was carried out overnight after closing constriction B, and, finally, the sheath was sealed off and removed from the vacuum system at constriction C.

6.3 Benzene-Water Displacements

The mutually saturated benzene and water used in these studies were prepared as described in Section 4.2. The liquids were introduced into the capillaries as follows: firstly, the ends of the evacuated microcapillary sheath were flamed clean, then one seal was broken under benzene, the other under water. In this way a benzene/water interface was formed with only a minimal risk of

contamination.

Two accurately bored rubber bungs were used to mount the microcapillary sheath into the thermostatically controlled cell as shown in Fig. 6.5. The cell was secured to the modified stage of the microscope and connected to the glycerol circulation system.

The manometer assembly shown in Fig. 6.6 was used to monitor the displacement pressure, Δp. It was connected to the benzene side of the sheath and comprised both water and mercury manometers, although only the latter was used with the 4μ bore capillary. The range of displacement pressures was set by opening tap A to a compressed air supply, and final adjustments were made by raising or lowering the mercury reservoir.

Displacements were performed at two, well spaced positions in each capillary. The exact locations were determined relative to one end of the tube to within ± 0.005 cm using the stage scale and vernier.

The interface was viewed through the microscope and velocity measurements were made by timing the interface between two divisions of a calibrated graticule. Times ranged between 1.5 and 30 sec. and were measured using a hand-operated stop watch to within 0.1 sec. Recorded velocities were the average of at least three separate displacements at the same Δp. Between such displacements, the

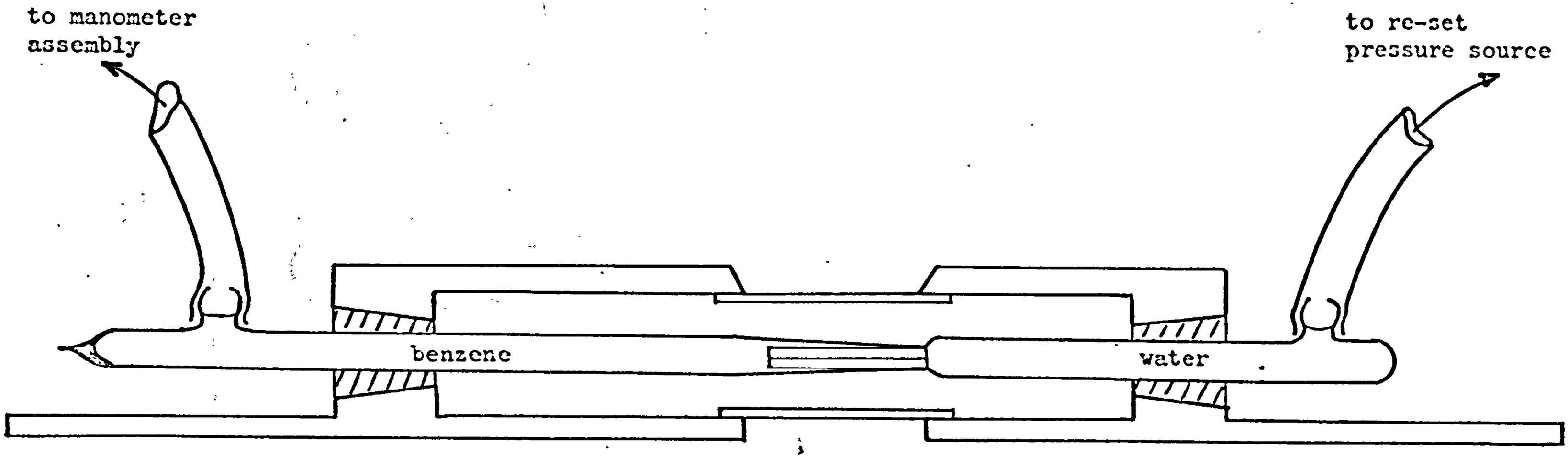

Fig. 6.5 Microcapillary assembly in cell

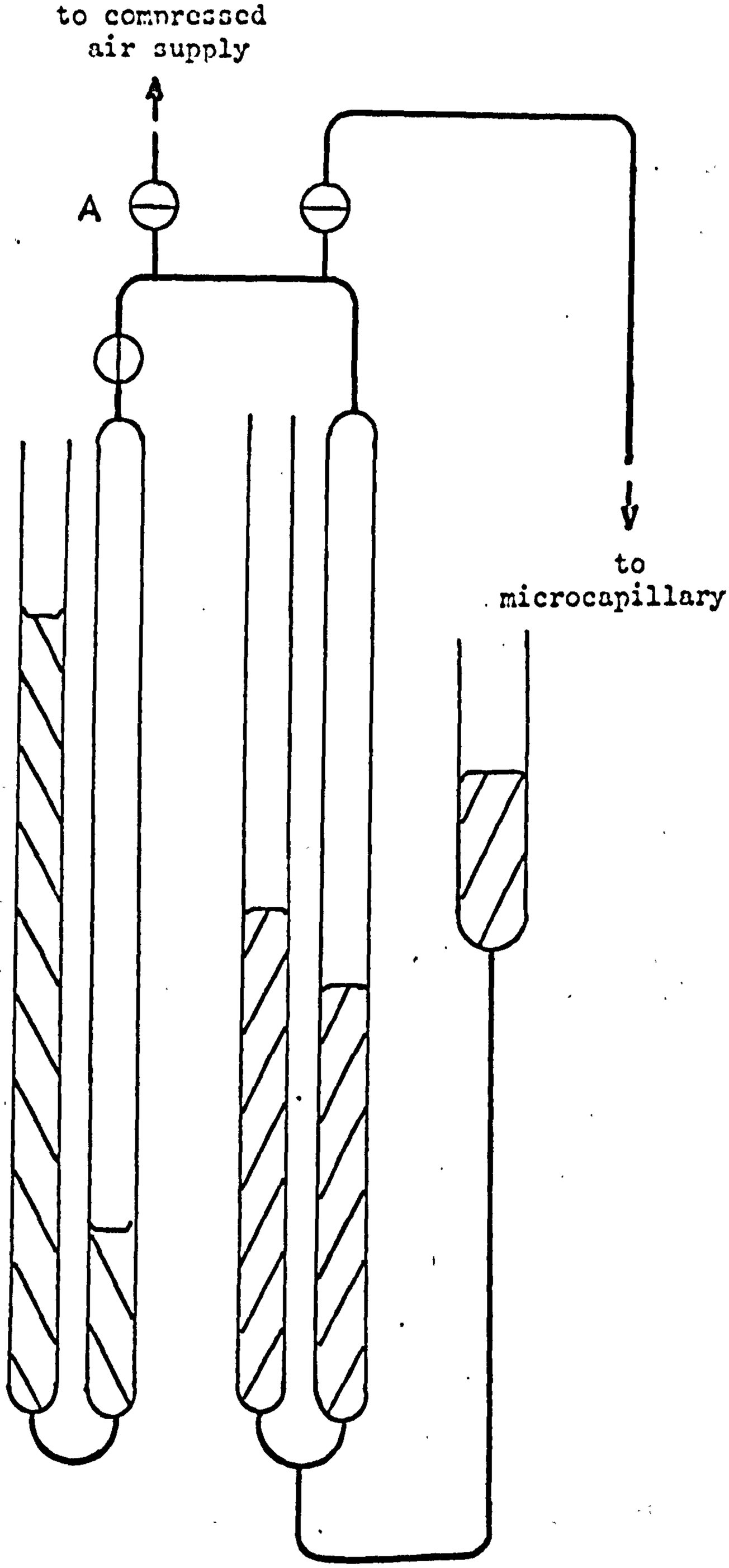

Fig. 6.6

meniscus was returned to the starting point by applying a slight pressure or suction to the water side of the sheath - thus avoiding the need to alter the pressure on the manometer side.

When determining Δp either the mercury manometer was read to the nearest 0.01 cm using a cathetometer, or the water manometer was read to the nearest 0.05 cm using a mirror scale.

The data obtained are shown in Tables 6.3 and 6.4.

6.4 Results and Discussion

The modified form of Eq. 3.3-2 for displacements in long capillaries of slightly varying diameter is

$$\dot{x} = \frac{\Delta p - 2\sigma_{12} \, r \cos \phi}{8r^2 \left[\eta_1 \int_0^x \frac{dx}{r^4} + \eta_2 \int_x^1 \frac{dx}{r^4} \right]} \qquad 6.4\text{-}1$$

A plot of $\dot{x}$ against Δp should therefore give a straight line of slope:

$$\frac{d(\Delta p)}{d\dot{x}} = 8r^2 \left[\eta_1 \int_0^x \frac{dx}{r^4} + \eta_2 \int_x^1 \frac{dx}{r^4} \right] \qquad 6.4\text{-}2$$

having a zero velocity intercept $\left(\frac{2\sigma_{12} \cos \phi}{r} \right)$

Figs. 6.7 and 6.8 show the data obtained with capillaries of respectively 2 and 10μ radius, plotted according to Eq. 6.4-1. The graphs show the expected linear relationship between $\dot{x}$ and Δp, and, furthermore, only small steps on the Δp-axis. There is thus no

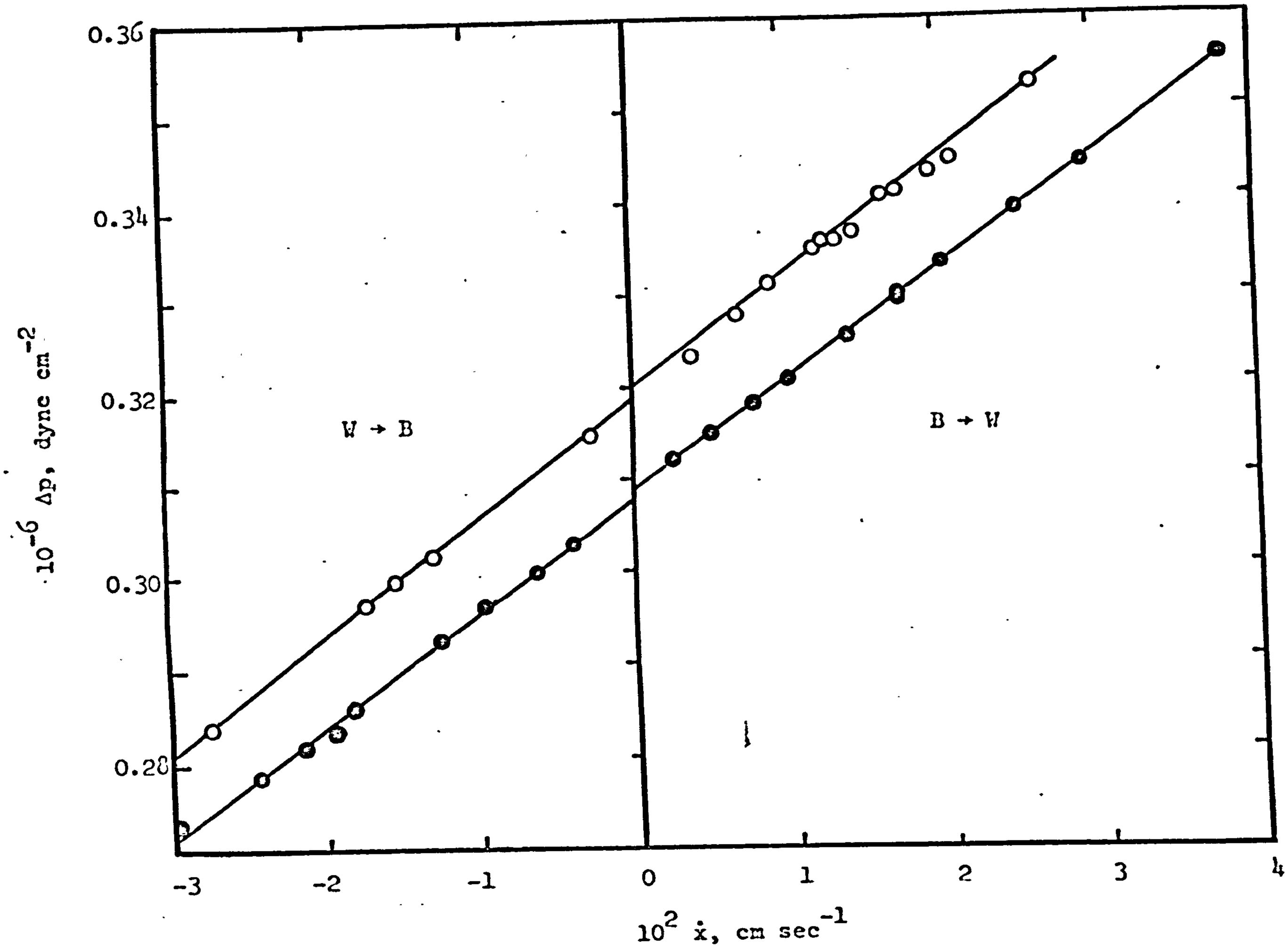

Fig. 6.7 O Run (i); ● Run (ii)

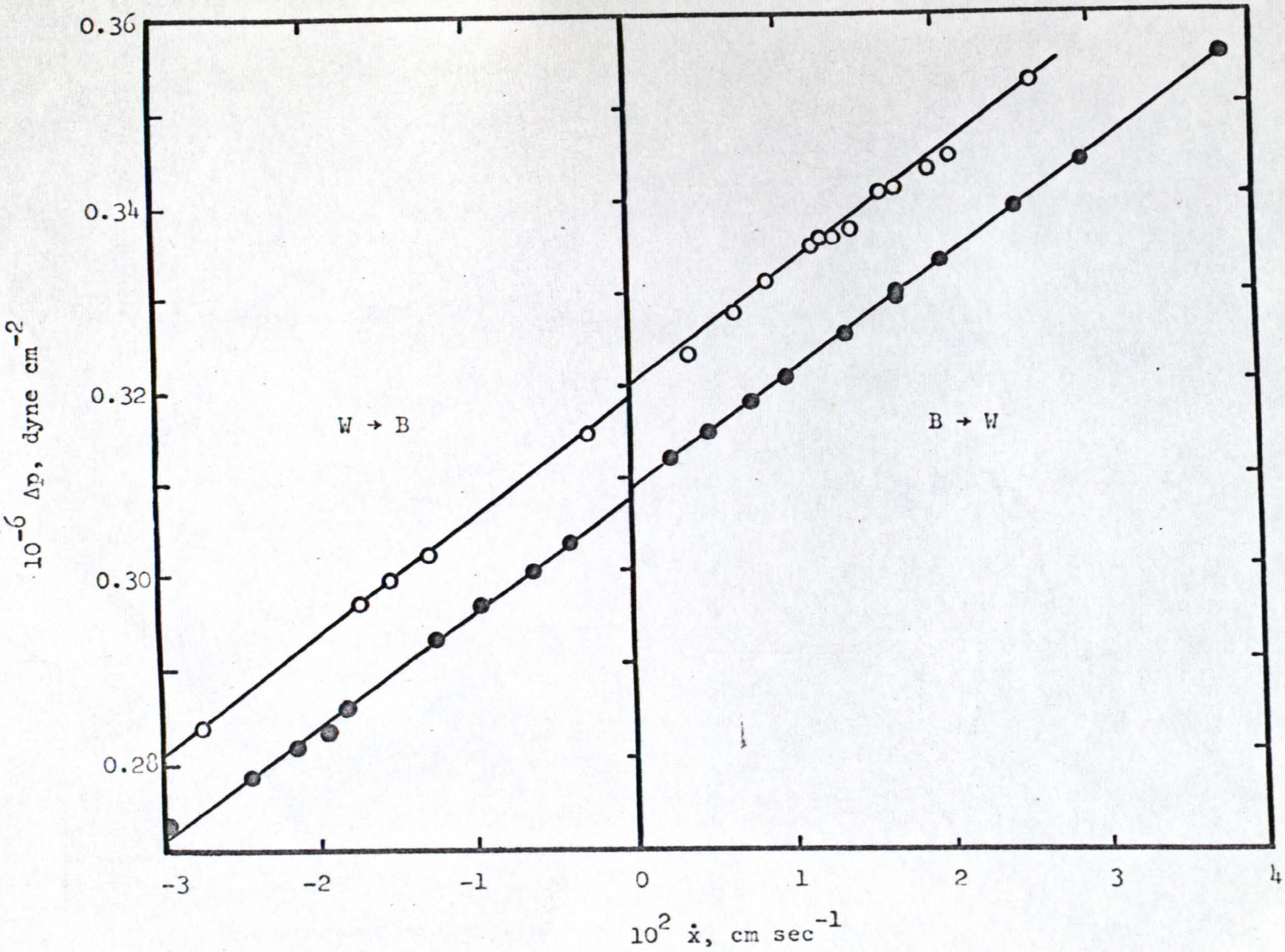

Fig. 6.7 ○ Run (i); ● Run (ii)

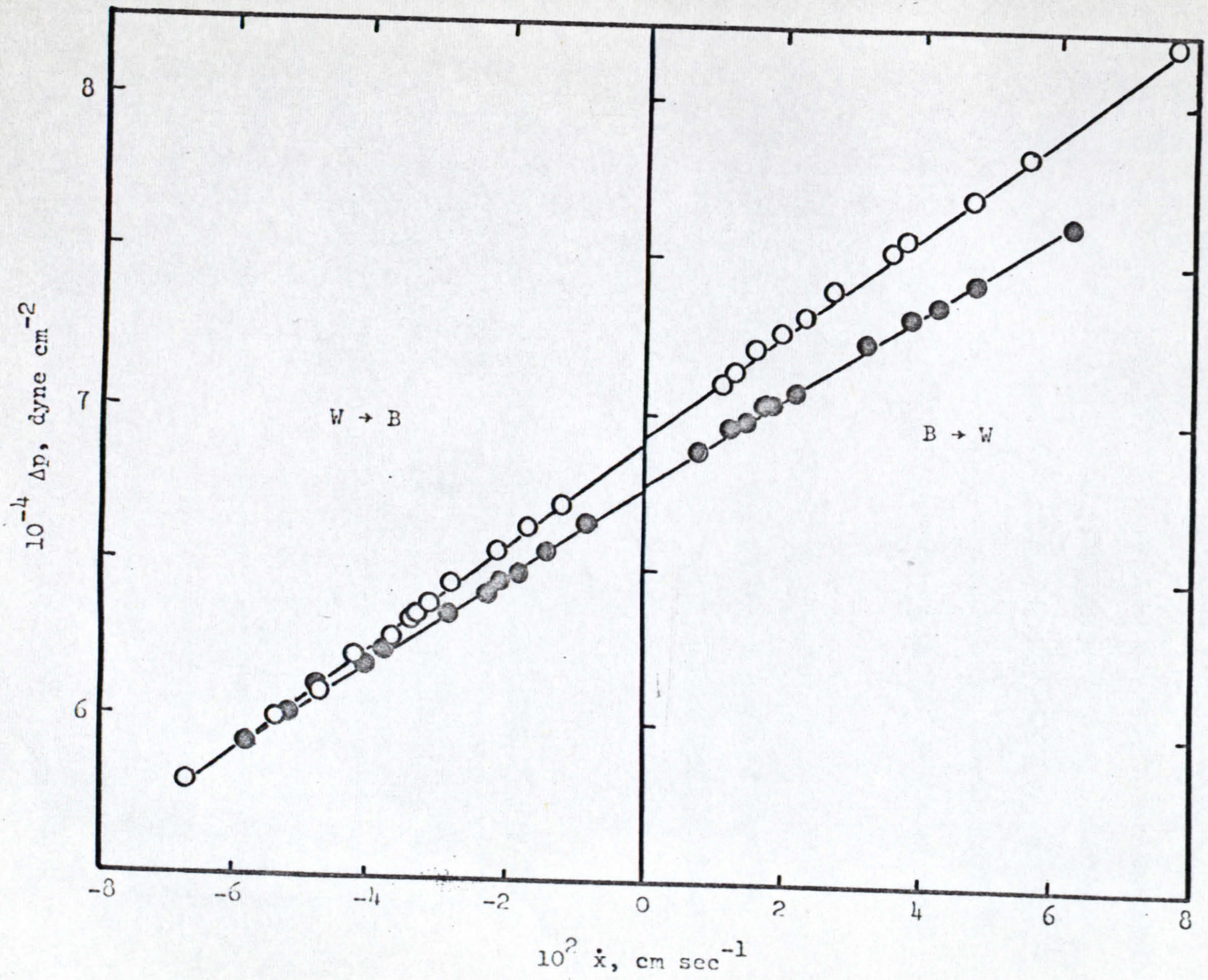

Fig. 6.8 ○ Run (i); ● Run (ii)

indication of significant contact angle velocity dependence or hysteresis. On the other hand, the use of Eq. 6.4-2 is open to the objection that if, as is assumed, the tube is completely wetted by water then the type of flow to be considered is concentric and not consecutive flow. However, providing $\frac{n\dot{x}}{\sigma} \ll 1$ this should present no additional problems. In fact, in these experiments, $\frac{n\dot{x}}{\sigma}$ was never greater than 2.3×10^{-4}. Slopes and intercepts were determined by the method of least squares.

Table 6.5 lists values of σ_{12} derived from the zero velocity intercepts, assuming $\cos \phi = 1$, together with the published value[147] and that obtained from a parallel, drop-weight experiment (Section 4.2).

TABLE 6.5: Benzene/Water Interfacial Tensions, σ_{12} dyne cm^{-1}

ICT[147] value	35.0	From Intercepts		
Drop-Weight value	34.9 ± 0.2	Run	W→B	B→W
20μ bore capillary		(i)	34.5	34.6
		(ii)	34.4	34.5
4μ bore capillary		(i)	34.9	35.0
		(ii)	34.8	34.9

Cohan and Meyer[165] have determined the surface tension of water and toluene in capillaries of similar bore. Whilst they were not able to detect any variation from the norm,

their accuracy was poor ($\pm 5\%$). In the present work, the values of σ_{12} found with the 20μ capillary are approximately 1% low; however, those obtained using the 4μ bore capillary are indistinguishable from the accepted value.

Table 6.6 shows both the experimental slopes and those predicted by Eq. 5.4-2 using values of r and $\int \frac{dx}{r^4}$ taken from Tables 6.1 and 6.2, and assuming that the viscosities of benzene and water (η_1 and η_2 respectively) have their normal bulk values[147].

TABLE 6.6: Slopes: $\frac{d(\Delta p)}{dt}$, dyne sec cm^{-3}

	Run	Predicted	Experimental	
			W→B	B→W
20μ bore capillary	(i)	1.488×10^5	1.514×10^5	1.478×10^5
	(ii)	1.262×10^5	1.272×10^5	1.236×10^5
4μ bore capillary	(i)	1.277×10^6	1.279×10^6	1.246×10^6
	(ii)	1.191×10^6	1.204×10^6	1.220×10^6

Correlation between experimental and predicted values is good, particularly so in the case of water displacing benzene (W→B). Such close agreement is, however, surprising. If the error estimates arrived at in Section 6.1 are realistic then a scatter of up to $\pm 7\%$ is to be expected. The fact that variations are nowhere greater than 2.1% suggests that the estimated uncertainty upon r ($\pm 1\%$) is too high.

A more appropriate value would seem to be ±0.3% (i.e. ± 60Å for r = 2μ)! The Fedyakin calibration technique is thus potentially very precise. By way of comparison, direct measurement of tube radius using conventional microscopy[138,139] cannot provide greater precision than ±0.1μ , i.e. the limits of resolution of the best optical microscopes[166].

One objection to the Fedyakin technique is that thick, disjoining pressure stabilized films may form on the capillary wall during calibration. Read and Kitchener[63], for example, report thick (0.1μ) stable films of dilute (2×10^{-5} M) aqueous electrolyte on carefully cleaned silica surfaces. Such films could produce large underestimates of microcapillary radii. Moreover, possible long-term corrosive attack by water[162], and gel formation, in the case of glass capillaries rich in Na_2O, produce additional uncertainties. In the present work, however, these effects appear to be either unimportant or fully compensated for by other, unsuspected phenomena.

In order to extract the maximum information from the results, the experimental slopes obtained at two points in the same tube have been combined with Eq. 6.4-2 to provide two simultaneous equations containing only n_1 and n_2 as unknowns. The solutions of these equations are tabulated below together with the viscosities obtained from the literature[147] (the effects of mutual saturation have been

ignored).

TABLE 6.7: Viscosities, cp.

	Benzene			Water		
	ICT[147]	Experimental		ICT[147]	Experimental	
		W → B	B → W		W → B	B → W
20 μ bore capillary	0.619	0.604	0.585	0.938	0.962	0.940
4 μ bore capillary	0.615	0.625	0.647	0.927	0.917	0.862

Unfortunately these solutions involve the difference of two quantities of similar magnitude so that scatter is much increased (although it is still not more than 3% for W → B). Nevertheless, the correlation is sufficient to indicate that, in glass capillaries of the size studied here, neither the viscosity of water nor that of benzene differs significantly from its bulk value. A similar conclusion was reached by Fedyakin[141] in 1957. However, more recently Derjaguin, Fedyakin and Talaev[65] have announced that if an index of water is introduced into a quartz capillary of this magnitude by condensation from its saturated vapour then its viscosity is greatly enhanced. Values of up to 22x the normal value are reported. In addition, it is stated that the viscosity is dependent upon how many times the liquid index is driven

along the tube, but not, apparently, upon how far or how fast the index was moved, since no changes in viscosity are recorded during a given displacement. Although it is difficult to fault this interpretation of their reported data with much certainty, each anomalous viscosity is apparently calculated on the strength of only two or three experimental points. Moreover, contact angle velocity dependence does not seem to have received sufficient attention. In the study reported here this latter objection has, it is believed, been overcome, and it is hoped that further work will resolve present uncertainties.

REFERENCES

1 BUFF, F. P., J. Chem. Phys., 23 (1955), 419.

2 YOUNG, T. Phil. Trans., 95 (1805), 65.

3 GIBBS, J. W., Collected Works, Vol. I (London, 1928).

4 DEFAY, R., PRIGOGINE, I., BELLEMANS, A., and EVERETT, D.H., "Surface Tension and Adsorption" (London, 1966).

5 KIRKWOOD, J. G. and BUFF, F. P., J. Chem. Phys., 17 (1949), 338.

6 BUFF, F. P., J. Chem. Phys., 19 (1951), 1591.

7 GUGGENHEIM, E. A., Trans. Far. Soc., 36 (1940), 397.

8 GUGGENHEIM, E. A., "Thermodynamics" (Amsterdam, 1949).

9 ARIS., R, "Vectors, Tensors and the Basic Equations of Fluid Mechanics" (Englewood Cliffs, 1962).
ESKINAZI, S., "Principles of Fluid Mechanics", Boston, 1962.

10 LAPLACE, P. S. "Mecanique, celeste", Book 10, second supplement (Paris, 1806).

11 BASHFORT, F., and ADAMS, J. C., "An Attempt to Test The Theories of Capillary Action" (Cambridge, 1883).

12 NEUMANN, F., "Vorlesungen über die Theorie der Capillarität" pp. 152-63 (Leipzig, 1894).

13 PITZER, K. S., and BREWER, L., revised edition: LEWIS, G. N., and RANDALL, M., "Thermodynamics" (New York, 1961).

14 ADAMSON, A. W., "Physical Chemistry of Surfaces" (New York, 1960).

15 ELEY, D. D., "Adhesion" (Oxford 1961).

16 MELROSE, J. C., J. Coll. Sci., 20 (1965), 801.

17 JOHNSON, R. E. Jr., J. Phys. Chem., 63 (1959), 1655.

18 See papers cited by ELEY[15], pp. 70-72, and DEFAY and co-authors[4] pp. 302-8.

19 SKAPSKI, A., BILLUPS, R., CASAVANT, D., J. Chem. Phys., 31 (1959), 4569.

20 THOMAS, D. G. and SAVELY, L. A. K., J. Chem. Soc. (1952), 4569.

21 TURNBULL, D., J. Appl. Phys. 21 (1950), 1022.

22 See ref. 11, pp. 4-6.

23 Discussion, Proc. 2nd. Int. Cong. Surf. Activity, 3 (1957), 187.

24 ADAM, N. K., Adv. Chem. Ser. 43 (1964), 52.

25 ADAMSON, A. W. and LING, I., ibid, 57.

26 MELROSE, J. C., ibid, 158.

27 BAKKER, G., "Kapillarität und Oberflächenspannung", in "Handbuch der Experimentalphysik", Vol. VI (Leipzig, 1928).

28 BOLTZMANN, L., Ann. Phys. 141 (1870), 582.

29 SEGNER, See ref. 11 pp. 4-6.

30 MONGE, See ref. 11 pp. 4-6.

31 DUPRE, A., "Théorie méchanique de la chaleur", p. 201 (Paris, 1869).

32 BANGHAM, D. H., and RAZOUK, R. I., Trans. Far. Soc. 33 (1937), 1459.

33 KITCHENER, J. A., Proc. 3rd Int. Cong. Surf. Activ ity (Cologne), 2 (1960), 426.

34 BIKERMAN, J. J., Proc. 2nd Int. Cong. Surf. Activity, 3 (1957), p. 125 and discussion pp. 187-90.

35 BIKERMAN, J. J., "Contributions to the Thermodynamics of Surfaces" published by the author (Massachusetts, 1961).

36 LESTER, G. R., J. Coll. Sci., 16 (1961), 315.

37 TABOR, D., and BAILEY, A. I., Proc. 2nd Int. Cong. Surf. Activity, 3 (1957), 189.

38 MICHAELS, A. S., and DEAN, S. W., J. Phys. Chem. 66 (1962), 1790.

39 PETHICA, B. A., and PETHICA, T. J. P., Proc. 2nd Int. Cong. Surf. Activity, 3 (1957), 131.

40 COLLINS, R. E., and COOKE, C. E., Trans. Far. Soc. 55 (1959), 1602.

41 DAVIES, J. T., and RIDEAL, E. K., "Interfacial Phenomena", 2nd. Edn., pp. 1-52 (New York, 1963).

42 (a) DEFAY, R., and PRIGOGINE, I., "Tension superficielle et Adsorption", (Liège, 1950).
(b) DUFOUR, L., and DEFAY, R., "Thermodynamics of Clouds", pp. 1-48 (New York, 1963).

43 ZISMAN, W. A., Adv. Chem. Ser., 43 (1964), pp. 1-51.

44 ELLIOTT, G. E. P., and RIDDIFORD, A. C., Rec. Progr. Surface Sci., 2 (1964), 111.

45 GRAY, V. R., Chem. Ind., (1965), 969.

46 GRAY, V. R., Proc. 2nd Int. Cong. Surf. Activity, 3 (1957), pp. 193-194.

47 SCHWARTZ, A. M., and MINOR, F. W., J. Coll. Sci., 14 (1959), 584.

48 BUFF, F. P., "The Theory of Capillarity", in "Handbuch der Physik", Vol. X, (Berlin, 1960).

49 BOYD, G. E., and LIVINGSTONE, H. K., J. Amer. Chem. Soc., 64 (1942), 2383.

50 BROWN, R. C., Proc. Phys. Soc., 59 (1947), 429.

51 GUASTALLA, J., Proc. 2nd. Int. Conf. Surf. Activity, 3 (1957), 143.

52 HARKINS, W. D., and LIVINGSTONE, H. K., J. Chem. Phys., 10 (1942), 342.

53 GANS, D. M., J. Phys. Chem., 68 (1945), 165.

54 JOHNSON, R. E., Jr. and DETTRE, R. H., J. Coll. Interface Sci. 21 (1966), 610.

55 HACKERMAN, N., and WADE, W. H., J. Phys. Chem., 69 (1965), 314.

56 MELROSE, J. C., S.C.I. Monograph No. 25, pp. 123-143 (London, 1967).

57 DERJAGUIN, B. V., and ZORIN, Z. M., 2nd. Int. Cong. Surf. Activity, Vol. II (1957), 145.

58 YOUNG, G. J., CHESSICK, J. J., HEALEY, F. H., and ZETTLEMOYER, A. C., J. Phys. Chem. 58 (1954), 313.

59 GRAHAM, D., J. Phys. Chem., 66 (1962), 1815.

60 FRUMKIN, A. N., Acta Physicochim, U.S.S.R., 9 (1938), 313.

61 DERJAGUIN, B. V., and KUSAKOV, M., Acta Physicochim, U.S.S.R., 10 (1939), 25, 153.

62 DERJAGUIN, B. V., Trans. Far. Soc. 36 (1940), 212.

63 READ, A. D., and KITCHENER, J. A., S.C.I. Monograph No. 25, pp. 300-313 (London, 1967).

64 DERJAGUIN, B. V., Disc. Far. Soc. 42 (1966), 109.

65 DERJAGUIN, B. V., FEDYAKIN, N. N., and TALAEV, (UDC 541.12.013.5), Translated Dokl. Acad. Nauk SSSR, 167 (1966), 376.

66 FEDYAKIN, N. N., ref. Chem. Abs. 53, 11938h.

67 SULMAN, H. L., Bull. Inst. Min. Met., (1919), 95.

68 STEPHENS, D. W., "Bibliography on gas/liquid and liquid/liquid interfaces", Vols. 1 and 2 (1962).

69 PETHICA, B. A., Rep. Prog. Appl. Chem., 46 (1961), 14.

70 MACDOUGAL, G., and OCKRENT, C., Proc. Roy. Soc., A 180 (1942), 151.

71 TIMMONS, C. O., and ZISMAN, W. A., J. Coll. Interface Sci., 22 (1966), 165.

72 GAUDIN, A. M., and WITT, A. F., Adv. Chem. Ser. 43 (1964), 202.

73 SHUTTLEWORTH, R., and BAILEY, G. L. J., Disc. Far. Soc., 3 (1948), 16.

74 GOOD, R. J., J. Amer. Chem. Soc., 74 (1952), 5041.

75 JOHNSON, R. E. Jr., and DETTRE, R. H., Adv. Chem. Ser. 43 (1964), 112.

76 JOHNSON, R. E. Jr., and DETTRE, R. H., J. Phys. Chem. 68 (1964), 1744; see also DETTRE, R. H., and JOHNSON, R. E. Jr., 69 (1965), 1507-15.

77 HANSEN, R. S., and MIOTTO, M., J. Amer. Chem. Soc., 79 (1957), 1765.

78 WENZEL, R. N., Ind. Eng. Chem. 28 (1936), 988; J. Phys. Coll. Chem. 53 (1949), 1466.

79 CASSIE, A. B. D., and BAXTER, S., Trans. Far. Soc. 40 (1944), 546.

80 GRAY, V. R., S.C.I. Monograph No. 25, pp. 99-115 (London, 1967).

81 BIKERMAN, J. J., J. Phys. Coll. Chem. 54 (1950), 553.

82 DETTRE, R. H., and JOHNSON, R. E. Jr., Adv. Chem. Ser. 43 (1964), 136

83 DETTRE, R. H., and JOHNSON, R. E. Jr., S.C.I. Monograph No. 25, pp. 144-155 (London, 1967).

84 BARTELL, F. E., and SHEPARD, J. W., J. Phys. Chem., 57 (1953), 211.

85 CASSIE, A. B. D., Disc. Far. Soc., 3 (1948), 11.

86 DOSS, K. S. G., and RAO, B. S., Proc. Indian Acad. Sci., 7A (1938), 113.

87 PEASE, D. C., J. Phys. Chem., 49 (1945), 107.

88 EDSER, E., 4th Coll. Rep. Brit. Assoc. Adv. Sci. p. 292 (London, 1922)

89 PHILIPS, M. C., and RIDDIFORD, A. C., Proc. Fourth Int. Congr. Surf. Activity (Brussels, 1964, in press).

90 ELLIOTT, G. E. P., and RIDDIFORD, A. C., J. Coll. Interface Sci. 23 (1967), 389

91 YARNOLD, G. D., and MASON, B. J., Proc. Phys. Soc. (London) B62 (1949), 125-128.

92 ELLIOTT, G. E. P., and RIDDIFORD, A. C., Nature, 195 (1962), 795.

93 FRENKEL, J., "Kinetic Theory of Liquids", (Oxford, 1946).

94 CLIFFORD, J., and LECCHINI, S. M. A., S.C.I. Monograph No. 25, pp. 174-195 (London, 1967).

95 LANGLOIS, W. E., "Slow Viscous Flow", (New York, 1964).

96 SLICHTER, C. S., 19th Ann. Rep., U.S. Geol. Survey, 1897-98, Part II, 295.

97 SMITH, W. O., "Physics", 3 (1932), 139.

98 LEVICH, V. G., "Physicochemical hydrodynamics" (Englewood Cliffs, 1962).

99 FAIRBROTHER, F., and STUBBS, A. E., J. Chem. Soc., 1 (1935), 527.

100 TAYLOR, G. I., J. Fluid Mech., 10 (1961), 161.

101 MERCHESSAULT, R. N., and MASON, S. G., Ind. Eng. Chem., 52 (1960), 79.

102 GOLDSMITH, H. L., and MASON, S. G., J. Coll. Sci., 18 (1963), 237.

103 BRETHERTON, F. P., J. Fluid Mech., 10 (1961), 166.

104 PLATEAU, J. "Statique experimentale et theorique des liquides soumis aux seules forces moleculaires" (Paris, 1873).

105 MAXWELL, J. C., "Capillary action", Encyclopaedia Brittanica, (9th Ed., 1876), 5 56-71, esp. 64-67.

106 HAYNES, J. M., Ph.D. Thesis, (Bristol, 1965).

107 GOREN, S. L., J. Fluid. Mech., 12 (1962), 309

108 GOLDSMITH, H. L., and MASON, S. G., J. Fluid Mech., 14 (1962), 42.

109 KARNIS, A., and MASON, S. G., J. Coll. Interface Sci., 23 (1967), 120.

110 BATAILLE, J., Comptes Rendus, A 262 (1966), 843.

111 TAYLOR, G. I., "Aeronautics and Astronautics", p. 12 (London, 1960).

112 MOFFAT, H. K., J. Fluid Mech., 18 (1964) 1.

113 GREGG, S. J., J. Chem. Phys., 16 (1948), 549.

114 ABLETT, R., Phil. Mag., (6) 46 (1923), 244.

115 BARTELL, F. E., and BRISTOL, K. E., J. Phys. Chem., 44 (1940), 86.

116 ADAM, N. K., and LIVINGSTONE, H. K., Nature, 182 (1958), 128.

117 BARTELL, F. E., and BJORKLUND, C. W., J. Phys. Chem., 56 (1952), 453.

118 ADAM, N. K., and JESSOP, G., J. Chem. Soc. (1925), 1863.

119 ROSE, W., and HEINS, R. W., J. Coll. Sci., 17 (1962), 39.

120 RAY, B. R., and BARTELL, F. E., J. Coll. Sci., 8 (1953), 214.

121 CHITTENDEN, D. H., and SPINNEY, D. V., J. Coll. Interface Sci., 22 (1966), 250.

122 SAKAR, N. and GAUDIN, A.M., J. Phys. Chem., 70 (1966), 2512

123 ROSE, W. D., Nature, 191 (1961), 242.

124 WEST, G. D., Proc. Roy Soc. A 86 (1912), 23.

125 YARNOLD, G. D., Proc. Phys. Soc., 58 (1946), 120.

126 BRITTIN, W. E., J. App. Phys., 17 (1946), 37.

127 DECHARME, C., Ann. Chim. Phys., 23 (1872), 228.

128 ELEY, D. D., and PEPPER, D. C., Trans. Far. Soc., 42 (1946), 697.

129 CALDERWOOD, C. F. N., and MARDLES, E. W. J., Proc. Phys. Soc., 67B (1954), 395.

130 JAMIN, J., C.r. hebd. Seanc. Acad. Sci., 50, 172 Paris 1860).

131 SCHWARTZ, A. M., RADER, C. A., and HUEY, E., Adv. Chem. Ser. 43 (1964), 251.

132 WASHBURN, E. W., Phys. Rev., 17 (1921), 273.

133 BOSANQUET, C. H., Phil Mag., 45 (1923), 525.

134 PEAK, R. L., and McLEAN, D. A., Ind. Eng. Chem. Anal. Ed.), 6 (1934), 85.

135 LIGENZA, J. R., and BERNSTEIN, R. B., J. Am. Chem. Soc., 73 (1951), 4636.

136 ROSANO, H. L., and GUASTALLA, J. C. R., Comptes Rendus Acad. Sci., Ser 43, p. 250 (Paris, 1950).

137 Le GRAND, E. J., and RENSE, W. A., J. App. Phys., 16 (1945), 843.

138 TEMPLETON, C. C., Trans. AIME, 201 (1954), 162.

139 TEMPLETON, C. C., ibid, 207 (1956), 211.

140 BLAKE, T. D., EVERETT, D. H., and HAYNES, J. M., S.C.I. Monograph No. 25 pp. 164-173 (London, 1967).

141 FEDYAKIN, N. N., NRC TT-995 (Canada), trans: Trudy Tekhol. Inst. Pishchevoi Prom., 8 (1957), 37.

142 FEDYAKIN, N. N., Russian J. Phys. Chem., 36 (1962), 776.

143 BASS, R. L., Chem. Ind., (1959), 912.

144 VANDERVORT, G. L., and WILLARD, J. E., J. Amer. Chem. Soc. 70 (1948), 3148.

145 EAKINS, W. J., S.P.E. Trans., (1962) 354.

146 HUNTER, M. J., GORDEN, M. S., BARRY, A. J., HYDE, J. F., and HEIDENREICH, R. D., Ind. Eng. Chem., 39 (1947), 1389.

147 "International Critical Tables", (New York, 1926).

148 GUTFREUND, K., WEBER, H. S., and BROWN, C., 15th R.P.D. Conf. S.P.I., Sec. 10-C (1960).

149 WHITE, T. E., Proc. Anniv. Tech. Conf. S.P.I. 3-B (1965), 15.

150 ARMISTEAD, C. G., and HOCKEY, J. A., Trans. Far. Soc. 63 (1967), 2549.

151 KITCHENER, J. A., Nature, 182 (1958), 1667.

152 HARKINS, W. D., and BROWN, F. E., J. Amer. Chem. Soc., 1 (1919), 499.

153 ISIRIKYAN, A. A., KISELEV, A. V., and USHAKOVA, E. V., (UDC 541.183.25) Translated from Koll. Zhr, 27 (1965), 690.

154 EIRICH, F. R., "Rheology, Theory and Applications". Vol. II (New York, 1958).

155 EYRING, H., J. Chem. Phys. 4 (1936), 283.

156 JOHNSON, F. H., EYRING, H., and POLISSAR, M., "The Kinetic Basis of Molecular Biology" (New York, 1954).

157 GLASSTONE, S., LAIDLER, K. J., and EYRING, H., "The Theory of Rate Processes" (New York, 1941).

158 MELROSE, J. C., and WADE, W. H., (to be published).

159 GRIFFITH, A. A., Phil. Trans. Roy. Soc., A 221 (1920). 163.

160 GORDON, J. E., MARSH, D. M., and PARATT, M., Proc. Roy. Soc. A 249 (1959), 65.

161 HOLLAND, L. "The Properties of Glass Surfaces" (London, 1964).

162 ZARZYCKI, J., and MEZARD, R., Proc. Euro. Reg. Conf. on Elect. Microscopy, Vol. I (Delft, 1960).

163 DERJAGUIN, B. V., and SHCHERBAKOV, L. M., Koll. Zhr., 23 (1961) 40.

164 OWEN, B. B., WHITE, J. R., and SMITH, J. S., J. Amer. Chem. Soc., 78 (1956), 3561.

165 COHAN, L. H., and MEYER, G. E., J. Amer. Chem. Soc. 62 (1940), 2715.

166 STARLING, S. G., and WOODALL, A. J., pp. 706 (London, 1958).

167 MUSCAT, M., "Physical Principles of Oil Production" (New York, 1949)

168 HOBSON, G. D., "Petroleum Geology" (Oxford, 1954).

169 SCHEIDEGGER, A. E., "The Physics of Flow Through Porous Media", Revised Ed. (Toronto, 1960).

170 COLLINS, R. V., "Flow of Fluids Through Porous Materials" (New York, 1961).

171 EYRING, H., J. Chem. Phys., 46 (1967), 1075.

A P P E N D I C E S

APPENDIX I

Table 4.1

Exp. P2: Benzene-Water Displacements in Uncoated Capillary

$T = 19.5^{\circ}C$

$l = 150$ cm

$x = 100$ cm (from benzene end)

$r = 0.45$ mm

W → B		B → W	
$-10^{-3}\Delta p$, dyne cm^{-2}	$-\dot{x}$, cm sec^{-1}	$10^{-3}\Delta p$, dyne cm^{-2}	$\dot{x}$, cm sec^{-1}
0.33	0.033	0.135	0.053
0.41	0.045	0.167	0.085
0.62	0.066	0.186	0.124
0.53	0.069	0.230	0.200
0.82	0.127	0.225	0.206
1.93	0.316	0.271	0.281
3.78	0.467		

Table 4.2

Exp. P3: Preliminary, Benzene-Water Displacements in Dimethyldichlorosilane-Treated Tubing.

$T = 19^{\circ}C$

$l = 27.41$ cm

$r = 0.20$ mm

$x = 23.50$ cm

$\Delta x = 2.41$ cm

B → W		W → B	
$10^4 \dot{x}$, cm sec^{-1}	$-10^{-3}\Delta p$, dyne cm^{-2}	$-10^4 \dot{x}$ cm sec^{-1}	$-10^{-3}\Delta p$, dyne cm^{-2}
14.6	1.05	3.8	3.37
22.8	0.98	55.1	3.39
36.2	0.89	282	3.54
108.5	0.72	433	3.63
148	0.40	1160	4.07
288	0.32		
355	0.20		
487	0.17		
648	0.04		
1590	-0.723		

Table 4.3

Exp. A1: Benzene-Water Displacements in Dimethyldichlorosilane-Treated Tubing.

$l = 12.71$ cm

$l_{eff} = l + 0.45 = 13.16$ cm

$x_{eff} = x + 0.22(5)$ cm

$r = 0.251$ mm

$T = 23.1^{\circ}C$

Stationary Interface

Δp, dyne cm^{-2}	ϕ_{cal}, deg	ϕ, deg
-6	90	90
+10	90	88
339	83	81
514	79	77
668	76	74
606	77	73
370	82	79
278	84	82
581	78	76
601	76	74
838	73	70

Table 4.3 (Cont.)

$$\Delta p \text{ (vis)} = \frac{8\dot{x}}{r^2}\{\eta_1 x + \eta_2(1 - x)\}$$

Moving Interface

Sense	x_{eff},	Δp, dyne cm^{-2}	$-10^4\dot{x}$, cm sec^{-1}	Δp(vis), dyne cm^{-2}	ϕ_{cal}, deg	ϕ, deg
B → W	9.53	1440	13	1	56	56
"	"	2043	450	55	45	41
"	"	2157	650	69	42	41
"	"	1994	150	18	45	43
" *	8.43	843	8	1	72	70
" **	9.53	2327	<1	-	33	32
" **	"	2412	<1	-	30	30
W → B	8.43	-674	-23	-3	105	99
"	"	-494	-2.2	-	100	99
"	"	-486	-30	-4	100	98
"	"	-549	-25	-3	101	101
"	9.53	-830	-740	-74	106	111
"	"	-1318	-1120	-140	115	113
"	"	-435	-42	-5	99	102
"	"	-295	-26	-3	96	99
" *	"	+343	-1	-	84	81

* Unsteady displacement

** Unsteady displacement following probable contamination.

Table 4.4

Exp. E1: Benzene-Water Displacements in Trimethylchlorosilane-Treated Tubing.

$r = 0.325$ mm

$T = 24^{\circ}C$

W → B First Displacement		W → B First Displacement After 1 hr	
$-10^4\dot{x}$, cm sec^{-1}	ϕ, deg.	$-10^4\dot{x}$, cm sec^{-1}	ϕ, deg.
9	158	88	150
175	158	366	153
122	160	19	146
18	159	755	154
105	161	226	150
47	158		
314	162		

Table 4.4 cont.

Second and Subsequent Displacements

W → B		B → W	
$-10^4\dot{x}$, cm sec^{-1}	ϕ, deg.	$+10^4\dot{x}$, cm sec^{-1}	ϕ, deg.
900	51	8	112
1	63	17	108
13	59	6	113
66	55	22	109
6900	47	16	109
2	119	124	103
		2	117
		210	100
		118	102
		54	105

Displacements after 3 WeeksSoak

W → B		B → W	
$-10^4\dot{x}$, cm sec^{-1}	ϕ, deg.	$+10^4\dot{x}$, cm sec^{-1}	ϕ, deg.
13	101	21	64
42	102	42	62
83	103	155	59
254	106	2	68
5	101	46	61
336	107	20	62
460	109	247	58
5	101	352	57
146	104	14	66

Table 4.5

Exp. E2: Benzene-Water Displacements in a Second Trimethylchlorosilane-Treated Tube.

$r = 0.35$ mm

$T = 24^{\circ}C$

B → W

First Displacement

$10^4\dot{x}$, cm sec^{-1}	ϕ, deg.
2	121
4	123
46	116
-274	115

B → W

Second and Subsequent Displacements during First 4 hr. Period

$10^4\dot{x}$, cm sec^{-1}	ϕ, deg.	$10^4\dot{x}$, cm sec^{-1}	ϕ, deg.	$10^4\dot{x}$, cm sec^{-1}	ϕ, deg.
5	128	316	109	36	116
410	107	970	103	140	113
296	110	1380	104	40	118
108	113	2200	102	124	115
186	112	6	123	202	113
34	116	8	121	162	113
218	111	24	118	106	468
186	111				

Table 4.5 (cont.)

W → B

Displacements During First ½ hr.

$-10^4\dot{x}$, cm sec^{-1}	ϕ, deg.
5	150
16	153
32	150
450	153
511	150

W → B

Subsequent Displacements

$-10^4\dot{x}$, cm sec^{-1}	ϕ, deg.
695	146
26	145
1020	148
1020	148
9	145
3	141
135	145
2	141
47	146
505	147
610	147
110	145

W → B

Displacements After 22 hr.

$-10^4\dot{x}$, cm sec^{-1}	ϕ, deg.
24	144
176	145
121	144
285	146
860	147
6170	149
24	143

Table 4.5 (Cont.)

B → W

Displacements After 20 hr.

$10^4\dot{x}$, cm sec^{-1}	ϕ, deg.	$10^4\dot{x}$, cm sec^{-1}	ϕ, deg.
14	116	596	107
58	114	40	115
258	112	336	109
162	113	842	106
196	112	696	108
198	112	368	110
190	110	324	111
390	109	324	112
40	115	1540	104

Table 4.6

Exp. F2: Benzene-Glycerol Displacements

$r = 0.325$ mm

$T = 23.5^{\circ}C$

B → G

$10^4\dot{x}$, cm sec^{-1}	ϕ, deg.
8	41
13	32
48	27
19	33
27	31
3	43
3	44
9	36

G → B

$-10^4\dot{x}$, cm sec^{-1}	ϕ, deg.	$-10^4\dot{x}$, cm sec^{-1}	ϕ, deg.
26	102	14	98
50	103	63	103
126	109	875	130
144	110	2160	140
698	129	1440	137
1220	131	158	109
1010	130	619	125
31	102	224	115
11	99		

Table 6.1

Computer Output for 20μ Bore Capillary

Coefficients of Polynomial V = V(X)

0	1.79398×10^{-3}
1	3.15062×10^{-6}
2	-1.46155×10^{-7}
3	6.36437×10^{-8}

X, cm	V, 10^{-3} cm^3	V = V(X), 10^{-3} cm^3	V - V(X) 10^{-8} cm^3
0.01264	1.79400	1.79402	-2.2
0.1454	1.79449	1.79444	+4.9
0.2440	1.79473	1.79474	-1.3
0.3540	1.79507	1.79508	-1.0
0.4677	1.79544	1.79543	-0.6
0.7205	1.79618	1.79620	-1.8
0.9859	1.79700	1.79701	-1.0
1.1882	1.79764	1.79763	+1.4
1.5042	1.79862	1.79861	+0.9
1.7064	1.79925	1.79925	-0.1
2.0350	1.80032	1.80033	-0.4
2.3131	1.80129	1.80128	+1.1
2.6038	1.80230	1.80232	-1.8
2.9704	1.80373	1.80372	+0.7

Table 6.1 (cont.)

X, cm	r, μ	$\frac{dV}{dX}, 10^{-6}$ cm^2	$\sum_{X=0}^{X} \frac{\delta X}{r^4}, 10^{12}$ cm^{-3}
0.0	10.01	3.15	0.0000
0.1	9.97	3.12	0.1002
0.2	9.93	3.10	0.2021
0.3	9.90	3.08	0.3054
0.4	9.87	3.06	0.4100
0.5	9.86	3.05	0.5155
0.6	9.84	3.04	0.6217
0.7	9.84	3.04	0.7284
0.8	9.84	3.04	0.8353
0.9	9.84	3.04	0.9420
1.0	9.85	3.05	1.0485
1.1	9.87	3.06	1.1543
1.2	9.89	3.07	1.2593
1.3	9.92	3.09	1.3631
1.4	9.96	3.12	1.4656
1.5	10.00	3.14	1.5666
1.6	10.04	3.17	1.6657
1.7	10.10	3.21	1.7629
1.8	10.16	3.24	1.8580
1.9	10.23	3.28	1.9508
2.0	10.30	3.33	2.0412
2.1	10.37	3.38	2.1290
2.2	10.45	3.43	2.2143
2.3	10.54	3.49	2.2969
2.4	10.63	3.55	2.3768
2.5	10.72	3.61	2.4539

Table 6.2

Computer Output for 4μ Bore Capillary

Coefficients of Polynomial V = V(X)

0	6.23310×10^{-5}
1	1.69230×10^{-7}
2	-3.06428×10^{-8}
3	1.37800×10^{-8}

X, cm	V, 10^{-5} cm^3	$\overline{V} = V(X)$, 10^{-5} cm^3	V - V(X) 10^{-9} cm^3
0.000	6.2330	6.2331	-1.0
0.034	6.2338	6.2337	+1.2
0.092	6.2347	6.2346	+0.9
0,175	6.2357	6.2360	-2.4
0.242	6.2370	6.2370	0
0.267	6.2375	6.2374	+0.7
0.301	6.2380	6.2380	+0.9
0.371	6.2390	6.2390	+0.1
0.448	6.2402	6.2402	-0.2
0.522	6.2414	6.2413	-0.5
0.662	6.2433	6.2434	-0.6
0.680	6.2437	6.2436	+1.2
0.786	6.2451	6.2452	-0.3
0.865	6.2463	6.2463	0.0
0.917	6.2471	6.2471	+0.1

Table 6.2 (cont.)

X, cm	r, μ	$\frac{dV}{dX}$, 10^{-7} cm^2	$\sum_{X=0}^{X} \frac{\delta X}{r^4}$, 10^{14} cm^{-3}
0.0	2.32	1.69	0.0000
0.1	2.28	1.64	0.3557
0.2	2.25	1.59	0.7354
0.3	2.22	1.55	1.1373
0.4	2.19	1.51	1.5587
0.5	2.18	1.49	1.9963
0.6	2.17	1.47	2.4461
0.7	2.16	1.47	2.9032
0.8	2.16	1.47	3.3628
0.9	2.17	1.48	3.8195
1.0	2.18	1.49	4.2685
1.1	2.20	1.52	4.7051
1.2	2.22	1.55	5.1251

Table 6.3

Benzene-Water Displacements in 20 Bore Tube.

	X,cm	x,cm	r,μ	$\sum_{x=0}^{x} \frac{x}{r^4}, 10^{12} cm^{-3}$	$\sum_{x}^{l} \frac{x}{r^4}, 10^{12} cm^{-3}$
Benzene End of Tube	0.26	0.00	9.92	0.0000	-
Water End of Tube	0.46	2.20	10.68	2.4231	-
Run (i)	0.58	0.32	10.04	0.3366	1.8224
Run (ii)	1.59(5)	1.335	9.84	1.3966	0.7624

$T = 23.0^{\circ}C$

$\Delta x = 0.127(5) cm$

Run (i)

B → W		W → B	
$10^{4}\frac{\Delta x}{t}$, cm sec^{-1}	$10^{-3}\Delta p$, dyne cm^{-2}	$-10^{4}\frac{\Delta x}{t}$, cm sec^{-1}	$10^{-3}\Delta p$, dyne cm^{-2}
-95.1	69.47	86.7	67.12
215	71.10	156.0	66.19
172	70.50	203	65.51
255	71.58	236	65.17
365	73.20	255	64.82
491	74.42	425	62.77
555	75.20	455	62.41
709	77.16	532	61.59
440	74.03	580	60.71
203	71.04	654	59.83
145	70.26	319	64.09
93.1	69.52		

Table 6.3 (cont.)

Run (ii)

B → W		W → B	
$10^4 \frac{\Delta x}{t}$, cm sec^{-1}	$10^{-3}\Delta p$ dyne cm^{-2}	$-10^4 \frac{\Delta x}{t}$ cm sec^{-1}	$10^{-3}\Delta p$ dyne cm^{-2}
129	71.78	386	63.79
153	72.17	412	63.35
194	72.80	472	62.67
232	73.44	532	61.49
272	74.03	607	60.61
319	74.91	750	58.56
412	76.08	370	63.99
440	76.57	349	64.43
543	77.94	315	65.07
638	79.32	236	66.19
880	83.04	187	66.98
		129	67.76

Table 6.4

Benzene-Water Displacements in 4μ Bore Tube.

	X, cm	x, cm	r, μ	$\sum_{x=0}^{x} \frac{x}{r^4}, 10^{14} cm^{-3}$	$\sum_{x}^{1} \frac{x}{r^4}, 10^{14} cm^{-3}$
Benzene End of Tube	1.04	0.00	2.19	0.0000	-
Water End of Tube	0.00	1.04	2.32	4.4431	-
Run (i)	0.16	0.86	2.26	3.8596	0.5835
Run (ii)	0.48	0.54	2.18	2.5343	1.9088

$T = 23.5^{\circ}C$

$\Delta x = 0.0627 cm$

Run (i)

B → W		W → B	
$10^4 \frac{\Delta x}{t}$, cm sec^{-1}	$10^{-6}\Delta p$, dyne cm^{-2}	$-10^4 \frac{\Delta x}{t}$, cm sec^{-1}	$10^{-6}\Delta p$, dyne cm^{-2}
174	0.3303	40.1	0.3030
203	0.3338	64.0	0.3000
251	0.3392	96.0	0.2964
292	0.3445	125	0.2928
384	0.3558	199	0.2831
174	0.3293	184	0.2853
141	0.3256	216	0.2811
100	0.3210	240	0.2780
78.4	0.3183	298	0.2728
50.8	0.3150		
25.7	0.3123		

Table 6.4 cont.

Run (ii)

B → W		W → B	
$10^4 \frac{\Delta x}{t}$, cm sec^{-1}	$10^{-6}\Delta p$, dyne cm^{-2}	$-10^4 \frac{\Delta x}{t}$, cm sec^{-1}	$10^{-6}\Delta p$, dyne cm^{-2}
209	0.3451	27.0	0.3152
119	0.3362	172	0.2970
157	0.3412	128	0.3023
119	0.3354	273	0.2837
89.7	0.3317	151	0.2997
69.0	0.3282		
39.5	0.3239		
261	0.3532		
196	0.3438		
174	0.3416		
146	0.3372		
157	0.3362		

APPENDIX II

The following paper is to be submitted for publication.

THE INTERACTION OF WATER WITH SILANE-TREATED POROUS GLASS

by

T. D. Blake and J. M. Haynes

INTRODUCTION

The reaction of halogenated alkyl or aryl silanes with hydrated silica surfaces, e.g.

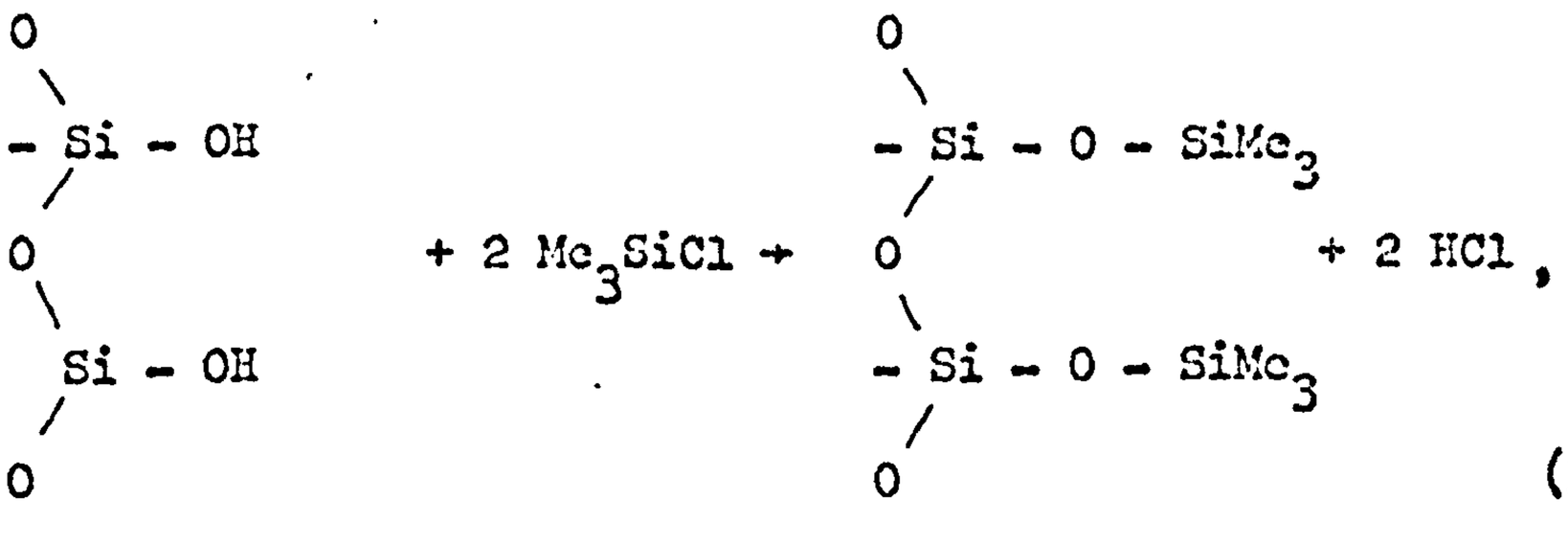

(1)

has often been used to produce surfaces described as hydrophobic[1,2,3] and organophilic[4]. This paper reports measurements showing that an increasingly hydrophilic character is imparted to the treated surface by subsequent exposure to water. Previously reported observations of benzene/water interfaces undergoing steady displacement in silane-treated glass capillaries[5] had first led to this conclusion, and the present work was undertaken to substantiate it.

EXPERIMENTAL

Water adsorption isotherms were measured at 30.0°C on a McBain balance (sensitivity 0.25 mm mgm^{-1}) within a grease-free high vacuum system. The porous glass sample (Vycor 7930), in the form of an annulus 15 mm in diameter, 2 mm thick and 6 mm long, was cleaned by heating in 100-vol. H_2O_2 solution before being suspended from the balance. It was then heated at 450°C for 4 hours in 3 cm Hg pressure of pure oxygen.

The cleaned sample was exposed to saturated water vapour at room temperature for 4 days, and finally, physically adsorbed water was removed by outgassing overnight at 110°C. The hydration process caused a weight gain (after outgassing) of 14.7 mgm gm^{-1}. A complete water adsorption isotherm was then measured (Fig.1, Run A). At the conclusion of this run, the sample returned to its original (hydrated) weight.

The sample was then exposed to the saturated vapour of trimethylchlorosilane purified by vacuum distillation and stored in glass break-seal bulbs; purity checked by v.p.c.). After pumping at room temperature for 48 hours to remove physically adsorbed silane and reaction products, a constant weight was attained, exceeding the hydrated weight by 25.4 mgm gm^{-1}. Three further water isotherms were then measured (Fig.1, Runs B, C and D). At the conclusion of Runs B and C the sample weight, after prolonged pumping at room temperature, exceeded that at the start of each run by 8.2 and 12.0 mgm gm^{-1} respectively.

DISCUSSION OF RESULTS

The water isotherms shown in Fig.1 closely resemble the results of some earlier unpublished measurements on similarly prepared samples.*

---

* Undertaken by Dr. E. Gonick whilst a visitor in this Department

Table I lists some numerical results obtained from the data. $\underline{w}_m$ and $\underline{c}$ are the two constants of the B.E.T. equation, derived in the usual way from data in the relative pressure range $0 \leq \underline{p}/\underline{p}^o < 0.35$. $\Delta\underline{w}_o$ is the relative change in sample weight between the beginning and end of a run and $\underline{w}_\infty$ is the weight uptake at $\underline{p} = \underline{p}^o$, relative to the sample weight at the beginning of a run.

The value of $\underline{w}_m$ for Run A yields a specific surface $S = 126\ m^2\ gm^{-1}$ ($H_2O = 10.8\ \text{Å}^2$ molecule^{-1}), in reasonable agreement with previously reported values[6,7]. Thus, the average surface density of hydroxyl groups resulting from the hydration reaction

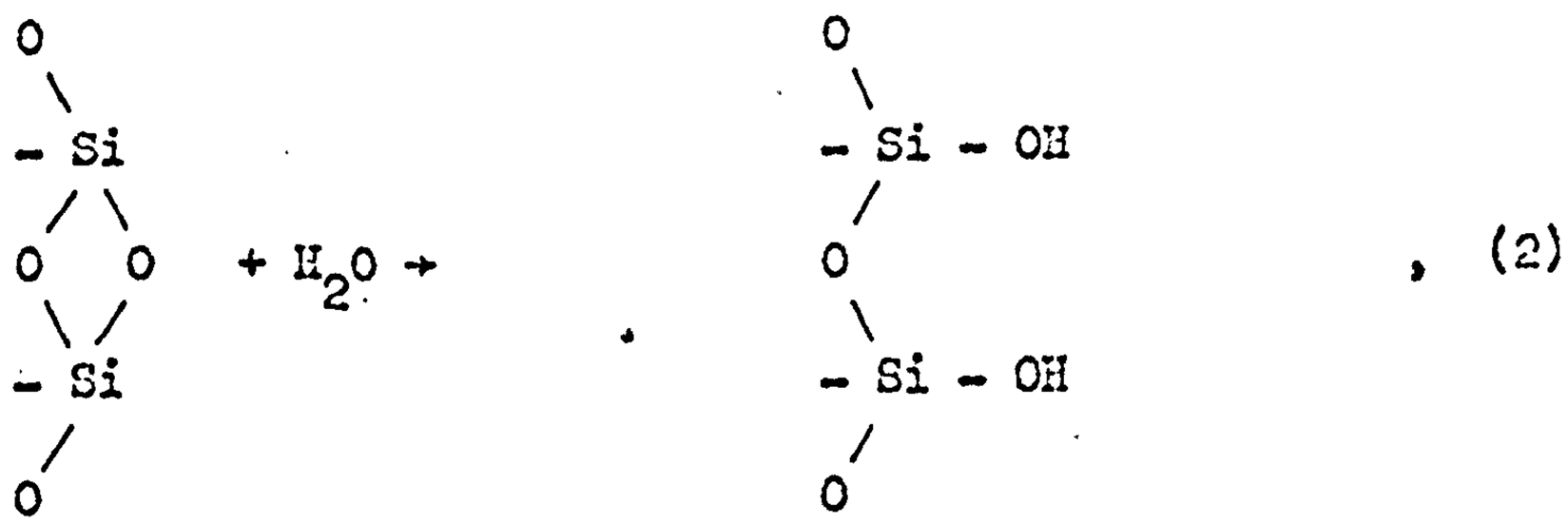

(2)

in which 14.7 mgm gm^{-1} was taken up, would be about one hydroxyl group to each 13 Å^2 of surface. The silane reaction (1), in which 25.4 mgm gm^{-1} was gained, therefore involved about 22% of the available sites; the comparable reaction with Aerosil surfaces was also found to be incomplete[3]. Studies of molecular models of Me_3SiCl suggest that more extensive coverage of the

hydroxylated surface by trimethylsilyl groups is improbable for steric reasons; most of the unreacted silanol groups will, however, still be accessible to small molecules, such as water.

The B.E.T. constants $\underline{v}_m$ and $\underline{c}$ for Run D indicate that whilst the monolayer capacity of the silane-treated glass was reduced to 54% of that of the untreated glass, the average net heat of adsorption in the first layer (taken to be proportional to log $\underline{c}$) had increased by about 7%. In other words, the available area for adsorption had decreased, but the affinity of the surface for water had increased.

A decrease in specific surface consequent upon pre-adsorption of the silane within the pores is to be expected[8], since part of the original pore space is now filled, and inaccessible to the subsequently adsorbed water. Wade's measurements of the B.E.T. area (to N_2) of a similar sample of porous glass containing pre-adsorbed water[9] suggest, however, that the specific surface should only have fallen from 126 to about 110 $m^2\ gm^{-1}$ for the quantity of silane pre-adsorbed.

It therefore appears that in the region of monolayer coverage (achieved at $\underline{p}/\underline{p}^\circ$ = 0.209 when $\underline{c}$ = 13.6), adsorption of water was restricted to the unreacted silanol sites and the decrease in $\underline{v}_m$ does not entirely represent a decrease in specific surface. The slight enhancement of adsorption energy may be attributed to the close proximity of the trimethylsilyl groups to water molecules adsorbed on surface silanol groups, which occupy declivities almost

3 Å deep. The relatively hydrophobic part of the surface appears to contribute negligibly to water adsorption in this relative pressure range.

In the capillary condensation region, however, Run B showed a large hysteresis effect, although displaced towards higher relative pressures compared with Run A. Studying a similarly-treated silica gel, Kiselev[10] found that capillary condensation of water was completely suppressed.

In the hysteresis region, the relative pressure is related to the curvature, $\underline{C}$, of the interface between capillary condensate and vapour (neglecting adsorption forces arising from the solid) by the Kelvin equation:-

$$\underline{R}\underline{T} \ln \underline{p}/\underline{p}^{o} = -\sigma \underline{v}\, \underline{C}, \qquad \text{(i)}$$

where σ is the surface tension of the capillary condensed liquid and $\underline{v}$ is its molar volume. $\underline{C}$ is in turn related to some linear dimension $\underline{r}$ of the pores containing the interfaces, through the equation

$$\underline{Cr} = \beta \cos\theta, \qquad \text{(ii)}$$

where θ is the contact angle formed in the condensate in contact with its vapour at the solid surface, and β is a shape factor. In the case of spherical interfaces within cylindrical capillaries of radius $\underline{r}$, $\beta = 2$. In non-cylindrical capillaries, if $\beta = 2$ is retained, then $\underline{r}$ becomes an equivalent cylindrical radius; alternatively, if $\underline{r}$ is chosen as a real dimension of the pore, β takes other values (generally < 2). β assumes different values

according to whether pores are filling or emptying, and in capillaries of non-uniform cross-section it is to be expected that β will be a function of θ, the nature of which depends on the detailed pore geometry. Melrose's analysis[11] shows, however, that for model porous media composed of packed equal spheres, variation of the contact angle has only a slight effect on the value of β appropriate to desorption. When capillary condensation occurs in pores of less than about 50 Å radius, it is customary[12] to "correct" the Kelvin radius $\underline{r}$ by adding to it the thickness of the adsorbed multilayer film on the pore walls, although this is unjustified in view of the explicit neglect of adsorption forces in applying the Kelvin equation, and the corresponding assumption of uniformity of interfacial curvature.

The curvature $\underline{C}_{\underline{d}}$ at the commencement of desorption was calculated, using the Kelvin equation, from the corresponding relative pressures in runs A, B and C, marked by arrows in Fig.1. The onset of desorption is readily observed on account of the concomitant increase in the turbidity of the adsorbent (Zsigmondy's "opacity point"[13]).

For comparison purposes, another measure of the pore "size" may be found in the hydraulic radius, $\underline{r}_{\underline{h}}$, defined as the ratio of pore volume to specific surface[14]. For cylindrical pores of radius $\underline{r}$, $\underline{r}_{\underline{h}} = \underline{r}/2$. More generally, $\underline{r}_{\underline{h}}$ will be related to some linear dimension $\underline{r}$ of a non-cylindrical pore by means of another shape factor, γ :-

$$\underline{r}_{\underline{h}} = \underline{r}/\gamma \qquad \text{(iii)}$$

It is therefore possible to gain information on variations in the contact angle following different surface treatments, by calculating the quantity

$$\underline{C}_{\underline{d}}\underline{r}_{\underline{h}} = (\beta \cos \theta/\underline{r})_{\underline{d}} \cdot (\underline{r}/\gamma).$$

On the assumptions (a) that the variation of β with θ for constant pore geometry may be neglected, (b) that the pore "size" which controls desorption, $\underline{r}_{\underline{d}}$, is not changed by the surface treatment, and (c) that the true specific surface is not significantly altered by silane treatment, then variations in $\underline{C}_{\underline{d}}\underline{r}_{\underline{h}}$, for a given adsorbent in different stages of surface modification, may be ascribed solely to variations in cos θ. If cos θ = 1 in Run A, for the desorption of water from clean porous glass, then corresponding values of θ may be calculated for Runs B and C, as in Table II.

That the contact angle is less than 90° is to be expected, since Runs B and C show evidence of extensive capillary condensation; this result is also consistent with those of direct contact angle studies at silane-treated glass surfaces[5,15]. The adsorption isotherms also show evidence of a slow, irreversible change in surface properties: additional water is taken up during each of Runs B and C, which cannot be removed by pumping at room temperature; $\underline{v}_{\underline{m}}$ reverts nearly to its original value after the first water adsorption on the treated surface; the uptake at saturation

also increases; and the contact angle shows a slight decrease. (Here it should be noted that the value of θ obtained from Run B may already have fallen from its maximum value, since it was obtained from the desorption isotherm, after the surface had been in contact for several days with water vapour concentrations up to saturation).

These findings are all consistent with the suggestion of Elliott and Riddiford[15] that water molecules may "penetrate" the hydrophobic surface layer formed by reaction with alkyl halo-silanes. It is not yet clear, however, whether the change in surface properties is simply due to the physical presence of intercalated water, or whether an actual hydrolysis reaction is involved. A spectroscopic study of the "irreversibly" adsorbed water would therefore be of particular interest.

CONCLUSIONS

(i) Trimethylmonochlorosilane reacts with slightly less than half of the available surface hydroxyl groups in fully hydrated porous glass.

(ii) The consequent reduction in B.E.T. monolayer capacity to water is attributed largely to the restriction of water adsorption, at relative pressures below about 0.2, to unreacted hydroxyl groups, and only slightly to an actual reduction in specific surface.

(iii) Subsequent exposure of the treated surface to water vapour causes its hydrophobic character to decline, in a way which is

consistent with contact angle observations.

REFERENCES

1. Hunter, M.J., Gordon, M.S., Barry, A.J., Hyde, J.F. and Heidenreich, R.D., Ind.Eng.Chem., 39, 1389 (1947)

2. Vanderwort, G.L. and Willard, J.E., J.Amer.Chem.Soc., 70, 3148 (1948)

3. Babkin, I.Yu., Vasil'eva, V.S., Drogaleva, I.V., Kiselev, A.V., Korolev, A.Ya., and Shcherbakova, K.D. Dokl.Akad.Nauk SSSR 129, 131 (1959)

4. Vasil'eva, V.S., Drogaleva, I.V., Kiselev, A.V., Korolev, A.Ya. and Shcherbakova, K.D., Dokl.Akad.Nauk SSSR 136, 852 (1961)

5. Blake, T.D., Everett, D.H. and Haynes, J.M. "Wetting" (S.C.I. Monograph No.25, London, 1967), 164.

6. Barrer, R.M. and Barrie, J.A. Proc.Roy.Soc. 213A. 250 (1952)

7. Amberg, C.H. and McIntosh, R., Can.J.Chem., 30, 1012 (1952)

8. Wade, W.H., J.Phys.Chem., 68, 1029 (1964)

9. Ferguson, C.B. and Wade, W.H., J.Coll.Interface Sci., 24, 366 (1967)

10. Kiselev, A.V., Kovaleva, N.V., Korolev, A.Ya. and Shcherbakova, K.D., Dokl.Akad.Nauk SSSR, 124, 617 (1959)

11. Melrose, J.C., J.Soc.Petrol.Eng., 5, 259 (1965)

12. De Boer, J.H., Proc.Colson Research Soc., 10, 68 (1958)

13. Zsigmondy, R., Z.anorgChemie, 71, 356 (1911)

14. Brunauer, S., Mikhail, R.Sh. and Bodor, E.E., J.Coll.Interface Sci., 24, 451 (1967)

15. Elliott, G.E.P. and Riddiford, A.C., J.Coll.Interface Sci., 23, 389 (1967)

TABLE I

Isotherm constants

Run	w_m/mgm-gm^{-1}	c	Δw_o/mgm-gm^{-1}	w_ω/mgm-gm^{-1}
A	37.6	11.4	0	207
B	20.5	13.6	8.2	189
C	35.8	10.9	12.0	198

TABLE 2

Calculation of contact angle from desorption isotherms

Run	C_d/cm^{-1}	r_h/Å	$C_d r_h$	cos 0	0/deg
A	1.21×10^7	16.5	2.00	(1.00)	(0)
B	0.506×10^7	15.0	0.76	0.38	68
C	0.583×10^7	15.7	0.92	0.46	63

CAPTION

Fig.1 Water adsorption on porous glass at 30.0°C - effect of Me_3SiCl treatment.

Open points, dotted lines - adsorption

Filled points, full lines - desorption

-O- Run A — before treatment.

-□- Run B

-Δ- Run C ↓ after treatment

-◇- Run D

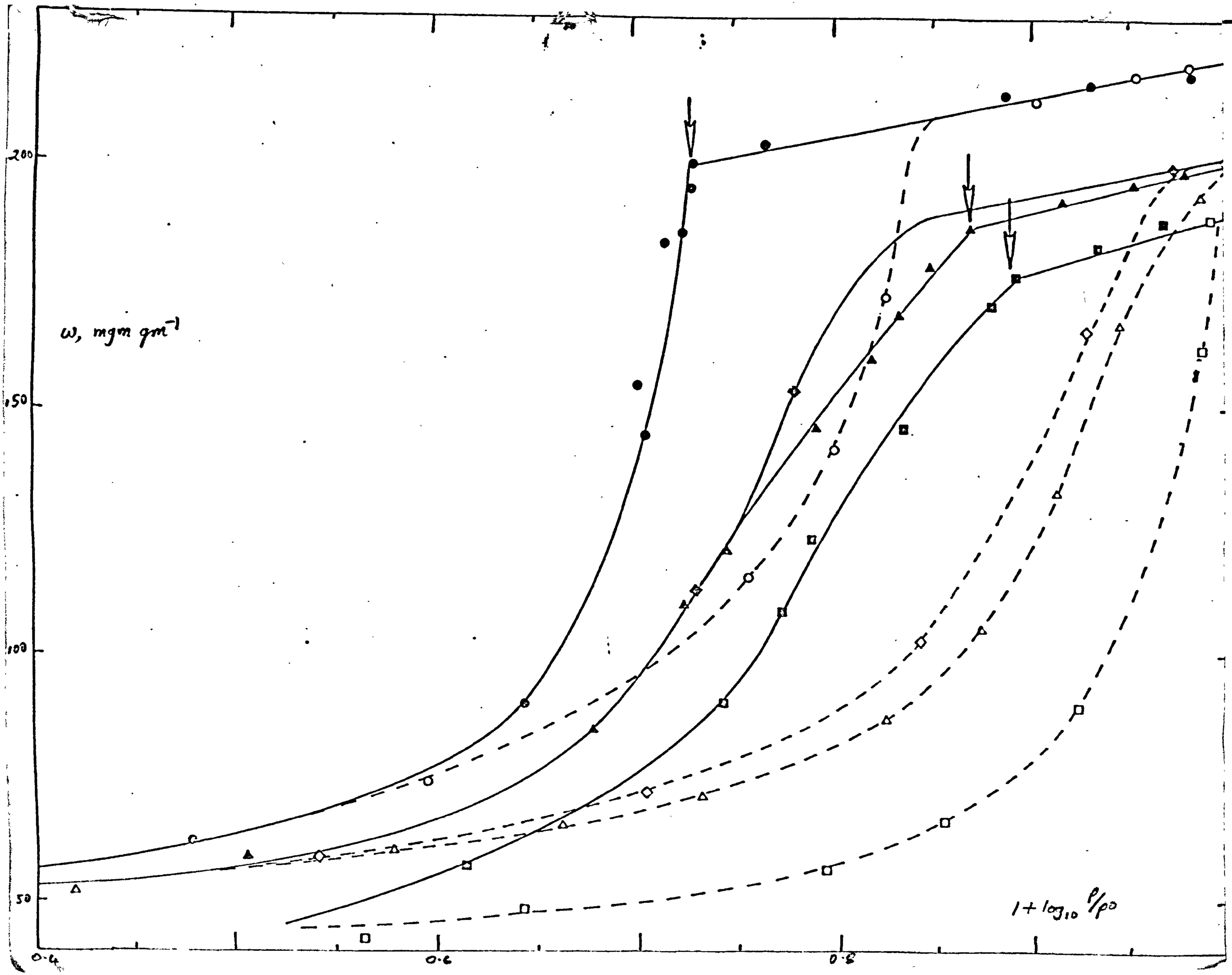
200
150
100
50
ω, mgm gm⁻¹
0·4
0·6
0·8
1 + log₁₀ p/p₀